Contamination of the environment with plastic debris

“Development, improvement, and evaluation of monitoring methods”

Kumulative Dissertation

zur Erlangung des akademischen Grades einer Doktorin

der Naturwissenschaften (Dr. rer. nat.)

in der Bayreuther Graduiertenschule für Mathematik und Naturwissenschaften

(BayNAT)

der Universität Bayreuth

vorgelegt von

Sarah Piehl

aus Fulda

Bayreuth, 2019

Die vorliegende Arbeit wurde in der Zeit von August 2014 bis Oktober 2019 in Bayreuth am Lehrstuhl Tierökologie I unter Betreuung von Herrn Professor Dr. Christian Laforsch angefertigt.

Vollständiger Abdruck der von der Bayreuther Graduiertenschule für Mathematik und Naturwissenschaften (BayNAT) der Universität Bayreuth genehmigten Dissertation zur Erlangung des akademischen Grades einer Doktorin der Naturwissenschaften (Dr. rer. Nat.).

Dissertation eingereicht am: 22.10.2019
Zulassung durch das Leitungsgremium: 30.10.2019
Wissenschaftliches Kolloquium: 15.05.2020

Amtierender Direktor: Prof. Dr. Markus Lippitz

Prüfungsausschuss:

Prof. Dr. Christian Laforsch (Gutachter)
Prof. Dr. Stefan Peiffer (Gutachter)
Prof. Dr. Holger Kress (Vorsitz)
Prof. Dr. Heike Feldhaar

Content

List of Abbreviations

ATR	Attenuated total reflection
BEPP	Basic enzymatic purification protocol
BSH	Backshore
cDOM	Colored dissolved organic matter
Chl-A	Chlorophyll-a
CNR-ISMAR	Consiglio Nazionale delle Ricerche- Istituto di Scienze Marine (National Research Council - Institute of Marine Science)
DLR	Deutsches Zentrum für Luft- und Raumfahrt
DW	Dry weight
EP	Epoxid
ETL	Extreme tide line
EU	European Union
FPA	Focal plane array
FTIR	Fourier Transform-infrared
GESAMP	Joint Group of Experts on the Scientific Aspects of Marine Environmental Protection
HELCOM	Baltic Marine Environment Protection Commission
HTL	High tide line
HZ	Hyporheic zone
LIPI	Lembaga Ilmu Pengetahuan Indonesia (Indonesian Institute of Science)
MARPOL	International Convention for the Prevention of Pollution from Ships
MP	Microplastic
MSFD	Marine Strategy Framework Directive
NOAA	National Oceanic and Atmospheric Administration

OSPAR	Convention for the Protection of the Marine Environment of the North-East Atlantic
PAN	Polyacrylonitrile
PBT	Polybutylene terephthalate
PE	Polyethylene
PES	Polyester
PET	Polyethylene terephthalate
PP	Polypropylene
PS	Polystyrene
PTFE	Polytetrafluoroethylene
PUR	Polyurethane
PVC	Polyvinyl chloride
Pyr-GC-MS	Pyrolysis-gas-chromatography-mass spectroscopy
RGB	Red-Green-Blue (color model)
SD	Standard deviation
SPM	Suspended particulate matter
STCZ	Sub-tropical convergence zone
SWIR	Short waved infrared
TED	Thermoextraction and desorption
TSG-ML	Technical Subgroup on Marine Litter
UAS	Unmanned aerial systems
UEPP	Universal enzymatic purification protocol
UV	Ultraviolet
WWTP	Wastewater treatment plant

Abstract

Improper disposal of plastics, coupled with their durability and low weight, has led to the widespread environmental pollution of plastic debris. For larger plastic debris negative ecological, cultural, economic, safety, and health impacts are reported and well known. For microplastics (particle size ≤5 mm), harmful effects are still a matter of debate. Nevertheless, microplastics are the distinct subject of national and international marine monitoring directives (i.e. MSFD, NOAA), due to their bioavailability to a wide range of organisms, their omnipresence in the marine environment, and the lack of removal techniques once introduced. Microplastic contamination levels have been intensively examined within marine habitats. And even though the relationship of human activities and plastic debris inputs are known, significant knowledge gaps exist on the sources, transport, and accumulation areas in terrestrial environments.

Thus, the first objective of this thesis was the *identification of potential sources, pathways, and accumulation areas of plastic debris in terrestrial environments*. Three case studies on overlooked, yet potentially plastic debris containing sources and accumulation areas, were carried out. As plastics frequently enter biowastes through misthrows, we exemplarily investigated organic fertilizer from biowaste fermentation and composting as input source of microplastic debris to farmlands. Our results indicate that, depending on receiving wastes, pretreatment of the substrate, and the technical state of the plant, organic fertilizers can contain high concentrations of microplastics. When applied to farmlands, a potential input of 35 billion to 2.2 trillion microplastic particles per year was calculated for German arable land. As around 50% of land use in Germany is agricultural, we further investigated plastic debris contamination of a farmland neither subjected to known plastic-containing fertilizer or to plastic applications. We detected 206 large plastic pieces, and 158,100 to 292,400 microplastic pieces per hectare. Additionally, we were the first to investigate the hyporheic zone of streambed sediments, a transition zone between fresh- and groundwater. Our exemplary study at the Rote Main river indicated that especially small microplastics (<50 µm) are infiltrated into sediments of the hyporheic zone of streambeds. Even though, results from this study are based on one sample, it points towards another temporal sink and relevant transportation pathway for microplastics.

The lack of sufficient sample replication is a common issue in microplastic studies, mainly due to the high costs of sampling, sample processing, and analytics. Consequently, the second objective was to *improve existing sampling and sample processing methods for microplastics*. Concerning sample processing, environmental samples often contain a high number of natural particles that impair spectroscopic identification of microplastics if not removed. Thus, I contributed to the development of a gentle sample purification protocol that is adaptable to a broad range of

environmental samples. With the application of a series of specific enzymes, we achieved high removal efficiencies of organic matter from surface water samples (>95%) and high recovery rates of microplastics (>80%). Yet, sample replication is still a compromise between representativeness and feasibility within a project. To assess sufficient sample replication for beaches, we studied the spatial distribution of microplastics in beach sediments of the Po River Delta, in northern Italy. Our analysis of microplastics >1 mm for three different accumulation areas suggests that for the high tide line, the recommendation by the "Technical Subgroup on Marine Litter" of five replicates is sufficient. If accumulation areas farther from the waterline are sampled, a minimum of 10 replicates should be taken. The highly variable polymer type distribution among the accumulation areas further indicated that for a comprehensive assessment of microplastic contamination, different accumulation areas need to be sampled. However, concerning water surface samples from coasts and the open ocean, a representative sampling will be limited simply because of their mere dimensions.

Hence, the third objective was the *development of alternative monitoring methods* that could provide additional information on sources, sinks, and transport pathways of buoyant plastic debris. A three-dimensional hydrodynamical model, coupled with a Lagrange particle tracking module, was utilized to forecast the transport of microplastics emitted by the Po River branches and subsequent off-washing onto adjacent beaches. A correlation with in-situ measured microplastic abundances on the beaches was not present. In another approach, we assessed if water constituents depictable from satellite images (e.g., chlorophyll-a, suspended particulate matter, and colored dissolved organic matter) could be used as proxy to indirectly map microplastic distribution. Under the assumption that microplastic transport is driven by similar processes, such as wind and currents, we tested if a correlation between microplastics and those water constituents exists. The results of three field data acquisitions on three different river systems showed no clear relationship, with only one data set showing a spatial correlation between microplastics and the proxy water constituents. Nevertheless, model simulations and remote sensing techniques are able to provide information on larger spatial and temporal scales, which is why the development of this methods should be followed in future.

Zusammenfassung

Die unsachgemäße Entsorgung von Plastikprodukten, die die Eigenschaft besitzen gleichzeitig leicht und stabil zu sein, hat zu einer globalen Verschmutzung der Umwelt mit Kunststoffmüll geführt. Für größeren Plastikmüll sind negative Einflüsse auf Ökologie, Kultur, Ökonomie, Sicherheit und Gesundheit dokumentiert und bekannt, wohingegen die Gefahren von Mikroplastik (Kunststoffpartikel ≤5 mm) noch kontrovers diskutiert werden. Allerdings hat die Bioverfügbarkeit dieser Partikel für Organismen an der Basis des Nahrungsnetzes, seine Omnipräsenz in der marinen Umwelt sowie das derzeitige Fehlen von Methoden zur Entfernung aus der Umwelt dazu geführt, dass Mikroplastik in nationalen und internationalen Richtlinien zum Erhalt und Verbesserung der marinen Umwelt (z.B. MSFD, NOAA) aufgenommen wurde. Die Kontamination mariner Systeme mit Mikroplastik wurde daher in den letzten Jahren gut untersucht. Doch auch wenn bekannt ist, dass das Auftreten von Kunststoffmüll in der Umwelt mit menschlichen Aktivitäten zusammenhängt, gibt es bisher kaum Studien zum Eintrag, Transport und Verbleib von Kunststoffmüll in terrestrischen Ökosystemen.

Daher war das erste Ziel der Doktorarbeit die *Identifizierung von potenziellen Quellen, Transportwegen und Akkumulationsgebieten von Kunststoffmüll in terrestrischen Ökosystemen*. Drei Fallstudien von bisher unberücksichtigten und potenziell durch Kunststoffmüll belasteten Quellen und Akkumulationsgebieten, wurden durchgeführt. Da Kunststoff durch Fehlwürfe in Bioabfälle gelangt, wurden Dünger von Bioabfallvergärungs- und Bioabfallkompostieranlagen als potenzieller Eintragspfad von Mikroplastik auf landwirtschaftliche Flächen untersucht. Unsere Ergebnisse zeigen, dass, abhängig vom zugeführten Substrat, dessen Vorbehandlung und der Art der Prozessierung, dieser einen relevanten Eintragspfad in die Umwelt darstellen kann. Wenn diese Düngemittel aus Bioabfallaufbereitungsanlagen auf Ackerland aufgebracht werden, würde sich aus unseren Ergebnissen ein potenzieller Eintrag von 35 Milliarden bis 2.2 Billionen Mikroplastikpartikeln pro Jahr in Deutschland ergeben. Da landwirtschaftliche Flächen ca. 50% der Landnutzung in Deutschland darstellen führten wir eine erste Untersuchung auf einem Ackerland in Süddeutschland durch. Auf diesem wurden weder potenziell Plastik-enthaltenen Düngemittel noch Plastikmaterialien als Hilfsmittel eingesetzt. Dabei wurden 206 größere Plastikteile und zwischen 158.100 und 292.400 Mikroplastikpartikel pro Hektar detektiert.

Darüber hinaus untersuchten wir exemplarisch am Roten Main zum ersten Mal die hyporeische Zone eines Flussbetts, als Verbindungszone zwischen Fluss- und Grundwasser. Die Ergebnisse legen nahe, dass vor allem sehr kleine Mikroplastikpartikel (<50 µm) in die hyporeische Zone des Flussbetts infiltriert werden. Auch wenn nur eine Probe untersucht werden konnte, deuten

unsere Ergebnisse auf eine weitere temporäre Senke und einen relevanten Transportweg bestimmter Mikroplastikpartikel hin.

Eine akzeptable Replikation von Umweltproben ist derzeit bei Studien zu Mikroplastik generell problematisch, was auf kosten- und arbeitsintensive Beprobungen, Probenaufbereitung und -analyse zurückzuführen ist. Daher war das zweite Ziel der Doktorarbeit die *Verbesserung bereits bestehender Methoden zur Probennahme und -aufbereitung von Mikroplastik*. Hinsichtlich der Probenaufbereitung dominieren in Umweltproben meist natürliche Partikel. Diese müssen aus der Probe entfernt werden, um anschließend die spektroskopische Identifizierung von synthetischen Polymerpartikeln nicht zu beeinträchtigen. Hierfür wurde ein Protokoll zur Aufreinigung der Mikroplastikproben entwickelt, welches auf ein breites Spektrum an Umweltproben anwendbar ist. Durch die aufeinander folgende Nutzung spezifischer Enzyme wurde organisches Material in Proben von der Wasseroberfläche effizient entfernt (>95%), bei einer gleichzeitig hohen Wiederfindungsrate von Mikroplastikpartikeln (>80%). Dennoch ist die Anzahl der Replikate zurzeit ein Kompromiss zwischen Repräsentativität und der Machbarkeit innerhalb eines Projektes. Um eine ausreichende Replikation von Sedimentproben an Stränden zu evaluieren, haben wir die räumliche Verteilung von Mikroplastik exemplarisch in Strandsedimenten des Poflussdeltas in Norditalien untersucht. Unsere Analyse von Mikroplastikpartikeln >1 mm für drei verschiedene Akkumulationszonen zeigt, dass für die aktuelle Hochwasserlinie der Vorschlag der "Technical Subgroup on Marine Litter“ von fünf Replikaten ausreichend ist, wohingegen mindestens 10 Replikate für höher gelegene Akkumulationszonen für eine repräsentative Probennahme nötig sind. Des Weiteren deutet eine höchst variable Verteilung der Polymertypen zwischen den Akkumulationszonen darauf hin, dass die alleinige Betrachtung einer einzelnen Akkumulationszone für eine vollständige Beschreibung der Mikroplastikkontamination eines Gebietes nicht ausreicht. Wenn man allerdings Wasseroberflächenproben in Küstengebieten und im offenen Ozean betrachtet, ist eine repräsentative Beprobung durch die enormen Dimensionen nicht möglich.

Um zusätzliche Informationen zu Quellen, Senken und dem Transport von auf der Wasseroberfläche treibendem Kunststoffmüll zu erhalten war die *Entwicklung alternativer Monitoringmethoden* das dritte Ziel der Doktorarbeit. Mittels eines dreidimensionalen hydrodynamischen Modells gekoppelt mit einem Lagrange-Partikel-Modell wurde Mikroplastik, welches durch die Poflussdelta-Mündungen entlassen wurde, verfolgt und dessen Anlandung an angrenzende Strände vorhergesagt. Allerdings ergab der Vergleich mit den Felddatenerhebungen von Mikroplastik keine Übereinstimmung mit den Modellvorhersagen. In einem weiteren Experiment untersuchten wir, ob Wasserparameter, deren Verteilung durch Satellitenbilder bestimmbar sind (z.B. Chlorophyll-a, Schwebstoffe und Gelbstoffe), als Indikatoren für die

Verteilung von Mikroplastik herangezogen werden können um dessen Verbreitungsmuster vorherzusagen. Unter der Annahme, dass Mikroplastik den gleichen Transportmechanismen (Wellen und Wind) wie den oben genannten Wasserparametern ausgesetzt ist, wurde eine mögliche Korrelation zwischen Mikroplastik und den Wasserparametern untersucht. Nur bei einer von insgesamt drei Feldkampagnen an drei verschiedenen Flusssystemen konnte ein räumlicher Zusammenhang von Mikroplastik und Wasserparametern gezeigt werden. Dennoch stellen sowohl hydrodynamische Modelle als auch Fernerkundungsdaten Informationen über größere räumliche Distanzen und höher aufgelöste Zeiträume bereit, weshalb die Entwicklung dieser Methoden in Zukunft weiterhin verfolgt werden sollte.

SYNOPSIS

Introduction

The plastic debris problem

Human activities and interactions with natural ecosystems are substantially changing the environment and leaving measurable impacts on earth. Hence, scientists propose the "Anthropocene" as a new geological epoch, starting in the mid-twentieth century (Waters et al. 2015, Zalasiewicz et al. 2015). Among proposed stratigraphic indicators marking the Anthropocene is one material which nowadays permeates all domains of our lives: plastics (Zalasiewicz et al. 2016). Alongside the proliferation of plastics came the emergence of "disposables"; single-use goods that spawned a new consumer behavior termed "throwaway living" (Life Magazine 1955). Since then, plastic production has steadily risen, and within the last 50 years the increase of plastic consumption has outpaced population growth by almost 50-fold (Andrady 2015).

Due to its adjustable diverse characteristics and low-cost production, plastic is superior to most other materials. Within the ~20 chemically distinct classes of synthetic polymers, only six account for commodity plastics (Andrady 2003). Of these six, polyethylene (PE; 36%), polypropylene (PP; 21%), and polyvinyl chloride (PVC; 12%), followed by polyethylene terephthalate (PET), polyurethane (PUR), and polystyrene (PS) (<10% each), represent the largest groups in total non-fiber plastic production, while polyester (mostly PET) has the highest share of the synthetic fiber production (70% of all acrylic fibers) (Geyer et al. 2017). Those six commodity plastics account for more than 80% of total plastic demand (Law 2017). Despite being used in nearly all market sectors, the largest demand for synthetic polymers comes from the packaging industry, which accounts for 40% within the EU (PlasticsEurope 2018). Due to the relatively short lifetime of plastic packaging products, the share of plastic on solid waste production has steadily increased, with a current sharing of 10-15% by weight (Andrady 2017). It is further estimated that globally 32% of the plastic packaging debris entering collection systems is leaking into the environment (World Economic Forum 2016). The combination of moderate growing polymer recycling rates and fast growing polymer production rates (Geyer et al. 2017) has turned environment plastic contamination into one of the fastest growing forms of pollution.

Given that it can take centuries for plastic debris to become mineralized (Andrady 2003), it is assumed that the majority of plastic debris that has escaped collection systems (since the start of mass production) is still present in the environment (Andrady 2015). Plastic litter visible to the

naked eye represents only a part of this contaminant pervading all ecosystems on earth. Chemical, physical, and biological processes break apart plastic debris, fragmenting it into smaller, microscopic particles. Those “microplastics” (MPs) of secondary origin are broadly defined as synthetic polymer particles ≤5 mm (Arthur et al. 2009), whereas the lower size limit is often set by sampling and analytical techniques with a lower size limit of 1 µm (Kershaw et al. 2019, Frias & Nash 2019). Besides MPs of secondary origin, primary MPs are intentionally produced within this size range to be used in cosmetic or cleansing products, for air-blasting and as drilling fluid (Auta et al. 2017), and even as film-coatings applied to agronomic seeds (Accinelli et al. 2019). Nevertheless, the majority of MPs in the environment arises through weathering of larger plastic debris. Plastic degradation refers to any process that leads to the chemical transformation of a material, changing its properties and resulting in discoloration, cracking, or erosion, among others (Singh & Sharma 2008). Exposure to UV radiation, which causes photo-oxidative degradation, is the major factor for degradation of plastic debris in the environment (Andrady 2017). Examples of other less influential mechanisms are thermal degradation, mechanochemical degradation, and biodegradation (Singh & Sharma 2008). Nevertheless, depending on the plastic debris location in the environment, the relative importance of those processes may change. For example, the fragmentation of plastic debris at beaches is greater than at a sea or lake bottom where neither solar radiation nor mechanical forces can contribute to fragmentation of the plastics.

The fate of plastic debris in the environment also determines their bioavailability to organisms. As synthetic polymer particles become smaller and smaller, the number of organisms capable of ingesting those particles grows. As a result, MPs are of special concern, as laboratory studies have shown that they can be ingested by organisms at the base of the food web (Cole et al. 2011, 2013). Moreover, it is known that nano-sized synthetic polymer particles are able to cross cell barriers (Hussain et al. 2001, Lehner et al. 2019). Potential harmful effects of MP ingestion for organisms at the base of the food web are thought to be similar to the effects observed for large plastic debris, but scientific evidence is currently lacking and controversially discussed (Ogonowski et al. 2018, Foley et al. 2018). Additionally, it often cannot be distinguished if observed effects are the result of the synthetic polymer itself or incorporated additives (Karami 2017, Schrank et al. 2019). Additives include a set of chemicals used to achieve the desired functions of the plastic product and can include, among others, plasticizer, flame retardants, stabilizers, antioxidants, and color pigments.

Thus, plastic debris constitutes not only a single material with defined characteristics, but a complex mixture of items differing in size, shape, density, and chemical composition. And with clear evidence for large plastic debris of direct negative impacts to a wide range of organisms (Sheavly & Register 2007, Gall & Thompson 2015) and the potential of MPs to pose a risk to human health (Sharma & Chatterjee 2017, Wang et al. 2019). Different interest groups have called for an immediate implementation of measures to curb plastic debris pollution. Therefore, a sound understanding about emission sources, transport patterns, and accumulation areas of plastic debris in the environment is required.

Occurrence of microplastic debris in the environment

Even though MPs are not easily visible by the naked eye, they were already observed in the marine environment around 50 years ago (Carpenter et al. 1972, Morris & Hamilton 1974, Colton et al. 1974). Nevertheless, at the beginning research focused on large marine plastic debris. With increasing awareness of the negative impacts to organisms and the economy, policies approaching the problem were formulated, leading to a subsequent decrease of studies in this field in the '90s (Bergmann et al. 2015). Within the last decade, the study of plastic debris has resumed, as MPs have been recognized as a potential risk to organisms and the environment (Browne et al. 2015). As with larger plastic debris, research on MPs began within marine environments. Due to the different densities of the various polymers (ranging from ~0.05 g cm^{-3} for expanded PS to 1.4 g cm^{-3} for PET and PVC; Bergmann et al. 2015), MPs are located throughout the entire water column, being affected by different transport processes. Thus, MPs have been identified from the water surface to the deep sea, and from Antarctic sea ice to tropical beaches (Cole et al. 2011, Auta et al. 2017, Peeken et al. 2018, Rezania et al. 2018). Sea bottom sediments have been largely proposed as a final sink (Fischer et al. 2014, Bergmann et al. 2017, Tekman et al. 2017), a reasonable conclusion given that the water cycle transports most of the land-based MP debris to the sea. During its residence time in aquatic systems, MP debris is subjected to density-changing processes, such as biofouling or agglomeration (Rummel et al. 2017, Michels et al. 2018), which initiates its sinking to the seafloor. As most plastic is produced and consumed on land, rivers were immediately addressed as major emission sources of plastic debris and MPs to the oceans (Browne et al. 2011, Rech et al. 2014, Wagner et al. 2014, Jambeck et al. 2015, Lebreton et al. 2017). The following studies on freshwater ecosystems revealed comparable quantities of MPs in lakes and rivers as in the marine environment (Imhof et al. 2013, Eerkes-Medrano et al. 2015, Li et al. 2017, Rezania et al. 2018), with lake sediments being proposed as a sink for MPs within the terrestrial environment (Schwarz et al. 2019).

Considering point sources of MPs for freshwater systems, wastewater and sewage sludge (Mintenig et al. 2016, Gatidou et al. 2019), as well as industrial sites (Lechner & Ramler 2015), were among the first identified. Nevertheless, a certain amount of MP debris in freshwater systems is introduced via diffuse sources from land, i.e. urbanized areas (Dris et al. 2015), agricultural farmland (Duis & Coors 2016, Horton et al. 2017), or atmospheric fallout (Dris et al. 2016). Improper disposal of plastic waste and its continuous fragmentation to MP particles is often the cause, but there is also a wide variety of applications for plastic products in the terrestrial environment, such as geotextiles (Wiewel & Lamoree 2016) or agricultural plastic applications (Briassoulis et al. 2010, Liu et al. 2014), where unintentional losses can occur. Yet, there is a considerable lack of studies targeting sources, transport, and sinks of plastic and MP debris in freshwater systems, especially in regard to the terrestrial environment.

Environmental monitoring of microplastic debris

Initial assessments of plastic and MP debris contamination levels are not only necessary to provide data on the current condition and to assess the relevance of this kind of pollution, but also to design and direct monitoring programs more effectively (Kershaw et al. 2019). In addition, environmental monitoring of plastic debris includes repeated measurements to assess pollution levels and to detect temporal and spatial trends as well as to evaluate whether prevention and/or mitigation strategies are successful, i.e. if plastic debris pollution decreases over time. For monitoring programs, several conditions are essential to ensure that the measurements are representative and comparable between studies, thus requiring the development of standardized monitoring protocols. One of the first attempts was made by the Technical Subgroup on Marine Litter (TSG-ML), who suggested methods for marine plastic debris monitoring based on the most often used techniques ("Guidelines for Monitoring of Marine Litter") and highlighted the need for further standardization (Hanke et al. 2013). Moreover, the relevance of prevention of sample contamination, due to the omnipresence of this contaminant, was already addressed and guidance given to apply precautions to minimize contamination of samples in the field and laboratory. Nevertheless, procedural blanks should accompany data acquisitions but was either not reported or not considered in many previous studies although an upward trend is indicated (Filella 2015). Contamination of samples is increasing with decreasing size class of particles and depending on the investigated size class of MP the magnitude of applied precautions may differ. Results from procedural blanks should be reported as well as how corrections to MP data were made. First advice on how to treat the results of procedural blanks in order to account for background contamination were published in the current GESAMP report (Kershaw et al. 2019).

Due to the novelty of MPs as environmental contaminants, the development of standardized monitoring protocols is still ongoing and improvements are compulsive, considering sample extraction techniques, sample preparation, and reliable identification and quantification methods. Thereby, several requirements for an operational monitoring should be fulfilled, with the most important two being cost- and labor-effective and ease of application. For example, large plastic debris can be visually identified, but visual identification of MPs leads to errors of up to 70% (Hidalgo-Ruz et al. 2012). Therefore, a reliable identification of MPs demands a chemical characterization. Currently, Fourier Transform-infrared (FTIR), Raman spectroscopy, or thermal analysis such as pyrolysis-gas-chromatography-mass spectroscopy (Pyr-GC-MS) and thermoextraction and desorption (TED), coupled with GC-MS, are the most prevalent methods used by scientists (Mai et al. 2018). The main difference between spectroscopy and thermal analysis is the reference unit yielding MP particle numbers for spectroscopy, whereas thermal analysis records the mass of MPs. A challenge for all analytical methods is the precedent sample purification process before the analysis. For a representative sample, large sample volumes need to be taken, resulting in high abundances of organic and inorganic materials that would interfere with subsequent spectroscopic analysis if not removed. Protocols for the separation of inorganic particles from MPs using high density solutions were already proposed in the early stages of MP research (Imhof et al. 2012, Hidalgo-Ruz et al. 2012). For the removal of organic matter, strong acidic or alkaline solutions, as well as oxidation agents, have later been reported in the literature (Book Chapter, Appendix). Nevertheless, those chemicals bear the danger of degrading sensitive polymer types (Enders et al. 2017). An alternative was proposed by Cole et al., (2015) using enzymes for a gentler treatment, but which is associated with high expenses and thus makes it impractical for operational monitoring activities. Thus, further progress in cost- and labor-efficient sample processing and analysis is essential to conduct spatio-temporal sufficient replicated MP contamination studies, and to draw general conclusions about the contamination level and contamination trends of a sampled area.

Considering sampling areas, plastic debris monitoring activities are imbalanced, as most studies have been conducted on sandy beaches and the sea surface, followed by bottom sediment samples and water column samples (Hidalgo-Ruz et al. 2012, Bergmann et al. 2015, Van Cauwenberghe et al. 2015, Duis & Coors 2016). The cost of sampling increases the further away from land the samples are taken (e.g., costly ship expeditions). The good accessibility of beaches makes them attractive areas for monitoring activities. Additionally, because beaches act as accumulation area for plastic debris, they allow for a relatively easy assessment of contamination trends. For large plastic debris, operational protocols for beach monitoring exist and are routinely applied (HELCOM 2008, OSPAR 2010, Kershaw et al. 2019). Nevertheless, different sampling designs are

applied for MPs (e.g., different beach areas, sample volumes, sample depth, size fractions, etc.), and as only a small proportion of the whole beach can be surveyed, comparison among studies are accompanied with high uncertainties (Filella 2015). In addition, the distribution of MPs is highly variable, causing high standard deviations in reported data; however in-depth investigations of the quantity of replicates needed to obtain an acceptable precision are rare.

Alternative monitoring methods

Generally speaking, MP abundance data for any environmental compartment is spatially and temporally limited as currently the demand of resources for MP sampling, sample preparation, and analysis are high. Albeit, MP studies revealed high spatio-temporal variability of MP abundance for small and large scales (Heo et al. 2013, Fisner et al. 2017, Imhof et al. 2017, Chubarenko et al. 2018), and transportation pathways and accumulation patterns are far away from being fully understood. Additional monitoring tools that cover larger areas and allow for a higher temporal replication are likewise needed for operational monitoring activities of plastic debris. Considering the vast dimensions of the oceans, for example, seawater motion can be mapped using hydrodynamical modelling approaches. Coupled with particle tracking models, any tracers transported by the seawater can be further tracked (van Sebille et al. 2018). Thereby, particle tracking models make use of velocity fields computed by hydrodynamical models to determine trajectories of virtual particles (van Sebille et al. 2018). Particle path can be tracked by using a numerical integration method to integrate through time and space. Model simulations on marine litter transport using Lagrangian particle tracking were already conducted in previous studies, identifying the formation of oceanic accumulation areas (Lebreton et al. 2012) or tracking debris released from a tsunami (Lebreton & Borrero 2012). Thereby, rivers and estuaries primarily have been implemented in model simulations as point sources (Lebreton et al. 2012, Siegfried et al. 2017), and only limited studies focused on modelling river transport, especially with regard to MPs (Besseling et al. 2017).

Besides numerical modelling approaches, another monitoring technology widely applied for environmental monitoring are remote sensing data acquisitions. Polymers exhibit specific absorption bands in the short waved infrared (SWIR) range and thus, a direct identification of plastic debris theoretically could be possible with remote sensors covering the SWIR range as applied in satellite sensors. Nevertheless, as the proportion of plastic debris is too low to significantly influence the signal reflected from the water surface, a direct identification of plastic debris at sea with remote sensing systems is currently not feasible (Mace 2012). Besides, other substances further influence the reflected signal such as suspended particulate matter (SPM) or

chlorophyll-a (Chl-A). Within this context, Pichel et al. (2007) first published an indirect approach, using water constituents as proxies for plastic accumulation areas within the oceans. For example, it is known that the sub-tropical convergence zone (STCZ) within the North Pacific is accumulating floating materials due to its circular current patterns and thus, plastic debris (Lebreton et al. 2012). Pichel et al., (2007) used satellite-derived information to study the STCZ and predicted plastic debris accumulation. Moreover, a spatial relationship could be detected for satellite-derived Chl-A, sea surface temperature and macroplastic debris (Pichel et al. 2007), but if this relationship also exists for MP particles was not investigated. Yet, the study demonstrated an application for an indirect monitoring approach of plastic debris through water constituents derived from satellite imagery.

Objectives of the thesis

My PhD thesis focused on MPs, due to the emerging significance of this contaminant in the environment. Large plastic debris was further addressed in some of the studies as the fragmentation of larger plastics generally is the major source for MP debris in the environment. In this thesis, MP is defined as synthetic polymer particles ≤5 mm and larger plastic debris considered as macroplastic. The thesis is structured into three chapters whose specific objectives are outlined here.

Identification of potential sources, pathways, and accumulation areas of plastic debris in terrestrial environments (Chapter A)

Considering plastic debris contamination, and specifically MP debris, terrestrial ecosystems are still understudied. At the beginning of this thesis only limited data on plastic debris and almost no studies on MP debris within terrestrial environments were published. Moreover, the initial perception of plastic debris pathways was often unidirectional, assuming inputs from land and continuous transport via rivers to the oceans. Likewise, few studies addressed ecotones between freshwater and terrestrial systems. Within this thesis three case studies were conducted on overlooked, yet potentially relevant plastic debris sources or accumulation areas in terrestrial environments. As plastic debris is correlated to human activities and agriculture comprises around 50% of land use in Germany (Statistisches Bundesamt 2019) we thus focused on arable land.

Sewage sludge had already been identified as potential pathway of MP debris to arable lands. Nevertheless, organic fertilizer from biowaste digestion, and composting was neglected as potential source and pathway of MP debris, despite the awareness that plastic debris is entering biowaste through frequent misthrows. Thus, we investigated for the first time the occurrence of large MP debris within organic fertilizer from 14 biowaste digestion and composting plants (Article A1). Knowing that arable land fertilized with sewage sludge or organic fertilizer from biowaste processing (Article A1) can thereby receive a high load of MP debris we were further interested to find out if farmlands, subjected neither to the above mentioned fertilizers nor plastic applications, are still susceptible to plastic debris contamination. Within a case study we assessed the contamination level of plastic debris and, for the first time, large MP debris, on a farmland in southeast Germany (Article A2). Furthermore, only a limited number of studies focused on transition zones of freshwater and adjacent terrestrial environments. The hyporheic zone was examined as an example for an ecotone, potentially depicting a temporal accumulation area as well as a pathway of MP debris between ecosystems. Concentrating on the Rote Main river in southeast Germany as study area, we investigated the occurrence of MP debris in the hyporheic zone of streambed sediments, for the first time (Article A3).

Moreover, an exemplary investigation, including MP sizes within the pore and sub-pore scale size (<50 µm), was conducted within this study, another novelty as this size class was mostly neglected in MP studies of streambed sediments due to elaborate sampling and analytical methods.

Improvement of existing sampling and sample processing methods for microplastics (Chapter B)

During the first three investigations challenges considering an efficient sampling, sample preparation and analysis of MP debris emerged. Moreover, for MPs efficient and applicable methods are still being developed, in contrast to larger plastic debris where standardized protocols exist and operational monitoring programs are already in place.

For instance, for a reliable identification of MP particles with spectroscopic methods, environmental samples (consisting of a mixture of diverse organic and inorganic materials) need to be efficiently purified, while leaving MP particles intact. To achieve this published protocols either use aggressive chemicals or expensive enzymes not affordable for routine applications (Book Chapter, Appendix). Thus, I supported the development of an enzymatic purification protocol, utilizing a series of technical grade enzymes, suitable for application within routine monitoring programs (Article B1). Especially beach sediments, which are the focus of operational monitoring programs due to their accessibility, often contain a high load of inorganic sediments, seashells, and organic washed-ashore materials. Here, initial considerations about the sampling design and sample replication are crucial to obtain achievable and representative results. As in-depth investigations of the spatial distribution and sample replication of MP debris on sandy shores were rare a case study on the spatial distribution of large MP at different accumulation areas on beaches of the Po River Delta was conducted (Article B2).

Development of alternative monitoring methods for buoyant plastic debris in aquatic systems (Chapter C)

Currently cost- and labor-intense sampling and analysis methods for MP debris hampers high resolved spatio-temporal in-situ data acquisitions. Thus, the concurrent development of alternative monitoring methods, providing additional information for monitoring attempts of plastic debris, was the third objective of this thesis. Within this thesis we focused exemplarily on the buoyant fraction of plastic debris.

Here, model simulations have already been proved to provide valuable data on plastic debris transport and accumulation for offshore environments. Nevertheless, due to their complex dynamics, coastal areas were mostly neglected. In our case study at the Po River Delta we followed two different approaches to predict coastal accumulation of buoyant MP particles emitted by the terminal branches of the Po River. Our first approach utilized a hydrodynamic model and

Lagrangian particle tracking module, whereas the second approach utilized remote sensing imagery of the river plume, represented by SPM (Article C1). Another monitoring strategy takes advantage of relationships between the contaminant of interest and proxy (i.e. indicator) parameters. Keeping track of the remote sensing approach from Article C1 we further investigated a potential relationship of water constituents depictable from satellite images and buoyant MP debris. Under the assumption that the distribution of water constituents (e.g., SPM, Chl-A, and colored dissolved organic matter (cDOM)) and buoyant MP debris is influenced by the same mechanisms (i.e. wind, currents) a case study on three different river systems was conducted to investigate spatial relationships of the proxy water constituents and MP debris (Article C2).

Overview of the thesis

Chapter A: Identification of potential sources, pathways, and accumulation areas of plastic debris in terrestrial environments

To determine the most effective measures for curbing plastic pollution in the environment, an identification of relevant input sources is crucial. The long prevailing marine perception of the issue has led to a considerable absence of studies on initial sources, pathways and accumulation areas of plastic debris (MP's especially) in terrestrial environments and their relevance.

Organic fertilizer as a vehicle for the entry of microplastic into the environment

Considering MPs, a neglected waste stream included organic fertilizers from biowaste fermentation and composting. Here, miss-sorting and contamination of biowaste with plastics is not unusual. Even though prior sorting and sieving procedures reduce those mistakes, a complete removal of contaminants is impossible. Most countries even allow a certain amount of contaminants in fertilizers with small foreign particles not considered within legislations (e.g., <2 mm in Germany). Thus, we investigated if organic fertilizers from biowaste composting plants and biowaste- and energy digesters are possible transporters of MP particles >1 mm to the environment (Article A1).

One biowaste composting plant and one biowaste digester were examined in detail (both receiving biowaste from households and green clippings from the area), and an agricultural energy crop digester used as reference point. Further, a commercially available fertilizer from a second biowaste digester (processing solely waste from commerce) and digestate samples from 10 agricultural biogas plants (processing feeds such as dung/manure, sunflowers, or waste from fruit processing together with the regular energy crops) were screened for large MP particles using attenuated total reflection (ATR)-based FTIR spectroscopy.

While all fertilizer samples from plants receiving biowaste contained MP particles, the amount and composition of MPs was dependent on the initial feeding substrates and the plant's technical state. High MPs abundances were observed in plants processing biowaste from households (14 to 146 MP particles per kg dry weight (DW)), as well as from commerce (895 MP particles per kg DW). Thereby, the composition of the fertilizer samples from plants receiving biowastes from households were dominated by PS and PE, polymers commonly used for food packaging. In contrast, it was primarily polyesters (PES) that were identified in plants processing commercial biowastes, likely emerging from protective containers and packaging.

Moreover, an in-depth analysis of one biowaste digestion plant (receiving mainly household biowaste, green clippings, and occasionally energy crops) revealed a divergent composition of MPs within composts matured for different time periods, pointing towards seasonal changes in biowaste composition. Concerning differences among plants, pre- and post-treatment processes are fundamental factors influencing the degree and variety of MP contamination in organic fertilizers. As MP degradation pathways are likely altered by oxygen availability, temperature, and exposure to UV radiation (Singh & Sharma 2008, Andrady 2017), MP composition will further be influenced depending on the plant's technology. Finally, during the process of anaerobic digestion the dry mass of the material will be reduced to a certain extent, leading to higher enrichment factors for MPs.

We only focused on particles >1 mm and further studies are crucial to gain knowledge on the abundance and composition of smaller particles. Nevertheless, an extrapolation based on this first study suggests that, in Germany alone there are between 35 billion and 2.2 trillion large MPs potentially being introduced via this pathway to arable land each year. Nevertheless, in contrast to sewage sludge (the use of which as fertilizer is evermore restricted due to associated foreign substances of concern), using biowastes as fertilizer is generally a sustainable way to return valuable nutrients back to the ecosystem and should further be practiced.

Identification and quantification of macro- and microplastics on an agricultural farmland

Farmlands using known MP-containing fertilizers potentially receive a constant input of MPs. This gives rise to the question of whether agricultural farmlands not subjected to known MP-containing-fertilizers (or plastic applications) are still susceptible to plastic debris contamination. Furthermore, a literature review revealed only a limited number of studies addressing plastic debris contamination within terrestrial habitats (Basnet 1993, Zylstra 2013, Huerta Lwanga et al. 2017), and only one study focused on large plastic debris on a farmland in China at that time (Liu et al. 2014). Thus, we focused on macro- as well as MP debris in our exemplary study on an agricultural farmland in southeast Germany, with a total area of 0.5-hectare (Article A2). The fertilizer used over the last five years included pig and cow manure and ammonium sulphate nitrate fertilizer. Crops cultivated on the farmland are wheat, barley, lucerne, triticale, white mustard, and corn. The farmland is regularly ploughed to a 20-30 cm depth, and neighboring farmlands receive similar agricultural treatment. The visual examination by two independent observers of the surface of the agricultural farmland identified 81 macroplastic pieces. For MPs, the analysis of 14 subsamples (each around five liters of soil) yielded 0.34 (±0.36 SD) MP particles per kg DW. Trough an extrapolation based on typical bulk densities for clayey soils, and

considering the sampled upper 5 cm of soil, it was estimated that the investigated soil contained between 158,100 and 292,400 MPs per hectare. Using ATR-based FTIR spectroscopy, we further identified that the majority of found large plastic debris was composed of the commodity plastics PE (68%), PS (14%), PP (8%), and PVC (5%). For MP particles PE (62.5%) dominated, followed by PP (25%), and PS (12.5%).

Even with information on the polymer type, identifying the sources of the plastic debris was not straightforward. Macroplastic pieces could accidently have been introduced into the pig and cow manure that was used as fertilizer. Only some pieces could be allocated to agricultural origin with a high certainty, such as an earmark from livestock. Wind driven diffuse inputs of low-density plastics from nearby sources could be another source. Most MPs were fragmentation products from larger plastic pieces. Weathering via UV radiation of plastic debris trapped at the field surface could be one explanation, as could mechanical breakdown through ploughing and other field cultivation activities. The Chinese study with long-term plastic film mulch covers found 50 to 260 kg per hectare (Liu et al. 2014), primarily composed of PVC. While the 0.066 kg per hectare found in our study is three to four orders of magnitude lower, it is composed of more diverse polymer types. The difference in abundance is not surprising, as we focused on an area not subjected to agricultural plastic applications. Even though we did not consider particles <1 mm, our study is the first one systematically investigating the contamination of plastic debris and large MP debris of an agricultural farmland in Germany. Considering even smaller MP particles, our results indicate that the found abundance of plastic debris represent a best-case scenario. On an international level, plastic demand in agriculture is growing (Scarascia-Mugnozza et al. 2012), as it increases quality and quantity of crop yield, e.g. plastic films are used on fields for temperature regulation and crop protection in the form of mulch films, greenhouses, and walk-in, low tunnel or silage covers (Espí et al. 2006). The short service life of many agricultural plastic materials, which is on average less than two years (Martín-Closas et al. 2017), in combination with poor recycling rates (Briassoulis & Dejean 2010) and fragmentation due to weathering and mechanical stress, leads to a severe contamination of arable soils (Liu et al. 2014). In addition, there is a growing demand for micro- and nanoplastics in agriculture. For example, as seed a coating to improve sowing (as seeds become more uniform), or to increase germination success (as nutrients, fungicides, and insecticides can be added to the seed pellet) (Taylor et al. 1998, Accinelli et al. 2016, 2019). Micro- and nano-sized polymers called “hydrogels” are further used as soil conditioners to influence, for example, aeration, temperature, and nutrient transport within soils (Rodrigues et al. 2014, Guilherme et al. 2015). First investigations of seed-film coating fragments indicate enhanced distribution of associated pesticides and reduced half-lives in conjunction with specific polymer types (Accinelli et al. 2019). Given that more than a third of the

global land use is agricultural (WORLDBANK 2015), further studies are needed to evaluate the overall budget of plastic debris contamination on arable land. Likewise, studies investigating interactions with chemicals used in agriculture, as well as effects on soils and organisms, are essential to evaluate the potential impact of this contaminant for those ecosystems and for food production.

Occurrence of microplastics in the hyporheic zone of rivers

Another overlooked area during my doctoral time were transition zones of freshwater and adjacent terrestrial systems. Moreover, river transport was often perceived as unidirectional pathway transporting MP debris from land to the oceans. A few studies on streambed sediments were conducted but focused on MP particles >300 µm (Castañeda et al. 2014, Hoellein et al. 2017). Thus, we exemplary analyzed the hyporheic zone (HZ) of streambed sediments (area beneath the streambed equally influenced by river- and groundwater flow dynamics) as further potentially relevant pathway and accumulation area of MP debris. Thereby, the extraction of undisturbed sediment samples to a certain depth below a water surface proved to be a specific challenge. To investigate MP abundance and composition down to a size of 20 µm in the HZ of streambed sediments, and whether those particles can be transported to deeper layers, we utilized freeze core samples (Article A3). Thereby, a hollow metal rod is pushed into the sediment and filled with dry ice which freezes the surrounding sediment matrix onto the metal rod for an undisturbed extraction of sediment and associated pore water. Within a case study from the Rote Main River close to Bayreuth, Germany, sediment samples up to a depth of 60 cm were taken from a riffle structure (including the HZ) downstream of a wastewater treatment plant (WWTP). The investigated sediments consisted mainly of sand, medium to fine gravel, and cobbles (Buffington & Montgomery 1999). Hence, particles with a size of 50-20 µm are similar to the size of the sediment pores or below and were considered as mobile pore scale particles.

In four of the five freeze cores, 14 large MP particles >500 µm could be detected down to a depth of 60 cm below the streambed using ATR-based FTIR spectroscopy. No pattern within the depth profile was detected, in regards to MP abundance, polymer composition, and/or particle shape. The found polymer types were diverse, including polyacrylonitrile (PAN), polytetrafluoroethylene (PTFE), PS, epoxide (EP), PUR, terpolymer, PE, and PP. An exemplary analysis of a subsample of one core for small MP particles (500-20 µm) using focal plane array (FPA)-based µFTIR spectroscopy revealed numbers exceeding 50,000 particles per kg DW for the upper 10 cm of sediment with pore scale MPs making up the majority with around 30,000 particles per kg DW. In contrast, for the depths 20-30 cm and 40-60 cm, the size class

100-500 µm dominated. Except the depth of 10-20 cm, MP abundance generally decreased with depth. The major identified polymer types were PP, PVC, and PET, with further identifications of PE, PS, polybutylene terephthalate (PBT), polycarbonate, and PAN.

The occurrence of low-density polymers such as PE and PP within the sediment can be explained by processes increasing particle density. Such processes include biofouling, aggregation, and incorporation into fecal pellets (Rummel et al. 2017, Besseling et al. 2017, Kaiser et al. 2017, Kooi et al. 2018, Michels et al. 2018), all of which can lead to sedimentation. For MP particles larger than the pore space of sediments an advective transported through the interstitial space of the streambed is not possible. Thus, sedimentation and burial seem to be the major processes leading to inputs of MP debris into streambed sediment. The observed non-uniform distribution of large MP particles among the five extracted cores points towards spatio-temporal variations in inputs, transport and sedimentation patterns. Thereby, MP particle properties play an important role and detected differences in polymer types among cores probably reflect the different transport and sedimentation behavior over time.

While the obtained data does not prove advection into sediments, the small size fraction of MPs displayed the potential to advectivley penetrate into the HZ with infiltrating stream water. Moreover, for mobile pore scale MPs within the interstitial space of the HZ, there exists a probability of reaching the shallow groundwater with infiltrating stream water or via mixing processes. Nevertheless, mobility of small MPs within the interstitial space can depend on a multitude of factors, such as pore water flow rates, aggregation with organic matter, and bioturbation (Gebhardt & Forster 2018, Michels et al. 2018). Furthermore, biofilms can affect surface properties, hydrophobicity, and attachment efficiencies (Rummel et al. 2017), parameters which influence the hydrodynamic behavior of MPs (Galloway et al. 2017). Even though we lack a detailed, mechanistic understanding of transport processes within streambed sediments, our results show that there is a retention capacity for MPs within rivers, and that the HZ can act as temporal sink for MPs in fluvial ecosystems.

Discussion on Chapter A

Through our investigation of MP debris within organic fertilizers we could identify an until then neglected source of large MPs to arable land (Article A1). And although the identification of a MP source is straightforward, the assessment of the general relevance requires a more differentiated recognition. For instance, one needs to consider the temporal and spatial component of a source. Microplastic-containing organic fertilizers would only be a relevant source for MP into the

environment where it is applied to agricultural soils. In addition, the emission of MPs through this source takes place at specific time points in contrast to temporal and spatial diffuse emissions from surroundings and on-site fragmentation of larger plastic debris as discussed for the investigated farmland (Article A2).

Our exemplary in-situ assessments of plastic debris and MP debris of an agricultural farmland in southeast Germany (Article A2) as well as MP debris within the HZ of streambed sediments at the Rote Main river (Article A3) revealed until then neglected temporal sinks on terrestrial ecosystems, thereby also pointing towards important transport routes for MP debris. Here, the specific properties of different plastic types (i.e. size, density, and shape) will influence both their transport pathways and accumulation areas within terrestrial and aquatic ecosystems. This, in turn, can affect their relevance as a contaminant for a given environmental location. For instance, a current discussion among scientists concerns the relevance of tire and road wear particles as a source for MP debris. Here, some studies indicate road wear particles to be an important source of MP debris into the oceans (Kole et al. 2017, Siegfried et al. 2017). Due to the generally higher density of those particles (compared to fresh- or saltwater), however, they are expected to primarily settle to sediments and soils following road runoff (Unice et al. 2013).

Our case studies (Article A1 and A2) as well as other recent published studies on terrestrial ecosystems reveal that they are likely as severely polluted with plastic debris as marine ecosystems, and therefore represent another important sink (Rochman 2018, Kawecki & Nowack 2019). Considering MP debris, most studies have concentrated on larger MPs (mostly >300 µm), as the methodology for MP analysis is still being developed. Our exemplary analysis of the HZ of streambed sediments (Article A3), in conjunction with other studies that include particles down to 20 µm, show that the majority of MPs are occurring within smaller sizes classes below 300 µm. Ultimately, this means that most reported numbers on MPs within the environment are probably underestimations. Thus, we are just beginning to understand the relevance of several sources and accumulation areas for MP debris within the environment.

Chapter B: Improvement of existing sampling and sample processing methods for microplastics

Encountering several difficulties while planning MP sampling campaigns and following sample extraction, preparation, and analysis of MP particles, the next step was to improve and develop sampling and sample preparation methods and protocols for MP monitoring in the environment.

Enzymatic purification of microplastics in environmental samples

To identify MP particle abundances, spectroscopic methods are routinely used and provide a reliable analysis of particles down to 1 µm (Bergmann et al. 2015). Larger MPs (>500 µm) are often extracted by sieving and visual sorting of potential synthetic polymer particles. The single particles can be subsequently chemically characterized with ATR-based FTIR spectroscopy, which is commonly applied and accepted to be sufficiently precise for MPs within this size class. For smaller MPs, however, visual identification can lead to errors of up to 70% (Hidalgo-Ruz et al. 2012) and thus, visual presorting steps are unreliable. Furthermore, as natural particles are generally the dominating fraction in environmental samples, an extraction and enrichment of MPs from the sample becomes necessary to facilitate an efficient and reliable identification of MPs with spectroscopic methods, such as FPA-based µFTIR (as applied in Article A3, C1, and C2) or Raman spectroscopy (Book Chapter, Appendix). Especially for bulk sediment samples, MPs have to be extracted from the inorganic sediment matrix. This is facilitated primarily by density separation (Hanvey et al. 2017). Subsequently, the organic material needs to be eliminated without damaging MP particles. Even though protocols for the purification of the sample from organic and inorganic materials were already published, they either used aggressive chemicals, which would not ensure that MPs are left intact during the purification process, or expensive enzymes (Book Chapter, Appendix) which are not feasible for routine monitoring programs. Thus, I contributed to the development of an enzymatic purification approach that (I) reduces the sample matrix to allow for a reliable analysis with FPA-based µFTIR spectroscopy; (II) conserve the composition of the MPs; and (III) is labor and cost-effective (Article B1).

The efficiency of the developed basic enzymatic purification protocol (BEPP) was tested on environmental samples from the North Sea, resulting in a high grade of purification (98.3 ± 0.1%) while simultaneously reaching a high recovery rate (84.5% ± 3.3%). Nevertheless, the samples that were purified contained high loads of diverse organic materials (e.g., algae, zooplankton, fragments of insects, and higher plants), and thus, the efficiency of single purification steps differed, depending on the amount of the target material present within the respective sample.

To ensure that the original quantity and composition of MPs within the sample was not influenced by the loss of materials (due to the used chemicals and sample handling during the different purification steps), two validation experiments were carried out. Analyses of IR spectra and weight loss on virgin films of eight common plastic polymers showed that the effects of the enzymatic purification with the enzymes and chemicals (H_2O_2) were negligible. Furthermore, the potential loss of MPs through sample handling was estimated by recovery experiments with artificially spiked samples using PE beads. Here, only a minor particle loss during the entire purification process was determined. Also knowing that every polymer type, size, shape and sample matrix will potentially have a unique recovery rate, both of our tests show that the developed BEPP allows for a realistic quantification of results.

For routine monitoring programs, sample purification processes need to be labor and time efficient. Even though up to 16 days are required for the incubation with the different enzymes and chemicals, the actual handling time is shorter (around 3–4 h per sample), and samples can be processed in parallel. Finally, the advantage of the BEPP is the use of different specialized technical grade enzymes, which are not only inexpensive but also allow for the digestion of different materials regardless of the sample type or prior knowledge of the exact content of the sample. Thus, further adjustments of the original BEPP – developed for seawater surface samples (Löder et al. 2015) – resulted in a universal enzymatic purification protocol (UEPP) applicable to a wide range of environmental samples. Additionally, if the matrix composition is known, unnecessary steps can be omitted, further increasing the efficiency of the protocol. With the UEPP, a relatively inexpensive and reliable purification protocol was developed that is universally applicable and thus suitable for routine monitoring studies on MPs.

Abundance and distribution of large microplastics (1-5 mm) within beach sediments at the Po River Delta, northeast Italy

Besides improvements for sample preparation and analysis of MP debris, studies investigating spatial distribution of MPs in different habitats are necessary to assess adequate sample replication to obtain an acceptable precision within the acquired data. Among different habitats, beaches are the most studied systems with regard to MP contamination (Van Cauwenberghe et al. 2015, Rezania et al. 2018), due to their accessibility and thus cost-effective sampling possibilities. Even though sediment sampling is most commonly performed (Van Cauwenberghe et al. 2015, Rezania et al. 2018) and some recommendations for spatial sample replication have been made (Hanke et al. 2013), no consensus exists to date. A high uncertainty remains regarding whether results of different studies can be compared, partly because of a lack of standardization.

Yet, most studies investigated the high tide line, which is susceptible to daily variation (Imhof et al. 2017). Moreover, the few studies examining distribution patterns of MPs on beaches primarily focused on specific items (e.g., pre-production pellets) or relied on visual identification.

In our study we investigated the distribution patterns of MPs of various types and shapes at three accumulation areas (i.e. driftlines) on three sandy beaches at the Po River Delta, northern Italy (Article B2). We sampled the recent high tide line, the extreme tide line (area with the highest amount of washed ashore material), and the backshore (area in front of dunes). We concentrated on large MPs (>1 mm), as this is currently the only size class feasible for routine monitoring programs. ATR-based FTIR spectroscopy revealed particle abundances from 2.92 (± 4.86 SD) to 23.30 (± 45.43 SD) MPs per kg DW between the beaches. Our hypothesis of increasing MP abundance with increasing distance to the waterline was not statistically confirmed, which is in accordance with a similar study by Lo et al., (2018). Nevertheless, most studies have shown increasing MP abundance towards the upper beach (Turner & Holmes 2011, Heo et al. 2013, Turra et al. 2014, Imhof et al. 2018), which is in agreement in our study for the uppermost accumulation area backshore for two sites, where foamed PS was the dominant polymer type found. Foamed PS particles have a very low density (~0.05 g cm^{-3}) and often occur as fragments or spherules having a relatively high windage. Transport of foamed PS towards the upper shore can occur quickly due to wind-driven transport processes (Heo et al. 2013, Imhof et al. 2018). Additionally, the further away MPs are deposited from the waterline the less impacted they are by wave action and tide cycles and thus, exported back to the sea. In contrast, the polymer types PE and PP (density around 0.9 g cm^{-3}) showed no clear accumulation patterns among the beaches. Distribution is probably more influenced by beach morphology and hydrodynamical factors. For example a smaller beach width could enhance redispersion through wave-action and sea-storm events, either moving particles to the upper shore (Chubarenko et al. 2018) or exporting particles within the intertidal zone back to sea. Frequent contact with water, occurring at the accumulation area nearest to the water, further results in direct input and output of MPs (Imhof et al. 2018). Apart from a generally strong along-shore patchiness of total MP abundance, the along-shore distribution of single polymer types was also highly variable. Along-shore distribution is influenced by hydrodynamic processes such as current circulation cells (Chubarenko & Stepanova 2017), beach morphology, and natural structures acting as traps for MPs like dunes, vegetation, or detritus (Turner & Holmes 2011, Imhof et al. 2018).

Furthermore, results of the sampling frequency analysis (after Besley et al., (2017)) within an accumulation area showed that the values were highly variable between sites and accumulation areas. Considering a standard deviation of 0.5 around the mean with a confidence level of 90% as sufficiently precise, around five replicates for the recent high tide line seems reasonable which is

in accordance with recommendations by the TSG-ML (Hanke et al. 2013). The obtained results for the accumulation areas extreme tide line and backshore in our study on the other hand suggest taking at least 10 replicates for accumulation areas further away from the waterline. This is in agreement with results by Besley et al., (2017), reporting that the confidence interval around the mean decreased rapidly after a replication of five, and 11 replicates would be sufficient. In our study we concentrated on 100 m long transects of a beach. Depending on the area of the investigated area, one has to further consider heterogeneities within a beach and probably also adjust transect replication (Fisner et al., 2017). Moreover, factors such as proximity to potential sources (e.g., cities, harbors, industry), ocean currents, and sampled sediment type, for example, need to be considered and reported, as they can influence the abundance and composition of MPs (Hanvey et al. 2017). Currently, sample replication is a compromise between representativeness and feasibility, as not only sampling can be time consuming but subsequent sample processing and analysis. Here, additional monitoring attempts, such as predictions on MP accumulation areas by model simulations, could support in-situ monitoring.

Discussion on Chapter B

The development of reliable and efficient MP monitoring methods is ongoing. For instance, sample purification protocols, either based on chemical degradation or on enzymatic digestion, are being constantly developed and improved (Zarfl 2019). Even though standardization of monitoring approaches is of utmost importance, a certain flexibility within extraction, purification, and analysis methods for MP analysis is reasonable. The adaption of the enzymatic treatment within the UEPP for example (Article B1) does not significantly influence the final MP composition and abundance. If the protocol is applied in a constant way for the investigated research question and adaptions are transparently reported, the obtained data are still comparable among other studies. One should further consider that different research questions require different monitoring strategies. and that in some cases specific methods could provide fast results with an acceptable accuracy. For instance, considering the investigation of beach sediments, if the standing stock of MP debris is the focus on needs to take different areas of the beach into account whereas a frequent investigation of the recent high tide line should be chosen to assess MP input rates. Or, if the goal is to assess the effectiveness of a measure targeting specific types of synthetic polymers or sources, it is still reasonable to apply analytical techniques that demonstrate high accuracy for those but may have lower accuracy for others. Here, Zhang et al., (2018) proposed an identification method for PE and PP based on the visual identification of their

specific melting products. Even though the technique will not reach the precision of chemical characterization of MP debris, the application of this method for monitoring programs targeting PE and PP plastic mulch film contamination of arable lands could be a time and cost-effective alternative. Albeit, monitoring activities should be re-evaluated at a regular basis as some plastic products will be replaced by other polymers or materials, with yet unknown consequences for the environment. For example, if current trends of replacing single-use plastics by biodegradable plastics continue, identification methods need to be likewise sensitive for biodegradable plastics.

Contrary to larger plastic debris, for MP particles in most cases it is not possible with current techniques to allocate them to a specific source as distinct features such as color (obscured by biofilms or faded due to sample processing), shape (mostly fragments or films of irregular shape), and other distinct structures or labels are either not present or no reliable features for those small particles. Further information on chemicals and dyes could provide valuable information but in turn would again increase monitoring efforts. Thus, alternative monitoring methods that allow for source allocation like hydrodynamic model simulations coupled with particle tracking modules could provide useful information to identify sources of MP debris.

Chapter C: Development of alternative monitoring methods for buoyant plastic debris in aquatic systems

Aquatic ecosystems exhibit especially high spatio-temporal variabilities, making the relationships between sources and sinks of plastic debris complex. While field data acquisitions are essential for assessment and monitoring of plastic debris contamination levels, they alone cannot capture those complex relationships. Thus, we further investigated the applicability of alternative monitoring tools which are able to provide additional information on sources, pathways, and accumulation areas of plastic debris.

Coastal accumulation of microplastic particles emitted from the Po River, Northern Italy: Comparing remote sensing and hydrodynamic modelling with in-situ sample collections

Through model simulations of plastic debris transport (Lebreton & Borrero 2012, Carson et al. 2013, Law et al. 2014, van Sebille et al. 2015) major accumulation areas within the oceans were described and their existence subsequently validated through in-situ measurements (Maximenko et al. 2012, Law et al. 2014, van Sebille et al. 2015). Sherman and van Sebille (2016) used a model based on satellite-tracked buoy observations (calibrated with literature data of plastic debris abundance) to simulate plastic debris transport, with the goal to identify optimal removal locations. Likewise, model simulations could be used to assess optimal removal and monitoring sites for plastic debris and especially for MP debris, where in-situ data collection involves high expenses. In cooperation with the Italian Institute of Marine Science (CNR-ISMAR), we aimed to predict coastal accumulation of virtually released large MP particles by the complex deltaic system of the Po River Delta over 1.5 years (utilizing a hydrodynamic model coupled with a Lagrangian particle tracking module) (Article C1). Within a second approach, SPM based on remote sensing imagery of the river plume was used as a proxy to predict river-induced MP accumulation on adjacent coastal areas.

The resulting MP accumulation maps from both approaches were validated against field samples at nine beaches with detected MP concentrations of up to 78 particles per kg DW. The distribution of recorded in-situ MP abundance, however, was not reflected in accumulation maps. Several factors could have led to the observed results. For the hydrodynamic model a particle was considered as beached when it reached the coastal grid cell being 250 m within the coastline. Near shore currents are very complex and currently not captured within the applied hydrodynamical model, which could have led to different beaching probabilities. Further processes leading to re-distribution of beached MP particles, such as wind-driven transport at the beach or washing-off from the beach, were also not included. While particle emission was held constant through the

model simulation period, it likely varies throughout the year, coupled to several factors, such as population density, plastic application activities (e.g., agricultural use), and differing environmental conditions influencing transport (e.g., washing-off from ground and transport to rivers depends on precipitation). Particle characteristics were chosen as to represent the most commonly found polymer types (PE, PP with a density ~0.9 g cm^{-3}), which was confirmed by our results, except for foamed PS particles with a much lower density (density ~0.05 g cm^{-3}). Nevertheless, excluding PS particles from the analysis did not result in an improved relationship between model results and in-situ measured MP abundances. Planar fragments were the predominant identified MP shape from in-situ samples, in contrast to the idealized spheres used in the model. A different shape can influence the sinking behavior of particles (Khatmullina & Isachenko 2016, Waldschläger & Schüttrumpf 2019), but its influence on horizontal transport should be negligible for small particles not exhibiting high windage. Other processes that change the density of the virtual MPs (and consequently their sinking behavior) seem to be more important. Microplastic particles released to the environment are subjected to several processes changing their density, as already stated above (Kowalski et al. 2016, Rummel et al. 2017, Waldschläger & Schüttrumpf 2019). Considering that beaching occurred primarily during the first three days, with a sharp decrease (remaining close to zero) in particle beaching after ten days, it needs to be assessed if those processes can have a significant influence on the model results.

The release of virtual MPs was coupled to the water discharge of the six major terminal river branches of the Po River Delta as no in-situ data on MP abundance at the different sites were available. An improved emission scenario of virtual MPs, including land- and sea-based MP sources and applying realistic ratios among the terminal river branches, would greatly benefit model results. Another aspect is the chosen sampling design. Considering the different accumulation areas as sites for in-situ validation of modelled particle accumulation, we decided to investigate the extreme tide line based on preliminary results of Article B2. Even though the extreme tide line showed the highest along-shore variability, the decision for this accumulation area was a compromise between representativeness for the model and feasibility of analysis within the project. The high tide line is more influenced by daily variations (Imhof et al., 2017) and thus not representative for longer accumulation periods (particle accumulation was modelled for 1.5 years). The analysis of backshore samples, on the other hand, appeared to be highly time consuming due to a large amount of interfering organic materials, which prolonged washing and sorting steps and analysis, making it infeasible within the project period.

Nevertheless, the median values (Table 1) of the three different accumulation areas for the three investigated beaches indicate the same trend: a decreasing MP abundance from north (Levante)

to south (Allagemento) which suggests that independent of the chosen accumulation area the same results would have been obtained.

Table 1: Median microplastic concentration per kilogram dry weight at the investigated beaches and for the different accumulation areas ± standard error (BSH: backshore, ETL: extreme tide line, HTL: high tide line).

	BSH	ETL	HTL	Total
Levante	9.28 ± 3.45	17.43 ± 21.34	5.29 ± 1.56	9.28 ± 7.91
Pila	9.08 ± 3.05	2.28 ± 2.88	3.94 ± 0.54	4.44 ± 1.48
Allagemento	6.22 ± 2.19	0.24 ± 0.17	0.51 ± 0.47	0.72 ± 0.94

A major factor that could have influenced our results, mentioned above, are additional nearby emission sources. Such sources include aquaculture within the lagoon (which is intensively practiced) and recreational activities on land and at sea. The Venice lagoon, which is known to be heavily contaminated with plastic debris (Vianello et al. 2013), is in the proximity. The Adige and Brenta, two highly urban-influenced rivers, discharge into the Northern Adriatic Sea directly above the delta. In addition, maritime traffic is high in the Northern Adriatic Sea, and further contributes to diffuse plastic debris inputs into the area.

Yet, the hydrodynamical model provided some general insights into the release and transport of buoyant MPs from the six distal branches of the Po River Delta and their accumulation probability to adjacent coastal beaches. For instance, only up to 18% of total released virtual MPs were beached within the simulation period in the investigated area (with the exception of the southernmost branch, where virtual MPs still beached after ten days). Generally, virtual MP accumulation remained quite local around each of the river mouth release points, except for the southernmost branch where beaching continued along the southward coast. Beaching rate estimates suggest that over 80% of the virtual MP particles released by the Po River Delta are dispersed to the Northern Adriatic Sea.

In contrast to the hydrodynamical model, where a continual track of released virtual MP particles is provided, the remote sensing approach provides actual snapshots of the river plume shape with a finer spatial resolution over a large area. The remote sensing approach captured the river mouth's relative strength and identified small structures not considered in the hydrodynamical model that likely influence MP transport. Nevertheless, it is difficult to translate the SPM concentration into MP concentration.

With the utilization of three-dimensional models, as well as an improved understanding of density changing processes for MP debris and near-shore hydrodynamic processes, the presented

approach is a promising monitoring tool for mapping MP distribution pathways in large aquatic ecosystems. Moreover, with the applicability of satellite-derived data of water constituents such as SPM to illustrate river plume dynamics we were further interested in another indirect monitoring approach for MP debris utilizing satellite imagery of proxy water constituents, which was the focus of the following study (Article C2).

Can water constituents be used as proxy to map microplastic dispersal within transitional and coastal waters?

In this study we tested if MP distribution follows the same movement pattern as passive buoyant water constituents derivable from satellite images, such as Chl-A, SPM, and cDOM (Article C2). The underlying assumption was that both, water constituents and buoyant MP debris is transported by the same driving mechanisms (i.e. wind and currents). As rivers are of particular interest as sources for marine MPs, we concentrated on the lower courses and river mouth of the Trave and Elbe Estuary in northern Germany and the Po River Delta in northern Italy.

The investigation of a spatial relationship of passive buoyant MP particles and water constituents depictable from satellite images was an innovative approach demanding complex field sampling methods. To obtain the final product of satellite maps showing MP distribution, several in-situ measurements and calibration methods are necessary as shown in Figure 1.

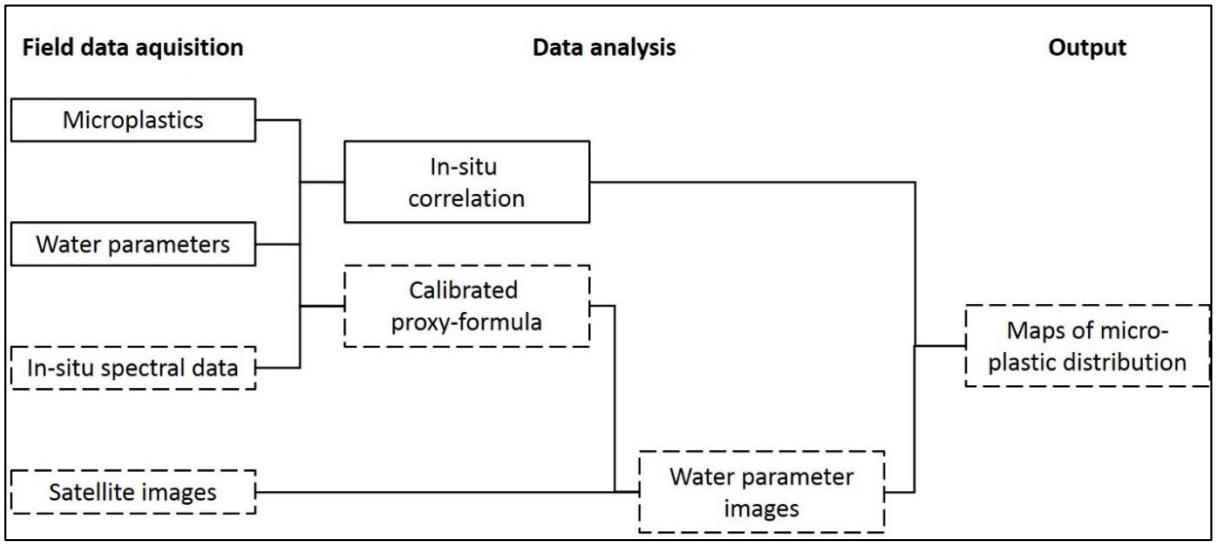

Figure 1: Data acquisition and calibration scheme for the proposed indirect monitoring approach of microplastic dispersal in coastal areas using proxy water constituents (e.g., suspended particulate matter) despicable from satellite images.

For the general approach the in-situ correlation of MPs and water constituents needed to be investigated in a first place, which was the focus of the present work. Therefore, 13 samples (MPs, water constituents, and in-situ spectral measurements) were taken at the Trave and 20 each at the Elbe Estuary and the Po River Delta. Microplastic samples were processed according to the developed UEPP (Article B1) with some modifications. For a full quantitative analysis of MPs down to a size of 300 µm potential MP particles were analyzed with ATR- and FPA-based µFTIR spectroscopy as well as with the hyperspectral imaging spectrometer HySpex SWIR-320m-e (Schmidt et al. 2018). For the investigation of water constituents Chl-A, SPM, and cDOM, two liter water samples were collected with glass flasks.

Results of regression analysis of water constituents and MP abundances for the three river systems revealed contrary results with only the Trave data showing a positive relationship between buoyant MPs and the investigated water constituents Chl-A, SPM, and cDOM. A possible explanation for these observations are differences in dominating MP sources as well as differences in water constituents sources.

Particularly, it was found that open-sea activities did not play a major role for plastic debris inputs to Baltic Sea beaches but land-based inputs dominated (Haseler et al. 2018). Thus, the lower MP water surface concentrations at the coastal area in contrast to the inner parts of the Trave River could be a dilution effect. In contrast, the study systems of the Elbe Estuary and the Po River Delta are highly influenced by sea-based debris inputs, e.g. shipping, fisheries, and aquaculture (Simeoni & Corbau 2009, Kammann et al. 2017). The increasing MP concentrations at the Elbe Estuary towards the coastal area maybe a consequence of both, additional inputs of sea-based sources as well as the tidal influence, increasing the residence times for particulate materials. The differing hydrodynamic conditions at the investigated sites, spanning from a mixed mesotidal estuary (Elbe) to nearly stratified systems (Trave, Po), generally influenced the transport and retention of water constituents as well as MP debris within the distal river branches and adjacent coastal areas. For instance, the Elbe Estuary exhibits a maximum turbidity zone (MTZ), which traps suspended matter. Accumulation of larger debris within the MTZ was already reported for an estuary in South America (Acha et al. 2003). During our field sampling at the Elbe in August we did not cover the MTZ. However, in a preliminary study on the Elbe in June the MTZ was covered and a correlation analysis showed a positive relationship between SPM and MPs. Considering SPM and MP relationships for the other two systems, the positive relationship at the Trave could be due to dominating riverine inputs for both, whereas the missing relationship at the Po delta could be the result of differing input sources of SPM and MPs among the distal branches. For the Po delta with its diverse terminal branches whose discharge is influenced by coastal currents differently, no pattern of MP abundance was observed.

Considering cDOM, which consists of decaying material of terrestrial origin and/or is the result of in-situ biological activity in the respective area, a spatial relationship with MPs was assumed as terrestrial inputs are thought to dominate the cDOM source in coastal areas (Harvey et al. 2015), as it is thought for plastic debris. Indeed, for the Trave cDOM explained most of the variance in coastal samples, but a relationship was absent for the other two systems. It needs to be considered that the field campaigns were conducted at different seasons. Processes leading to higher cDOM concentrations in spring and summer vary with higher inputs due to melt-water run-off from rivers in spring (Ferrari & Dowell 1998, Massicotte et al. 2017) and higher photo-bleaching input in summer (Vodacek et al. 1997). Whereas the latter could counteract potential relationships of river induced relationships of cDOM and MPs. Additionally, the contradictory results obtained for the investigated rivers can further be explained by differing cDOM dynamics among systems. For example, Berto et al., (2010) has shown an influence on cDOM dynamics on a monthly and sub-monthly time scale at the Po River Delta. Harvey et al., (2015) although found differing behaviors of the optical signals between the seasons of the investigated two sub-areas of the Baltic Sea. Regarding the investigated water constituent Chl-A, i.e. algae, a relationship with MPs was found for the Trave. Nevertheless, due to the low replication at this site the obtained results need further validation. Contrarily, a relationship for Chl-A and MPs was absent at the Po River Delta. A drawback of Chl-A as proxy water constituent for MPs could be the seasonal influence on the relationship, which would not allow for a continuous monitoring. Moreover, algae communities vary among different habitats and some algae are also able to influence their vertical position in the water column (Raven & Doblin 2014), which consecutively influences their potential relationships with MP debris.

In coastal systems remote sensing of water constituents is influenced by the overlapping spectral signals from different optical components. The Trave for example provided the clearest cDOM signal, concurrent with relatively low SPM concentration, whereas for the Po River Delta a contrary situation was observed. Fulfilling the most important requirements for an operational monitoring in being cost- and labor -effective, as well as easy to assess, SPM seems to be most promising as a proxy water constituent for MPs. Moreover, a relationship between MP concentrations and organic matter deposition has recently been reported wherein particles <100 µm made up >95% of the MP concentration but more importantly, particles >500 µm showed different spatial distribution patterns (Haave et al. 2019). This points towards the importance of MP particles <300 µm not covered by our MP sampling method. Thus, it would be interesting in future studies to test the relationship of SPM and MPs with recently developed pumping systems which are able to extract MPs down to 1 µm (Lenz & Labrenz 2018). In conjunction with the development of faster identification methods of MPs higher sample replication can be achieved, resulting in more precise model results.

Even though a clear relationship among passive tracers and MP could not be identified for all three investigated river systems, it showed that in some cases a relationship may exist. Those can further be spatially limited and depending on the estuary type potentially occur within both, a river course (e.g., Elbe) as well as the coastal zone (e.g., Trave). Considering the investigated water constituents, the applicability of SPM as proxy water constituent should be verified in future studies using improved MP sampling methods. Through the utilization of remote sensing imagery of water constituents as proxy for MPs current existing single point measurements could be extrapolated to large spatial scales. This would greatly benefit our understanding of transport mechanisms as well as accumulation areas of MP debris in aquatic systems.

Preliminary study on the applicability of drones as monitoring tool for floating plastic debris

Considering large plastic debris, currently a direct identification with satellite imagery is not feasible (Mace 2012). Here, the ongoing technical development of cameras and unmanned aerial systems (UAS) opens up new possibilities for monitoring approaches. Kako et al., (2010) and Nakashima et al., (2011) were among the first to use an unmanned aerial system equipped with a camera to conduct a full-scale analysis of beach macrolitter. An automated approach to identify plastic debris within the images, using the color difference between target objects and the background, was further proposed by Kako et al., (2012). Nevertheless, the helium balloon used needs to be manually towed, either by volunteers on the beach or by boat on the water, limiting a flexible application.

Within the DLR project Sentinels4MarinePlastics, we established a cooperation with the Indonesian Institute of Science (LIPI) to use drone imagery to quantify plastic debris floating at the Citarum river surface in Java, Indonesia. Data acquisition was conducted with a GoPro4 silver camera mounted to a 3DR solo drone. To increase image quality, the original camera lens was replaced by a FishEye lens with a low-distortion objective (Backbone, 1/2.3", 4.4mm, low distortion, M12). To cover a certain area with the drone imagery, the flight path of the drone was programmed with the software Mission Planner (Version 1.3.40, Fig. 2).

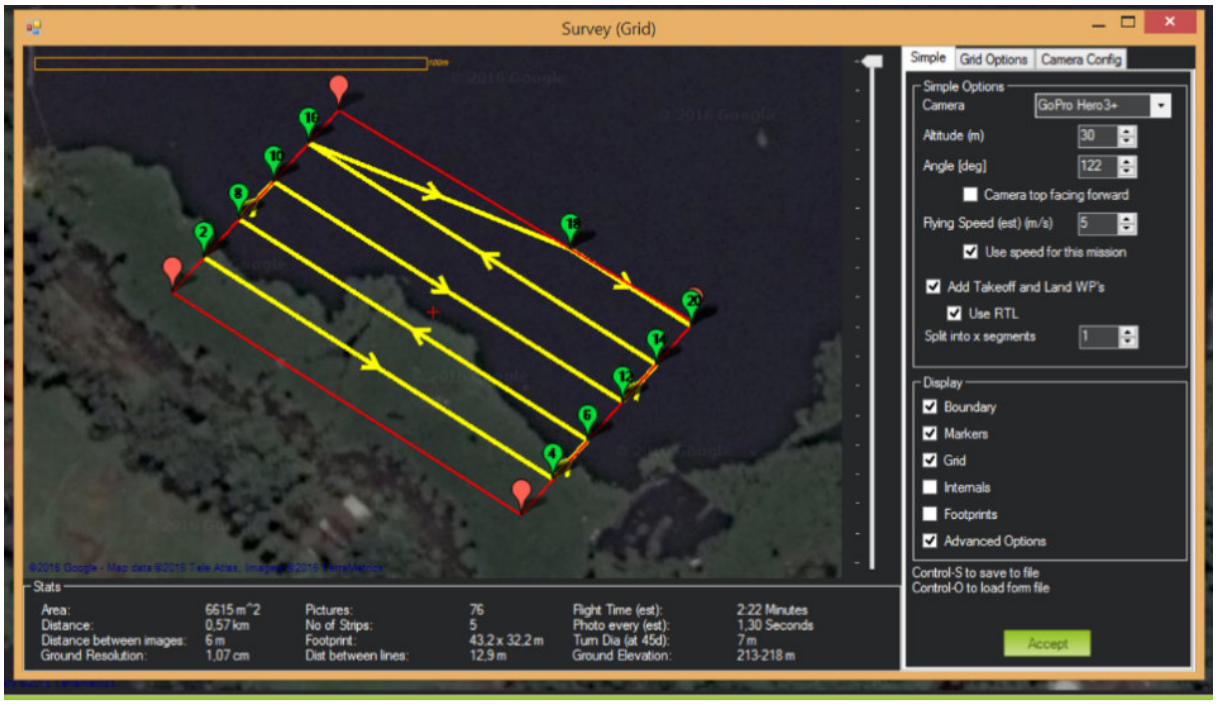

Figure 2: Example of a preset flight path for the image acquisition with the drone using the Mission planner software (Version 1.3.40).

To achieve a pixel resolution of around 1 cm, a flight height of 30 m and speed of 7 m/s were chosen. For later compiling of the images to a orthophoto a horizontal image overlap of 85 % and a lateral overlap of 60 % was set. In total, data for 8 river sections were obtained during the field campaign (Fig. 3).

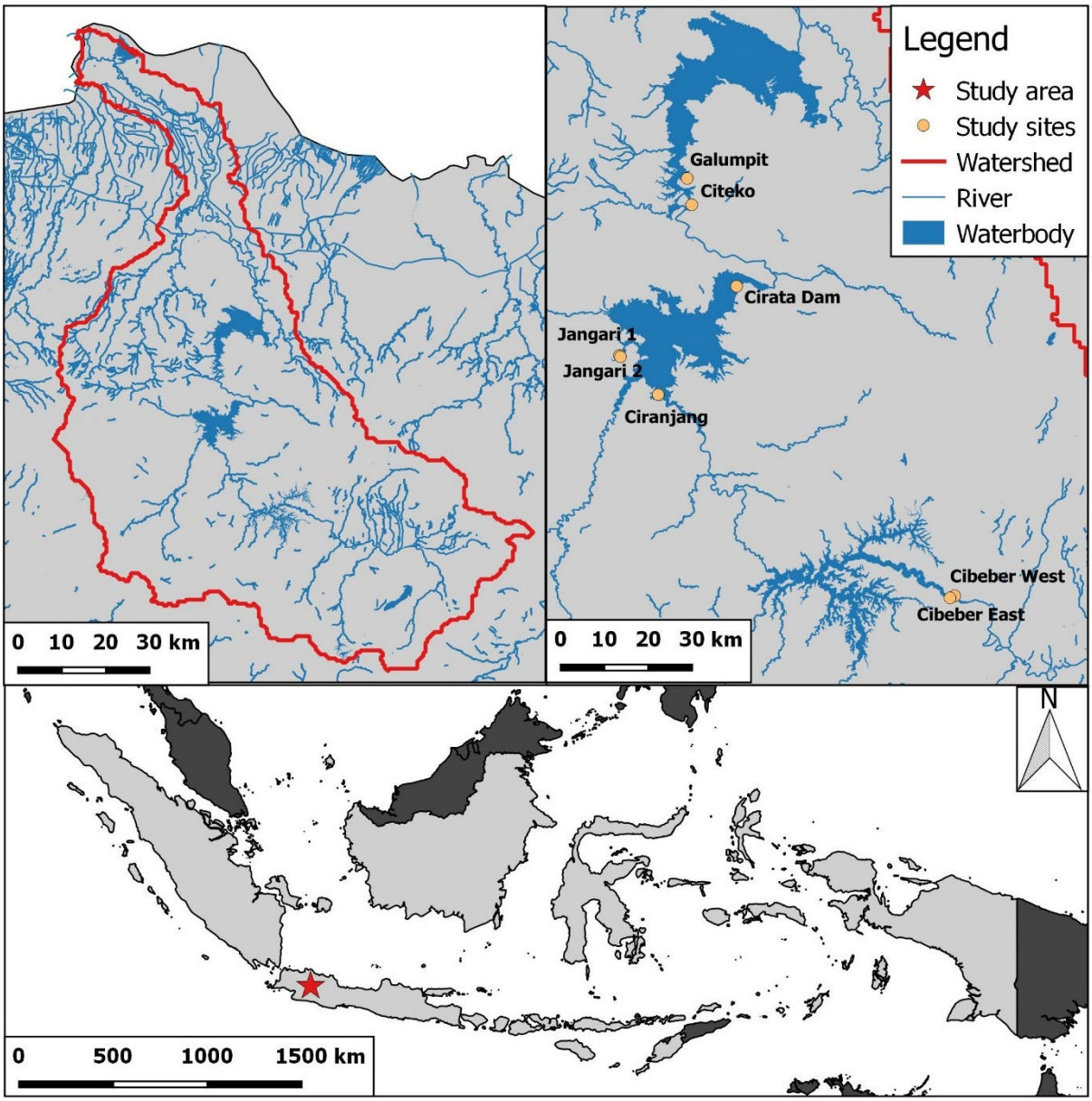

Figure 3: Sampling area in Indonesia (lower panel), watershed of the investigated area of the Citarum river (upper left panel), and study sites for drone image acquisition (upper right panel). Data source: GADM (v3.6), OSM project.

The following processing of the data was conducted by our project partner RSS GmbH (Elizabeth Catherine Atwood and Sabela Rodríguez Castaño). To transform single images of a study site to orthophoto mosaics, the software packages Agisoft PhotoScan Professional (Version 1.2.6) and

ERDAS IMAGINE 2014 were used. Images were classified with a hierarchical object-based algorithm (eCognition Developer 9.2, Trimble). Based on the RGB data in the visible spectrum, a classification between the following floating objects was conducted: debris (plastic debris), vegetation (wood, bamboo, hydrophytes, and other organic debris), water, and sunglint (Fig. 4).

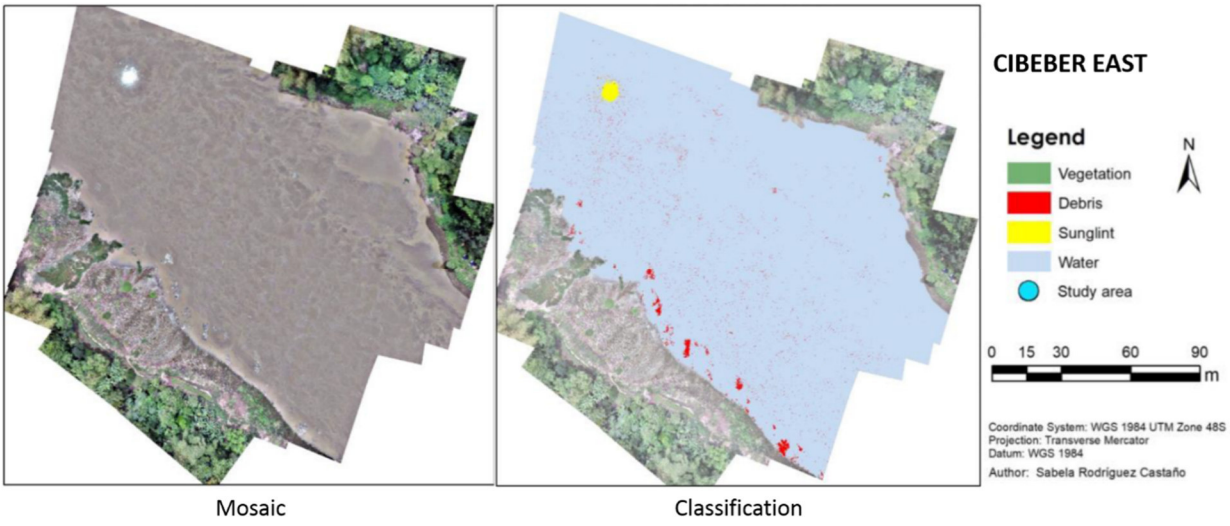

Figure 4: Orthophoto of processed drone image (left panel) and classified image (right panel) © Sabe Sabela Rodríguez Castaño.

The ground control points used (Fig. 5) were categorized by independent persons without background knowledge of the eCognition classification scheme into the same classes. A confusion matrix was used to analyze the comparison of ground control points with the classification scheme.

Figure 5: Examples of classified ground control images by independent persons to assess accuracy of the applied automatic classification algorithm of eCognition Developer software.

Our results showed that drone acquired RGB images can be used for the identification of areas heavily impacted by floating debris, as well as the extension of the impacted area. Together with in-situ measurements, the amount of plastic debris can be extrapolated. For example, at the most impacted site, Jangari 1, additional videos from a boat were taken, showing that around 50% of the flotsam consisted of plastic debris (Fig. 5). Thus, the site would be covered with 1,558 m^2 of large plastic debris.

To conclude, using a costume RGB camera already provided useful information. Further developments of drones equipped with sensors with a wider spectral range (providing more detailed information, such as SWIR sensors), could greatly improve this technique. Known accumulation hotspots and inaccessible coastlines could thus be monitored on a regular basis with only a minor time investment.

Discussion on Chapter C

With an improved understanding of MP transport processes, as well as better model resolution and computing capacity, hydrodynamical models coupled with Lagrangian particle tracking is a promising monitoring tool. Going forward, a crucial factor will be the parameterization of the

processes that influence particle movement. It is known that particle size, density, and shape are major influencing factors for particle transport (Waldschläger & Schüttrumpf 2019). Moreover, MP density modifications that influence transport behavior are further caused by biological, chemical, and mechanical processes (Kowalski et al. 2016, Rummel et al. 2017), which are variable for different types of MPs (Fazey & Ryan 2016, Halle et al. 2016). Here, supportive laboratory experiments that consider the processes influencing MP transport will be essential for future modeling efforts (Hardesty et al. 2017, Kaiser et al. 2019).

Furthermore, particle tracking modules can be implemented offline, i.e. when velocity fields are stored, which allows a backward simulation of particles (Neumann et al. 2014, Krelling et al. 2017). This theoretically allows for source allocation of specific items found during in-situ sampling campaigns, for example, and could serve as an alternative method for identifying MP particle sources. Besides a mechanistic understanding of transportation pathways, model results can further help to identify suitable sites and time frames for monitoring activities, as well as optimal removal sites for plastic debris (Sherman & van Sebille 2016).

Considering larger plastic debris, remote sensing approaches, satellite imagery data, and unmanned aerial systems (UAS, e.g., drones), are currently under review for their applicability. Our approach using RGB imagery taken from a drone has shown promising results. Nevertheless, higher resolution sensors that cover the SWIR range, as currently utilized by satellite sensors, would greatly improve the accuracy of remote identification of plastic debris by UAS.

A drawback of satellite imagery is the large distance between the object of interest and the sensor, as the atmosphere can influence the spectral signal. In regards to plastic debris floating at the water surface, sun glint or whitecaps can further impact the spectral signal. Fortunately, there exist some recommendations to overcome those issues. For example, using specific atmospheric and sun glint correction algorithms, as well as acquiring data during low wind conditions (Goddijn-Murphy et al. 2018). In addition, a recent study showed the potential of multi- to hyperspectral sensors to detect floating plastic debris from UAS as well as satellite imagery and suggests future directions for research priorities (Topouzelis et al. 2019).

Taken together, the huge diversity of plastic debris in terms of physical (size, shape, and density) and chemical (associated additives and adsorbed chemicals) properties, all of which can vary non-linearly over time due to biofouling, weathering, and interactions with organisms, cause their distribution to be fast, extensive, and difficult to predict. Thus, combined monitoring approaches, including in-situ data acquisitions, model simulations, and remote sensing should be applied to gain a comprehensive understanding of sources, sinks, and transportation pathways

Contributions and contributors to this PhD work

For the presented work many samples were taken and an extensive amount of time spend for MP sample preparation and analysis. The extensive data sets for the presented seven studies would not have been obtained without the assistance of students, research and technical assistants, colleagues, and cooperation partners. For field sampling and sample preparations Julia N. Möller, Carolin Elbel, and Alexandra Preiß played important roles for Article A1, Anna Leibner for Article A2, and Laura Wilhelm and Jennifer Krutzke for Article A3. Veronika Mitterwallner and Lena Löschel did most of the visual pre-sorting and FTIR measurements of potential MP particles from the sediment samples for Article B2 and C1. Ursula Wilczek, Heghnar Martirosyan, and Marion Preiß supported sample preparation, measurements, and analysis and helped with initial trainings of research assistants. Moreover, Dr. Francesco M. Falcieri from ISMAR-CNR provided the hydrodynamic model simulations for Article C1 and Reza Muhammed Cordova from RCO-LIPI supported the field work in Indonesia. Further credits are assigned to Sabe Sabela Rodríguez Castaño from RSS GmbH for the processing of the drone images. For our in-situ measurements for Articles B2, C1, and C2 the crew of the sailing ships Aldebaran and Anna-Lisa von Wischhafen are thanked, as well as the boat captains for the field sampling at the Po River Delta in Italy.

The following contributions to the work are estimated:

Article A1

Authors: Nicolas Weithmann, Julia N. Möller, Martin G.J. Löder, Sarah Piehl, Christian Laforsch, Ruth Freitag

Title: Organic fertilizer as a vehicle for the entry of microplastic into the environment

Status: Published at the Journal Science Advances

Own contribution: sampling design 30%, microplastic sample preparation 30%, analysis of microplastic samples 20%, data analysis and figures 20%, discussion of results 25%, manuscript writing 25%.

The study was designed by CL and RF. Field sampling was done by NW, JNM, and MGJL. Sample preparation and microplastic identification was done by NM, JNM, SP with the support from three technical assistants as well as two former Bachelor students. MGJL and SP analyzed the data. NW, MGJL, SP, CL, and RF interpreted and discussed results. Figures and tables were created by NW

and SP. NW wrote the first draft of the manuscript. Revision and rewriting of the manuscript was done by NW, MGJL, SP, CL, and RF.

CL is the corresponding author.

Article A2

Author: Sarah Piehl, Anna Leibner, Martin G. J. Löder, Rachid Dris, Christina Bogner, Christian Laforsch
Title: Identification and quantification of macro- and microplastics on an agricultural farmland
Status: Published at the Journal Scientific Reports

Own contribution: concept and study design 35%, microplastic data acquisition 50%, microplastic sample preparation 75%, analysis of microplastic samples 75%, data analysis and figures 100%, discussion of results 35%, manuscript writing 80%.

The study was designed by SP, AL, and CL. AL and SP performed the field sampling. Microplastic sample preparation and identification was done by AL and SP with support of one student intern. AL and SP analyzed the data. Figures and tables were created by SP. All authors interpreted and discussed results. SP wrote the first draft of the manuscript. Revision and rewriting of the manuscript was done by all authors.

CL is the corresponding author.

Article A3

Author: Sven Frei, Sarah Piehl, Ben S. Gilfedder, Martin G. J. Löder, Jennifer Krutzke, Laura Wilhelm, Christian Laforsch
Title: Occurrence of microplastics in the hyporheic zone of rivers.
Status: accepted by Scientific Reports

Own contribution: analysis of microplastic samples 50%, data analysis and tables 25%, discussion of results 25%, manuscript writing 25%.

The study was initiated and designed by SF, BSG, and CL. Field sampling was carried out by JK and LW. Microplastic sample preparation and identification was done by SP and MGJL with the help of two technical assistants. Data was analyzed, interpreted and discussed by SF, SP, BSG, MGJL, and CL. Figures and tables were created by SF, BSG, and SP. SF wrote the first draft of the manuscript. Revision and rewriting of the manuscript was done by all authors.

SF is the corresponding author.

Article B1

Author: Martin G. J. Löder, Hannes K. Imhof, Maike Ladehoff, Lena A. Löschel, Claudia Lorenz, Svenja Mintenig, Sarah Piehl, Sebastian Primpke, Isabella Schrank, Christian Laforsch and Gunnar Gerdts
Title: Enzymatic Purification of Microplastics in Environmental Samples
Status: Published by the Journal Environmental Science and Technology

Own contribution: data acquisition 10%, analysis of samples 10%, discussion of results 10%, manuscript writing 10%.

The study was designed by MGJL, GG, and ChL. Field sampling was conducted by MGJL and ML. MGJL, HKI, ML, LAL, ClaL, SM, SaP, SeP, and IS performed the experiments. Further experiments were conducted by ASA Spezialenzyme GmbH. Data was analyzed by MGJL and ML as well as discussed and interpreted by all authors. Figures and tables were created by MGJL. MGJL wrote the first draft of the manuscript. Revision and rewriting of the manuscript was done by all authors.

MGJL, CL, and GG are the corresponding authors.

Article B2

Author: Sarah Piehl, Veronika Mitterwallner, Elizabeth C. Atwood, Mathias Bochow, Christian Laforsch
Title: Abundance and distribution of large microplastics (1–5mm) within beach sediments at the Po River Delta, northeast Italy.
Status: Accepted by the Journal Marine Pollution Bulletin

Own contribution: concept and study design 40%, data acquisition 35%, analysis of samples 30%, data analysis and figures 90%, discussion of results 70%, manuscript writing 80%.

The study was designed by SP, ECA, MB, and CL. Field sampling was conducted by SP ECA, and MB. Sample preparation and identification of microplastics was done by SP and VM with the help of two student interns and one technical assistant. Data were pre-proceeded by VM. Data was analyzed by SP and discussed and interpreted by SP, ECA, MB, and CL. Figures and tables were created by SP. SP wrote the first draft of the manuscript. Revision and rewriting of the manuscript was done by all authors.

CL is the corresponding author.

Article C1

Author: Elizabeth C. Atwood, Francesco M. Falcieri, Sarah Piehl, Mathias Bochow, Michael Matthies, Jonas Franke, Sandro Carniel, Mauro Sclavo, Christian Laforsch, Florian Siegert
Title: Coastal accumulation of microplastic particles emitted from the Po River, Northern Italy: Comparing remote sensing and hydrodynamic modelling with in situ sample collections
Status: Published by the Journal Marine Pollution Bulletin

Own contribution: concept and study design 25%, data acquisition 35%, analysis of microplastic water samples 90%, analysis of microplastic sediment samples 30%, analysis of water constituents 65%, data analysis and figures 35%, discussion of results 25%, manuscript writing 10%.

The study was designed by ECA, SP, MB, MM, JF, CL, and FS. Field sampling was conducted by ECA, SP, and MB. Development of the hydrodynamical model and particle tracking was done by ECA, SP, FMF, MM, SC, and MS. Hydrodynamical modelling and particle tracking was done by FMF. The RS model (including the development of near-range spectral measurement cal/val methodology) was created by ECA while image processing was supported by three technical assistants. Microplastic sample preparation was done by SP with the help of three student interns and two technical assistants. Microplastic particle identification with FTIR spectroscopy was done by SP. MB developed and completed the SWIR microplastic particle identification. Data was analyzed, discussed, and interpreted by ECA, FMF, SP, MB, JF, CL, and FS. Figures and tables were created by ECA and FMF. ECA wrote the first draft of the manuscript. Revision and rewriting of the manuscript was done by ECA, FMF, SP, MB, MS, JF, CL, and FS.

ECA is the corresponding author.

Article C2

Author: Sarah Piehl, Elizabeth C. Atwood, Mathias Bochow, Hannes K. Imhof, Jonas Franke, Florian Siegert, Christian Laforsch
Title: Can water constituents be used as proxy to map microplastic dispersal within transnational and coastal waters?
Status: Final form as brief research report for submission to the Journal Frontiers in Marine Science

Own contribution: concept and study design 20%, data acquisition 35%, analysis of microplastic samples 90%, analysis of water constituents 65%, data analysis and figures 80%, discussion of results 50%, manuscript writing 80%.

MB, JF, FS, and CL initiated the study. The study was designed by all authors. Field sampling was conducted by SP, ECA, MB, and HKI. Microplastic sample preparation was done by SP with the help of two technical assistants. Microplastic particle identification with FTIR spectroscopy was done by SP. MB developed and completed the SWIR microplastic particle identification. Chl-A analysis was done by HKI and SP in the laboratories of the Aquatic Ecology of the Ludwig-Maximilians University of Munich and the Department of Hydrology of the University Bayreuth. SPM analysis was done by HKI and SP partly in the department of Animal Ecology II of the University of Bayreuth. Analysis of cDOM was done by MB at Section 1.4 Remote Sensing and Geoinformatics at GFZ Potsdam. Data were analyzed by SP and discussed and interpreted by SP, ECA, MB, HKI, JF, and CL. Figures and tables were created by SP and ECA. SP wrote the first draft of the manuscript. Revision and rewriting of the manuscript was done by all authors.

CL is the corresponding author.

Chapter A

Chapter A: Identification of potential sources, pathways, and accumulation areas of plastic debris in the terrestrial environment

Article A1: Organic fertilizer as a vehicle for the entry of microplastic into the environment

Weithmann N, Möller JN, Löder MGJ, Piehl S, Laforsch C, Freitag R (2018)

Science Advances 4: 1-7

SCIENCE ADVANCES | RESEARCH ARTICLE

ENVIRONMENTAL STUDIES

Organic fertilizer as a vehicle for the entry of microplastic into the environment

Nicolas Weithmann,[1] Julia N. Möller,[2] Martin G. J. Löder,[2] Sarah Piehl,[2] Christian Laforsch,[2]* Ruth Freitag[1]

The contamination of the environment with microplastic, defined as particles smaller than 5 mm, has emerged as a global challenge because it may pose risks to biota and public health. Current research focuses predominantly on aquatic systems, whereas comparatively little is known regarding the sources, pathways, and possible accumulation of plastic particles in terrestrial ecosystems. We investigated the potential of organic fertilizers from biowaste fermentation and composting as an entry path for microplastic particles into the environment. Particles were classified by size and identified by attenuated total reflection-Fourier transform infrared spectroscopy. All fertilizer samples from plants converting biowaste contained plastic particles, but amounts differed significantly with substrate pretreatment, plant, and waste (for example, household versus commerce) type. In contrast, digestates from agricultural energy crop digesters tested for comparison contained only isolated particles, if any. Among the most abundant synthetic polymers observed were those used for common consumer products. Our results indicate that depending on pretreatment, organic fertilizers from biowaste fermentation and composting, as applied in agriculture and gardening worldwide, are a neglected source of microplastic in the environment.

INTRODUCTION

Plastics are an integral part of everyday life. They fulfill a wide variety of functions, primarily packaging (39.9% of the total plastics used in Europe in 2016) (*1*). Additional applications are in building and construction; the electrical, electronic, automotive, and agriculture sectors; and, to a lesser extent, consumer and household appliances, furniture, sport, health, and safety (*1*). Despite its varied applications, approximately 80% of the produced plastic falls into six categories: polyethylene (PE), polypropylene (PP), polyvinyl chloride (PVC), polyurethane (PUR), PE terephthalate (PET), and polystyrene (PS). Worldwide plastic production has increased steadily since 1950, reaching an annual production of 322 million metric tons worldwide in 2015, of which approximately 40% was used in one-way products (*1*). Not surprisingly, because of inadequate end-of-life treatment, plastics are increasingly found as contaminants in the environment (*2*). Recently, the World Economic Forum estimated that 32% of plastic packaging is leaking into the environment (*3*), and models suggest that up to 12.7 million metric tons of plastic litter enters the oceans from land-based sources each year (*4*). Therefore, the G7 has acknowledged that "plastic litter poses a global challenge" (*5*). Accordingly, scientists have suggested to "classify plastic waste as hazardous" because it may have "significant ecological impacts, causing welfare and conservation concerns" (*6*). Among the plastic materials found in the aquatic environment, so-called microplastic particles (MPPs; <5 mm)—mainly fragments, fibers, and spheres—have attracted particular attention (*7*, *8*) because harmful effects of MPPs on various aquatic organisms have been proposed (*6*, *8*–*11*), linked either to the presence of MPPs per se, to toxic additives, or to potentially harmful microorganisms or chemicals enriched onto them. However, theoretical predictions based on models and empirical studies are often contradictory, and it is not known how effects reported for individual organisms may affect ecosystems (*12*).

[1]Process Biotechnology and Centre for Energy Technology, University of Bayreuth, 95440 Bayreuth, Germany. [2]Animal Ecology I and BayCEER, University of Bayreuth, 95440 Bayreuth, Germany.
*Corresponding author. Email: christian.laforsch@uni-bayreuth.de

Because of their small size, MPPs may presumably also enter the food web (*10*) and thus potentially end up in human food (*13*). There, they pose a risk that is not yet predictable, because the interaction of MPPs with tissue and cells is poorly understood. Investigation of the interaction is further complicated by the fact that MPPs are not single compounds but constitute mixtures of different plastic types, each often consisting of a blend of synthetic polymers, residual monomers, and chemical additives. Furthermore, their morphology (for example, fragments, fibers, or spheres) may influence their effects. In this context, a distinction is typically made between industrially manufactured primary MPPs, originating from cosmetics, household cleaners and other products to which they were purposely added, and secondary MPPs that originate from the disintegration of larger plastics caused by ultraviolet (UV) radiation, mechanical abrasion, and biological degradation (*14*, *15*).

MPPs are detected ubiquitously in aquatic environments across the globe (*16*–*19*), reaching values of up to 100,000 particles per cubic meter, with predominantly secondary origin (*8*). Little is known about the exact origin of this significant contamination, although several pathways through which MPPs may enter surface water have been discussed. Most studies assume a transfer from land, including, but not restricted to, improper disposal of plastic waste, wind distribution, and municipal, as well as industrial wastewater and sewage sludge (*10*, *18*, *20*). However, detailed studies regarding MPP production and initial entry into terrestrial ecosystems are currently lacking.

Here, we investigated organic fertilizers (composts, digestates, and percolate-leachates from digestion, which is used as liquid fertilizer) from recycled biowaste as possible vehicles for the entry of MPPs >1 mm into the environment. According to best current practice, after separate collection, organic waste from households and industry is either directly composted or partially digested for biogas/energy production in an anaerobic biogas fermenter, typically followed by composting of the remaining digestates. The recycling of organic waste through composting or fermentation and subsequent application on agricultural land is, in principle, an environmentally sound practice to return nutrients, trace elements, and humus to the soil. However,

most household and municipal biowaste is contaminated by plastic material. Sieving and sifting procedures can significantly reduce, but never completely remove, these contaminants. Moreover, most countries allow a certain amount of foreign matter such as plastics in fertilizers; for example, Germany, which has one of the strictest regulations on fertilizer quality worldwide, allows up to 0.1 weight % (wt %) of plastics. In this regulation, particles smaller than 2 mm are not even considered (*21*). Thus, organic fertilizers may be a source of environmental MPPs that should not be overlooked. Our study is a first attempt to estimate the significance of this entry pathway to the terrestrial environment.

RESULTS

In this investigation, one biowaste composting plant (plant A; aerobic treatment) and one biowaste digester (plant B, "biogas plant"; anaerobic treatment) were studied in detail. The biowaste composting plant (plant A) processes the biowaste from households with a nearly equal amount of green clippings from the area. The plant removes potential nonbiodegradable material, including plastics, as thoroughly as possible by a series of sieving (80 mm), metal separation, and manual sorting steps. The remaining material is subsequently transferred into a box composter for rotting. The plant offers two types of commercial, quality-controlled, certified compost [composting plant (CP) 8 and CP 15 mm], sieved through 8- and 15-mm meshes, respectively. Both composts were sampled. The batch biowaste digester (parallel boxes, plant B) mainly processed biowaste from households with the addition of some green clippings and occasionally energy crops. The mixture is introduced directly into the digester without pretreatment. Instead, the operators remove contaminating materials from the final compost using one or two sieving steps (see Materials and Methods). From plant B, two mature composts ("Digest A" and "Digest B"), a nonmatured fertilizer ("Digest C"), and the pooled percolate ("Digest D") from the parallel boxes were analyzed.

An agricultural energy crop digester (plant C) processing only energy crops and no biowaste served as a reference. In plant C, the sample ("Energycrop") was taken from the postdigester outlet, corresponding to an end-of-process sample. This agricultural biogas plant processes energy crops such as corn/grass silage and, to a lesser extent, ground wheat. Ground wheat and silage arrive in plastic encasings, but these are removed before the substrate is passed through the shredder and entered into the fermenter. In addition, a commercially available fertilizer from a second biowaste digester (plant D, processing solely waste from commerce) located in the same area, as well as end-of-process digestate samples from 10 additional agricultural biogas plants (plants E to N), processing feeds such as dung/manure, sunflowers, or waste from fruit processing, together with the regular energy crops, were screened for MPPs.

Quantity of MPPs

With only 20 (CP 8 mm) and 24 (CP 15 mm) particles per kilogram dry weight (Table 1), the MPP load of the certified composts from the biowaste composting plant (plant A) was almost an order of magnitude lower than that determined in the samples from the biowaste digester (plant B), where up to 146 particles per kilogram dry weight were found in the fresh digestate-fertilizer (Digest C). Mature compost from the same biowaste digester (Digest A and Digest B) contained similar amounts of MPPs (70 and 122 particles per kilogram dry weight, respectively), whereas the pooled percolate sample (Digest D) was somewhat less contaminated, containing only 14 particles per kilogram dry weight. In the agricultural energy crop digester (plant C), which served as a "blank" fermenter, no plastic particles were found in the end-of-process digestate (sample Energycrop) (Table 1). The end-of-process samples of digestates from the additional 10 agricultural biogas plants (plants E to N) included in the screening contained only negligible numbers of particles: The samples from eight plants contained no particle, whereas the samples from the other two plants contained one particle each, resembling a maximum of 11 MPPs per kilogram dry weight. In contrast, with 895 MPPs per kilogram dry weight, the sample from the second biowaste digester (plant D) included in the screening contained even higher numbers of MPPs than found in composts (Digests A to C) from the biowaste digester (plant B), despite the fact that plant B processed biowaste collected from households, whereas plant D processed biowaste directly supplied by commerce.

Polymer size, type, and morphology

Before further analysis, samples were gently fractionated using sieves with mesh sizes of 5, 2, 1, and exceptionally also 0.5 mm. Analysis of MPP size showed that most of the particles collected from the various samples were between 2 and 5 mm (Fig. 1). Only the pooled percolate sample (Digest D) from the biowaste digester (plant B) contained MPPs mostly from 1 to 2 mm. In some samples, we also found MPPs as small as 250 μm. However, because these data are not fully quantitative, we only present data in the size range of 1 to 5 mm. All MPPs were categorized by shape into three subgroups: fragments, fibers, and spheres. Examples are shown in Fig. 2. Most of the MPPs (75 to 100%) were fragments, followed by fibers (0 to 8%) and spheres (0 to 8%).

Attenuated total reflection (ATR)–Fourier transform infrared (FTIR) spectroscopy analysis identified 11 polymer types in the samples: styrene-based polymers (PS, acrylonitrile butadiene styrene, and styrene acrylonitrile), polyester (PES), PE, PP, PET, PVC, PUR, polyvinylidene chloride (PVDC), polyamide (PA), and latex- and cellulose-based polymers (Table 2). Most of the particles found in the high-quality composts from the biowaste composting plant (plant A) were styrene-based polymers (60%; 42%), followed by PE (30%; 33%) for the CP 8- and CP 15-mm samples, respectively. The most abundant polymer types in Digest A (73%) and Digest B (80%) from the biowaste digester (plant B) were also styrene-based polymers, whereas most of the MPPs found in the Digest C from this digester were PES with 38% and PE with 21%. The few polymers found in the additional energy crop digesters (plant E to N) were PP and PVC.

DISCUSSION

Organic waste from private households and industry is increasingly seen as a valuable source of both fertilizer and energy. Processing organic waste by fermentation and/or composting is a sustainable means of producing organic fertilizer for agriculture and private gardening, thereby reducing the need for chemical fertilizers. An initial anaerobic fermentation step (production of biogas) before composting is often proposed because this produces energy in a sustainable manner and helps to economically run a plant (production of electricity and heat) while avoiding the drawbacks of conventional biogas production from energy crops (monocropping, rivalry to esculents). Moreover, an initial fermentation step reduces the amount of methane—a more potent greenhouse gas than carbon dioxide—released into the atmosphere, as compared to composting alone.

Table 1. Overview of plants and compartments. The total number of particles is shown as particles >1 mm per kilogram of dry weight.

	Plant A			Plant B			Plant C	Plant D	Plants E to N
Type	Biowaste composting			Biowaste digestion			Energycrop digestion	Biowaste digestion	Agricultural digestion
Sampled	CP 8 mm	CP 15 mm	Digest A	Digest B	Digest C	Digest D	End-of-process	Commercial binding	End-of-process
Particles per kilogram	20	24	70	122	146	14	0	895	0 to 11

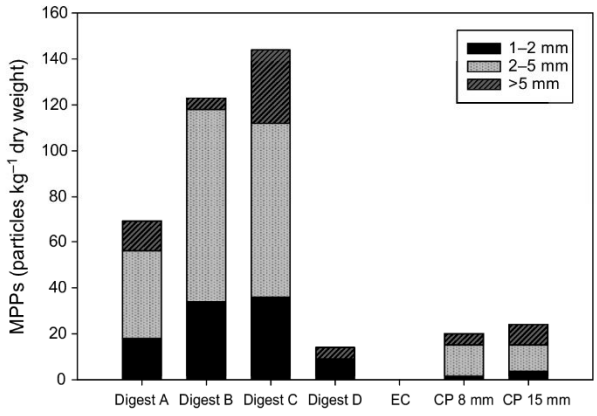

Fig. 1. Size fractions of MPPs in different fertilizers. Digests A/B/C/D, biowaste digester; EC, energy crop digester; CP 8 mm/15 mm, biowaste composting plant.

Current practice for collecting organic waste fractions from private households calls for separate collecting bins. Theoretically, a pure organic fraction very suitable to composting/biogas fermentation should be obtained. However, in practice, most biowaste contains contaminants, often including plastics. Organic materials from commercial sources, such as the food and drink industries, tend to be less contaminated by plastics, but in particular, unsold food items often arrive in packaged form, some parts of which may then also enter the respective biowaste processing plant. The fact that all the samples from biowaste processing plants investigated in this study contained a certain number of MPPs is therefore not surprising, although a detailed quantitative analysis has been lacking so far. Most of the MPPs were "fragments," most likely secondary MPPs produced through breakdown of larger plastic materials, such as bags and containers, used for packaging. This hypothesis is corroborated by the fact that styrene-based polymers and PE tended to predominate among the identified materials (that is, materials used mainly for packaging and wrapping). In contrast, none of the samples from the investigated agricultural energy crop digesters contained significant amounts of MPPs, indicating that agricultural crops are only rarely contaminated with plastic items.

However, the relative distribution of MPPs among the different polymer types was not necessarily consistent for all samples from a given plant. For example, although polymer distribution was similar in Digests A and B from the biowaste digester (plant B), a different distribution was found in Digest C from the same plant. The three composts/fertilizers (Digests A to C) from plant B were sampled simultaneously. Because they had matured for differing lengths of time, the observed differences in MPP composition may very well reflect seasonal changes in biowaste composition. However, because no samples of the original feed substrate were available, this aspect could not be further investigated.

The final processing step for compost is typically sieving using 8-, 10-, or even 15-mm mesh sizes. MPPs, defined as particles smaller than 5 mm, will therefore pass through these sieves and enter the compost. Here, samples were gently fractionated using sieves with mesh sizes of 5, 2, 1, and exemplarily 0.5 mm before the analysis. In most samples, MPP sizes ranged between 2 and 5 mm. The only exception was the percolate sample (Digest D) from plant B, which mainly contained particles between 1 and 2 mm. This may be because the percolate is filtrated because it passes through the fermenter content, and retention increases with particle size. This may also explain why the percolate sample contained a comparatively low number of MPPs compared to the other samples from plant B.

Although particles as small as 250 µm were found in some of the fractions, most likely because they had attached to larger fragments and were therefore retained, the smallest MPP size that could be examined with certitude in this study was 1 mm. At present, quantitative evaluation of smaller particles via the existing methodology is very difficult because the removal of the high organic load is extremely challenging and hampers reliable analysis (*22*). Hence, quantitative results are presented in this study only for the size range of 1 to 5 mm. Studies focusing on aquatic environments have reported that sites contaminated by MPPs in the range of 1 to 5 mm typically also contain an even higher amount of particles <1 mm, presumably created through further fragmentation of larger MPPs (*23*). However, fragmentation into a size <1 mm is perhaps more likely in the natural environment, where mechanical forces act (for example, wave action at a beach), than in biowaste treatment plants. Nevertheless, it cannot be excluded at present writing that MPPs <1 mm are produced during biowaste treatment as well (for example, due to the mechanical forces present during the various sieving steps), indicating that actual MPP numbers in fertilizer originating from biowaste may be much higher. This needs further study, particularly in view of the intended use of the material as organic fertilizer.

Although all samples from the biowaste treatment plants contained MPPs, significant differences in the level of contamination were observed. High-quality compost ("quality seal" label) from the biowaste composting plant (plant A) contained less than 25 MPPs per kilogram dry weight, whereas the contamination of the composts/digestates from the biowaste digester (plant B) was nearly an order of magnitude higher. Several factors may have contributed to this result. Although aerobic rotting (composting) reduces the dry mass of the material by approximately 50%, anaerobic conversion to biogas, followed by composting, will often achieve a reduction of more than 80%. Nondigested material, such as MPPs, is therefore enriched by a factor of 5 during anaerobic biowaste digestion but by only a factor of 2 during simple composting.

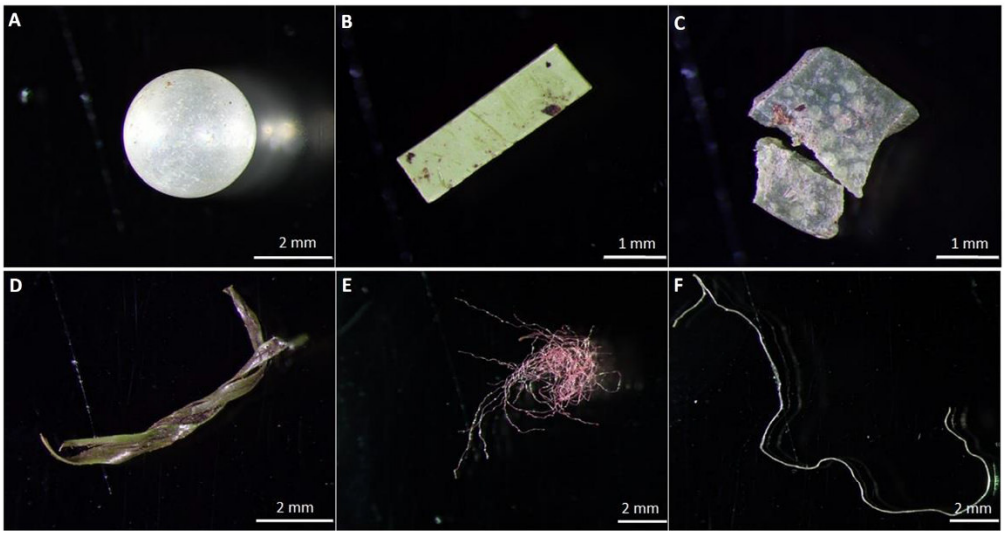

Fig. 2. Examples of MPPs of various shapes found in samples. (**A**) PE sphere. (**B**) PVC fragment. (**C** and **D**) PE fragments. (**E**) PES fiber. (**F**) PP fiber.

Table 2. MPP abundances in different samples. Digests A/B/C/D, biowaste digester; EC, energy crop digester, CP 8 mm/15 mm, biowaste composting plant; MPP per kilogram of dry weight; A, proportion of polymer type in specific sample.

	CP 8 mm		CP 15 mm		Digest A		Digest B		Digest C		Digest D		EC	
	MPP per kilogram	A (%)	MPP per kilogram	A (%)	MPP per kilogram	A (%)	MPP per kilogram	A (%)	MPP per kilogram	A (%)	MPP per kilogram	A (%)	MPP per kilogram	A (%)
Styrene-based polymer	12	60	10	42	51	73	97	80	10	7	0	0	0	0
PES	1	5	0	0	2	3	2	2	56	38	14	100	0	0
PE	6	30	8	33	6	9	3	2	31	21	0	0	0	0
PP	0	0	4	17	3	4	2	2	24	16	0	0	0	0
PET	0	0	1	4	0	0	0	0	16	11	0	0	0	0
Cellulose-based polymer	0	0	0	0	6	9	11	9	5	3	0	0	0	0
PVDC	0	0	0	0	2	3	0	0	0	0	0	0	0	0
PVC	1	5	1	4	0	0	5	4	2	1	0	0	0	0
Latex	0	0	0	0	0	0	0	0	1	1	0	0	0	0
PUR	0	0	0	0	0	0	0	0	1	1	0	0	0	0
PA	0	0	0	0	0	0	2	2	0	0	0	0	0	0
Σ MPP	20		24		70		122		146		14		0	

Concomitantly, in the biowaste composting plant (plant A), biowaste from private households was mixed with at least equal amounts of green clippings. The latter is typically much less contaminated with plastics and thus dilutes the MPP contamination. In addition, an elaborate substrate preparation protocol is in place at the biowaste composting plant (plant A), which attempts to remove contaminating materials as thoroughly as possible before the substrate enters the composter. Finally, temperatures of up to 75°C are reached during aerobic rotting (composting as in plant A), whereas most anaerobic biowaste digesters, such as plant B, are operated between 45° and 55°C. This will directly influence, for example, the fraction of cellulose-based MPPs found in the final compost, which, in consequence, was nondetectable in the samples from the composting plant (plant A). In addition to the lower temperature, a lack of oxygen and UV radiation will also block potential MPP

degradation pathways in the anaerobic biowaste digesters, such as plant B, compared to aerobic composting, as in plant A. A recent study testing the degradability of PE and PET in an active anaerobic environment at 50°C showed no appreciable degradation of polymers over the investigation period of 500 days (*24*). In particular, PE and PS, which were detected in all samples from the biowaste treatment plants, are known to be highly persistent in the environment. It is therefore likely that these particles, once released, will accumulate in nature over time.

In Germany alone, which has one of the strictest regulations on fertilizer quality worldwide, more than 12 million metric tons of biowaste were either composted or passed through municipal biogas plants in 2013 (*25*). This quantity of biowaste translates into more than 5 million metric tons of compost from these plants, most of which is used in traditional agriculture and gardening. We recorded particle counts varying from 14 to 895 particles per kilogram dry weight (when conservatively calculated, 1-kg compost contains approximately 50% dry weight content) for MPPs larger than 1 mm, together with a yet unquantified number of smaller particles. Although our data may not be representative of all biowaste treatment plants, an extrapolation based on our results suggests that, in Germany alone, although counting only particles >1 mm, between 35 billion and 2.2 trillion MPPs are potentially introduced via this pathway into the environment each year.

An evaluation of our data is difficult because there is no other quantitative study on MPPs in compost available. However, our data can at least be compared with similar potential sources of MPPs such as sewage sludge, which is also used for fertilization of agricultural land. When considering only MPPs >1 mm, recent studies on the MPP contamination of sewage sludge have found concentrations ranging between 0 and 300 particles per kilogram dry weight in the analyzed samples (*26*, *27*). The highest concentration found for sewage sludge in the latter study is by a factor of 3 lower than the highest concentration found in the compost samples in our study. However, as stated above, sewage sludge may be contaminated with an even higher amount of smaller MPPs (<1 mm) indicated by recent studies, which have found between 1000 and 24,000 particles per kilogram dry weight (*26*, *27*). For various reasons, sewage sludge is in the public opinion increasingly seen as problematic waste inappropriate for redistribution into the environment, probably not least because of the contamination with heavy metals, residual pharmaceuticals, and also artificial fibers. The latter was detectable in agricultural soils up to 15 years after application of sewage sludge (*28*). This abandonment is not the case for composts and digestates from biowaste processing plants, which, in principle, do constitute valuable organic fertilizers.

However, compared to sewage sludge, which, in Germany, is routinely incinerated, fertilizer contaminated with MPPs from biowaste processing plants inevitably enters the environment. Because Germany has one of the strictest regulations on fertilizer quality worldwide, we here report only on the "best case scenario," whereas the MPP contamination in countries with less strict regulations may be even higher.

However, advantages and disadvantages of the continuation of using biowaste for fertilizer production need to be carefully balanced, particularly because studies on the impact of MPPs on terrestrial life forms are still inconclusive. It cannot be excluded that, analogous to aquatic systems, MPPs can accumulate in the soil detrital food web (*29*). At least one study has shown that (pristine) PE particles mixed with litter and offered to earthworms for uptake led to higher mortality and a reduced growth rate (*30*). Another study showed that polybrominated diphenyl ether, a substance mixed into polymers as a flame retardant, is bioaccessible and can enter soils after volatilization or polymer deterioration. Accumulation in earthworms was shown, and transfer to higher trophic levels is likely (*31*). However, it is unknown whether these additives are still present in secondary MPPs after fermentation and/or composting. In addition, it cannot be excluded that MPPs in the investigated size range, or smaller, exert a direct influence on active microbiota in biowaste treatment plants or soils, which has not been considered yet in the literature. Hence, further studies on the possible consequences and impacts of MPP contamination of fertilizers originating from biowaste treatment plants for soil quality and soil life forms are necessary before any risk assessment can be undertaken.

MATERIALS AND METHODS

Biowaste composting plant (aerobic treatment), plant A

The biowaste compositing plant (plant A) processes approximately 8000 metric tons per year (t/a) of biowaste solely from households, together with approximately 12,000 t/a of green clippings. The plant commercializes quality-controlled, certified composts of two compost qualities (sieving with 8- and 15-mm sieves), both of which were sampled. Arriving biowaste was initially sieved using an 80-mm mesh. The fraction <80 mm was passed through the metal separator and then directly placed into the rotting containers for fast initial decomposition. The fraction >80 mm was sorted manually to remove stones, metals, plastics, and glass. Afterward, the material was mechanically shredded and again added to the sieving drum. In the rotting container, temperatures >70°C were reached. After initial rotting, the compost was left to mature and stabilize in open piles for several months, followed by a final sieving step to reach the desired final corn sizes of below 8 and 15 mm, respectively.

Biowaste digester (anaerobic treatment), plants B and D

The investigated biowaste digester (plant B) was a nonstirred, discontinuous box fermentation system. The plant comprised several quadrangular box digesters, each with a volume of 945 m^3 and a filling capacity of 500 m^3, which corresponds to a mass of 350 metric tons of organic material. All boxes were equipped with a floor heating and operated at temperatures between 40° and 45°C. The substrate consisted of a pourable mixture of biowaste (11,000 t/a, solely from households) and green clippings (3000 t/a) with a water content below 15 wt %. The composition of the substrate follows seasonal changes. In the winter, the substrate is occasionally supplemented with energy crops.

To initiate the fermentation in the box, fresh substrate was predigested via aerobic digestion for several days and mixed with two volumes of fermenter content. The mixture was added into a fermenter box using an excavator. Afterward, the box was locked, assuring anaerobic conditions, and inoculated by sprinkling with percolate from other boxes. No mechanical treatment or manual presorting took place. After 28 days of fermentation, the box was emptied, 30 volume percent (volume %) of the digestate was removed, and the rest was mixed with 30 volume % of fresh substrate. Subsequently, the digestate was sieved (20-mm mesh) to remove impurities, such as stones, larger plastics, and metals, before it is processed to fertilizer and potting soil using an aerobic composting process. To produce high-quality compost, digestates were matured for 11 to 13 months and sieved using a 10-mm mesh. Lower-quality fertilizer was matured for only 8 to 9 months, and no additional sieving step was performed at 10 mm.

In addition, to expand the range and verify our findings, 1.5 liters of liquid fertilizer for private and agricultural use produced by another anaerobic plant (plant D) was screened for MPPs. This plant processes

16,000 t/a biowaste from commerce, particularly waste from the local market, as well as waste from food and drink industries.

Energy crop digester, plant C and plants E to N

The agricultural energy crop digester (plant C) serving as a presumably uncontaminated reference in this study was a standard two-stage "wet-digester" tank system consisting of a 30-m^3 unit for feeding, a 400-m^3 plug-flow fermenter with spool agitators, and a 1000-m^3 agitated post-digester. The fermenter and postdigester were equipped with heating aggregates and operated between 42° and 45°C. The plant converts approximately 3200 t/a of corn silage and 200 t/a of ground wheat, together with varying amounts of grass silage, and produces approximately 950,000 Nm^3 of biogas per year. Before feeding, the silage was removed from its plastic encasing and passed through a mechanical shredder. Enough water was added to ensure pumpability. In addition, similar end-of-process samples were taken from 10 additional agricultural biogas plants (plants E to N), with feeds ranging from dung/manure, sunflowers, or waste from fruit processing, together with regular energy crops; none of these plants processed any biowaste. Whatever material arrived in plastic encasings was taken from these foils before being either mechanically shredded or directly entered into the digester.

Sampling

All samples were stored in glass jars to avoid contamination by plastics. In the case of the energy crop digester (plant C), a 2-liter sample was taken from the outlet pipe of the postdigester after a certain amount of digestate was discharged to avoid clotted residues. The 10 additional agricultural biogas plants (plants E to N) included in the study were sampled in the same way as the agricultural biogas plant (plant C).

Four 0.75-liter subsamples were taken from the biowaste digester (plant B) and pooled from a compost (Digest A) matured for 11 months and a compost (Digest B) matured for 13 months. Both were sieved with a mesh size of 10 mm. In addition, one compost (Digest C) sample, which had not been matured beforehand, was sieved with a mesh size of 20 mm. For each compost sample, four subsamples were taken equidistantly at a constant height per heap according to the heap size (50 cm for heap A, 30 cm for heap B, and 1.5 m for heap C). The first subsample was always taken at a distance of 1 m from the wall, and every subsequent subsample was taken at an interval of 1 m from the previous subsample. Compost heap C was sampled from the rightmost end to the middle to maintain the greatest possible distance from the adjacent heap (which had not yet undergone sieving) to avoid contamination with objects that would not have passed the sieving process. In addition to the compost, 5.5-liter samples were taken from the percolate at the outlet of the pipeline pooling the percolate from all fermenter boxes (Digest D). In the second anaerobic biowaste digestion plant (plant D) in the study, a representative sample was drawn from commercially available 5-liter bindings.

In the case of the biowaste composting plant (plant A), two 40-liter batches of compost were purchased and subsampled to a 3-liter volume. One batch was sieved with a mesh size of 8 mm ("CP 8 mm"), and the other was sieved with a 15-mm mesh ("CP 15 mm").

Isolation of MPPs

For MPP isolation, samples were wet-sieved through three stacked stainless steel sieves with mesh sizes of 5, 2, and 1 mm and exemplarily 500 µm (see below). Objects >5 mm were thoroughly rinsed over the sieves with filtered water and filtered ethanol (30%) to remove any attached MPPs. The material remaining on the sieves was visually presorted under a Leica M50 stereomicroscope. Potential plastic particles were photographed, sized at a magnification of ×40 with a digital camera for microscopy (Olympus DP26), and stored for further analysis using ATR-FTIR spectroscopy (see below). Additional samples from 10 agricultural biogas plants and one liquid fertilizer were treated equally, with the exception of sieving with mesh sizes of 1 mm and 500 µm.

FTIR spectroscopy

A Bruker Tensor 27 FTIR spectrometer equipped with a germanium crystal for measurements in the ATR mode was used for spectral analysis of the putative MPPs. Following 16 background scans, 16 sample scans were performed with a spectral resolution of 8 cm^{-1} within a range of 3940 to 800 cm^{-1}. The measured spectra were identified by comparison with reference spectra from a custom-made spectral polymer library. The library includes 131 records and contains not only the most common plastic polymers but also natural materials such as silicate, chitin, cotton, or keratin (*32*).

Determination of dry weight

For standardization, the dry weight of each pooled sample (n = 5) was determined by weighing before and after drying at 60°C to a constant weight.

REFERENCES AND NOTES

1. *Plastics - The facts 2016, An Analysis of European Plastics Production, Demand and Waste Data* (PlasticsEurope, 2016).
2. *Green Paper - On a European Strategy on Plastic Waste in the Environment* (European Commission, 2013).
3. L. Neufeld, F. Stassen, R. Sheppard, T. Gilman, Eds., *The New Plastics Economy: Rethinking the Future of Plastics* (World Economic Forum, 2016).
4. J. R. Jambeck, R. Geyer, C. Wilcox, T. R. Siegler, M. Perryman, A. Andrady, R. Narayan, K. L. Law, Plastic waste inputs from land into the ocean. *Science* **347**, 768–771 (2015).
5. G7 leaders, *Leaders' Declaration* (2015); www.g7germany.de/Content/EN/_Anlagen/G7/2015-06-08-g7-abschluss-eng_en.pdf?__blob=publicationFile&v=3.
6. C. M. Rochman, M. A. Browne, B. S. Halpern, B. T. Hentschel, E. Hoh, H. K. Karapanagioti, L. M. Rios-Mendoza, H. Takada, S. Teh, R. C. Thompson, Policy: Classify plastic waste as hazardous. *Nature* **494**, 169–171 (2013).
7. J. A. Ivar do Sul, M. Costa, The present and future of microplastic pollution in the marine environment. *Environ. Pollut.* **185**, 352–364 (2014).
8. S. L. Wright, R. C. Thompson, T. S. Galloway, The physical impacts of microplastics on marine organisms: A review. *Environ. Pollut.* **178**, 483–492 (2013).
9. A. McCormick, T. J. Hoellein, S. A. Mason, J. Schluep, J. J. Kelly, Microplastic is an abundant and distinct microbial habitat in an urban river. *Environ. Sci. Technol.* **48**, 11863–11871 (2014).
10. M. A. Browne, P. Crump, S. J. Niven, E. Teuten, A. Tonkin, T. Galloway, R. Thompson, Accumulation of microplastic on shorelines woldwide: Sources and sinks. *Environ. Sci. Technol.* **45**, 9175–9179 (2011).
11. D. Lithner, Å. Larsson, G. Dave, Environmental and health hazard ranking and assessment of plastic polymers based on chemical composition. *Sci. Total Environ.* **409**, 3309–3324 (2011).
12. T. S. Galloway, M. Cole, C. Lewis, Interactions of microplastic debris throughout the marine ecosystem. *Nat. Ecol. Evol.* **1**, 0116 (2017).
13. L. van Cauwenberghe, C. R. Janssen, Microplastics in bivalves cultured for human consumption. *Environ. Pollut.* **193**, 65–70 (2014).
14. A. L. Andrady, Microplastics in the marine environment. *Mar. Pollut. Bull.* **62**, 1596–1605 (2011).
15. M. Cole, P. Lindeque, C. Halsband, T. S. Galloway, Microplastics as contaminants in the marine environment: A review. *Mar. Pollut. Bull.* **62**, 2588–2597 (2011).
16. H. K. Imhof, N. P. Ivleva, J. Schmid, R. Niessner, C. Laforsch, Contamination of beach sediments of a subalpine lake with microplastic particles. *Curr. Biol.* **23**, R867–R868 (2013).
17. M. Zbyszewski, P. Corcoran, Distribution and degradation of fresh water plastic particles along the beaches of Lake Huron, Canada. *Water Air Soil Pollut.* **220**, 365–372 (2011).
18. M. Wagner, C. Scherer, D. Alvarez-Muñoz, N. Brennholt, X. Bourrain, S. Buchinger, E. Fries, C. Grosbois, J. Klasmeier, T. Marti, S. Rodriguez-Mozaz, R. Urbatzka, A. Dick Vethaak,

M. Winther-Nielsen, G. Reifferscheid, Microplastics in freshwater ecosystems: What we know and what we need to know. *Environ. Sci. Eur.* **26**, 12 (2014).
19. D. Eerkes-Medrano, R. C. Thompson, D. C. Aldridge, Microplastics in freshwater systems: A review of the emerging threats, identification of knowledge gaps and prioritisation of research needs. *Water Res.* **75**, 63–82 (2015).
20. K. Duis, A. Coors, Microplastics in the aquatic and terrestrial environment: Sources (with a specific focus on personal care products), fate and effects. *Environ. Sci. Eur.* **28**, 2 (2016).
21. B. Kehres, *H&K Aktuell, Änderung der Düngemittelordnung* (BGK e.V., 2015).
22. M. G. J. Löder, H. K. Imhof, M. Ladehoff, L. A. Löschel, C. Lorenz, S. Mintenig, S. Piehl, S. Primpke, I. Schrank, C. Laforsch, G. Gerdts, Enzymatic purification of microplastics in environmental samples. *Environ. Sci. Technol.* **51**, 14283–14292 (2017).
23. H. K. Imhof, C. Laforsch, A. C. Wiesheu, J. Schmid, P. M. Anger, R. Niessner, N. P. Ivleva, Pigments and plastic in limnetic ecosystems: A qualitative and quantitative study on microparticles of different size classes. *Water Res.* **98**, 64–74 (2016).
24. S. Selke, R. Auras, T. A. Nguyen, E. Castro Aguirre, R. Cheruvathur, Y. Liu, Evaluation of biodegradation-promoting additives for plastics. *Environ. Sci. Technol.* **49**, 3769–3777 (2015).
25. Federal Statistical Office (2017); www.destatis.de/EN/Homepage.html.
26. S. M. Mintenig, I. Int-Veen, M. G. J. Löder, S. Primpke, G. Gerdts, Identification of microplastic in effluents of waste water treatment plants using focal plane array-based micro-Fourier-transform infrared imaging. *Water Res.* **108**, 365–372 (2017).
27. A. M. Mahon, B. O'Connell, M. G. Healy, I. O'Connor, R. Officer, R. Nash, L. Morrison, Microplastics in sewage sludge: Effects of treatment. *Environ. Sci. Technol.* **51**, 810–818 (2017).
28. K. A. V. Zubris, B. K. Richards, Synthetic fibers as an indicator of land application of sludge. *Environ. Pollut.* **138**, 201–211 (2005).
29. M. C. Rillig, Microplastic in terrestrial ecosystems and the soil? *Environ. Sci. Technol.* **46**, 6453–6454 (2012).
30. E. Huerta Lwanga, H. Gertsen, H. Gooren, P. Peters, T. Salánki, M. van der Ploeg, E. Besseling, A. A. Koelmans, V. Geissen, Microplastics in the terrestrial ecosystem: Implications for *Lumbricus terrestris* (Oligochaeta, Lumbricidae). *Environ. Sci. Technol.* **50**, 2685–2691 (2016).
31. M. O. Gaylor, E. Harvey, R. C. Hale, Polybrominated diphenyl ether (PBDE) accumulation by earthworms (*Eisenia fetida*) exposed to biosolids-, polyurethane foam microparticle-, and Penta-BDE-amended soils. *Environ. Sci. Technol.* **47**, 13831–13839 (2013).
32. M. G. J. Löder, M. Kuczera, S. Mintenig, C. Lorenz, G. Gerdts, Focal plane array detector-based micro-Fourier-transform infrared imaging for the analysis of microplastics in environmental samples. *Environ. Chem.* **12**, 563–581 (2015).

Acknowledgments: We want to thank U. Wilczek, H. Martirosyan, and M. Preiss for help with the experiments. Furthermore, we want to thank the editor and the anonymous reviewers for valuable and helpful comments on the manuscript and B. Trotter for linguistic improvements. Institutional Review Board and/or Institutional Animal Care and Use Committee guidelines were followed with human or animal subjects. **Funding:** The authors acknowledge that they received no funding in support of this research.
Author contributions: C.L. and R.F. designed the study. N.W., J.N.M., M.G.J.L., and S.P. performed the experiments. N.W., M.G.J.L., S.P., C.L., and R.F. wrote and revised the manuscript.
Competing interests: The authors declare that they have no competing interests.
Data and materials availability: All data needed to evaluate the conclusions in the paper are present in the paper. Additional data related to this paper may be requested from the authors.

Submitted 28 August 2017
Accepted 14 February 2018
Published 4 April 2018
10.1126/sciadv.aap8060

Citation: N. Weithmann, J. N. Möller, M. G. J. Löder, S. Piehl, C. Laforsch, R. Freitag, Organic fertilizer as a vehicle for the entry of microplastic into the environment. *Sci. Adv.* **4**, eaap8060 (2018).

Article A2: Identification and quantification of macro- and microplastics on an agricultural farmland

Piehl S, Leibner A, Löder MGJ, Dris R, Bogner C, Laforsch C (2018)

Scientific Reports 8

SCIENTIFIC REPORTS

OPEN

Received: 31 May 2018
Accepted: 8 November 2018
Published online: 18 December 2018

Identification and quantification of macro- and microplastics on an agricultural farmland

Sarah Piehl[1], Anna Leibner[1], Martin G. J. Löder[1], Rachid Dris[1], Christina Bogner[2] & Christian Laforsch[1]

Microplastic contamination of aquatic ecosystems is a high priority research topic, whereas the issue on terrestrial ecosystems has been widely neglected. At the same time, terrestrial ecosystems under human influence, such as agroecosystems, are likely to be contaminated by plastic debris. However, the extent of this contamination has not been determined at present. Via Fourier transform infrared (FTIR) analysis, we quantified for the first time the macro- and microplastic contamination on an agricultural farmland in southeast Germany. We found 206 macroplastic pieces per hectare and 0.34 ± 0.36 microplastic particles per kilogram dry weight of soil. In general, polyethylene was the most common polymer type, followed by polystyrene and polypropylene. Films and fragments were the dominating categories found for microplastics, whereas predominantly films were found for macroplastics. Since we intentionally chose a study site where microplastic-containing fertilizers and agricultural plastic applications were never used, our findings report on plastic contamination on a site which only receives conventional agricultural treatment. However, the contamination is probably higher in areas where agricultural plastic applications, like greenhouses, mulch, or silage films, or plastic-containing fertilizers (sewage sludge, biowaste composts) are applied. Hence, further research on the extent of this contamination is needed with special regard to different cultivation practices.

Plastic debris is ubiquitous in all ecosystems on earth[1] and yet, only a fraction of this environmental issue is visible. Through chemical, physiochemical, and biological processes, plastic debris disintegrates into smaller particles in the environment[2]. When those particles reach a size below five millimetres, they are called "microplastics". It is commonly distinguished between fragments of larger plastic items, so called secondary microplastics, and primary microplastics which are specifically produced within a small size for a variety of applications, like cosmetic products or household cleaners. Many organisms are known to ingest microplastic particles (MPPs), with reported adverse effects from the molecular level up to the behavioural level[3] and yet unknown consequences for environmental and human health[4].

Research on microplastics started in the marine environment over a decade ago[5], whereas the question of the origin of plastic debris addressed continental sources, especially rivers, as the main input route[6,7]. This led the scientific community to recently carrying out progressive work on freshwater ecosystems[8]. While both freshwater (including water surface and sediments) and atmospheric environments[9,10] were investigated regarding microplastic contamination, there is a large gap of knowledge on the extent to which terrestrial ecosystems are affected[1]. This is even more surprising, as plastic is already suggested as a stratigraphic indicator for the Anthropocene Era due to its suspected omnipresence in soils[11]. Recent literature[8,12–14] illustrated several pathways for plastic debris entering terrestrial soils. In this context, Hurley and Nizzetto[14] differentiated between three main categories of sources: (I) fragmentation of plastic debris already present in the environment, (II) deposition and runoff from the surroundings, and (III) inputs from agricultural practices. Thereby, fragmentation of intentional or unintentional discarded plastic debris is one of the major input routes, with estimates that around 32% of the world plastic packaging debris can escape collection systems[15]. These macroplastics further represents a constant input source for secondary microplastics to the environment if not removed. In addition, aeolian transport constitutes a possible distribution route for small microplastics from their source to remote areas where deposition to soils (due to rain, declining wind, or barriers) could occur[10,16]. Runoff from the surrounding environment is also

[1]Animal Ecology I and BayCEER, University of Bayreuth, 95440, Bayreuth, Germany. [2]Ecological Modelling and BayCEER, University of Bayreuth, 95440, Bayreuth, Germany. Correspondence and requests for materials should be addressed to C.L. (email: christian.laforsch@uni-bayreuth.de)

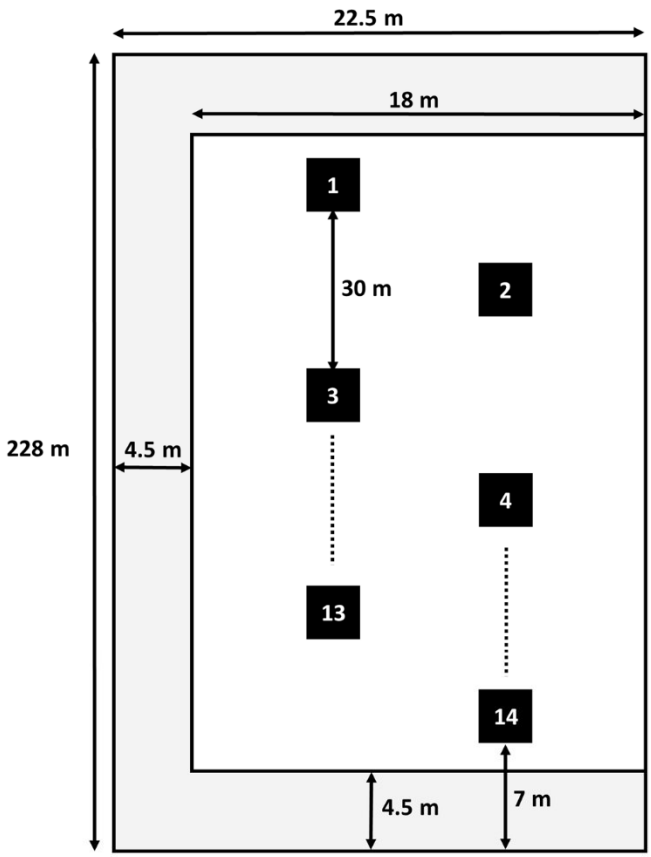

Figure 1. Schematic drawing of the investigated agricultural farmland with length specifications and placing of the samples for microplastic analysis (1 to 5 mm). The margin is shown in grey, the sampled area for macroplastics in white. On the site bordering another similar cultivated agricultural field, no margin was applied. Black dots indicate further sampling plots not shown in the figure.

a potential pathway, but its influence is yet unknown. While it is widely discussed for microplastics[17], field studies quantifying it are lacking[13]. Next to those sources, it has recently been suggested that fertilizers originating from sewage sludge[18] and bio-waste[19] processed from households or commercial bindings, may act as a further major input route of microplastics to soils and thus, especially agricultural soils are prone to microplastic contamination. For instance it is assumed that between 63,000 and 430,000 tons of microplastics are added via sewage sludge to European farmlands annually[18]. Nevertheless, the main source of nitrogen input to agricultural lands within the EU is mineral fertilizer and livestock manure, accounting for 83.2%[20]. Consequently, the question arises if also a conventionally treated agricultural farmland not subjected to potentially microplastic-containing fertilizers, could still be contaminated with plastic debris.

We therefore collected data on the amount of macro- and microplastic debris on an agricultural farmland in southeast Germany. We chose a study site which only receives conventional agricultural treatment (rain-fed, ploughing, harrowing, sowing, fertilization, herbicide application, harvesting) and is not subjected to microplastic-containing fertilizers (for example sewage sludge, organic fertilizers) or agricultural plastic applications (for example mulching films, greenhouses, nets). Therefore, our study is the first report on macro- and microplastic contamination of an agricultural farmland in rural areas which only receives conventional agricultural treatment.

Results

An agricultural farmland in Middle Franconia, southeast Germany with a total area of 0.5 ha (Fig. 1) served as the study site. Geographically, it can be assigned to the supra-region "Southwest German Scarplands". This is a wide flat open cultural landscape shaped by arable land. The exact coordinates of the field cannot be provided in order to respect the privacy of the owner. The soils in this area are predominantly Entisols and Vertisols (both USDA soil taxonomy and FAO WRB) with a high clay content[21]. The site is located approximately 316 m above mean sea level and has a slope of ~6%, facing north-northwest. It is bordered by field roads on three sides and surrounded by fields owned by the same person (i.e. receiving similar agricultural treatment). The closest inhabited area is located 1.5 km distance away and the next bigger city of Nuremberg around 50 km. Within the last five years, the investigated field was fertilized with pig and cow manure as well as ammonium sulphate nitrate fertilizer. No agricultural plastic was used for cultivation practices on the field and cultivated crops include wheat, barley, lucerne, triticale, white mustard, and corn. The farmland was regularly ploughed to 20 to 30 cm depth. Barley was sowed two weeks prior to our sampling and at sampling seedlings had reached a height of around 5 to 10 cm. To

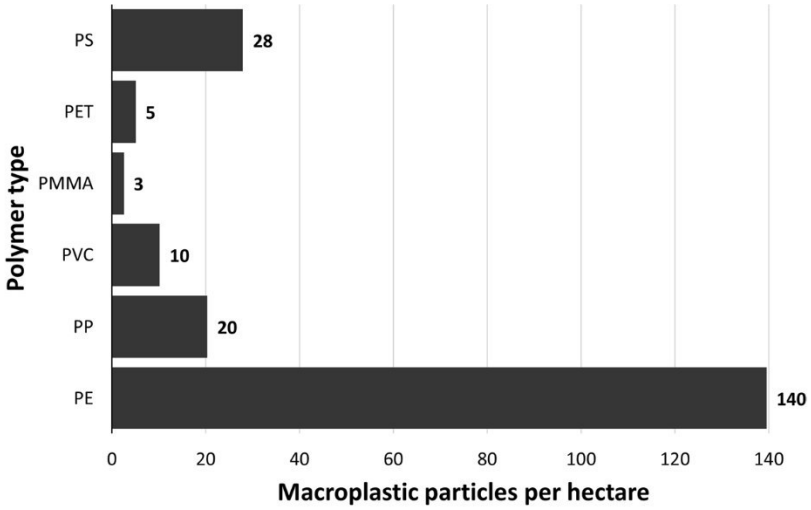

Figure 2. Abundance of polymer types within the detected macroplastic particles on the investigated agricultural farmland. Particles are separated by polymer type on the y-axis and show particle numbers per hectare at the end of each bar. Polymer types are sorted by polymer application amounts for European agriculture (no data for PET and PS)[28], which decrease from bottom to the top of the y-axis. PE, polyethylene; PP, polypropylene; PVC, polyvinyl chloride; PMMA, polymethyl methacrylate; PET, polyethylene terephthalate; PS, polystyrene.

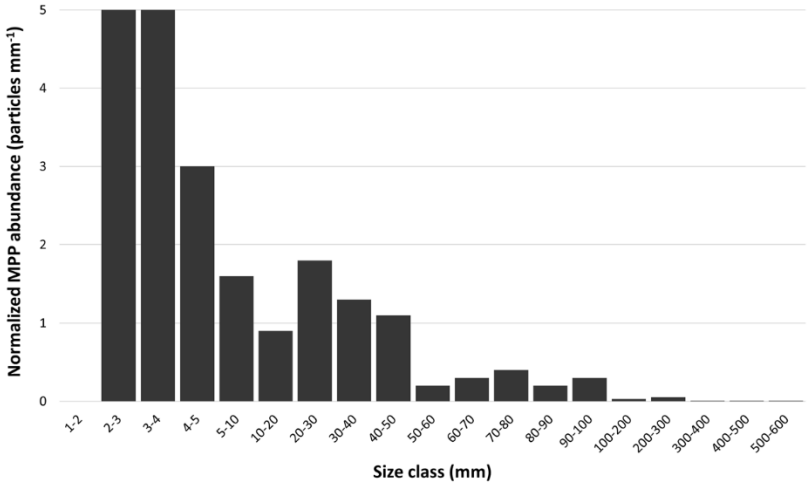

Figure 3. Size distribution of plastic debris detected on the investigated agricultural farmland. Normalized particle abundances (particle abundance of a size class divided by the width of that size class in millimetre) are shown on the y-axis and size classes in millimetre on the x-axis. Particle length was used to sort particles into size classes.

exclude an influence from the surroundings, a margin of 4.5 m was left out along three sides adjacent to a field road during sampling, according to the guidelines for sampling of arable soil[22], thus a total area of 0.4 ha was analysed. Macroplastic debris was collected from the soil surface, whereas for microplastics (1 to 5 mm), 14 samples were taken from the top 5 cm of soil within 32 × 32 cm quadrates, resulting in a sample volume of approximately 5 litres per sample (see Methods).

Macroplastic contamination. Using attenuated total reflection (ATR)-Fourier transform infrared (FTIR) spectroscopy we identified 81 macroplastic pieces collected within the investigated area which extrapolates to 206 particles per hectare. In total, six different plastic polymers were identified. The most common polymer type found was polyethylene (PE) with 67.90% (55 particles) of all macroplastic pieces, followed by polystyrene (PS; 13.58%, 11 particles) and polypropylene (PP; 9.88%, 8 particles). Pieces of polyvinyl chloride (PVC; 4.94%, 4 particles), polyethylene terephthalate (PET; 2.47%, 2 particles), and polymethyl methacrylate (PMMA; 1.24%, 1 particle) were also found (Fig. 2). Size distribution analysis revealed that over two-thirds (72.84%) of all macroplastic pieces were in the size range of 5 to 50 mm and only three pieces >300 mm were found (Fig. 3). The calculated total surface area of the found macroplastic pieces corresponds to approximately 0.18 m^2. The

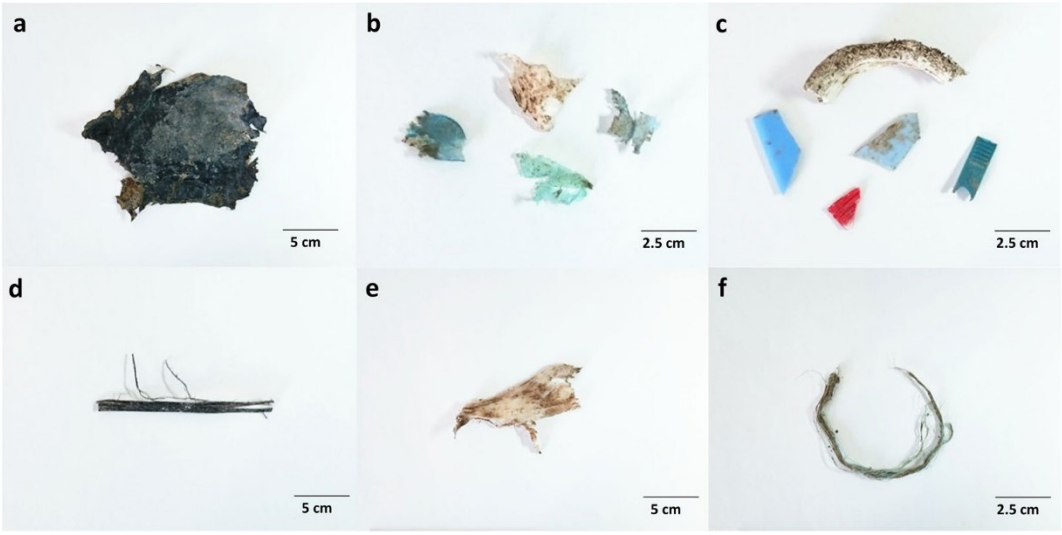

Figure 4. Exemplary pictures of macroplastic debris detected on the investigated agricultural farmland. Particles were grouped into three different shape categories: films (**a**,**b**), fragments (**c**), and others (**d**–**f**).

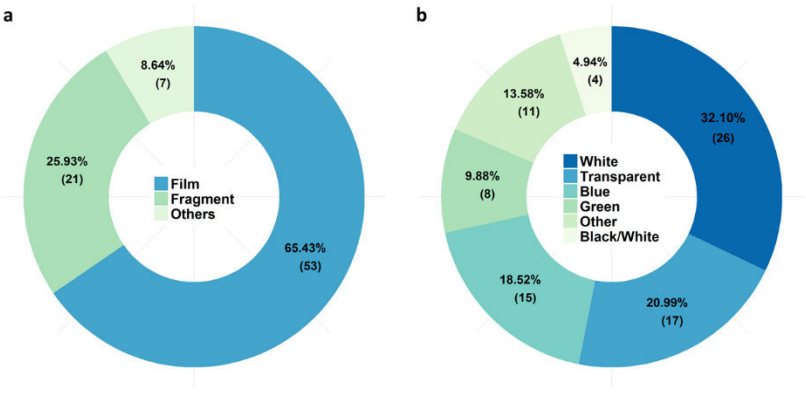

Figure 5. Relative proportions of shape (**a**) and colour (**b**) of macroplastic particles found on the investigated agricultural farmland with absolute numbers in brackets. Black/White refers to bicoloured films, featuring a black and a white side.

measured total weight added up to 26.25 grams. As for the number of particles, PE is also predominant in terms of mass with 16.39 grams (62.43%), followed by PS (15.80%, 4.15 grams), PP (8.57%, 2.25 grams), PVC (7.99%, 2.10 grams), PET (3.88%, 1.02 grams), and PMMA (1.34%, 0.35 grams). Most of the found plastic debris were in the shape of films (65.43%), which together with fragments (25.93%) comprised 91.36% of all found macroplastic pieces (Figs 4 and 5A). Other shapes like rope, strapping tape, and fabric rests were grouped together in the category "others" with a 8.64% contribution. The found colours were more diverse, with white (32.10%), transparent (20.99%), and blue (18.52%) being the most common ones (Figs 4 and 5B), followed by green and bicoloured particles which often featured a black and a white side.

Microplastic contamination. In total, 16 MPPs (5 to 1 mm) were identified via ATR-FTIR spectroscopy in ~50 kg dry weight (DW) of the sampled soil. Particle abundances in samples ranged from 0 to 1.25 MPPs per kilogram DW with a mean abundance of 0.34 ± 0.36 MPPs per kilogram DW (Table 1). Using the typical bulk densities for clayey soils (between 0.93 and 1.72 g cm^{-3} [23]) and considering the sampled upper 5 cm of soil we can transform the average abundance of MPPs per weight (0.34 MPPs per kilogram DW) to the average abundance of MPPs per area. Thus, we can estimate that the soil contains between 158,100 and 292,400 MPPs per hectare. This must be seen as a rough extrapolation, considering the high standard deviation of the average abundance of MPPs.

Polyethylene was the polymer type most often found (62.50%, 10 particles), followed by PP (25.00%, 4 particles), and PS (12.50%, 2 particles) (Table 1). The total weight of the found MPPs added up to 0.005 grams. With 43.75% each, fragments and films were the most common shapes of MPPs (Fig. 6A). Only two polymer fibres (12.50%) were identified within the samples (Fig. 6A). The majority of MPPs were white (62.50%). Only a few MPPs with a transparent, blue, or green colour were found (Fig. 6B). According to size measurements, no particles below 2 mm length were found within the samples (Fig. 3). Two fibres and one particle slightly longer than

Sample ID	Polymer type			MPPs per sample	Weight of sample in kilogram	MPPs per kilogram
	PE	PP	PS			
Plot 01	0	0	0	0	3.7991	0
Plot 02	1	3	0	4	3.2099	1.2461
Plot 03	1	0	1	2	3.4249	0.5840
Plot 04	1	1	0	2	3.5579	0.5621
Plot 05	1	0	0	1	2.9504	0.3389
Plot 06	0	0	0	0	3.3204	0
Plot 07	1	0	0	1	3.2635	0.3064
Plot 08	1	0	0	1	3.2539	0.3073
Plot 09	2	0	0	2	3.6726	0.5446
Plot 10	2	0	0	2	2.9978	0.6672
Plot 11	0	0	1	1	4.3150	0.2317
Plot 12	0	0	0	0	4.7340	0
Plot 13	0	0	0	0	3.4402	0
Plot 14	0	0	0	0	3.4414	0
Mean	0.7143	0.2857	0.1429	1.1429	3.5272	0.3420
SD	0.7263	0.8254	0.3631	1.1673	0.4883	0.3585

Table 1. Microplastic particle (MPP) abundances in absolute numbers of polymer type found within the samples and total MPP abundances per sample and per kilogram dry weight. PE, polyethylene; PP, polypropylene; PS, polystyrene.

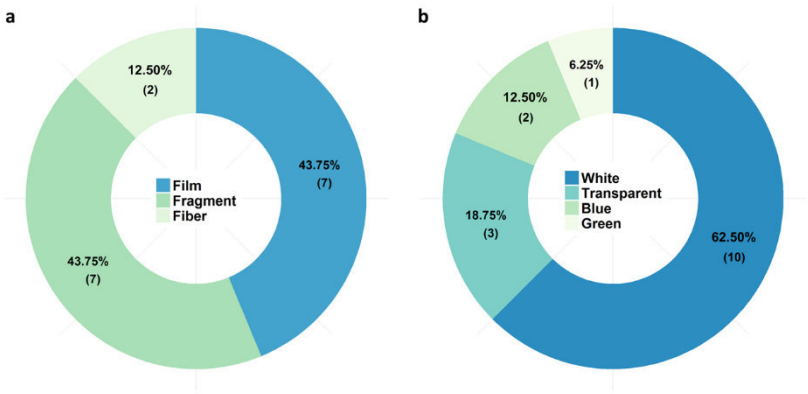

Figure 6. Relative proportions of shape (**a**) and colour (**b**) of microplastic particles found on the investigated agricultural farmland with absolute numbers in brackets.

5 mm were included in the microplastic fraction as they passed the mesh size of 5 mm. No plastic particles were detected in the negative control.

Discussion

Macroplastic contamination. In our study we found a concentration of 206 macroplastic pieces per hectare. Although, the site was screened by two independent observers for macroplastic debris, we cannot completely rule out that some macroplastic pieces, especially when covered with soil, were overlooked. Thus, our reported number is rather conservative. To our best knowledge, there are only a few quantitative studies on macroplastic debris in terrestrial ecosystems and no full quantitative study for agroecosystems. This lack of data limits the possibilities to interpret and compare the results of the present study. Zylstra[24] examined an area within the Sonoran Desert National Park, southern Arizona, which is relatively unaffected by human littering but still found macroplastic densities ranging between 0.056 and 0.627 pieces per hectare. However, they only focused on plastic bags and balloons. In contrast, Basnet[25] selected a hotspot within the Sagarmatha (Mt. Everest) National Park and counted solid waste on tourist trekking trails as well as camp disposal sites. They detected 0 to 1,769,870 macroplastic pieces per hectare with a mean value of 141,190.56 ± 372,651.96 pieces per hectare. A similar order of magnitude for plastic debris was found by Huerta Lwanga *et al.*[26]. They focused on house waste disposal sites (50 × 50 m) within home gardens in a rural environment in Mexico and quantified 744,000 ± 204,000 PE bottles and 74,000 ± 65,000 plastic pieces per hectare. Our results lie between those reported numbers and reflects contamination in a region with intensive agricultural land use and proximity to rural communities. Besides, investigations of arable lands with long-term plastic film mulch covers revealed soil residual plastic mulch levels from 50 to 260 kilograms per hectare[27], primarily composed of PVC. The calculated weight of the found macroplastic

debris within our study amounts only to 0.066 kilogram per hectare and is composed of more diverse polymer types. This indicates, that plastic contamination is to a considerable degree higher on farmland where plastic materials are applied on a regular basis, compared to farmland where no agricultural plastic is used for cultivation practices.

Besides PET the identified polymer types are among the most commonly used polymers in agriculture, such as PE, followed by PP, PVC, ethylene vinyl acetate (EVA), PMMA, and polycarbonate (PC)[28]. Nevertheless, only few particles can be linked to agricultural origin, such as bicoloured fragments of black and white (4.94%), which may originate from so called white-on-black mulches or silage films that are frequently used in agriculture[29]. Even less common were distinct particles like an ear tag from livestock or an animal feed packaging fragment. It is possible that the applied pig and cow manure contained plastic debris, as plastic materials are omnipresent at farms, and unintentional breakdown of materials and spreading may introduce plastic debris into farmyard manures. Furthermore, plastic debris unintentionally attached to agricultural equipment (i.e. tractors), as for example white-on-black films, may be transferred to the agricultural soils. As all neighbouring farmlands are owned by the same person, receiving the same agricultural treatments, transfer of plastic debris from those farmlands is probably a minor route. In addition, careless disposal and displacement of plastic by wind were supposed to be the major routes for input to the national park in the Sonoran Desert[24] and are further possible pathways relevant for this study.

Microplastic contamination. The found mean abundance of 0.34 ± 0.36 MPPs per kilogram DW is a conservative measurement as we cannot completely rule out that microplastic particles could have been overlooked during visually pre-sorting for subsequent ATR analysis. Nevertheless, visual pre-sorting has been suggested for larger particles[30,31] and is commonly applied[32]. It further needs to be considered that the found numbers represent only a part of the whole microplastic contamination due to the applied lower size limit of 1 mm.

The presence of microplastics in agricultural soils was already suggested by a study that investigated the potential to use synthetic fibres as an indicator of sewage sludge application[33]. The study considered all fibres as synthetic if displaying certain characteristics under a polarized light microscope but did not identify the chemical nature of these fibres. However, pure visual identification of synthetic materials is often error-prone since particles of natural origin can have the same appearance as synthetic fragments[6,8]. Hence, the present study used FTIR spectroscopy to quantify the presence of plastic particles in soils. Fibres accounted only for 12.50% of the microplastics within this study, indicating that all shapes of microplastics have to be considered if analysing the microplastic contamination on farmlands. The low amount of fibres could be related to the fact that on the studied site no sewage sludge was deployed as fertilizer. A more recent study investigated two different soil horizons but only PE and PP were considered[34]. Both polymer types were identified based on an observation of the melting products before/after heating the samples at 130 °C for 3–5 seconds. As this is a new method which cannot address the chemical nature of the object under consideration, it still requires further validation and its efficiency needs to be determined. The study suggests that PE and PP particles down to <50 µm in size were present in an agricultural soil where plastic mulch was applied for at least 20 years. In the present study, plastic types were chemically identified and a wider variety of plastic materials have been found. The fact that plastic mulch was not used in the studied farmland shows the existence of other potential microplastic sources for agricultural fields.

Input via runoff from adjacent areas is unlikely at our study site, as the field is located on top of a hill. Additionally, the drainage systems surrounding the study site exhibit another barrier for input via runoff from adjacent areas. Atmospheric deposition of microplastics was shown in a study from Dris *et al.*[9], predominantly finding fibres in the size range of 200 to 600 µm in the atmospheric fallout of urban and sub-urban sites. Regarding particles, atmospheric suspension of quartz grains occurs at a particle size <70 µm[35]. Atmospheric transport of the investigated polymers >1 mm (densities of 0.9 to 1.4 g cm^{-3}) seems therefore rather unlikely, even if considering the higher density of quartz (2.65 g cm^{-3}). However, we cannot rule out that transport way completely. Regarding particle motion processes, only pushing or rolling over the surface (so called "surface creep") could be an aeolian process accounting for microplastic transport in the investigated size class.

Another apparent source for the found MPPs in this study could be the onsite degradation of macroplastic debris on the field. This assumption is supported by our results: PE films were most often identified for macroplastics (56.10%, 46 particles) and concordantly most of the identified microplastics were PE films (43.75%, 7 particles) and fragments (18.75%, 3 particles). Moreover, this is reflected by the identified colours: 65.22% of the macroplastic PE films where transparent (17 particles) or white (13 particles); in accordance 50.00% of the microplastic PE films and fragments were transparent (3 particles) or white (5 particles). For example, ploughing could entrap macroplastic debris at the soil surface, thereby increasing its residence time on the field. Partly trapped macroplastics at the soil surface are directly exposed to UV light, initiating photo-degradation which is recognized as a major process for decomposition of polymer materials[36,37]. If already brittle, further mechanical disintegration, caused by application of shearing forces, can occur through several mechanisms like freeze-thaw-cycles, pressure due to burial under soil or snow, or damage caused by interactions with organisms[38,39]. Further, shearing forces on plastic debris in agricultural soils could act when the farmland is ploughed and other tillage work is done. If macroplastics are present on the agricultural farmland, all the processes described above will lead to a constant production of new microplastics through fragmentation.

Rough estimations of plastic debris abundances within the upper 5 cm of soil further suggest that MPPs (1 to 5 mm – 158,100 to 292,400 particles per hectare) are several orders of magnitude more abundant than macroplastics (>5 mm – 276 to 510 pieces per hectare if similar approximations are made for the upper 5 cm, backed up by observations that several pieces were partly buried within the soil). If transferring the particle numbers to mass, macroplastics were more abundant with 0.066 kilogram per hectare, compared to 0.035 kilogram microplastics per hectare, considering only the sampled surface area for microplastics. Moreover, the size distribution of the found plastic debris is left-skewed (increasing abundances with decreasing size, see Fig. 3), which can be

explained by progressive fragmentation of larger pieces into more and smaller pieces[40]. Understanding of particle size distribution of MPPs is still limited due to a lack of comparable data. It is assumed that particle abundance is increasing logarithmically with decreasing particle size as already observed for natural particles[32].

Further studies are necessary to understand transportation processes of plastic debris on soil surfaces and within soils to determine the fate and possible sinks for plastic debris. Microplastics present at the soil surface presumably are transported by wind or are transferred into surface waters by run off after rain events[17]. Only two studies have demonstrated that microplastics could be transported along the soil profile by earthworms and via preferential flow paths[41,42]. Soil structure of agroecosystems is very dynamic in the ploughed horizon and macroporosity, necessary for preferential flow, is regularly destroyed by tillage. However, the lower soil below the tillage pan could still be hydraulically connected to the upper soil, in particular in clayey soils that tend to shrink when drying[43]. Thus, at sites with a shallow groundwater and soils with a shrink-swell potential, for example, a downward transport of microplastics to the groundwater could be possible.

Conclusions

The ubiquitous contamination of the environment with microplastics has recently attracted a great deal of public and scientific attention. Surprisingly, only little is known for terrestrial ecosystems although it is a crucial missing link in the global understanding of plastic distribution in the environment. This study presents first quantitative and qualitative data of plastic contamination in an agricultural soil which only receives conventional agricultural treatment. It therefore provides important data on microplastic contamination for agricultural areas where microplastic-containing fertilizers and agricultural plastic applications are not used. However, our results are probably at the lower end of possible contamination levels in agricultural farmlands, as much higher levels can be expected in areas where plastic application is common[44]. Since agricultural land covers more than one third of the global land area[45], this issue should be treated with the same global importance as marine and freshwater ecosystems. Whether the presence of plastic debris in agricultural soils has implications for economy and environmental health is already under discussion. For instance, studies on residual plastic mulch levels within agricultural soils report negative effects on crop emergence, root growth, and salinization[27]. Further effects on moisture and nutrient transport in soils are hypothesized[27]. Hence, further research on agroecosystems and other terrestrial ecosystems will shed light on the significance of this contamination on land and pave the way to rethink the current paradigm that the oceans are the only sink for plastic debris.

Methods

Macroplastic sampling. The field survey was conducted on 13th October 2015. To account for potential influences from the adjacent field roads (through farm tractors or pedestrians), we split the study site into two areas: margin and centre area (Fig. 1). A minimum distance of 4.5 m from the edge of the field was chosen to account for any influences of the surroundings. Macroplastic debris (all visible particles >0.5 cm) was collected by two persons as follows: the total area was divided into 13 transects with a distance of one arm length (approximately 80 cm) in between. Each transect was walked by one observer, whereas the distance between transects allowed observation of the whole area by both observers. All potential plastic fragments were collected from the soil surface (pieces per hectare) and transferred into freezer bags for further analysis in the laboratory. Macroplastic particles were then photographed (Canon Digital Ixus 50), measured, and analysed via ATR-FTIR (attenuated total reflectance – Fourier transform infrared) spectroscopy as described below.

Microplastic sampling. Microplastic sampling was performed on the same day as the macroplastic sampling and according to the protocol developed by the MSFD Technical Subgroup on Marine Litter with some adaptations[46]. We took 14 evenly distributed samples aligned in two transects within the centre area of the farmland (Fig. 1). Each sample was taken from a 32 × 32 cm quadrate made of stainless steel and the upper 5 cm of soil extracted. Thus, at each sampling plot around five litres of soil were transferred into PE barrels using metal spatula. To account for possible contamination by the PE barrels, we prepared one negative control by adding de-ionized water to the barrel and treated it like all other samples.

To normalize microplastic abundance to kilogram soil, the dry weight of each sample was first determined. To do so, the wet weight of a subsample (100 to 200 g) from each sample was determined on a laboratory scale (Sartorius 1219 MP), followed by drying (at 60 °C) until a stable weight was reached. Afterwards each subsample was analysed for microplastics as described below.

Microplastic sample purification. A challenge in any microplastic study is to overcome the problem of very heterogenous sample matrices which interfere with the MPP detection. Considering both, the highly labour-intensive analysis of particles <1 mm and the large area of the investigated site we decided on taking large sample volumes and thus to focus on particles >1 mm. As we concentrated on MPPs with a size range of 1 to 5 mm, we first conducted a volume reducing step where all material smaller than one millimetre was discarded.

A simple wet-sieving of the clayey soil was not possible, as soil aggregates could not be destroyed despite soaking samples over several days with de-ionized water. Therefore, samples were transferred into glass beakers and soil aggregates were dissolved as follows: 500 ml of sample was covered with de-ionized water and 20 ml of hydrogen peroxide was added. After the reaction (formation of bubbles, gasification) stopped, size fractioning was done with two combined sieves with a mesh size of five and one millimetre respectively. Those steps were repeated until all soil aggregates were dissolved (maximum of three times). The residual potential MPPs on the sieves were optically sorted under a magnifying lamp, further viewed under a stereomicroscope (Leica M50), photographed (Olympus, DP 26), and stored in Eppendorf tubes for subsequent ATR-FTIR analysis.

Analysis. For identification and quantification, all potential plastic particles were analysed with a Tensor 27 FTIR spectrometer (Bruker Optik GmbH) further equipped with a Platinum-ATR-unit (Bruker Optik GmbH).

For the measurement of each particle, 16 background scans were pooled, followed by 16 sample scans with a spectral resolution of 8 cm^{-1} in a wavenumber range from 4000 cm^{-1} to 400 cm^{-1}. Obtained spectra were analysed with the software OPUS 7.5 (Bruker Optik GmbH) through comparison with polymer reference spectra from a custom-made database containing the most common polymers as well as natural materials[47]. Besides polymer type, colour and shape of each particle were recorded. Measurements of macroplastic area and length measurements for micro- and macroplastic were conducted with the image processing program ImageJ (version 1.51j8). If macroplastic pieces exhibited holes, those areas were subtracted from the total area. As the width of the size classes for particle size distribution analyses were not uniform, the particle numbers were normalized by dividing the total particle numbers of each size class by the width of the size class (in mm). Finally, to obtain the dry weight of the particles, each particle was carefully cleaned under de-ionized water and dried (at 40 °C) until stable weight, which was obtained with a precision scales (Ohaus Explorer EX225D/AD ± 0.1 mg).

Contamination prevention. Between all steps, the equipment was rinsed with filtered de-ionized water and 35% ethanol (0.2 μm membrane filter, Whatman). During work laboratory coats made of cotton were worn and all samples not in use were covered with either aluminium foil or glass ware. During field sampling, we first took the microplastic samples to avoid influences of our own presence on the field, regarding microplastic contamination. One negative control was initiated during sampling and underwent all laboratory procedures.

Data Availability

All data needed to evaluate the conclusions in the paper are present in the paper. Additional data related to this paper may be requested from the authors.

References

1. Rochman, C. M. Microplastics research—from sink to source. *Science.* **360**, 28–29 (2018).
2. Fotopoulou, K. N. & Karapanagioti, H. K. Degradation of Various Plastics in the Environment, 1st edt. [Barceló, D., Kostianoy, A. G. (ed.)] *The Handbook of Environmental Chemistry* 41–53 (Springer, 2017).
3. Galloway, T. S., Cole, M. & Lewis, C. Interactions of microplastic debris throughout the marine ecosystem. *Nat. Ecol. Evol.* **1**, 0116 (2017).
4. Koelmans, A. A. *et al.* Risks of Plastic Debris: Unravelling Fact, Opinion, Perception, and Belief. *Environ. Sci. Technol.* **51**, 11513–11519 (2017).
5. Thompson, R. C. Lost at Sea: Where Is All the Plastic? *Science.* **304**, 838–838 (2004).
6. Wagner, M. *et al.* Microplastics in freshwater ecosystems: what we know and what we need to know. *Environ. Sci. Eur.* **26**, 12 (2014).
7. Lebreton, L. C. M. *et al.* River plastic emissions to the world's oceans. *Nat. Commun.* **8**, 15611 (2017).
8. Horton, A. A., Walton, A., Spurgeon, D. J., Lahive, E. & Svendsen, C. Microplastics in freshwater and terrestrial environments: Evaluating the current understanding to identify the knowledge gaps and future research priorities. *Sci. Total Environ.* **586**, 127–141 (2017).
9. Dris, R., Gasperi, J., Saad, M., Mirande, C. & Tassin, B. Synthetic fibers in atmospheric fallout: A source of microplastics in the environment? *Mar. Pollut. Bull.* **104**, 290–293 (2016).
10. Dehghani, S., Moore, F. & Akhbarizadeh, R. Microplastic pollution in deposited urban dust, Tehran metropolis, Iran. *Environ. Sci. Pollut. Res.* **24**, 20360–20371 (2017).
11. Zalasiewicz, J. *et al.* The geological cycle of plastics and their use as a stratigraphic indicator of the Anthropocene. *Anthropocene* **13**, 4–17 (2016).
12. de Souza Machado, A. A., Kloas, W., Zarfl, C., Hempel, S. & Rillig, M. C. Microplastics as an emerging threat to terrestrial ecosystems. *Glob. Chang. Biol.* **24**, 1405–1416 (2018).
13. Bläsing, M. & Amelung, W. Plastics in soil: Analytical methods and possible sources. *Sci. Total Environ.* **612**, 422–435 (2018).
14. Hurley, R. R. & Nizzetto, L. Fate and occurrence of micro(nano)plastics in soils: Knowledge gaps and possible risks. *Curr. Opin. Environ. Sci. Heal.* **1**, 6–11 (2018).
15. World Economic Forum, Ellen MacArthur Foundation and McKinsey & Company, The New Plastics Economy — Rethinking the future of plastics (2016, http://www.ellenmacarthurfoundation.org/publications).
16. Dris, R. *et al.* A first overview of textile fibers, including microplastics, in indoor and outdoor environments. *Environ. Pollut.* **221**, 453–458 (2017).
17. Nizzetto, L., Bussi, G., Futter, M. N., Butterfield, D. & Whitehead, P. G. A theoretical assessment of microplastic transport in river catchments and their retention by soils and river sediments. *Environ. Sci. Process. Impacts* **18**, 1050–1059 (2016).
18. Nizzetto, L., Futter, M. & Langaas, S. Are Agricultural Soils Dumps for Microplastics of Urban Origin? *Environ. Sci. Technol.* **50**, 10777–10779 (2016).
19. Weithmann, N. *et al.* Organic fertilizer as a vehicle for the entry of microplastic into the environment. *Sci. Adv.* **4**, eaap8060, https://doi.org/10.1126/sciadv.aap8060 (2018).
20. EUROSTAT, European Commission, http://ec.europa.eu/eurostat/statistics-explained/index.php?title=Agriculture_and_environment_-_pollution_risks, accessed on 2018-07-31, (2018).
21. Bavarian Environment Agency, https://www.lfu.bayern.de/boden/boden_daten/uebk25/index.htm, accessed on 2018-04-01, (2018).
22. ÖNORM L 1055, Austrian Standards International, *Sampling of arable soil* 7 pp (2004).
23. Blume, H.-P. *et al.* Physical Properties and Processes [Blume, H.-P. *et al.* (ed.)] *Scheffer/Schachtschabel Soil Science* 175–283 (Springer Berlin Heidelberg, 2016).
24. Zylstra, E. R. Accumulation of wind-dispersed trash in desert environments. *J. Arid Environ.* **89**, 13–15 (2013).
25. Basnet, K. Solid Waste Pollution Versus Sustainable Development in High Mountain Environment: A Case Study of Sagarmatha National Park of Khumbu Region, Nepal. *Contrib. Nepalese Stud* **20**, 131–139 (1993).
26. Huerta Lwanga, E. *et al.* Field evidence for transfer of plastic debris along a terrestrial food chain. *Sci. Rep.* **7**, 14071 (2017).
27. Liu, E. K., He, W. Q. & Yan, C. R. 'White revolution' to 'white pollution'—agricultural plastic film mulch in China. *Environ. Res. Lett.* **9**, 091001 (2014).
28. Scarascia-Mugnozza, G., Sica, C. & Russo, G. Plastic materials in European agriculture: actual use and perspectives. *J. Agric. Eng.* **42**, 15 (2012).
29. Steinmetz, Z. *et al.* Plastic mulching in agriculture. Trading short-term agronomic benefits for long-term soil degradation? *Sci. Total Environ.* **550**, 690–705 (2016).
30. Löder, G. J. M. & Gerdts, G. Methodology Used for the Detection and Identification of Microplastics—A Critical Appraisal [Bergmann, M., Gutow, L., Klages, M. (ed.)] Marine Anthropogenic Litter 201–227 (Springer, 2015).
31. Hidalgo-Ruz, V., Gutow, L., Thompson, R. C. & Thiel, M. Microplastics in the Marine Environment: A Review of the Methods Used for Identification and Quantification. *Environ. Sci. Technol.* **46**, 3060–3075 (2012).

32. Filella, M. Questions of size and numbers in environmental research on microplastics: methodological and conceptual aspects. *Environ. Chem.* **12**, 527 (2015).
33. Zubris, K. A. V. & Richards, B. K. Synthetic fibers as an indicator of land application of sludge. *Environ. Pollut.* **138**, 201–211 (2005).
34. Zhang, S. *et al.* A simple method for the extraction and identification of light density microplastics from soil. *Sci. Total Environ.* (2017).
35. Nickling, W. G. & McKenna Neuman, C. Aeolian Sediment Transport [Parsons, A. J. & Abrahams, A. D. (ed.)] *Geomorphology of Desert Environments* 517–555 (Springer Netherlands, 2009).
36. Williams, A. T. & Simmons, S. L. The degradation of plastic litter in rivers: Implications for beaches. *J. Coast. Conserv.* **2**, 63–72 (1996).
37. Singh, B. & Sharma, N. Mechanistic implications of plastic degradation. *Polym. Degrad. Stab.* **93**, 561–584 (2008).
38. Rillig, M. C. Microplastic in Terrestrial Ecosystems and the Soil? *Environ. Sci. Technol.* **46**, 6453–6454 (2012).
39. Lambert, S., Sinclair, C. & Boxall, A. Occurrence, Degradation, and Effect of Polymer-Based Materials in the Environment [Whitacre, D. M. (ed.)] *Reviews of Environmental Contamination and Toxicology* **227**, 1–53 (Springer International Publishing, 2014).
40. Lee, J. *et al.* Relationships among the abundances of plastic debris in different size classes on beaches in South Korea. *Mar. Pollut. Bull.* **77**, 349–354 (2013).
41. Huerta Lwanga, E. *et al.* Incorporation of microplastics from litter into burrows of *Lumbricus terrestris*. *Environ. Pollut.* **220**, 523–531 (2017).
42. Rillig, M. C., Ziersch, L. & Hempel, S. Microplastic transport in soil by earthworms. *Sci. Rep.* **7**, 1362 (2017).
43. Bogner, C., Mirzaei, M., Ruy, S. & Huwe, B. Microtopography, water storage and flow patterns in a fine-textured soil under agricultural use. *Hydrol. Process.* **27**, 1797–1806 (2013).
44. Ng, E. L. *et al.* An overview of microplastic and nanoplastic pollution in agroecosystems. *Sci. Total Environ.* **627**, 1377–1388 (2018).
45. WORLDBANK. https://data.worldbank.org/indicator. World Development Indicators. (2015), accessed on 2018-07-31 (2018).
46. Galgani, F. *et al.* Guidance on Monitoring of Marine Litter in European Seas. *JRC Scientific and Policy Reports*, doi:10.2788/99475 (2014).
47. Löder, M. G. J., Kuczera, M., Mintenig, S., Lorenz, C. & Gerdts, G. Focal plane array detector-based micro-Fourier-transform infrared imaging for the analysis of microplastics in environmental samples. *Environ. Chem.* **12**, 563 (2015).

Acknowledgements

We thank two anonymous reviewers for their valuable comments on the manuscript. The authors further thank Lena Löschel for assistance with sample preparation and Jens Diller for conducting weight measurements of soil samples. For linguistic improvements we want to thank Elizabeth Catherine Atwood and Julia Naima Möller. The authors acknowledge that they received no funding in support of this research.

Author Contributions

A.L., S.P. and C.L. designed the study; A.L. and S.P. performed the experiments; S.P., R.D., M.L., C.B. and C.L. wrote the manuscript.

Additional Information

Competing Interests: The authors declare no competing interests.

Publisher's note: Springer Nature remains neutral with regard to jurisdictional claims in published maps and institutional affiliations.

Article A3: Occurrence of microplastics in the hyporheic zone of rivers

Frei S, Piehl S, Gilfedder BS, Löder MGJ, Krutzke J, Wilhelm L, Laforsch C

Scientific Reports 9

SCIENTIFIC REPORTS
nature research

Occurence of microplastics in the hyporheic zone of rivers

S. Frei[1*], S. Piehl[3], B. S. Gilfedder[2], M.G.J. Löder[3], J. Krutzke[1], L. Wilhelm[1] & C. Laforsch[3]

Although recent studies indicate that fluvial systems can be accumulation areas for microplastics (MPs), the common perception still treats rivers and streams primarily as pure transport vectors for MPs. In this study we investigate the occurrence of MPs in a yet unnoticed but essential compartment of fluvial ecosystems - the hyporheic zone (HZ). Larger MP particles (500–5,000 µm) were detected using attenuated total reflectance (ATR) - Fourier-transform infrared (FTIR) spectroscopy. Our analysis of MPs (500–5,000 µm) in five freeze cores extracted for the Roter Main River sediments (Germany) showed that MPs were detectable down to a depth of 0.6 m below the streambed in low abundances (≪1 particle per kg dry weight). Additionally, one core was analyzed as an example for smaller MPs (20–500 µm) with focal plane array (FPA)- based µFTIR spectroscopy. Highest MP abundances (~30,000 particles per kg dry weight) were measured for pore scale particles (20–50 µm). The detected high abundances indicate that the HZ can be a significant accumulation area for pore scale MPs (20–50 µm), a size fraction that yet is not considered in literature. As the HZ is known as an important habitat for invertebrates representing the base of riverine food webs, aquatic food webs can potentially be threatened by the presence of MPs in the HZ. Hyporheic exchange is discussed as a potential mechanism leading to a transfer of pore scale MPs from surface flow into streambed sediments and as a potential vector for small MPs to enter the local aquifer. MPs in the HZ therefore may be a potential risk for drinking water supplies, particularly during drinking water production via river bank filtration.

Rivers and streams represent a primary input vector for microplastics (MPs) into marine ecosystems[1,2]. In contrast to marine environments, still little is known about the fate and behavior of MPs in fluvial ecosystems[1]. Only recently MP research has begun to shift its focus from a marine-centric viewpoint towards freshwater and terrestrial systems. MP particles enter fluvial systems from e.g. waste water treatment plant (WWTP) effluents[3], sewer overflows during heavy rain events, agricultural runoff, aerial input/atmospheric fallout[4,5], road runoff or via fragmentation of plastic litter[6–8]. WWTPs alone are estimated to contribute up to 520,000 tons per year of MPs to rivers and streams in Europe[6].

The hyporheic zone (HZ) is an ecologically essential and sensitive compartment of fluvial ecosystems and is defined as the area below the streambed interface that is equally influenced by surface and groundwater flow dynamics[9]. The HZ is known as an important habitat for various invertebrates, being representative for the lower level of the riverine food web and as an important fish spawning area[10]. Although not investigated up to now, compared to MPs that are transported in the open channel flow, MPs located in the HZ should face a much longer retention and thus exposure time to benthic organisms. Although clear evidence is still missing, it is possible that MPs in the HZ are taken up by benthic organisms and are transferred to higher trophic levels in the food web. Thus, the HZ potentially functions as an additional entry point of MPs into riverine food webs. An uptake of MPs in freshwater organisms of different feeding guilds has already been demonstrated[11], however, data on the effects of MPs on freshwater species is scarce[12]. MPs are known to contain a multitude of chemical additives such as flame retardants or plasticizers that are often carcinogenic or hormone-active, exhibiting a high potential for leaching[13] and accumulation in higher trophic levels[12]. In addition, environmental contaminants of concern (e.g. heavy metals or pesticides) may adsorb to the surface of the particles[14–16] and can be transferred to the respective organisms after ingestion[17]. However, the environmental relevance of MPs as a vector for harmful substances is still discussed controversially in the scientific community[16,18]. Furthermore, pathogens or harmful microorganisms may be a component of the biofilm covering MP particles[19–21] especially after transit through WWTPs.

[1]Department of Hydrology, Bayreuth Center of Ecology and Environmental Research (BAYCEER), University of Bayreuth, Bayreuth, Germany. [2]Limnological Research Station, Bayreuth Center of Ecology and Environmental Research (BAYCEER), University of Bayreuth, Bayreuth, Germany. [3]Department of Animal Ecology I, Bayreuth Center of Ecology and Environmental Research (BAYCEER), University of Bayreuth, Bayreuth, Germany. *email: sven.frei@uni-bayreuth.de

River	Particle abundance (dry weight) [kg^{-1}]	Detected particle size [µm]	Reference
Rhine River (Germany)	228–3,763	63–5,000	Klein *et al.*[22]
Main River (Germany)	786–1,368	63–5,000	Klein *et al.*[22]
Lake Ontario tributaries (Canada)	average 760 max: 28,000	250–5,000	Ballent *et al.*[24]
River Thames (UK)	185–660	1,000–4,000	Horton *et al.*[23]
Beijiang River (China)	178–554	?-5,000	Wang *et al.*[25]
Mersey/Irwell River (UK)	300–75,000	63–5,000	Hurley *et al.*[43]

Table 1. Measured MP abundances in streambed sediments for different fluvial systems.

Until now only few studies have addressed the accumulation of MPs in streambed sediments (Table 1). For the Rhine/Main catchment Klein *et al.*[22] investigated MP contamination of stream sediments at the confluence between the Main and the Rhine Rivers. MP abundances ranged from 228–3,763 particles per kg dry weight (in the latter referred to as particles/kg) for the Rhine and 786–1,368 particles/kg for the Main River sediments. In the river Thames (UK) average particle abundances in the sediments ranged from 185–660[23] particles/kg, similar values (on average 760 particles/kg) were measured for lake Ontario tributaries[24] (Canada) and for the Bijiang River[25] (178–554 particles/kg) in China. With 75,000 particles/kg[26], very high MP abundances were measured at contamination hot spots in the Mersey/Irwell River catchment (UK). All these studies show that streambed sediments can contain a much higher contamination than river surface waters and that streambed sediments are significant accumulation areas for MPs in fluvial ecosystems[4].

In the studies listed in Table 1 MP particles <50 µm were not included, most likely due to the high effort necessary to detect this particle size fraction. Particles with an effective size of 50 µm and below can be classified as pore scale and sub-pore scale MPs. This upper limit roughly represents the maximum in the pore size distribution of a medium-grained sand[27]. Evidence for the presence of pore scale MPs in streambed sediments currently is missing in literature. Mainly because the extraction, purification and detection of this size fraction in natural sediments is extremely time and labor intensive and requires spectroscopic techniques for producing reliable data. Ingestion of MP particle sizes at the pore scale by organisms living in the HZ, may involve the potential biological risk of MPs translocation into organs[28–30] and tissues[26,28,31] leading to a risk for bioaccumulation, as shown for marine and freshwater food webs[32–35]. Thus data on MP contamination of the HZ are necessary to assess if it represents a potential environmental risk for benthic organisms as well as for freshwater food webs.

To contribute towards a better and improved understanding of the fate and behavior of MPs in fluvial ecosystems and to account for the missing data on pore scale MPs, we investigated the depth specific occurrence of MP particles in-between a size of 20–5,000 µm. We extracted five freeze cores from the Roter Main River sediments (southeast Germany), taken from a 5 m × 5 m riffle area located downstream of a WWTP (Fig. 1). To investigate the depth specific MP contamination of the HZ, the cores were sliced into different depth segments. After further sample preparation using sequential filtration the analysis of the larger MPs (500–5,000 µm) was performed with state-of-the-art ATR-FTIR spectroscopy. One core was analyzed as an example for smaller particles (20–500 µm) including pore scale MPs (20–50 µm) with µFTIR spectroscopy after enzymatic purification and extraction. Although we did not perform a detailed MP examination of the Roter Main River sediments over time, our results - for the first time – (1) show depth specific data on the occurrence of MPs in the HZ and (2) further provide first insights in the depth-specific distribution of MP polymer types and size fractions in streambed sediments and the HZ.

Results

MPs 500–5,000 µm. MP particles >500 µm were detected in four of the five extracted cores down to a maximum depth of 60 cm below the streambed interface. All five cores were extracted from a 5 × 5 m area of the riffle structure located close to the outlet of the nearby WWTP (Fig. 1). Extracted material for all five cores in general consisted of coarse sediments with a high fraction of sand, medium to fine gravels and cobbles (classification system after Buffington and Montgomery[36]). For core 1, 2, 4 and 5, no sediment material could be extracted for the deepest core segment (40–60 cm), due to the coarse material present there. All cores were analyzed for MPs > 500 µm by using ATR-FTIR spectroscopy. The verified particle number was normalized to the dry weight of the different segment samples (Fig. 2). Detected MP abundances for the five cores ranged from 0 to 2.2×10^{-3} particles/kg. We found no clear pattern in MP contamination as particles in the analyzed cores were non-uniformly distributed with respect to (1) depth specific abundances, (2) polymer compositions and (3) particle shapes (Fig. 2). For several depth segments of the cores no MP particles were found and core 2 was entirely free from MPs > 500 µm.

Based on the extrapolated depth specific abundances obtained from ATR-FTIR spectroscopy a mean value and standard deviation could be estimated (Fig. 2) for the different depth classes. As we only were able to extract one single replicate for the 40–60 cm segment from core 3, a corresponding mean and standard deviation for this segment could not be estimated. The low mean values for MP abundances, ranging from 0.5×10^{-4} to 4.4×10^{-4} particles/kg, in combination with the high standard deviations reflect the non-uniform MP accumulation in the five cores for particles >500 µm. Plastic polymers detected for MPs > 500 µm in the core segments were polyacrylonitrile (PAN, mean: 9.83×10^{-4} particles/kg), polystyrene (PS, mean: $1.81–7.43 \times 10^{-4}$ particles/kg), epoxide (EP, mean: 5.56×10^{-4} particles/kg), polytetrafluoroethylene (PTFE, mean: $1.08–2.18 \times 10^{-4}$ particles/kg), polypropylene (PP, mean: 1.85×10^{-4} particles/kg), polyurethane (PUR, mean $1.08–1.81 \times 10^{-4}$ particles/

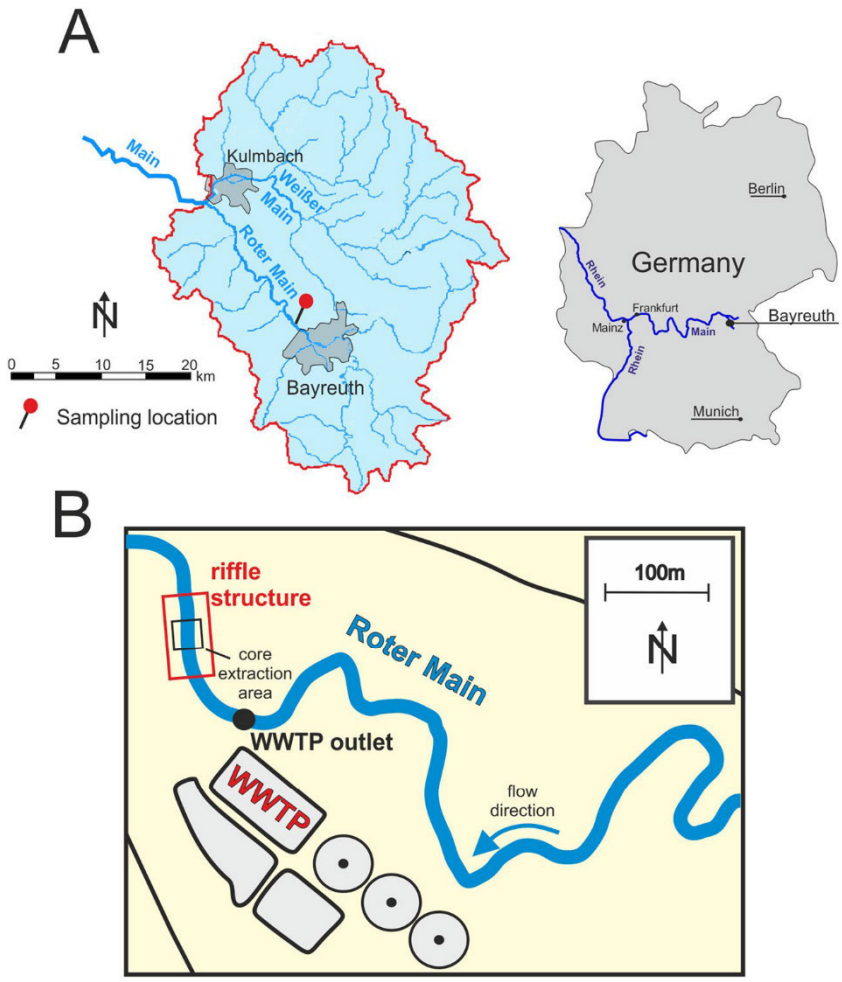

Figure 1. (**A**) Catchment of the Main River tributaries Roter Main River and Weißer Main River. (**B**) Location of the sampling site close to the WWTP north of Bayreuth. All five freeze cores were extracted within an area of 5 × 5 meters.

kg), terpolymer (mean: 1.08×10^{-4} particles/kg), and polyethylene (PE, mean: 0.93×10^{-4} particles/kg) (Fig. 2). Expect for PE and PP all detected polymers are non-buoyant. Most of the detected particles >500 µm were irregularly shaped fragments and to a lesser extent fibers (Fig. 2). Fibers made of PAN and PS were exclusively found in core 3 for the shallowest (0–10 cm) and deepest segment (40–60 cm), respectively.

Size fraction 20–500 µm. As an example for pore scale MPs, core 3 was analyzed for MPs in the range of 20–500 µm using FPA-based µFTIR spectroscopy. The depth specific distribution of MPs in this size range is shown in Figs 3 and 4. A classification of the extracted streambed materials for core 3 is provided in Fig. 3B, according to the classification system proposed by Buffington and Montgomery[36]. In general, MP accumulation decreased with increasing depth. Highest MP accumulation for particles in-between 20–500 µm was found for the upper 10 cm of the core (exceeding 50,000 particles/kg) while lowest particle abundance (~10,000 particles/kg) was detected for the 10–20 cm segment. High MP abundances, ranging from 4,500–30,000 particles/kg, were detected for pore scale MPs (20–50 µm) in the different core segments (Fig. 4A). With ~30,000 particles/kg pore scale MPs especially dominated the superficial core segment (0–10 cm) (Fig. 4A). The size class 100–500 µm displayed the highest abundance in the core segments 20–30 cm and 40–60 cm. In the analyzed core, with the exception of the 10–20 cm segment, there seems to be a tendency towards a lower accumulation of MPs with increasing depth.

The most abundant plastic polymers found in the size range of 20–500 µm particles were PP, polyvinyl chloride (PVC) and polyethylene terephthalate (PET). Non-buoyant polymer types represented a major fraction of detected particles and were found in every depth segment. An exceptionally high number of PP fibers (45%) was found in-between 20 and 30 cm below the streambed interface (Fig. 3C). With increasing particle size, the percentage of fibers increases from 0% for the 20–50 µm class to 3% for the 50–100 µm class and 16% for the 100–500 µm class (Fig. 4B). Majority of the pore scale MPs (20–50 µm) detected for the upper 10 cm of the core were identified as PET particles (~15,000 particles/kg) (Fig. 4A). Other polymer types, beside PET, identified for pore scale MPs (20–50 µm) were PP, and to a lesser extent PVC, PS and PE. All detected pore scale particles were fragments (Fig. 4B). For MPs of the size fraction 50–100 µm and 100–500 µm, PVC and PP were the most

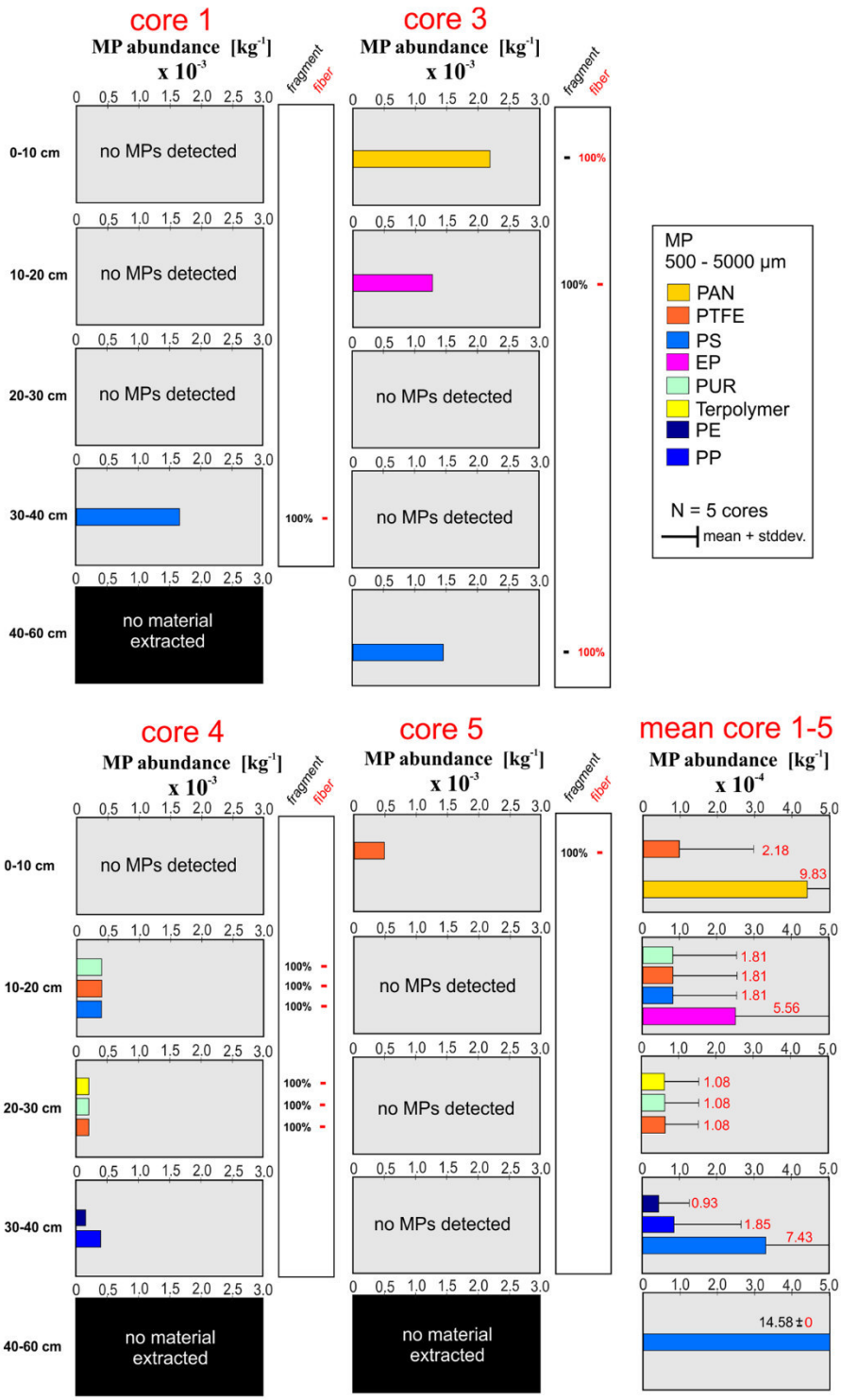

Figure 2. Depth specific distribution of MP particles 500–5,000 µm (per kg dry weight), extracted from the five freeze cores of the river Roter Main River (PAN = polyacrylonitrile, PTFE = polytetrafluoroethylene, PS = polystyrene, EP = epoxide, PUR = polyurethane, PE = polyethylene, PP = polypropylene). Corresponding dry weights of the sub-samples are presented in the Supplementary Material. The red numbers inside the bar plots represent the estimated standard deviation. Results for core 2 are not shown as no MPs (500–5,000 µm) were detected for this core.

abundant polymers that could be verified for almost every depth segment of the analyzed core. Additionally to MP particles <500 µm, some fibers/particles >500 µm were found in the samples, which were excluded as potential contamination and thus not considered further.

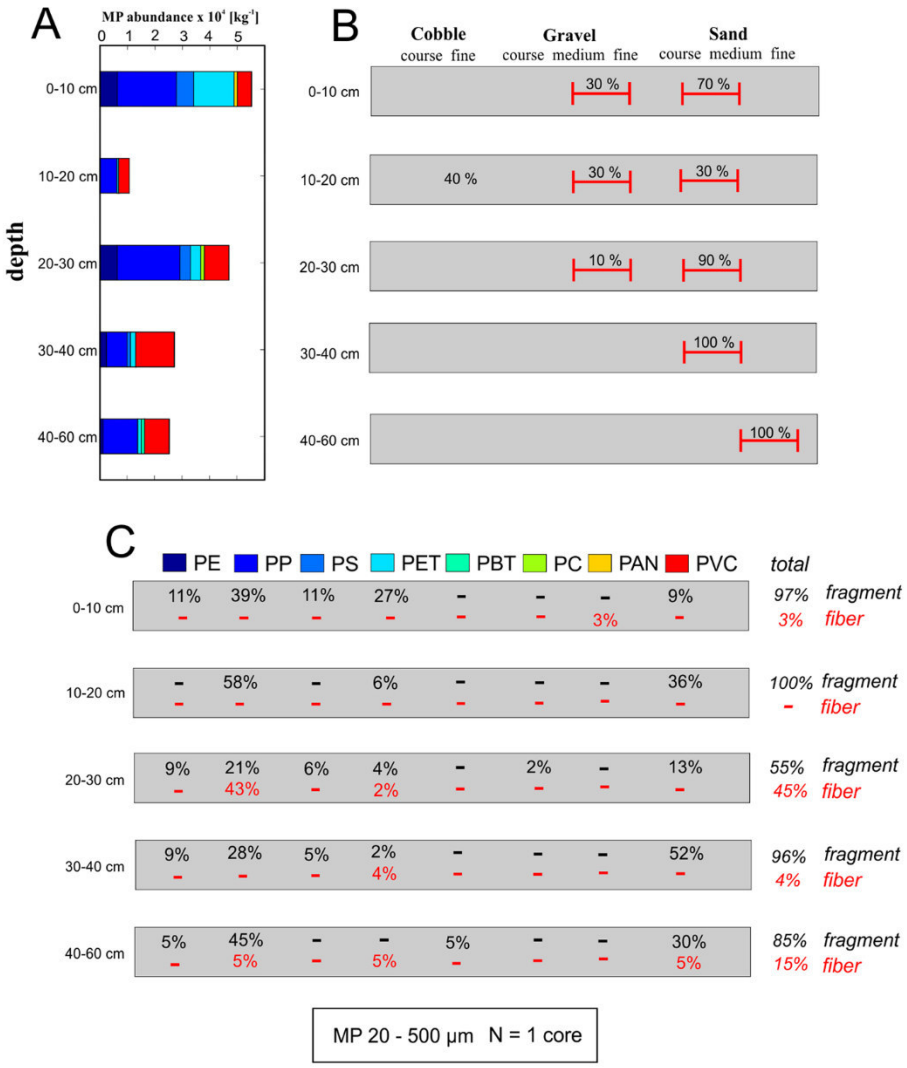

Figure 3. (**A**) Depth specific abundances (per kg dry weight) for MP particles (20–500 µm) in one sediment core of the Roter Main River. Corresponding dry weights of the sub-samples are presented in the Supplementary Material (for color code see C). (**B**) Textural properties of the sediments extracted with the freeze core technique, classification according to Buffington and Montgomery[36] for hyporheic sediments. (**C**) Depth specific material (PE = polyethylene, PP = polypropylene, PS = polystyrene, PET = polyethylene therephthalat, PBT = polybutylene terephthalate, PC = polycarbonate, PAN = polyacrylonitrile, PVC = polyvinyl chloride) and shape composition for the detected particles. Figures 3 and 4 present data analyzed from the same freeze core.

Discussion and Implications

In fluvial systems, MPs - similar to natural particles - are not uniformly transported. Mechanisms and timescales of transport depend on the hydrodynamic properties of the MP particles such as particle size, shape, density, surface roughness, and the hydrodynamic transport conditions in the open channel flow. Currently there is only a rudimentary understanding of the relevant mechanisms that control the transfer of MPs from surface flow into streambed sediments. Settling of suspended MPs due to the influence of gravity (sedimentation) seems to be the most obvious mechanism leading to a translocation of MPs from the stream into the HZ (Fig. 5). Sedimentation can also affect buoyant MPs after density modification processes occurring in aquatic environments leading to higher gross densities of the respective particles. Such density modification processes include aggregation with other MP particles, sediments or organic matter[37,38], photo-degradation and biofouling[39], ingestion and excretion of MPs in fecal pellets by organisms[37] (Fig. 5).

Small particles such as pore scale MPs are more affected by aggregation processes, as the surface to volume ratio and thus the associated surface reactivity is much higher compared to larger particles[40]. For buoyant synthetic polymers detected in the sediments of the Roter Main River (PE and PP) density modification processes can explain the high abundancies in the HZ. Although abundances for PP and PE particles <500 µm are highest for the upper 10 cm of the extracted core, both lightweight polymers were found in almost every depth segment. For the core analyzed for MPs < 500 µm, including pore scale particles (20–50 µm), buoyant polymers represent a major fraction (depth averaged fractions: 61% for 20–50 µm particles, 63% for 50–100 µm particles and 35% for

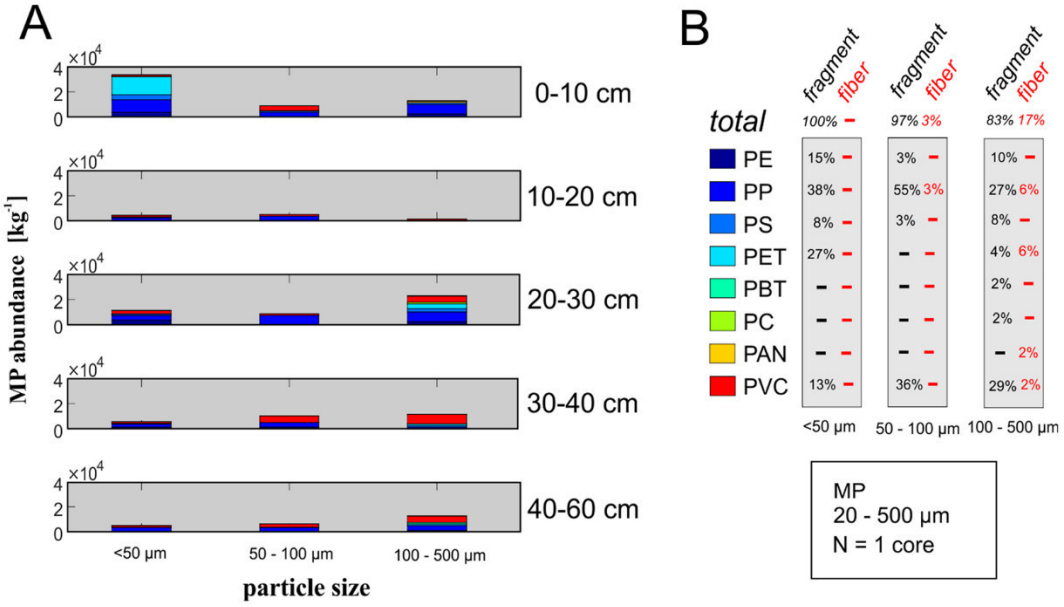

Figure 4. (**A**) MPs-abundances (per kg dry weight) for the different particle size fraction of the sediment core was analyzed down to 20 µm. Corresponding dry weights of the sub-samples are presented in the Supplementary Material. Particles below 50 µm are considered as pore scale and sub-pore scale MPs (for color code see **B**). (**B**) Material and shape composition for the different particle size fractions. Figures 3 and 4 present data obtained from the same freeze core. MP abundances were extrapolated to the dry weights of the samples. (PE = polyethylene, PP = polypropylene, PS = polystyrene, PET = polyethylene therephthalat, PBT = polybutylene terephthalate, PC = polycarbonate, PAN = polyacrylonitrile, PVC = polyvinyl chloride).

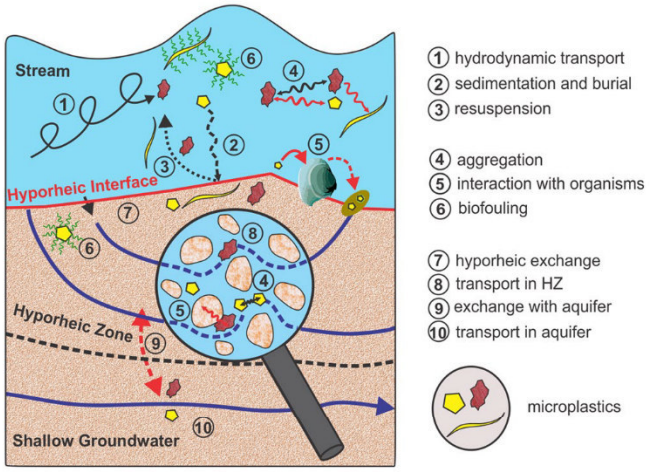

Figure 5. Potential processes that control the transport and redistribution of microplastic particles in fluvial systems.

100–500 µm particles) of the detected particles and additionally were found among larger MP particles >500 µm (depth averaged fractions: 20%).

In the sediments of the Roter Main River particles >500 µm were found in 4 of the 5 freeze cores and were non-uniformly distributed for the different depth segments. An advective transfer of particles, across the streambed interface due to hyporheic exchange (Fig. 5), can be excluded for MPs exceeding the average pore size of the streambed material (>50 µm). Beside interactions with organisms, sedimentation and burial seems to be the only plausible transfer mechanism for MP particles >50 µm that has led to an accumulation over time in the sediments of the Roter Main River. Hydrodynamic conditions, controlling the transport and sedimentation behavior of natural particles and MP particles alike, in rivers and streams are non-stationary and can vary spatially on very small scales such as a few centimeters[41]. Temporal and spatial variations in transport and sedimentation patterns along the streambed interface can explain the non-uniform distribution of MP particles >500 µm observed for the different cores. Even for the small sampling area (5 m × 5 m) for which the cores were extracted, conditions for sedimentation of MPs were non-uniform and affected by the dynamical variations of the streambed interface

and the hydrodynamic characteristics of open channel flow. As the depth specific sediment composition of the core segments indicate previous sedimentation conditions in the stream, the sporadic presence of MPs > 500 µm in the core likely also reflects these non-stationary sedimentation characteristics. Here the different polymer types (MPs > 500 µm) detected in the cores likely were affected differently in the past regarding their transport and accumulation behavior before the particles where immobilized in the HZ.

Once in the streambed sediments larger MPs are temporarily immobilized likely resulting in a higher exposure time to benthic organisms increasing the probability for uptake. Uptake and excretion of MPs by benthic organisms can reverse the extent of biofouling of MP particles by digesting biofilms in which case polymers like PP and PE may regain their buoyancy[42]. Re-mobilization of MP in streambed sediments can occur during high flow events where high flow conditions lead to streambed erosion (Fig. 5). Such high flow events can have a dramatic effect on MP contamination in streambed sediments, as has been shown recently for the Mersey and Irwell Rivers, where around 70% of the MP loads stored in the riverbed were flushed during a single high flow event[43]. For larger MPs > 500 µm it was reported that those particles were found within the cases of benthic organisms such as the caddisfly larva[44]. Binding of sediments with silk strands from the caddisfly can have a stabilizing effect on the surrounding sediments[45] providing a mechanism where MPs are retained in the sediments during high flow conditions[44].

Based on the results obtained for the single core analyzed as an example for MPs < 500 µm, extrapolated abundances increase considerably with decreasing particle size. Highest abundance was estimated for pore scale particles (~30,000 particles/kg) for the superficial segment of the analyzed core. Although clear evidence is still missing, the hypothesis that MP particles at the pore and sub-pore scale can be transferred advectivley via hyporheic exchange (Fig. 5) into the streambed sediments is suggested. For the streambed of the Roter Main River we hypothesize that the accumulation of MPs is controlled by a combination of (1) sedimentation and (2) advective transfer of pore scale particles across the streambed interface. In this context, the observed depth specific accumulation of MPs, where both pore scale and larger particles are equally detectable in high numbers, can be interpreted as the result of both accumulation mechanisms. Hyporheic exchange of water between the stream and the HZ -and likely also of pore scale MPs- is controlled by site specific characteristics such as the morphological shape of the streambed[9], the influence of local groundwater[46,47], material heterogeneities in the HZ[48] and the turbulent conditions in the stream[47]. Pore scale MPs can further decay into nano-sized particles[49], and for these particles an advective transfer across the hyporheic interface is even more likely. For pore scale MP particles capable of entering the pore system of the HZ, hyporheic exchange represents an additional transfer mechanism that has not yet been recognized.

As part of this study we only analyzed five different freeze cores to investigate the depth specific occurrence of MPs of different size ranges and polymer compositions in the HZ of the Roter Main River. Each of the cores was sliced into five different depth segments and respectively analyzed for MPs. Results of detected MPs were normalized to kg dry weight. For the single core, which was analyzed for MPs < 500 µm, only subsamples of the different depth segments were measured by FPA-based µFTIR spectroscopy. Here the standard normalization procedure results in large extrapolation factors resulting in the high presented MP abundances. Thus, findings for MPs < 500 µm from this single freeze core sample only provides a first insight into the depth specific distribution of pore scale MPs in the HZ and cannot be interpreted as an universally valid assumption. However, our data - to our knowledge - are the first one that investigate the depth specific occurrence of MPs and additionally addresses pore size MPs.

Beside its ecological function, the HZ also is an important interface between the stream and the shallow groundwater system. For rivers and streams, the exchange between surface- and groundwater can be highly non-uniform in space and time[50]. Stream sections or entire river reaches can either gain or lose water from or to the local aquifer[50,51]. Under permanent loosing conditions infiltrating stream water first has to pass through the streambed sediments before it reaches the local aquifer. Thus, mobile pore scale MPs in the HZ can then theoretically be transferred advectivley into the aquifer (Fig. 5). That MP particles at the pore scale can principally be mobile in porous environmental media has already been shown for soils[52,53]. Infiltrating river water is commonly used for drinking water supplies[54] (induced bank filtration technique) and mobile MPs in shallow groundwater therefore can be seen as a potential threat for drinking water production.

WWTPs are widely recognized as potential point sources for the entry of MPs into aquatic environments[3]. Although a fraction of the MPs may be retained in the sewage sludge, a considerable number of particles leave with the cleaned water as only a very limited number of WWTPs possess the ability to filter particles at the end of the cleaning process. As the study site is located close to the headwater area of the Roter Main River, besides the inlet of the WWTP no other point sources for MPs are present in the catchment suggesting that the MPs we found primarily may stem from the nearby WWTP.

Our data clearly indicate a tendency of increasing MP abundances with decreasing particle size. Compared to data obtained further downstream in the Rhein/Main catchment[22] (>10 particles/kg for the confluence area of the Main River and Rhein River), the sediments of the Roter Main River show a relatively low MP contamination for particles >500 µm (depth averaged: ≪1 particles/kg). Abundances for the Roter Main River sediments however increase severely (>50,000 particles/kg), for particles <500 µm, whereas for the confluence area maximum reported values lie around 1,100 particles/kg for particles in-between 63–500 µm[22]. Highest MP abundance (~30,000 particles/kg) was estimated for pore scale particles (20–50 µm) in the sediments of the Roter Main River. Other studies dealing with MP contamination of streambed sediments did not analyze particles below 63 µm (Table 1), thus a direct comparison with our data is only possible to a limited extent. However, compared to the abundances of the river systems listed in Table 1, total MP abundances exceeding 50,000 particles/kg estimated for the Roter Main River sediments are close to abundances measured at contamination hot spots in the Mersey/Irwell River sediments[43] (~75,000 particles/kg). Our results indicate that especially pore scale MPs (~30,000 particles/kg) may represent the dominant size fraction in the HZ of the Roter Main River. Based on these findings

the assumption that the number of MP particles of the river systems listed in Table 1 would increase significantly if pore scale MPs were additionally considered is likely and intensive research on this issue is imperative. Furthermore, our data show that although we used the best methodology currently available, especially the development of methods that allow for the analysis of a larger sample amounts must be fostered in future research to reduce uncertainties by large extrapolation factors.

Summary and Conclusions

Our data indicate that the HZ represents an important accumulation zone - and thus a temporal sink - for MPs of various plastic polymer types and particle size fractions in fluvial ecosystems. Besides data on MPs > 500 µm the results obtained from one sediment core serves as an example suggesting that pore scale MPs < 50 µm potentially represent the most abundant size fraction in the sediments of the Roter Main River. As it is highly unlikely that this is only the case for the Roter Main River, we conclude that the importance of MPs of a size at the pore scale and below is given for other river systems as well. We strongly assume that by accounting for MPs < 50 µm, the hitherto presented abundances of MPs in streambed sediments dramatically would increase by orders of magnitudes. We hypothesize that accumulation of MPs in streambed sediments beside sedimentation is additionally controlled by advective transfer of pore scale and sub-pore scale particles across the streambed interface. Under loosing conditions MPs with sizes of or below the pore scale may even reach the shallow groundwater. Up to now freshwater systems have received only limited attention concerning the fate and behavior of MPs. However, it is imperative to address the mechanistic behavior of MPs in future research to better understand the threat MPs poses to fluvial ecosystems and additionally drinking water security.

Material and Methods

Study site and freeze core sampling. The Roter Main River is part of the headwater catchment of the Main River. The study site is located close to the city of Bayreuth in southeast Germany (Fig. 1). Previously, the Main River was identified as a major source of MPs for the river Rhine, with WWTPs identified as the major contributor to MP loads[22]. Sampling for MPs in the Roter Main River was performed in May 2016 and August 2017 and involved extracting five freeze cores down to a maximum depth of 60 cm from a natural riffle structure. Freeze core sampling was chosen mainly because the streambed materials involved larger gravels and fragments. For the freeze core extraction, a stainless-steel pipe was hammered into the sediments and filled with a mixture of dry ice and ethanol. The pipe was removed as soon as the surrounding sediments froze on the metal surface of the pipe (~20 minutes). For all cores a cylindrical shaped sediment core was extracted from the riverbed sediments. All five cores where extracted and analyzed for MPs in the size range 500 to 5,000 µm using ATR-FTIR spectroscopy and one core was additionally investigated for MP particles in the size range 20–500 µm which includes pore scale and sub-pore scale particles (20–50 µm) using focal plane array FPA-based µFTIR spectroscopy.

Sample preparation. The freeze cores were sliced into 10 cm depth segments prior to thawing and sample preparation. For the freeze core that was analyzed for 20–500 µm MPs the last 20 cm had to be combined into a single segment as not enough material was extracted. Each freeze core segment sample was then dried (50 °C) until a constant weight was reached (Sartorius 3802MPS) to allow for a normalization of MP concentrations to kg dry weight. Next, the samples were wetted with filtered de-ionized water and 20 ml of 30% H_2O_2 was added. After an incubation time of approximately one hour the samples were sieved sequentially over a 500 and 10 µm stainless steel sieve cascade using filtered de-ionized water. The sample material on the 500 µm mesh was visually inspected under the microscope and every particle that looked like a potential synthetic particle, i.e. had no clear mineral or organic appearance, was sorted out for ATR-FTIR measurement. Those particles were then consequently photographed and transferred into Eppendorf tubes for ATR-FTIR analysis.

In one core sampled in August 2017 the remaining material on the 10 µm mesh was further analyzed for MP particles <500 µm. The sample material was again dried (50 °C) to increase the efficiency of the density separation and a subsample of approximately 50 g (Sartorius LC1201S) of each 10 cm segment was taken. To remove inorganic material from the subsamples a density separation in a separating funnel was conducted with zinc chloride solution with a density of 1.6–1.7 kg/l. After a settling time of 24 hours the heavy sediment material was discarded, and the low-density material including MPs was filtered through a 10 µm stainless steel filter. To remove residual zinc chloride the filter was then rinsed with 98% ethanol and transferred into a laboratory beaker using filtered de-ionized water. Organic material was removed using wet peroxide oxidation (Fenton's reagent: 0.05 M Fe^{2+} solution and 30% H_2O_2)[55]. To allow for an undisturbed spectroscopic analysis[56,57] a subsample of 1/64 of each 10 cm segment was filtered onto aluminum oxide filters (Anodisc, Whatman) for subsequent FPA-based µFTIR spectroscopy. Subsampling was performed on each final stainless-steel filter via specially designed sample dividing pliers that divides the filter into two equal parts and ensures a maximum of representativeness of the subsamples. One obtained half was then re-suspended in filtered de-ionized water and the filtration onto a stainless-steel filter repeated. This procedure was carried out until 1/64 of each sample was extracted which was subsequently filtered onto aluminum oxide filters for a reliable FPA-based µFTIR measurement.

Measures against contamination included the inclusion of glass and stainless-steel materials wherever possible, filtering of all chemicals and water during sample preparation, constant coverage of samples with aluminum foil or glass lids and the wearing of laboratory coats made of cotton. Possible contamination during laboratory analysis was further monitored using four negative controls, containing filtered de-ionized water only and receiving the same treatment as the samples. The results of the negative controls were subtracted from the sample results and a detailed table including polymer types, forms and size classes of MPs detected within the blanks is provided within Table S2 (Supplementary Material).

Detection of MPs > 500 µm. Analysis of MPS > 500 µm was conducted using ATR-FTIR spectroscopy[56] after sample preparation. The FTIR spectra were measured using a Tensor 27 FTIR spectrometer equipped with a Platinum-ATR-unit (Bruker Optics GmbH). The IR spectrum of each potential MP particle was recorded as an average spectrum of 16 co-added scans in the spectral range between 4000–400 cm^{-1} with a spectral resolution of 8 cm^{-1} with the software OPUS 7.5 (Bruker Optik GmbH). The background was measured against air. The sample spectra were compared to reference spectra of a self-made polymer library containing the most common polymers, as well as natural materials and has more than 130 entries[56]. The analyses have been conducted by staff with a long expertise in FTIR analysis. Fouling and other impurities at the particle surfaces may be represented in the spectra, as the ATR-FTIR technique measures the surface of the particles. In such cases the particle surface was cleaned mechanically or by alcohol to receive pure polymer spectra. Only particles that showed clear polymer spectra after cleaning were considered as MPs.

Detection of MPs < 500 µm. The aluminum oxide filters of the subsamples and negative controls were placed onto a calcium fluoride window in a customized sample holder and measured in transmittance mode with a Hyperion 3000 FTIR microscope (Bruker Optics GmbH) equipped with a 15 × Cassegrain objective and a 64 × 64 FPA detector. All measurements were performed with the settings published in Löder *et al.*[56] in a spectral range of 3,600–1,250 cm^{-1}, with a spectral resolution of 8 cm^{-1} and 6 co-added scans as well as 4 × 4 binning. The analysis of the obtained large, high-resolution chemical imaging datasets was performed with the software ImageLab and a fast and automated analysis via Random Decision Forest Classifiers[58] for the eleven most important polymers. All selected automatically analyzed particles were again manually checked against the reference database as stated above in cases of unclear spectra.

Received: 18 July 2017; Accepted: 8 October 2019;
Published online: 24 October 2019

References

1. Duis, K. & Coors, A. Microplastics in the aquatic and terrestrial environment: sources (with a specific focus on personal care products), fate and effects. *Environmental Sciences Europe* **28**, 2 (2016).
2. Lebreton, L. C. M. *et al.* River plastic emissions to the world's ocean. *s. Nature communications* **8**, 15611 (2017).
3. Mintenig, S. M., Int-Veen, I., Löder, M. G. J., Primpke, S. & Gerdts, G. Identification of microplastic in effluents of waste water treatment plants using focal plane array-based micro-Fourier-transform infrared imaging. *Water Research* **108**, 365–372 (2017).
4. Dris, R. *et al.* Beyond the ocean: contamination of freshwater ecosystems with (micro-) plastic particles. *Environmental Chemistry* **12**, 539–550 (2015).
5. Dehghani, S., Moore, F. & Akhbarizadeh, R. Microplastic pollution in deposited urban dust, Tehran metropolis, Iran. *Environmental science and pollution research international* **24**, 20360–20371, https://doi.org/10.1007/s11356-017-9674-1 (2017).
6. Horton, A. A., Walton, A., Spurgeon, D. J., Lahive, E. & Svendsen, C. Microplastics in freshwater and terrestrial environments: evaluating the current understanding to identify the knowledge gaps and future research priorities. *Science of the Total Environment* **586**, 127–141 (2017).
7. Ziajahromi, S., Neale, P. A. & Leusch, F. D. L. Wastewater treatment plant effluent as a source of microplastics: review of the fate, chemical interactions and potential risks to aquatic organisms. *Water science and technology* **74**, 2253–2269 (2016).
8. Estahbanati, S. & Fahrenfeld, N. L. Influence of wastewater treatment plant discharges on microplastic concentrations in surface water. *Chemosphere* **162**, 277–284 (2016).
9. Boano, F. *et al.* Hyporheic flow and transport processes: Mechanisms, models, and biogeochemical implications. *Reviews of Geophysics* (2014).
10. Boulton, A. J., Findlay, S., Marmonier, P., Stanley, E. H. & Valett, H. M. The functional significance of the hyporheic zone in streams and rivers. *Annual Review of Ecology and Systematics* **29**, 59–81 (1998).
11. Imhof, H. K., Ivleva, N. P., Schmid, J., Niessner, R. & Laforsch, C. Contamination of beach sediments of a subalpine lake with microplastic particles. *Current biology* **23**, R867–R868 (2013).
12. Wagner, M. *et al.* Microplastics in freshwater ecosystems: what we know and what we need to know. *Environmental Sciences Europe* **26**, 1–9 (2014).
13. Thaysen, C. *et al.* Leachate From Expanded Polystyrene Cups Is Toxic to Aquatic Invertebrates (Ceriodaphnia dubia). *Frontiers in Marine Science* **5**, 71 (2018).
14. Holmes, L. A. Interactions of trace metals with plastic production pellets in the marine environment (2013).
15. Turner, A. & Holmes, L. A. Adsorption of trace metals by microplastic pellets in fresh water. *Environmental Chemistry* **12**, 600–610 (2015).
16. Rochman, C. M. *et al.* Policy: Classify plastic waste as hazardous. *Nature* **494**, 169–171 (2013).
17. Bakir, A., Rowland, S. J. & Thompson, R. C. Transport of persistent organic pollutants by microplastics in estuarine conditions. *Estuarine, Coastal and Shelf Science* **140**, 14–21 (2014).
18. Koelmans, A. A., Besseling, E., Wegner, A. & Foekema, E. M. Plastic as a carrier of POPs to aquatic organisms: a model analysis. *Environmental Science & Technology* **47**, 7812–7820, https://doi.org/10.1021/es401169n (2013).
19. McCormick, A., Hoellein, T. J., Mason, S. A., Schluep, J. & Kelly, J. J. Microplastic is an abundant and distinct microbial habitat in an urban river. *Environmental Science & Technology* **48**, 11863–11871 (2014).
20. Zettler, E. R., Mincer, T. J. & Amaral-Zettler, L. A. Life in the "plastisphere": microbial communities on plastic marine debris. *Environmental Science & Technology* **47**, 7137–7146 (2013).
21. Kirstein, I. V. *et al.* Dangerous hitchhikers? Evidence for potentially pathogenic Vibrio spp. on microplastic particles. *Marine environmental research* **120**, 1–8 (2016).
22. Klein, S., Worch, E. & Knepper, T. P. Occurrence and spatial distribution of microplastics in river shore sediments of the Rhine-Main area in Germany. *Environmental Science & Technology* **49**, 6070–6076 (2015).
23. Horton, A. A., Svendsen, C., Williams, R. J., Spurgeon, D. J. & Lahive, E. Large microplastic particles in sediments of tributaries of the River Thames, UK–Abundance, sources and methods for effective quantification. *Marine pollution bulletin* **114**, 218–226 (2017).
24. Ballent, A., Corcoran, P. L., Madden, O., Helm, P. A. & Longstaffe, F. J. Sources and sinks of microplastics in Canadian Lake Ontario nearshore, tributary and beach sediments. *Marine pollution bulletin* **110**, 383–395 (2016).
25. Wang, J. *et al.* Microplastics in the surface sediments from the Beijiang River littoral zone: composition, abundance, surface textures and interaction with heavy metals. *Chemosphere* **171**, 248–258 (2017).
26. van Cauwenberghe, L. & Janssen, C. R. Microplastics in bivalves cultured for human consumption. *Environmental Pollution* **193**, 65–70 (2014).

27. Minagawa, H. *et al*. Characterization of sand sediment by pore size distribution and permeability using proton nuclear magnetic resonance measurement. *J. Geophys. Res.* **113**, 317, https://doi.org/10.1029/2007JB005403 (2008).
28. Moos, N., von, Burkhardt-Holm, P. & Köhler, A. Uptake and effects of microplastics on cells and tissue of the blue mussel Mytilus edulis L. after an experimental exposure. *Environmental Science & Technology* **46**, 11327–11335 (2012).
29. Browne, M. A., Dissanayake, A., Galloway, T. S., Lowe, D. M. & Thompson, R. C. Ingested microscopic plastic translocates to the circulatory system of the mussel, Mytilus edulis (L.). *Environmental Science & Technology* **42**, 5026–5031 (2008).
30. Farrell, P. & Nelson, K. Trophic level transfer of microplastic: Mytilus edulis (L.) to Carcinus maenas (L.). *Environmental Pollution* **177**, 1–3 (2013).
31. Watts, A. J. R. *et al*. Uptake and retention of microplastics by the shore crab Carcinus maenas. *Environmental Science & Technology* **48**, 8823–8830 (2014).
32. Barboza, L. G. A., Vethaak, A. D., Lavorante, B. R., Lundebye, A.-K. & Guilhermino, L. Marine microplastic debris: An emerging issue for food security, food safety and human health. *Marine pollution bulletin* **133**, 336–348 (2018).
33. Fonte, E., Ferreira, P. & Guilhermino, L. Temperature rise and microplastics interact with the toxicity of the antibiotic cefalexin to juveniles of the common goby (Pomatoschistus microps): post-exposure predatory behaviour, acetylcholinesterase activity and lipid peroxidation. *Aquatic toxicology* **180**, 173–185 (2016).
34. Carbery, M., O'Connor, W. & Palanisami, T. Trophic transfer of microplastics and mixed contaminants in the marine food web and implications for human health. *Environment International* **115**, 400–409 (2018).
35. Ferreira, G. V. B. *et al*. High intake rates of microplastics in a Western Atlantic predatory fish, and insights of a direct fishery effect. *Environmental Pollution* **236**, 706–717 (2018).
36. Buffington, J. M. & Montgomery, D. R. A Procedure for classifying textural facies in gravel-bed rivers. *Water Resour. Res.* **35**, 1903–1914, https://doi.org/10.1029/1999WR900041 (1999).
37. Kooi, M., Besseling, E., Kroeze, C., van Wenzel, A. P. & Koelmans, A. A. In *Freshwater Microplastics*, pp. 125–152 (Springer 2018).
38. Besseling, E., Quik, J. T. K., Sun, M. & Koelmans, A. A. Fate of nano-and microplastic in freshwater systems: A modeling study. *Environmental Pollution* **220**, 540–548 (2017).
39. Rummel, C. D., Jahnke, A., Gorokhova, E., Kühnel, D. & Schmitt-Jansen, M. Impacts of biofilm formation on the fate and potential effects of microplastic in the aquatic environment. *Environmental Science & Technology Letters* **4**, 258–267 (2017).
40. Fazey, F. M. C. & Ryan, P. G. Biofouling on buoyant marine plastics: An experimental study into the effect of size on surface longevity. *Environmental Pollution* **210**, 354–360 (2016).
41. Kessler, A. J., Glud, R. N., Cardenas, M. B. & Cook, P. L. M. Transport zonation limits coupled nitrification-denitrification in permeable sediments. *Environmental Science & Technology* **47**, 13404–13411 (2013).
42. Ye, S. & Andrady, A. L. Fouling of floating plastic debris under Biscayne Bay exposure conditions. *Marine pollution bulletin* **22**, 608–613, https://doi.org/10.1016/0025-326X(91)90249-R (1991).
43. Hurley, R., Woodward, J. & Rothwell, J. J. Microplastic contamination of river beds significantly reduced by catchment-wide flooding. *Nature Geoscience* **11**, 251 (2018).
44. Tibbetts, J., Krause, S., Lynch, I. & Sambrook Smith, G. Abundance, Distribution, and Drivers of Microplastic Contamination in Urban River Environments. *Water* **10**, 1597, https://doi.org/10.3390/w10111597 (2018).
45. Cardinale, B. J., Gelmann, E. R. & Palmer, M. A. Net spinning caddisflies as stream ecosystem engineers: the influence of Hydropsyche on benthic substrate stability. *Functional Ecology* **18**, 381–387 (2004).
46. Cardenas, M. B. Surface water-groundwater interface geomorphology leads to scaling of residence times. *Geophysical Research Letters* **35**, L08402 (2008).
47. Trauth, N., Schmidt, C., Maier, U., Vieweg, M. & Fleckenstein, J. H. Coupled 3-D stream flow and hyporheic flow model under varying stream and ambient groundwater flow conditions in a pool-riffle system. *Water Resources Research* **49**, 5834–5850 (2013).
48. Craig, J. R. Analytical solutions for 2D topography-driven flow in stratified and syncline aquifers. *Advances in Water Resources* **31**, 1066–1073 (2008).
49. Hüffer, T., Praetorius, A., Wagner, S., Kammer von der, F. & Hofmann, T. Microplastic exposure assessment in aquatic environments: learning from similarities and differences to engineered nanoparticles. *Environmental Science & Technology* (2017).
50. Frei, S., Fleckenstein, J. H., Kollet, S. J. & Maxwell, R. M. Patterns and dynamics of river–aquifer exchange with variably-saturated flow using a fully-coupled model. *Journal of Hydrology(Amsterdam)* **375**, 383–393 (2009).
51. Fleckenstein, J. H., Niswonger, R. G. & Fogg, G. E. River-Aquifer Interactions, Geologic Heterogeneity, and Low-Flow Managment. *Groundwater* **44**, 837–852 (2006).
52. Torkzaban, S., Bradford, S. A., van Genuchten, M. T. & Walker, S. L. Colloid transport in unsaturated porous media: the role of water content and ionic strength on particle straining. *Journal of contaminant hydrology* **96**, 113–127, https://doi.org/10.1016/j.jconhyd.2007.10.006 (2008).
53. Hoggan, J. L., Sabatini, D. A. & Kibbey, T. C. G. Transport and retention of TiO2 and polystyrene nanoparticles during drainage from tall heterogeneous layered columns. *Journal of contaminant hydrology* **194**, 30–35, https://doi.org/10.1016/j.jconhyd.2016.10.003 (2016).
54. Hiscock, K. M. & Grischek, T. Attenuation of groundwater pollution by bank filtration. *Journal of Hydrology* **266**, 139–144, https://doi.org/10.1016/S0022-1694(02)00158-0 (2002).
55. Masura, J., Baker, J. E., Foster, G. D., Arthur, C. & Herring, C. Labo ratory methods for the analysis of microplastics in the marine environment: recommendations for quantifying synthetic particles in waters and sediments (2015).
56. Löder, M. G. J., Kuczera, M., Mintenig, S., Lorenz, C. & Gerdts, G. Focal plane array detector-based micro-Fourier-transform infrared imaging for the analysis of microplastics in environmental samples. *Environmental Chemistry* **12**, 563–581 (2015).
57. Löder, M. G. J. *et al*. Enzymatic purification of microplastics in environmental samples. *Environmental Science & Technology* **51**, 14283–14292 (2017).
58. Hufnagl, B. *et al*. A methodology for the fast identification and monitoring of microplastics in environmental samples using random decision forest classifiers. *Analytical Methods* **11**, 2277–2285 (2019).

Acknowledgements

The authors would like to thank both Heghnar Martirosyan and Ursula Wilczek for microplastic sample preparation and FTIR measurements. This research was conducted in the context of SFB 1357 - funded by the German Research Foundation (DFG) under the project number 391977956 and the University of Bayreuth in the funding programme Open Access Publishing. We furthermore thank the Oberfankenstiftung for funding the project "Automatisiertes Verfahren zur Analyse der Kontamination von Süßgewässern mit Mikroplastikpartikeln und Anwendung am Ökosystem Main".

Author contributions

S. Frei, B.S. Gilfedder and C. Laforsch initiated and supervised the field campaign carried out by two former Bachelor students (J. Krutzke and L. Wilhelm). Sample preparation and identification of MP particles in the sediment samples was done by S. Piehl and M. Löder. All authors discussed the results and implications and commented on the manuscript.

Competing interests
The authors declare no competing interests.

Additional information
Supplementary information is available for this paper at https://doi.org/10.1038/s41598-019-51741-5.

Correspondence and requests for materials should be addressed to S.F.

Reprints and permissions information is available at www.nature.com/reprints.

Publisher's note Springer Nature remains neutral with regard to jurisdictional claims in published maps and institutional affiliations.

Article A3: Supplementary information

Table S1: Dry weights of the freeze core segments and the identified MP-particles

Freeze Core [-]	Depth Segement [cm]	Dry Weight [kg]	MP > 500 µm [-]	MP <500 µm detected on Anodisc (FTIR) 50/64 g [-]
1	10-20	2.47	3	not analyzed
1	20-30	4.11	3	not analyzed
1	30-40	4.83	3	not analyzed
1	40-50	2.02	0	not analyzed
2	0-10	2.05	1	not analyzed
2	10-20	2.32	0	not analyzed
3	10-20	2.03	0	not analyzed
3	20-30	2.28	0	not analyzed
3	30-40	0.6	1	not analyzed
4	0-10	1.19	0	not analyzed
4	10-20	1.5	0	not analyzed
4	20-30	2.86	0	not analyzed
5	0-10	0.45	1	44
5	10-20	0.80	1	10
5	20-30	0.5	0	37
5	30-40	0.26	0	22
5	40-60	0.69	1	20

Table S2: Polymer types, shapes, and size classes of MPs detected within the blanks.

		FRAGMENTS								FIBERS		
Sample ID	Size class	PE	PP	PS	PET	PBT	PC	PA	Total size class	PET	PAN	Total size class
Blank_1	20 - 50 µm	4	1	0	7	0	1	0		0	0	
Blank_2	20 - 50 µm	0	5	1	12	0	0	0		0	0	
Blank_3	20 - 50 µm	3	3	0	14	0	0	0		0	0	
Blank_4	20 - 50 µm	2	1	1	32	0	0	0		0	0	
TOTAL		2.25	2.5	0.5	16.25	0	0.25	0	21.75	0	0	0
STD		1.707825	1.9148542	0.57735	10.90489	0	0.5	0	6.696263666	0	0	0
Blank_1	50 -100 µm	1	2	0	4	3	0	0		0	0	
Blank_2	50 -100 µm	0	1	1	8	0	0	0		0	1	
Blank_3	50 -100 µm	1	3	0	6	3	0	0		0	0	
Blank_4	50 -100 µm	3	0	0	5	0	0	1		0	0	
TOTAL		1.25	1.5	0.25	5.75	1.5	0	0.25	10.5	0	0.25	0.25
STD		1.258306	1.2909944	0.5	1.707825	1.732051	0	0.5	2.134374746	0	0.5	0.353553391
Blank_1	100 - 500 µm	1	1	2	0	0	1	0		0	0	
Blank_2	100 - 500 µm	0	0	0	1	1	0	0		2	1	
Blank_3	100 - 500 µm	1	0	0	0	1	0	0		1	0	
Blank_4	100 - 500 µm	0	0	0	0	0	0	1		1	0	
TOTAL		0.5	0.25	0.5	0.25	0.5	0.25	0.25	2.5	1	0.25	1.25
STD		0.57735	0.5	1	0.5	0.57735	0.5	0.5	0.55872114	0.816497	0.5	0.744023809
Blank_1	500 - 1000 µm	0	0	0	0	0	0	0		0	0	
Blank_2	500 - 1000 µm	0	0	0	0	0	0	0		0	0	
Blank_3	500 - 1000 µm	0	0	0	0	0	0	0		0	0	
Blank_4	500 - 1000 µm	0	0	0	0	0	0	1		1	0	
TOTAL		0	0	0	0	0	0	0.25	0.25	0.25	0	0.25
STD		0	0	0	0	0	0	0.5	0.188982237	0.5	0	0.353553391

Chapter B

Chapter B: Improvement of existing sampling and sample processing methods for microplastics

Article B1: Enzymatic purification of microplastics in environmental samples

Löder MGJ, Imhof HK, Ladehoff M, Löschel L, Lorenz C, Mintenig S, Piehl S, Primpke S, Schrank I, Laforsch C, Gerdts G (2017)

Environmental Science and Technology 51: 14283–14292

Environmental Science & Technology

Article

Cite This: Environ. Sci. Technol. 2017, 51, 14283−14292

pubs.acs.org/est

Enzymatic Purification of Microplastics in Environmental Samples

Martin G. J. Löder,*[,†,§] Hannes K. Imhof,[‡] Maike Ladehoff,[†,∥] Lena A. Löschel,[‡] Claudia Lorenz,[†] Svenja Mintenig,[†,⊥] Sarah Piehl,[‡] Sebastian Primpke,[†] Isabella Schrank,[‡] Christian Laforsch,*[,‡] and Gunnar Gerdts*[,†]

[†]Biologische Anstalt Helgoland, Alfred-Wegener-Institut, Helmholtz-Zentrum für Polar- und Meeresforschung, P.O. Box 180, 27483 Helgoland, Germany

[‡]Department of Animal Ecology I and BayCEER, University of Bayreuth, Universitätsstrasse 30, 95440 Bayreuth, Germany

Supporting Information

ABSTRACT: Micro-Fourier transform infrared (micro-FTIR) spectroscopy and Raman spectroscopy enable the reliable identification and quantification of microplastics (MPs) in the lower micron range. Since concentrations of MPs in the environment are usually low, the large sample volumes required for these techniques lead to an excess of coenriched organic or inorganic materials. While inorganic materials can be separated from MPs using density separation, the organic fraction impedes the ability to conduct reliable analyses. Hence, the purification of MPs from organic materials is crucial prior to conducting an identification via spectroscopic techniques. Strong acidic or alkaline treatments bear the danger of degrading sensitive synthetic polymers. We suggest an alternative method, which uses a series of technical grade enzymes for purifying MPs in environmental samples. A basic enzymatic purification protocol (BEPP) proved to be efficient while reducing 98.3 ± 0.1% of the sample matrix in surface water samples. After showing a high recovery rate (84.5 ± 3.3%), the BEPP was successfully applied to environmental samples from the North Sea where numbers of MPs range from 0.05 to 4.42 items m^{-3}. Experiences with different environmental sample matrices were considered in an improved and universally applicable version of the BEPP, which is suitable for focal plane array detector (FPA)-based micro-FTIR analyses of water, wastewater, sediment, biota, and food samples.

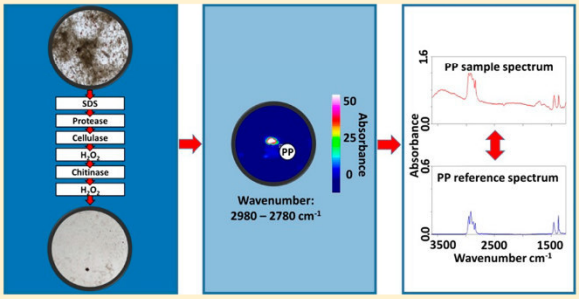

INTRODUCTION

To date, plastic debris is almost ubiquitous in aquatic habitats. Plastic particles <5 mm, so-called microplastics (MPs), have been reported to be present in various marine[1−4] and freshwater ecosystems.[5,6] As a result of this omnipresence, accompanied by the potential hazards of MPs to the environment, organisms, and human health, the contamination of the ocean with plastic debris has been characterized as one of the top emerging global issues,[7,8] and a similar risk for freshwater environments is anticipated.[9]

Although the problem has been recognized, to date, a universal standard operating procedure for identifying and quantifying MPs does not exist, which hampers comparing MPs data.[10] Nevertheless, technical advancements using state-of-the-art spectroscopic techniques allow for the reliable identification and quantification of MPs, even in the lower micron range.[11−13] The analysis of small MPs (<500 μm) with micro-FTIR spectroscopy[14] or Raman microspectroscopy[10,15] mandatorily requires concentrating the samples on filter membranes. By applying these techniques in combination with chemical imaging and analysis, MPs can be characterized in terms of their composition, quantity, and size.[13,14,16]

Generally, all spectroscopic approaches are constrained by a mostly unfavorable target (MPs) to nontarget (organic or inorganic particles) ratio in the samples. Hence, analyses are usually hampered by an excess of organic (e.g., algae, plankton, and natural debris) or inorganic particles (e.g., sand and silt) as their signal overlays MPs spectra. Therefore, the purification of MPs from environmental samples is an essential part of sample processing and a crucial step prior to conducting an identification and quantification analysis via chemical imaging.

As a prerequisite, the purification approach should (1) efficiently remove the organic and inorganic material from the samples while not affecting the synthetic polymers, (2) facilitate the concentration of the purified samples on filters with a small pore size (<1 μm) that is suitable for spectroscopic measurements, and 3) be cost and labor effective.

To date, diverse purification approaches have been developed to purify environmental samples for analyses of MPs. Inorganic particles in, e.g., sediment samples, are removed

Received: July 3, 2017
Revised: October 27, 2017
Accepted: November 6, 2017
Published: November 7, 2017

DOI: 10.1021/acs.est.7b03055
Environ. Sci. Technol. 2017, 51, 14283−14292

using density separation with different solutions of high density, which leads to a significant reduction in the sample volume.[17−21]

Organic material, often present in high loads in plankton, sediment, or tissue samples, is usually digested by strong acidic[11,12,22,23] or alkaline solutions,[23−26] oxidation agents,[19,27,28] or a combination of these agents.[24,29]

These digestion approaches, however, are limited by the chemical susceptibility of the MPs, and sensitive synthetic polymers can be lost during digestion,[22−24,26,29,30] which is furthermore dependent on their size, shape (e.g., fragment, fiber, film, sphere), age, and oxidation.

An alternative, plastic-conserving and expedient approach is to purify environmental samples using enzymes.[23,30,31] The use of a single enzyme (proteinase-K) to isolate MPs from seawater samples with a high content of planktonic organisms was first suggested by Cole et al.[23] Although a high grade of purification was reached, a significant drawback of the approach is the high cost for the enzyme that is usually used in molecular biology approaches. Meanwhile, inexpensive enzymes have been successfully used for the purification of plastic particles from mussel tissue samples.[30,31] Unfortunately, none of the studies determined whether their enzymatic approach is suitable for different sample matrices and appropriate for chemical imaging of MPs concentrated on filters.

This underlines the urgent need for a purification protocol that is "plastic-conserving" and applicable for different environmental sample matrices while meeting the above-mentioned prerequisites for spectroscopic analyses.

To overcome the existing limitations, the overall aim of our study was to develop a protocol for the reduction of organic and inorganic sample matrices of different environmental origins or types (plankton, sediment, and biota), while leaving all synthetic polymers unaffected. The grade of purification should be suitable for reliably identifying and quantifying MPs using an FPA-based micro-FTIR analysis accompanied by chemical imaging.[13,14,32]

In the first step, we developed a basic enzymatic purification protocol (BEPP) based on the sequential application of a detergent, technical grade enzymes, an oxidizing agent, and a density separation step, and evaluated the protocol for its purification efficiency and applicability for FPA-based FTIR imaging of MPs in the size range of 20−500 μm. In the second step, the recovery rate of the MPs after the application of the entire purification process was determined. In the final step, important improvements in the BEPP, based on tests conducted with different sample matrices, are described leading to an optimized universal enzymatic purification protocol (UEPP) that is suitable for different environmental matrices, including plankton samples, sediment samples, and biota samples.

■ MATERIALS AND METHODS

General Precautions To Prevent Sample Contamination. All laboratory equipment and materials were thoroughly rinsed with prefiltered (0.2 μm) deionized water (Milli-Q) and 35% ethanol before and during all working steps to prevent sample (cross-) contamination. The enzymes were filtered through a 0.45 μm filter before usage. All materials were covered whenever possible with glass lids or aluminum foil to prevent airborne contamination. Wherever possible, equipment made of plastic was replaced with glass or metal components. Within the laboratory, cotton lab coats and only non-synthetic clothing were worn. To monitor possible sample contamination, blank samples (Milli-Q water) that underwent the same procedure as the environmental samples were used.

MPs Sampling. Marine plankton samples were obtained from the North Sea by sea surface sampling with a neuston catamaran using a plankton net with a 100 μm mesh size during cruise "HE409" on the "*Heincke*" research vessel in September 2013 (Table S1). The samples were carefully transferred to PVC Kautex Bottles (Kautex Textron GmbH & Co. KG, Bonn, Germany) and frozen prior to purification with the BEPP and the subsequent FPA-based micro-FTIR analysis.

Basic Enzymatic Purification Protocol (BEPP). The BEPP is based on the results from preliminary purification experiments of plankton samples with commercial enzymatic mixtures produced for organic washing agents (Biozym SE & Biozym F, Spinnrad GmbH, Bad Segeberg, Germany), which contain a detergent, amylase, protease, and lipase. Combined with a preceding detergent step with sodium dodecyl sulfate (SDS) and a subsequent chitinase step, the approach proved to be efficient for the purification of marine surface water samples and mussels.

To increase the efficiency of the purification process, the enzyme mixtures were replaced with technical grade enzymes (protease, cellulase, chitinase; ASA Spezialenzyme GmbH, Wolfenbüttel, Germany) that were applied at their optimum pH and temperature (for detailed information on the used enzymes please refer to the section "Detailed Description of the Sequential Purification Steps" and the Supporting Information). All enzymes were specifically chosen according to the potential corresponding major components of organic material in the environmental samples. Similar to the preliminary experiments, the BEPP included an incubation step with SDS prior to the three enzymatic steps and was additionally combined with a hydrogen peroxide treatment that was performed twice and a final density separation step using a $ZnCl_2$ solution. As a result, the BEPP involves seven consecutive purification steps (Figure 1), which are described in detail below.

General Procedure. In the first step the samples were defrosted and subdivided into two size fractions using a 500 μm stainless steel sieve. The fraction >500 μm was visually sorted for potential MPs, and they were individually analyzed using attenuated total reflection (ATR) FTIR spectroscopy (Figure 1, data not shown). The sample fraction <500 μm was purified using the BEPP.

The general handling procedure for all samples was as follows for all sequential steps: Each sample was filtered through a stainless steel filter (47 mm diameter, mesh size 10 μm, Wolftechnik Filtersysteme GmbH & Co. KG, Weil der Stadt, Germany) with a bottle top filtration device (Thermo Fisher Scientific Inc., Waltham, MA, USA). One single filter per sample was used consecutively during the whole procedure. All equipment that came into contact with the sample was rinsed thoroughly with Milli-Q water to avoid particle losses. After filtration, the filtrate was discarded, and the filter with the residues was placed in a 100 mL laboratory glass bottle (DURAN Group GmbH, Mainz, Germany). Next, the respective enzyme or chemical solution was added as described in Figure 1. The sequence of the enzymes was chosen according to the lability of the targeted biological substrates − first proteins followed by cellulose and then chitin (for more information refer to the paragraph "Detailed Description of the Sequential Purification Steps"). During each filtration step rinsing with Milli-Q water took place to exclude an interference

DOI: 10.1021/acs.est.7b03055
Environ. Sci. Technol. 2017, 51, 14283−14292

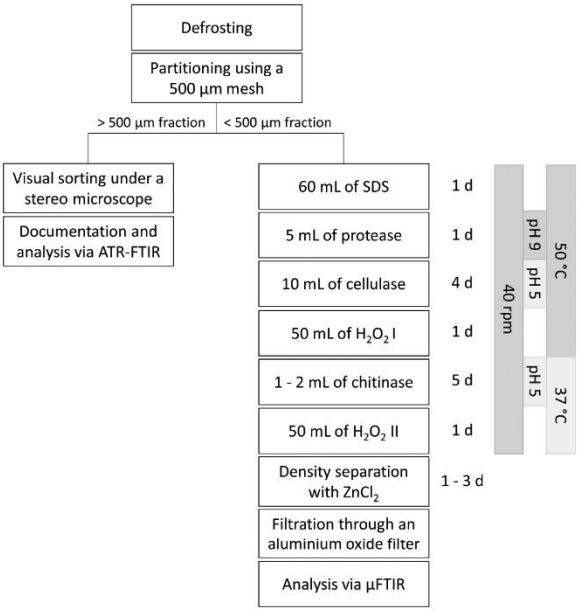

Figure 1. Flowchart of the basic enzymatic purification protocol used for the efficiency validation, determination of the recovery rate determination, and determination of the MPs in the plankton samples.

of the next enzyme with the enzyme rests of the previous step. The samples were incubated in a Multitron shaking incubator (Infors AG, Bottmingen, Switzerland) at 40 rpm with the respective incubation time and temperature. After the incubation, the stainless steel filter was removed from the bottle, and all remaining residues on the filter were thoroughly rinsed back into the bottle using Milli-Q water. Then, the clean stainless steel filter was remounted on the bottle-top filtration system, and the corresponding sample in the bottle was filtered again to remove the enzyme/chemical solution. The filter with the residue was placed back into the incubation bottle, the filtration equipment was rinsed with the corresponding buffer solution, and the next enzyme or chemical solution was added (Figure 1). After the six purification steps, a final density separation process was included (detailed description below). The residual sample was filtered through aluminum oxide filters (25 mm diameter, 0.2 μm pore size, Anodisc, Whatman, GE Healthcare, Chicago, IL, United States) for the FPA-based FTIR analysis. Here, a specially manufactured filter system, consisting of an acrylic glass filter funnel with a 9 mm diameter mounted on a 25 mm supporting plate and pressed on the fritted stainless steel support base with a laboratory clamp, was used to reduce the final filtration area with respect to the FPA-based micro-FTIR analysis.[14]

Detailed Description of the Sequential Purification Steps. Sodium Dodecyl Sulfate (SDS) Treatment. The initial incubation was performed using SDS, which is an anionic surfactant. SDS macerates planktonic organisms and animal and plant residues and increased the contact surface for the following enzymatic treatments. A solution of 5% (w/w) SDS with a volume of 60 mL per incubation bottle was applied. The samples were incubated for approximately 24 h at 50 °C in the incubator.

Protease Treatment. The first enzymatic purification was conducted with protease. Protease catalyzes the decomposition of protein chains into easily dissolved and dispersed peptides and thus further macerates planktonic organisms and cell residues. Protease A-01 (subtilisin, EC 3.4.21.62, ASA Spezialenzyme GmbH, Wolfenbüttel, Germany) was applied, which attains its optimum activity at pH 9.0 and 50 °C. The enzymatic activity is specified as 1,100 U/mL. In total, 5 mL of protease was added to the sample matrix in the laboratory glass bottles, and 25 mL of phosphate-buffered saline (PBS) solution was added. The PBS solution was set to pH 9.0 by adding sodium hydroxide. The samples were incubated at 50 °C for 24 h.

Cellulase Treatment. The cellulase treatment targets the maceration of phytoplankton cell walls and other plant residues. Cellulase TXL (EC 3.2.14, ASA Spezialenzyme GmbH, Wolfenbüttel, Germany) was applied, which is an endo-1,4-β-glucanase with a high "C1" activity. It cleaves the ß-1,4-bonds within cellulose molecules and is used to decompose all kinds of cellulose. Cellulase TXL attains its optimum reaction activity at pH 5.0 and 50 °C and had an activity of >30 U/mL. For this purification step, 10 mL of Cellulase TXL and 50 mL of the PBS solution, set to pII 5.0 by adding hydrochloric acid, were added. The samples were incubated at 50 °C for 4 days.

Hydrogen Peroxide Treatment I. The exoskeletons of crustaceans contain not only chitin but also a protective coating of proteins and calcium carbonate, which makes them very robust and difficult to digest. To facilitate better contact between the chitinase and chitin (in the subsequent step), the samples were initially treated with 50 mL of 35% stabilized hydrogen peroxide (Merck KGaA, Darmstadt, Germany), which is a well-established process for the destruction of organic materials.[20,33] The samples were incubated for 24 h at 50 °C.

Chitinase Treatment. High amounts of chitin-containing materials were anticipated to be present in both, marine and freshwater environmental samples. The chitinase used (EC 3.2.1.14, ASA Spezialenzyme GmbH, Wolfenbüttel, Germany) has a specific activity of >50 U/mL. It consists of chitodextrinase, 1,4-ß-poly-*N*-acetylglucosaminidase, and poly-ß-glucosaminidase. These hydrolytic enzymes break down the glycosidic bonds within chitin. The chitinase reaches its maximum enzyme activity at a pH of 5.6 and 37 °C. Depending on the amount of PBS buffer (pH 5) needed to rinse the equipment after filtration (between 15 and 30 mL), a total of 1 to 2 mL of Chitinase were added, and the samples were incubated for 5 days at 37 °C.

Hydrogen Peroxide Treatment II. A second application of hydrogen peroxide (50 mL) was performed to further degrade the partly dissolved organic material. The samples were treated for 24 h at 37 °C.

Density Separation. Frequently, considerable amounts of inorganic material (e.g., sand and diatom frustules) were present in the samples after the enzymatic treatment. Therefore, the samples underwent density separation using a $ZnCl_2$ solution at a density of 1.7 g/cm^3. After the last filtration step, the filter cake was flushed in a small 50 or 100 mL beaker using a prefiltered zinc chloride solution. Then, the samples were transferred into 50 or 100 mL separation funnels where they remained between 1 and 3 days. Every few hours (4−12 h), the settled portion was carefully discarded. When necessary, the separation funnels were carefully swayed to support the separation process and overcome the surface tension. As soon as sedimentation was no longer observed, the separation funnels were carefully emptied until just a few mL of solution,

DOI: 10.1021/acs.est.7b03055
Environ. Sci. Technol. 2017, 51, 14283−14292

containing the light fraction with the MPs, were left. This fraction was finally filtered through aluminum oxide filters (0.2 μm, Anodisc, Whatman, GE Healthcare, Chicago, IL, United States) for FPA-based micro-FTIR spectroscopy.

Efficiency Validation of the Enzymatic Purification. The efficiency of the BEPP was determined using representative environmental samples obtained in July 2014 northeast of the coast of Helgoland island, North Sea, German Bight. A plankton net with a mesh size of 100 μm was towed two times at the surface for several minutes resulting in a highly concentrated plankton sample of approximately 10 L that contained a sample matrix with a high content of phytoplankton and zooplankton, such as diatoms, ciliates, flagellates, and copepods as well as organic detritus (marine snow) and sand particles. The sample was mixed and homogeneously divided into 24 aliquots, each with a 250 mL volume. Further, each incubation bottle was doped with a small amount of polypropylene (PP) particles (<150 μm, abrasion from a blue screw cap, Duran group, Wertheim, Germany). The PP doping was conducted to test whether the sample matrix reduction after the purification was sufficiently high to facilitate analyzing the MPs via FPA-based micro-FTIR spectroscopy. As described above, the plankton samples were filtered, and the filter cake of each replicate was transferred into 100 mL laboratory glass incubation bottles for subsequent purification using the BEPP.

The efficiency of the enzymatic purification process was evaluated according to the weight loss of the remaining filter cake after each purification step using a gravimetric analysis. Prior to the experiments, all filter substrates (21 clean 10 μm stainless steel filters and three 0.2 μm aluminum oxide filters) were dried for 48 h at 60 °C and weighed with a laboratory precision scale (d = 0.01 mg, Sartorius AG, Göttingen, Germany). All sample aliquots were treated according to the BEPP described above. Prior to the purification and after each purification step, three replicates were filtered through preweighted stainless steel filters, and after the last step (density separation), aluminum oxide filters were used for the subsequent FPA-based micro-FTIR spectroscopy tests. The filters with the residual samples were dried for 48 h at 60 °C and weighed, and the purification efficiency was calculated using the initial mean dry weight per sample aliquot of 94.77 mg. Additionally, the appearance of the residual sample was documented using a stereomicroscope (Olympus SZX16, Olympus Europa Holding GmbH, Hamburg, Germany). Prior to the photos, the filter residue has always been resuspended in the same volume of Milli-Q to facilitate a comparison. No photos have been taken after the density separation step, because due to the 0.2 μm aluminum oxide filters used for the subsequent FPA-based micro-FTIR analysis it was important to keep the filtered volume as small as possible to keep the filtration time at a minimum (compare paragraph "Density Separation" above). Thus, a resuspension in a larger amount of Milli-Q as necessary for the comparison with the previous steps was impossible.

The applicability of the BEPP for FPA-based micro-FTIR chemical imaging was tested on the PP doped samples, as described below.

FPA-Based Micro-FTIR Imaging. The suitability of the BEPP for chemical imaging was tested on a sample from the efficiency validation. The measurements were performed using FPA-based micro-FTIR spectroscopy with a Hyperion 3000 FTIR microscope equipped with a FPA detector coupled to a Tensor 27 spectrometer (Bruker Optik GmbH, Ettlingen, Germany), similar to the setup in Löder et al.[14] The dried sample on the aluminum oxide filter was placed on a CaF_2 filter holder under the IR microscope and measured in transmission mode at a final magnification of 150×. The FTIR measurement was performed in the wavenumber range of 3600−1250 cm^{-1} at a resolution of 8 cm^{-1} and a coaddition of 32 scans. The background was acquired on the blank filter material using the same parameters. Exemplarily, a filter area of approximately 2.5 × 1.6 mm was measured by combining 126 FPA tiles. The FTIR system was operated, and the data were processed using OPUS 7.5 software (Bruker Optik GmbH). For chemical imaging the wavenumber range between 2980 and 2780 cm^{-1}, corresponding to the C−H stretching vibrations in PP, was integrated. The measured spectra were compared to those from a polymer library generated by the Alfred Wegener Institute, Helgoland, Germany.[14]

The measurements of the purified samples from cruise "HE409" were performed using the same system; the measurement settings and the parameters for the subsequent analyses were chosen according to Löder et al.[14] (The measurement time for a filter area of around 10 × 10 mm with a pixel resolution of around 10.6 μm is 10−12 h; the time needed for the analysis of the spectra depends on the amount of potential particles present and can be several hours).

Determination of the Recovery Rate. Bright red polyethylene (PE) beads (density 1.072 g/cm^{-3}, size 180−212 μm, REDPMS-1.070, Cospheric, Santa Barbara, CA, USA) were counted (109, 84, and 86), picked out under a microscope (Olympus SZX16), and transferred into three laboratory glass bottles filled with 1 L of Milli-Q water. These three samples went through the entire BEPP as described above. Finally, the recovered PE beads were counted under the stereomicroscope, and the recovery rates were calculated.

Development of an Universal Enzymatic Purification Protocol (UEPP). During the daily lab routine, the enzymatic purification approach has been applied during several studies on MPs for samples containing different environmental matrices.[13,14,32,34] In addition to marine surface water samples, these matrices have included freshwater surface water samples from rivers and lakes, marine and freshwater sediment and beach samples after density separation, wastewater samples, tissue samples of mussels, daphnia, and fish, and commercial fish food samples. During these studies, several modifications in the BEPP were necessary to adjust for the different chemical compositions of each sample matrix, and all samples underwent an enzymatic purification and were concentrated through filters for subsequent analyses of MPs via FPA-based micro-FTIR spectroscopy and chemical imaging.

The experiences of these investigations resulted in an improved universal enzymatic purification protocol (UEPP), which is mainly based on the following main modifications in the BEPP: changing the buffer used, including two optional enzymatic steps (amylase and lipase), and optimizing the incubation conditions and enzyme concentrations, which were developed in cooperation with the enzyme manufacturer (ASA Spezialenzyme GmbH, Wolfenbüttel, Germany). These comprehensive adjustments for the proposed UEPP are not included in the Results section but are suggested in the Discussion, whereas the detailed changes are described in the Supporting Information (SI).

DOI: 10.1021/acs.est.7b03055
Environ. Sci. Technol. 2017, 51, 14283−14292

RESULTS

Efficiency Validation of the Enzymatic Purification. During the whole purification process, the initial sample mass (dry weight) was reduced by 98.3 ± 0.1% (standard deviation = SD), which was equal to a mean reduction of 93.18 ± 0.1 mg for an initial mean dry weight of 94.77 ± 3.8 mg (Figure 2).

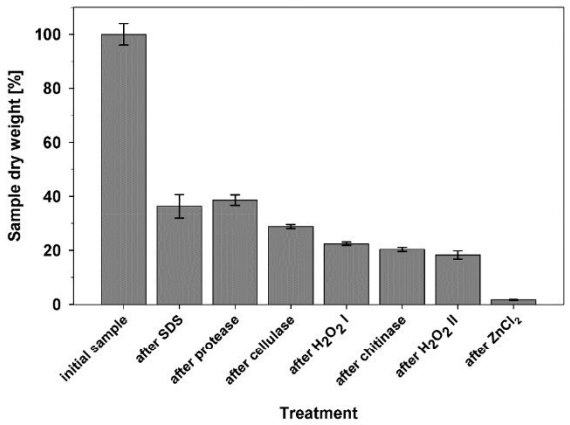

Figure 2. Changes in the sample dry weight in percent after each purification step (SD: n = 3 for all results; after $ZnCl_2$, SD: n = 2).

Within the single treatment steps, the largest reduction in the natural matter content was observed after the first treatment with SDS. During this step, the sample mass was reduced by 63.7 ± 4.3%. With the exception of the protease treatment, the sample mass was continuously reduced by the subsequent enzymatic and hydrogen peroxide purification steps (Figure 2), resulting in a further halving of the sample mass. This was also reflected in the reduced amount of visible residual material in the microscopic picture (Figure 3). The second highest mean reduction value (16.6 ± 0.1%) was attained during the final zinc chloride density separation, which removed high-density particles, mainly sand grains. The result of this last treatment was based on two instead of three replicates, because one sample was lost due to a leakage in the filtration device.

Suitability Test of the BEPP for FPA-Based Micro-FTIR Imaging. The above-mentioned prerequisites for a successful analysis of MPs via FPA-based micro-FTIR chemical imaging were clearly fulfilled. The chemical imaging based on the integration of the wavenumber range between 2980 and 2780 cm^{-1}, corresponding to the C−H stretching vibrations, allowed for the clear discrimination of the doped PP particles (Figure 4). Only minimal amounts of organic residues were present, which are also highlighted by the integration within this wavenumber range. The efficiency of the BEPP was very high and resulted in a good contrast between the background and PP particles due to the reduced intrinsic interference background signals from the residuals of the organic matrix (Figure 4). The residual sample matrix showed only a very weak signal in the wavenumber ranges between 1500 and 1800 cm^{-1} and between 3000 and 3600 cm^{-1} (Figure 4). The high grade of purification furthermore facilitated the visualization of PP particles smaller than 20 μm.

Determination of the Recovery Rate. The determined recovery rate for the red fluorescent MPs in the three water samples processed with the BEPP yielded a mean value of 84.5

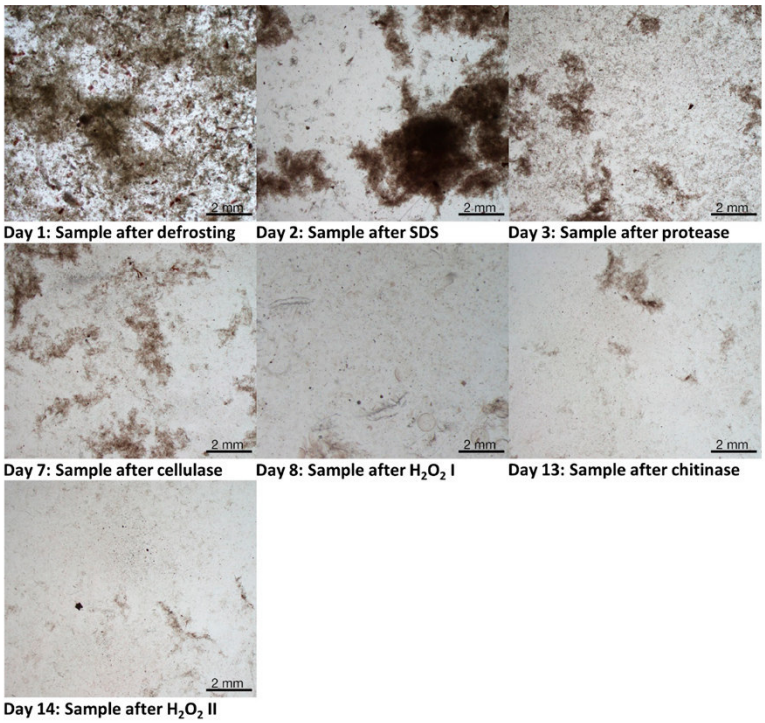

Figure 3. Digestion efficiency evaluation after each consecutive purification step. Due to differences in sample treatment, the final density separation step was not documented.

DOI: 10.1021/acs.est.7b03055
Environ. Sci. Technol. 2017, 51, 14283−14292

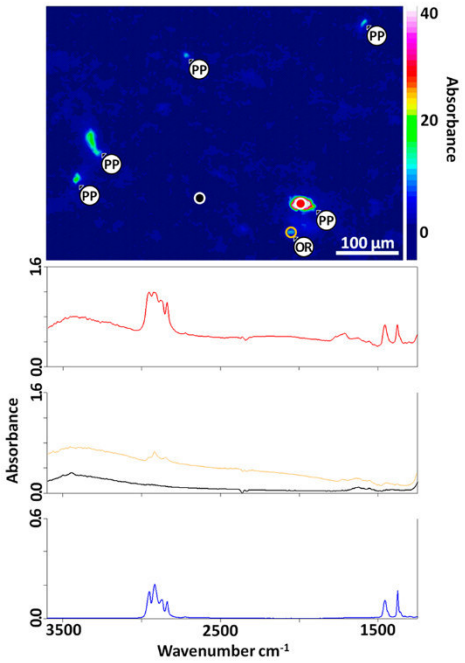

Figure 4. FPA-based micro-FTIR chemical imaging of a sample after the purification process. Upper figure: Chemical image of the wavenumber range from 2980−2780 cm^{-1}, corresponding to the C−H stretching vibrations. The particles marked with PP are the polypropylene particles from the sample doping; OR is an organic residue. The color bar represents the intensity of the integrated band region. Particles with peaks in the integrated region are highlighted according to their peak height. The scale bar corresponds to 100 μm. Lower figure: The red spectrum was measured at the location marked by the red point in the upper figure and identified as PP; the black spectrum was measured at the location of the black point in the upper figure and represents the background signal; the orange spectrum was measured at the location of the organic residue which is encircled in orange, and the blue spectrum is a PP reference spectrum from the reference database.

± 3.3%. Approximately 15% of the beads were lost during the purification process (see Table 1).

Table 1. Recovery Rate

replicate	no. of beads added	no. of beads recovered	recovery rate [%]
1	109	89	81.65
2	84	74	88.10
3	86	72	83.72
average ± SD			84.5 ± 3.3

Determination of MPs in the Plankton Samples. Sea surface plankton samples from the northern German Bight sampled during cruise "HE409" were purified using the BEPP. The geographic positions and further additional data are provided in the Supporting Information (Table S1).

In all samples, MPs < 500 μm were found, and the concentrations of the total polymer content and assigned polymer types are summarized in Table 2. MPs were found in concentrations between 0.05 and 4.42 particles m^{-3}, the particles were only fragments. The most abundant polymers found were PE and polystyrene (PS). The samples were corrected for a possible MP sample contamination during the purification by the values of three procedural blanks. Only one polyamide particle and one polyethylene terephthalate fiber were found in the procedural blanks. However, we found a relatively high number of PP particles in the procedural blanks that could be later traced back to the screw caps of the glass bottles the enzymes were stored in. Thus, PP was excluded from the analysis, and the screw caps were replaced by aluminum foil in subsequent studies.

■ DISCUSSION

Basic Enzymatic Purification Protocol (BEPP). The main aim of the enzymatic purification approach was (1) to reduce the sample matrix to allow for a reliable analysis during FPA-based micro-FTIR imaging and, simultaneously, (2) to conserve the natural composition of the MPs.

The samples that were purified with the BEPP contained a great variety of microalgae (e.g., diatoms and dinoflagellates) and crustaceans (e.g., copepods and decapod larvae), as well as small fragments of insects, macroalgae, and higher plants, that were not removed by the 500 μm sieving step. Despite the high load of organic material, the described BEPP efficiently reduced the natural matter during the enzymatic and oxidative purification steps, whereas inorganic material (mainly sand) was removed during the final density separation step. This resulted in a minimum amount of inorganic and organic particles on the aluminum oxide filters and facilitated the successful and time efficient identification and quantification of MPs down to a size of 20 μm using FPA-based micro-FTIR spectroscopy according to Löder et al.[14]

Although the BEPP reached in total a general high grade of purification in our efficiency validation, the efficiency of the single purification steps was of different magnitude (compare Figure 2). This is certainly dependent on the amount of the targeted substrata which is present in the respective sample. For example, no weight loss was observed for the protease step during our purification of the plankton samples. In this case, probably most of the proteins were already degraded by the previous SDS step. However, during the purification of other samples the protease step led to a significant reduction of organic material.

FPA-based micro-FTIR spectroscopy according to Löder et al.[14] facilitates the reliable analysis of particles down to a size of at least 20 μm, thus we used 10 μm stainless steel filters during the purification process. Nevertheless, only aluminum oxide filters allow for good quality FPA-based micro-FTIR measurements in transmission mode, as this filter material is IR transparent in the wavenumber range important for microplastic analyses.[14] Due to the fact that during the purification process we excluded small particles that are not in the measurable size range, 10 μm filters would be theoretically appropriate for FPA-based micro-FTIR measurements; however, unfortunately no aluminum oxide filters with a higher porosity than 0.2 μm are standardly available.

A great advantage of an enzymatic approach as proposed herein is the ability to conserve the sensitive synthetic polymers, as already described by Cole et al.,[23] Catarino et al.,[30] and Courtene-Jones et al.[31] In contrast, in several studies in which strong acid, alkaline, or oxidative treatments were applied, detrimental effects on sensitive synthetic polymers were observed.[22−24,26,29,30] Furthermore, the usage of aggressive chemicals increases the risk of further fragmenting the

DOI: 10.1021/acs.est.7b03055
Environ. Sci. Technol. 2017, 51, 14283−14292

Table 2. Abundances and Polymer Types of MPs < 500 μm Found at the Stations of the Cruise "HE 409" in Units of Number of Items m^{-3}[a]

station	total	PS	PE	PA	ABS	PVA	PET	PUR	EVA
1	0.266		0.061	0.051	0.061		0.061	0.031	
2	0.096		0.072		0.024				
3	0.437	0.309	0.077	0.051					
4	0.049				0.049				
5	1.815	1.210	0.519		0.043				0.043
6	0.551	0.551							
7	4.415	1.766	1.876		0.221	0.552			
8	0.209	0.070	0.139						
9	0.137	0.023	0.092				0.023		
10	1.762	0.576	0.105	0.977	0.052		0.052		

[a]PS = polystyrene, PE = polyethylene, PA = polyamide, ABS = acrylonitrile butadiene styrene, PVA = poly(vinyl alcohol), PET = polyethylene terephthalate, PUR = polyurethane, and EVA = ethylene vinyl acetate.

MPs, thus potentially falsifying the analysis results regarding the quantity of MPs.[22,23]

In addition to using SDS and enzymes, hydrogen peroxide was used in our protocol to degrade the organic matrices. Nuelle et al.[19] reported visible changes in MPs, which became more transparent and thinner, after exposure to 30% hydrogen peroxide over 7 days. In contrast to that, our samples were never treated longer than 24 h with hydrogen peroxide; however, we investigated the influence of the enzymatic purification protocol – including the two hydrogen peroxide steps – on films of eight different plastic polymers (polypropylene (PP), polyethylene (PE), polyvinyl chloride (PVC), polyurethane (PUR), polyamide (PA), polyethylene terephthalat (PET), polystyrene (PS), polycarbonate (PC)) in terms of IR spectra and weight loss. The effects of the enzymatic purification on all polymers, even on the sensitive polymers like PA, PET, PC, PUR, and PS, were negligible, while these polymers were strongly affected by other treatments with acids or bases (own unpublished data). We are aware that synthetic fibers with their higher surface area to volume ratio, very small aged, and oxidized particles or paint particles are probably more sensitive to the enzymatic purification approach with the two hydrogen peroxide steps than the virgin polymer films tested. However, the fact that we regularly find such MPs in the environmental samples that were processed with the enzymatic purification protocol suggests that the influence on these types of MP is also negligible.

Concerning the efficiency of the enzymatic purification approaches, it was previously reported in Courtene-Jones et al.[31] that the digestion of mussel tissues with trypsin reached a purification efficiency of 88%. In contrast, Catarino et al.[30] reported that mussel tissues could obviously be 100% digested using protease, which is similar to the digestion achieved using acidic or alkaline treatments. Cole et al.[23] reported that an enzymatic treatment with proteinase-K reached a higher purification efficiency for biota-rich plankton samples than using acid or alkaline treatments. The efficiency of our BEPP (98.3%) is similar to the values reported by Cole et al.[23] for proteinase-K (>97%) used for the purification of plankton samples. However, the BEPP requires an incubation time of up to 16 days instead of hours. While the BEPP requires a long duration, the actual handling time to filtrate and add new solutions is of course much shorter (in total around 3–4 h per sample), and many samples can be processed in parallel, which relativizes the time requirement. In contrast, our protocol does not require – besides filtration – any pretreatment steps, such as drying and grinding the sample as reported in Cole et al.,[23] which bears the risk of fragmenting the larger and brittle MPs into smaller pieces and thus potentially biasing the results.

A further advantage of our approach is the use of technical grade enzymes that are comparably inexpensive. Concerning the costs, a direct comparison with the other studies that used an enzymatic purification is difficult, as we used a series of enzymes and the other studies only one. However, the technical grade protease we used, for example, is by a factor of around 20,000 cheaper than e.g. proteinase-K. Furthermore, the use of a modular approach with different specialized enzymes allows for the digestion of different matrices regardless of the sample type. Our approach was additionally combined with a final density separation step with $ZnCl_2$, which proved to be important for the efficient elimination of the remaining inorganic residues. To reduce costs, the $ZnCl_2$ can be recycled by filtration. The total costs for the purification of one sample with the BEPP including all chemicals and enzymes lie in the single-digit euro range.

Although we were able to show that the BEPP is a very effective approach for the purification of MPs in environmental samples, the multiple filtration and rinsing steps involved in the purification protocol pose the risk of losses of MPs during processing. We thus estimated the potential equipment-specific loss of MPs during the purification process without the additional effect of an environmental sample matrix. We therefore purposely chose Milli-Q water as matrix and PE beads as reference MPs. We are aware that every different sample matrix will potentially have its own intrinsic recovery rate, which is potentially different for different polymers and size classes of MPs. Nevertheless, the determination of the equipment-specific recovery rate with Milli-Q as sample matrix revealed that only minor particle losses can occur during the entire purification process, thus allowing realistic quantification results. Careful rinsing during the sample processing can further mitigate the potential losses of MPs.

A series of environmental samples from the German Bight, in which a high amount of water was filtered (12.7–61.2 m^3) – resulting in a high load of organic matrix – were processed successfully with the BEPP and showed different numbers of MPs ranging from 0.05 to 4.42 items m^{-3}. To compare these values to numbers reported in other studies, it has to be mentioned that a mesh size of 100 μm was used. However, the determined numbers were comparable to the results from studies performed in the Northern Atlantic (mesh size 250 μm, 0–22.5 items m^{-3}),[35] the English Channel (mesh size 200 and

DOI: 10.1021/acs.est.7b03055
Environ. Sci. Technol. 2017, 51, 14283–14292

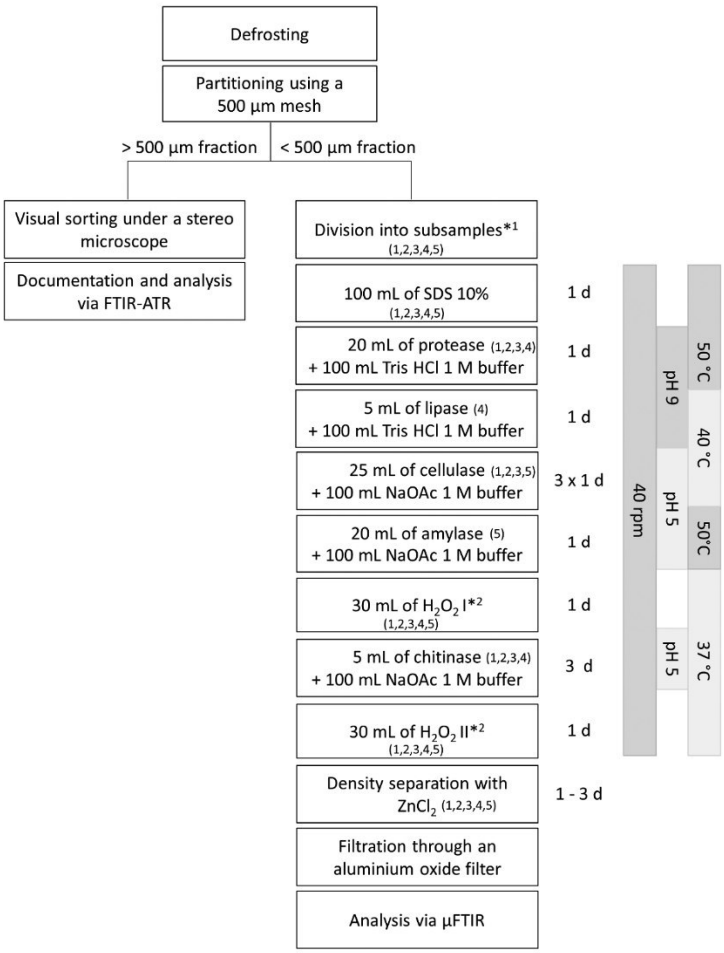

Figure 5. Universal enzymatic purification protocol. The optimized protocol (detailed description of the modifications in the SI) is suitable for purifying MPs from a wide range of different environmental matrices including plankton, extracted sediment, and biota. The incubation times represent the minimum values. The numbers represent the types of samples that are suggested to be purified with the respective purification step: 1 − plankton samples, 2 − extracted sediment samples, 3 − wastewater samples, 4 − lipid-rich biota samples (e.g., mussels, fish gut content, etc.) and other lipid-rich samples, 5 − samples with a high polysaccharide content, e.g. food samples, samples with high loads of plant material or algae. *1 Depending on the amount of matrix present, the samples can be divided before purification; depending on the amount of residue present, they can be reunified for analysis after purification. *2 The hydrogen peroxide steps can be replaced with wet peroxide oxidation, as described below.

500 μm, 0.26−0.31 items m^{-3}),[23] the Atlantic Ocean (mesh size 250 μm, 0−8.5 items m^{-3}),[36] and the Portuguese coast (mesh size 180−335 μm, 0−0.04 items m^{-3}),[37] in which the particles were also reliably identified using FTIR or Raman microspectroscopy.

Universal Enzymatic Purification Protocol (UEPP). Although the BEPP was originally developed for seawater surface samples,[14] in modified versions, it can be used to purify other environmental sample matrices, including freshwater plankton samples,[34] extracted sediment samples, wastewater samples,[32] tissue samples of mussels, daphnia, and fish organs,[38] and commercial fish food (partly unpublished data). The general procedure of filtration and incubation as described above remains the same; however, slight adjustments in the BEPP were necessary while considering the chemical composition of each sample matrix.

The final changes in the BEPP that resulted in the UEPP (Figure 5) are described here briefly, whereas a detailed description of the methods and results from the experiments that led to these adjustments is available in the SI (Optimization procedures). Experiments regarding the application of the enzymes were conducted in cooperation with the manufacturer of the enzymes (ASA Spezialenzyme GmbH).

Important improvements that led to the UEPP are suggested here as follows: (1) larger incubation bottles were used, (2) an optional subdivision of the samples was conducted prior to the purification for cases with high loads of the sample matrix, (3) the SDS concentration was increased to 10% (w/w), (4) the used buffers were replaced with tris(hydroxymethyl)-aminomethane (Tris) buffer (pH 9) and sodium acetate buffer (pH 5), (5) two optional steps (lipase and amylase) for samples with a high content of lipids or polysaccharides were added (e.g., food, biota samples, and water samples with a high organic plant or algae content; lipase is applied after the protease step, to account for lipids released during the digestion of e.g. tissue; amylase is applied after the cellulase step to further digest degradation products of the previous step), (6) the incubation conditions were changed to improve the

DOI: 10.1021/acs.est.7b03055
Environ. Sci. Technol. 2017, 51, 14283−14292

efficiency of the enzymatic purification (higher turnover/less time required), and (7) an option to replace both hydrogen peroxide steps with a wet peroxide oxidation protocol was added.

Generally, the modified version – the UEPP – incorporates all the above-mentioned advantages of the BEPP. However, improvements made by experience facilitate now the purification of a broader range of environmental sample matrices and their final concentration through filters for a subsequent reliable analyses via FPA-based micro-FTIR spectroscopy. The UEPP has thus a great potential to be implemented as a standard operation protocol for purifying samples during routine monitoring studies on MPs. Nevertheless, the samples that are purified with the UEPP should be examined carefully for their matrix composition. The necessary steps strongly depend on this composition, and the relevant steps for a sample type given in Figure 5 are just a suggestion, e.g. if a sample does not contain heavy material like sand a density separation with zinc chloride is not necessary.

■ ASSOCIATED CONTENT

Supporting Information

The Supporting Information is available free of charge on the ACS Publications website at DOI: 10.1021/acs.est.7b03055

Sample stations of RV Heincke cruise "HE409" and optimization procedures for the universal enzymatic purification protocol (UEPP) (PDF)

■ AUTHOR INFORMATION

Corresponding Authors

*Phone: +49(0)921/552209. Fax: +49(0)921/552784. E-mail: martin.loeder@uni-bayreuth.de.

*Phone: +49(0)921/552650. Fax: +49(0)921/552784. E-mail: christian.laforsch@uni-bayreuth.de.

*Phone: +49(0)4725/8193245. Fax: +49(0)4725/8193283. E-mail: gunnar.gerdts@awi.de.

ORCID

Martin G. J. Löder: 0000-0001-9056-8254

Hannes K. Imhof: 0000-0003-4992-5357

Present Addresses

§Department of Animal Ecology I and BayCEER, University of Bayreuth, Universitätsstrasse 30, 95440 Bayreuth, Germany.

∥Soil & More International B.V., Buttstraße 3, 22767 Hamburg, Germany.

⊥Copernicus Institute of Sustainable Development, Environmental Science Group, Utrecht University, P.O. Box 80115, 3508 TC Utrecht, The Netherlands.

Notes

The authors declare no competing financial interest.

■ ACKNOWLEDGMENTS

The authors would like to thank the German Federal Ministry of Education and Research and the Alfred Wegener Institute - Helmholtz Centre for Polar and Marine Research (AWI) for funding the projects MICROPLAST (BMBF grant 03F0631A) and BASEMAN (BMBF grant 03F0734A). Equally, we would like to thank the Bavarian State Ministry of the Environment and Consumer protection for funding the project "Eintragspfade, Vorkommen und Verteilung von Mikroplastikpartikeln in bayerischen Gewässern sowie mögliche Auswirkungen auf aquatische Organismen". Furthermore, we would like to thank ASA Spezialenzyme GmbH for their support with the optimization of the enzyme incubation conditions, Ursula Wilczek for her support in the laboratory, and finally, all the members of the MPs groups of the AWI and University of Bayreuth for fruitful discussions.

■ REFERENCES

(1) Barboza, L. G. A.; Gimenez, B. C. G. Microplastics in the marine environment: Current trends and future perspectives. *Mar. Pollut. Bull.* **2015**, *97* (1–2), 5–12.

(2) Cózar, A.; Echevarría, F.; González-Gordillo, J. I.; Irigoien, X.; Úbeda, B.; Hernández-León, S.; Palma, Á. T.; Navarro, S.; García-de-Lomas, J.; Ruiz, A.; Fernández-de-Puelles, M. L.; Duarte, C. M. Plastic debris in the open ocean. *Proc. Natl. Acad. Sci. U. S. A.* **2014**, *111* (28), 10239–10244.

(3) Browne, M. A.; Chapman, M. G.; Thompson, R. C.; Amaral Zettler, L. A.; Jambeck, J.; Mallos, N. J. Spatial and temporal patterns of stranded intertidal marine debris: Is there a picture of gobal change? *Environ. Sci. Technol.* **2015**, *49* (12), 7082–7094.

(4) Hidalgo-Ruz, V.; Gutow, L.; Thompson, R. C.; Thiel, M. Microplastics in the Marine Environment: A Review of the Methods Used for Identification and Quantification. *Environ. Sci. Technol.* **2012**, *46* (6), 3060–3075.

(5) Eerkes-Medrano, D.; Thompson, R. C.; Aldridge, D. C. Microplastics in freshwater systems: A review of the emerging threats, identification of knowledge gaps and prioritisation of research needs. *Water Res.* **2015**, *75*, 63–82.

(6) Dris, R.; Imhof, H. K.; Sanchez, W.; Gasperi, J.; Galgani, F.; Tassin, B.; Laforsch, C. Beyond the ocean: Contamination of freshwater ecosystems with (micro-) plastic particles. *Environ. Chem.* **2015**, *12* (5), 539–550.

(7) GESAMP *Sources, fate and effects of microplastics in the marine environment: A global assessment*; 90; IMO/FAO/UNESCO-IOC/UNIDO/WMO/IAEA/UN/UNEP/UNDP Joint Group of Experts on the Scientific Aspects of Marine Environmental Protection: 2015.

(8) Vethaak, A. D.; Leslie, H. A. Plastic Debris Is a Human Health Issue. *Environ. Sci. Technol.* **2016**, *50* (13), 6825–6826.

(9) Wagner, M.; Scherer, C.; Alvarez-Muñoz, D.; Brennholt, N.; Bourrain, X.; Buchinger, S. Microplastics in freshwater ecosystems: what we know and what we need to know. *Environ. Sci. Eur.* **2014**, *26* (1), 12.

(10) Löder, M. G. J.; Gerdts, G. Methodology used for the detection and identification of microplastics – a critical appraisal. In *Marine Anthropogenic Litter*; Bergmann, M., Gutow, L., Klages, M., Eds.; Springer: Berlin, 2015; DOI: 10.1007/978-3-319-16510-3_8.

(11) Enders, K.; Lenz, R.; Stedmon, C. A.; Nielsen, T. G. Abundance, size and polymer composition of marine microplastics ≥ 10 μm in the Atlantic Ocean and their modelled vertical distribution. *Mar. Pollut. Bull.* **2015**, *100* (1), 70–81.

(12) Imhof, H. K.; Laforsch, C.; Wiesheu, A. C.; Schmid, J.; Anger, P. M.; Niessner, R.; Ivleva, N. P. Pigments and plastic in limnetic ecosystems: A qualitative and quantitative study on microparticles of different size classes. *Water Res.* **2016**, *98*, 64–74.

(13) Primpke, S.; Lorenz, C.; Rascher-Friesenhausen, R.; Gerdts, G. An automated approach for microplastics analysis using focal plane array (FPA) FTIR microscopy and image analysis. *Anal. Methods* **2017**, *9* (9), 1499–1511.

(14) Löder, M. G. J.; Kuczera, M.; Mintenig, S.; Lorenz, C.; Gerdts, G. Focal plane array detector-based micro-Fourier-transform infrared imaging for the analysis of microplastics in environmental samples. *Environ. Chem.* **2015**, *12* (5), 563–581.

(15) Lenz, R.; Enders, K.; Stedmon, C. A.; Mackenzie, D. M. A.; Nielsen, T. G. A critical assessment of visual identification of marine microplastic using Raman spectroscopy for analysis improvement. *Mar. Pollut. Bull.* **2015**, *100* (1), 82–91.

(16) Käppler, A.; Fischer, D.; Oberbeckmann, S.; Schernewski, G.; Labrenz, M.; Eichhorn, K.-J.; Voit, B. Analysis of environmental

DOI: 10.1021/acs.est.7b03055
Environ. Sci. Technol. 2017, 51, 14283–14292

microplastics by vibrational microspectroscopy: FTIR, Raman or both? *Anal. Bioanal. Chem.* **2016**, *408* (29), 8377−8391.
(17) Claessens, M.; De Meester, S.; Van Landuyt, L.; De Clerck, K.; Janssen, C. R. Occurrence and distribution of microplastics in marine sediments along the Belgian coast. *Mar. Pollut. Bull.* **2011**, *62* (10), 2199−204.
(18) Imhof, H. K.; Schmid, J.; Niessner, R.; Ivleva, N. P.; Laforsch, C. A novel, highly efficient method for the separation and quantification of plastic particles in sediments of aquatic environments. *Limnol. Oceanogr.: Methods* **2012**, *10*, 524−537.
(19) Nuelle, M.-T.; Dekiff, J. H.; Remy, D.; Fries, E. A new analytical approach for monitoring microplastics in marine sediments. *Environ. Pollut.* **2014**, *184* (0), 161−169.
(20) Van Cauwenberghe, L.; Devriese, L.; Galgani, F.; Robbens, J.; Janssen, C. R. Microplastics in sediments: A review of techniques, occurrence and effects. *Mar. Environ. Res.* **2015**, *111*, 5−17.
(21) Thompson, R. C.; Olsen, Y.; Mitchell, R. P.; Davis, A.; Rowland, S. J.; John, A. W. G.; McGonigle, D.; Russell, A. E. Lost at Sea: Where Is All the Plastic? *Science* **2004**, *304* (5672), 838.
(22) Claessens, M.; Van Cauwenberghe, L.; Vandegehuchte, M. B.; Janssen, C. R. New techniques for the detection of microplastics in sediments and field collected organisms. *Mar. Pollut. Bull.* **2013**, *70* (1−2), 227−33.
(23) Cole, M.; Webb, H.; Lindeque, P. K.; Fileman, E. S.; Halsband, C.; Galloway, T. S. Isolation of microplastics in biota-rich seawater samples and marine organisms. *Sci. Rep.* **2015**, *4*, 4528.
(24) Dehaut, A.; Cassone, A.-L.; Frère, L.; Hermabessiere, L.; Himber, C.; Rinnert, E.; Rivière, G.; Lambert, C.; Soudant, P.; Huvet, A.; Duflos, G.; Paul-Pont, I. Microplastics in seafood: Benchmark protocol for their extraction and characterization. *Environ. Pollut.* **2016**, *215*, 223−233.
(25) Foekema, E. M.; De Gruijter, C.; Mergia, M. T.; van Franeker, J. A.; Murk, A. J.; Koelmans, A. A. Plastic in North Sea Fish. *Environ. Sci. Technol.* **2013**, *47* (15), 8818−8824.
(26) Karami, A.; Golieskardi, A.; Choo, C. K.; Romano, N.; Ho, Y. B.; Salamatinia, B. A high-performance protocol for extraction of microplastics in fish. *Sci. Total Environ.* **2017**, *578*, 485−494.
(27) Collard, F.; Gilbert, B.; Eppe, G.; Parmentier, E.; Das, K. Detection of Anthropogenic Particles in Fish Stomachs: An Isolation Method Adapted to Identification by Raman Spectroscopy. *Arch. Environ. Contam. Toxicol.* **2015**, *69* (3), 331−339.
(28) Tagg, A. S.; Harrison, J. P.; Ju-Nam, Y.; Sapp, M.; Bradley, E. L.; Sinclair, C. J.; Ojeda, J. J. Fenton's reagent for the rapid and efficient isolation of microplastics from wastewater. *Chem. Commun.* **2017**, *53* (2), 372−375.
(29) Enders, K.; Lenz, R.; Beer, S.; Stedmon, C. A. Extraction of microplastic from biota: recommended acidic digestion destroys common plastic polymers. *ICES J. Mar. Sci.* **2017**, *74* (1), 326−331.
(30) Catarino, A. I.; Thompson, R.; Sanderson, W.; Henry, T. B. Development and optimization of a standard method for extraction of microplastics in mussels by enzyme digestion of soft tissues. *Environ. Toxicol. Chem.* **2017**, *36*, 947−951.
(31) Courtene-Jones, W.; Quinn, B.; Murphy, F.; Gary, S. F.; Narayanaswamy, B. E. Optimisation of enzymatic digestion and validation of specimen preservation methods for the analysis of ingested microplastics. *Anal. Methods* **2017**, *9*, 1437−1445.
(32) Mintenig, S. M.; Int-Veen, I.; Löder, M. G. J.; Primpke, S.; Gerdts, G. Identification of microplastic in effluents of waste water treatment plants using focal plane array-based micro-Fourier-transform infrared imaging. *Water Res.* **2017**, *108*, 365−372.
(33) Vandermeersch, G.; Van Cauwenberghe, L.; Janssen, C. R.; Marques, A.; Granby, K.; Fait, G.; Kotterman, M. J. J.; Diogène, J.; Bekaert, K.; Robbens, J.; Devriese, L. A critical view on microplastic quantification in aquatic organisms. *Environ. Res.* **2015**, *143* (Part B), 46−55.
(34) Mani, T.; Hauk, A.; Walter, U.; Burkhardt-Holm, P. Microplastics profile along the Rhine River. *Sci. Rep.* **2016**, *5*, 17988.
(35) Lusher, A. L.; Burke, A.; O'Connor, I.; Officer, R. Microplastic pollution in the Northeast Atlantic Ocean: Validated and opportunistic sampling. *Mar. Pollut. Bull.* **2014**, *88* (1−2), 325−333.
(36) Kanhai, L. D. K.; Officer, R.; Lyashevska, O.; Thompson, R. C.; O'Connor, I. Microplastic abundance, distribution and composition along a latitudinal gradient in the Atlantic Ocean. *Mar. Pollut. Bull.* **2017**, *115* (1−2), 307−314.
(37) Frias, J. P. G. L.; Otero, V.; Sobral, P. Evidence of microplastics in samples of zooplankton from Portuguese coastal waters. *Mar. Environ. Res.* **2014**, *95*, 89−95.
(38) Fischer, M.; Scholz-Böttcher, B. M. Simultaneous Trace Identification and Quantification of Common Types of Microplastics in Environmental Samples by Pyrolysis-Gas Chromatography−Mass Spectrometry. *Environ. Sci. Technol.* **2017**, *51* (9), 5052−5060.

DOI: 10.1021/acs.est.7b03055
Environ. Sci. Technol. 2017, 51, 14283−14292

Article B1: Supplementary information

Sample stations

Table S1. Sample stations investigated in this work from the RV Heincke cruise "HE409" in September 2013

Sample	Station "HE409"	Date	Duration [min]	Starting Position N	Starting Position E	Ending Position N	Ending Position E	Distance [m]	Filtered Volume [m^3]
1	1	19.09.2013	15	54°04.43	7°26.73	54°4.46	7°28.90	1524.0	45.72
2	3	19.09.2013	18	53°51.99	6°21.77	53°52.83	6°22.44	1946.1	58.38
3	6	20.09.2013	6	53°19.48	7°00.1	53°19.31	7°00.41	604.8	18.14
4	8	21.09.2013	8	53°52.95	7°36.16	53°53.13	7°37.37	955.8	28.67
5	9	21.09.2013	12	53°41.72	8°04.05	53°42.05	8°03.82	1080.3	32.41
6	10	21.09.2013	13	53°33.05	8°10.68	53°32.77	8°10.63	1016.1	30.48
7	11	22.09.2013	6	53°33.28	8°33.06	53°33.31	8°33.03	423.0	12.69
8	13	22.09.2013	11	53°50.14	8°08.12	53°50.14	8°07.99	671.4	20.14
9	15	22.09.2013	16	54°08.79	7°49.92	54°08.83	7°51.19	2038.5	61.16
10	17	23.09.2013	15	54°41.36	7°55.91	54°41.32	7°55.30	892.2	26.77

Optimization procedures

Incubation bottles

The 100 mL glass bottles were replaced with 250 mL glass jars with glass lids during the purification process.

Division into subsamples

Environmental samples with high loads of a sample matrix are difficult to process. We suggest dividing the samples into subsamples with an equal load of matrix prior to the enzymatic purification process to increase the efficiency of the purification. After purification, the samples can be combined again prior to the spectroscopic analysis depending on the amount of sample residue that remains.

Increase in the SDS concentration

We suggest increasing the concentration of the SDS solution from 5 to 10 % (w/w) in the first purification step as this has been proven to yield even better purification results.

Buffer

A PBS solution in water has a pH of 7.4, and the pH can be adjusted by adding NaOH or HCl, but the buffer capacity will be lost. Therefore, we suggest the use of more appropriate buffer systems for optimizing the pH for enzymes. For pH 9, we suggest using a tris(hydroxymethyl)aminomethane (Tris) buffer, and for pH 5, we suggest using a sodium acetate buffer (NaOAc). Both are well established in biology and biochemistry laboratory applications, they are low cost and easy to prepare, and furthermore, they ensure a stable pH regime during the time of incubation.

pH 9: Tris HCl 1 M buffer

For a 1 L buffer solution, 121.14 g of Tris is dissolved in 800 mL of ultrapure water, and a pH value of 9 is achieved using concentrated HCl. After, the solution is filled to 1 L.

pH 5: NaOAc (C2H3NaO2) 1 M buffer

For 1 L buffer solution, 82.03 g of NaOAc (anhydrous) is dissolved in 800 mL of ultrapure water, and a pH value of 5 is achieved using concentrated acetic acid. The solution is filled to 1 L.

Additional treatments for the purification of samples with a high lipid or polysaccharide content

For samples with a high content of lipids or polysaccharides (e.g. food, biota samples, water samples with a high organic plant or algae content), we suggest including additional enzymes in the purification protocol as such samples are only partially purified with the BEPP, leading to undesired sample residues. For this reason, two optional enzymatic purification steps are included in the UEPP: one step with lipase and one step with amylase.

In particular, biota samples can have a high lipid content; thus, we included a lipase step after the proteinase step into the UEPP in order to digest the lipids in such samples. The application of amylase after the cellulase step was found to be helpful for samples with a high polysaccharide content as it is frequently present in food samples or water samples with a high organic plant content or algae concentration.

Lipase

The lipase treatment targets the digestion of lipids in samples usually containing high amounts of lipids, e.g., the tissues of different biota. Lipase FE-01 (EC 3.1.1.3, ASA Spezialenzyme GmbH, Wolfenbüttel, Germany) was used, which is a triacylglycerol acylhydrolase that is obtained from the fungus *Aspergillus oryzae.* The Lipase splits lipids into glycerol and fatty acids. Lipase FE-01

attains its optimum reaction activity at pH 10.5 and 40 °C. During this purification step, 5 mL of Lipase FE-01 (activity >13.000 U/mL) was used, and 100 mL of a Tris HCl 1 M buffer solution, set to pH 9.0 by adding hydrochloric acid, was added. The samples were incubated at 40 °C for one day.

Amylase

In particular, freshwater samples with high loads of plant material after the cellulose step or samples of agricultural products, such as fish food, can contain polysaccharides, which can be reduced by amylase enzymes. Amylase FL was used (EC 3.2.1.1, ASA Spezialenzyme GmbH, Wolfenbüttel, Germany), which has a specific activity of >40.000 U/mL and was obtained from *Aspergillis niger.* It consists of 1,4-α-D-glucan glucanohydrolase, which cleaves the α-1,4-bonds in starch. The amylase reaches its maximum enzyme activity at a pH of 5.0 and a temperature of 45-55 °C. A total of 20 mL of amylase was added to 100 mL of a NaOAc (C2H3NaO2) 1 M buffer, at pH 5, for 1 day of incubation at 50 °C.

Enzyme incubation conditions

Enzyme activity

In the preliminary enzymatic purification protocol, enzymes were applied for up to 5 days. However, the efficiency of an enzyme reduces with time, the number of turn-over cycles and the increasing concentration of the end products (end product inhibition). Therefore, after a certain time period, the solution had to be filtered, and new enzymes were added to achieve an efficient purification. In cooperation with the manufacturer of the enzymes (ASA Spezialenzyme GmbH), the enzymatic activity (U/mL) was tested over 24 h (0 h, 2 h, 4 h, 7 h and 24 h) to reveal the optimal point for enzyme exchange. This was performed for protease (5 mL of Protease A-01 + 25 mL of Tris HCl buffer, pH 9, 50 °C), lipase (1 mL of Lipase FE-01 + 25 mL of Tris HCl buffer, pH 9, 50 °C), amylase (5 mL of Amylase TXL + 25 mL of NaOAc buffer, pH 9, 50 °C), cellulase (1 mL of Cellulase TXL + 25 mL of NaOAc buffer, pH 5, 50°C) and chitinase (1 mL of chitinase + 25 mL of NaOAc buffer, pH 5, 35 °C).

The activities of chitinase and lipase were nearly unaffected after 24 h. The cellulase activity was reduced to approximately 50 % after this time period, the protease activity reduced more than 50 % after 2 h, and the amylase activity reduced more than 95 % after 2 h (Table S2). Therefore, protease and cellulase should be exchanged with a new enzyme solution within 24 h. If necessary the amylase step should be repeated after 4 h, or a different amylase should be used.

Table S2. Enzymatic activity of the protease, lipase, amylase, cellulase and chitinase according to the incubation time

Enzyme solution	pH	T (°C)	Enzymatic activity (U/ml)				
			0 h	2 h	4 h	7 h	24 h
5 mL of Protease A-01 + 25 of mL Tris-HCl buffer	9	50	569	363	254	182	96
1 mL of Lipase FE-01 + 25 of mL Tris-HCl buffer	9	50	552	576	499	600	504
5 mL of Amylase TXL + 25 mL of NaOAc buffer	5	50	3574	128	10	0	0
1 mL of Cellulase TXL + 25 mL of NaOAc buffer	5	50	3,3	3,0	2,8	2,5	1,8
1 mL of Chitinase + 25 mL of NaOAc buffer	5	35	3,2	3,6	3,0	3,4	3,3

Simultaneous use of different enzymes

To reduce the number of purification steps, a combination of enzymes with the same optimum temperature and buffer would be useful. Therefore, we investigated, in cooperation with the manufacturer of the enzymes (ASA Spezialenzyme GmbH), the activity of the enzymes after 0 h, 2 h, 4 h, 7 h and 24 h, using two enzymes simultaneously. First, 5 ml of Protease A-01 was combined with 1 mL of Lipase FE-01 (25 mL Tris HCl buffer, pH 9, 50 °C), and 5 mL of Amylase TXL was used together with 1 mL of Cellulase XTL (25 mL NaOAc buffer, pH 5, 50°C).

The combination of lipase and protease reduced the activity of lipase after 2 h, and the activity of protease is reduced by approximately 80 % (Table S3). The combination of amylase and cellulase reduced the cellulase activity to approximately 85 %, whereas the amylase activity was not affected. Therefore, it is not possible to combine enzymes to decrease the necessary time of incubation.

Table S3. Enzymatic activity of the combined enzymes according to the incubation time

Enzyme solution	pH	T (°C)	Enzymes	Enzymatic activity (U/ml)				
				0 h	2 h	4 h	7 h	24 h
5 mL of Protease A-01 + 1 mL of Lipase FE-01 + 25 mL of Tris-HCl buffer	9	50	Protease	516	340	294	172	104
			Lipase	348	12	12	0	0
5 mL of Amylase TXL + 1 mL of Cellulase TXL + 25 mL of NaOAc buffer	5	50	Amylase	3433	120	9	0	0
			Cellulase	4,3	2,4	1,9	1,4	0,68

Temperature stability of the cellulase

Although cellulase (Cellulase TXL, ASA Spezialenzyme GmbH) is active in the temperature range of 35 – 60 °C with an optimum at 50 °C, enzyme flocculation can be observed at 50 °C. This can have a negative impact on the filtering capacity of the used stainless steel filters and thus hinder the entire process and subsequent analysis. Therefore, in cooperation with the manufacturer of the enzymes (ASA Spezialenzyme GmbH), we tested the flocculation of the cellulase by incubating 20 mL of cellulase for 24 h in a water bath at a lower temperature (40 °C) in comparison with the optimal temperature (50 °C). To investigate the activity at both temperatures, 2.5 mL of Cellulase TXL and 12.5 mL of 0.1 M NaOAc (pH 5) were incubated at 40 °C and 50 °C, respectively, for 72 h. After 24 h and 48 h, an additional 2.5 mL of cellulase was added. The "C1"-activity of the cellulase (U/mL) and the substrate conversion (µmol/min) in the samples were determined after the following time points: 0 h, 24 h (before and after adding further cellulase), 28 h (before and after adding further cellulase), and 72 h.

The flocculation test showed 5 % flocculation at a temperature of 40 °C and 40 % flocculation at 50 °C (Table S4). At 50 °C, 100 % of the substrate in the sample was converted compared to 81.6 % at 40 °C, and the activity (U/mL) was over 30 % higher at 50 °C. Cellulase should be used at 40 °C to avoid flocculation, which disturbs the filtration process and the analysis. A disadvantage of using this temperature is that the activity is reduced compared to 50 °C. Therefore, the cellulase step should be repeated three times with an accordingly higher concentration, and the cellulase solution should be renewed every 24 h.

Table S4. Cellulase activity ("C1"-activity) and substrate conversion in the sample at 40 °C and 50 °C

Incubation time	"C1"- activity of the cellulase (U/mL)			
	40 °C		50 °C	
	Measured in the sample (U/mL)	Substrate conversion (µmol/min)	Measured in the sample (U/mL)	Substrate conversion (µmol/min)
0 h	6.5	4.4	10.9	10.9
24 h (before adding more cellulase)	6.2	4.2	3.8	3.8
24 h (after adding more cellulase)	22.9	15.7	23.6	23.6
48 h (before adding more cellulase)	21.2	14.5	14.2	14.2
48 h (after adding more cellulase)	34.1	23.3	30.6	30.6
72 h	34.4	23.5	21.7	21.7
Substrate conversion after 72 h (µmol)		61.6		75.5
Substrate conversion after 72 h (%)		81.6%		100 %
"C1"-activity of Cellulase TXL (U/mL)	44.1		64.5	

Wet peroxide oxidation

To further increase the efficiency, we suggest replacing both hydrogen peroxide steps with a wet peroxide oxidation step using Fenton's reagent, as described by Baker, et al. [1] This is a solution of hydrogen peroxide with ferrous iron as the catalyst. A detailed description of its application is also available in Masura, et al. [2] This method has been used to successfully purify MPs from wastewater without showing detrimental effects on the MPs itself [3]. The catalytic reaction is an exothermic reaction that can lead to an increase in the incubation temperature above 70 °C, at which some synthetic polymers, such as polyethylene, start to melt. To avoid damaging the MPs, we thus strongly suggest cooling the incubation bottles in a water bath at a maximum temperature of 40 °C after the catalytic reaction has started.

References:

(1) Baker, J. E.; Foster, G. D.; Masura, J. E. Methods for the analysis of microplastics in water samples. George Mason University: Fairfax, VA, **2011**.

(2) Masura, J.; Baker, J. E.; Foster, G.; Arthur, C.; Herring, C. *Laboratory methods for the analysis of microplastics in the marine environment: Recommendations for quantifying synthetic particles in waters and sediments*; Technical Memorandum NOS-OR&R-48; **2015**.

(3) Tagg, A. S.; Harrison, J. P.; Ju-Nam, Y.; Sapp, M.; Bradley, E. L.; Sinclair, C. J.; Ojeda, J. J. Fenton's reagent for the rapid and efficient isolation of microplastics from wastewater. *Chemical Communications* **2017,** *53*, (2), 372-375.

Article B2: Abundance and distribution of large microplastics (1-5 mm) within beach sediments at the Po River Delta, northeast Italy

Piehl S, Mitterwallner V, Atwood EC, Bochow M, Laforsch C (2019)

Marine Pollution Bulletin 149

Marine Pollution Bulletin 149 (2019) 110515

Contents lists available at ScienceDirect

Marine Pollution Bulletin

journal homepage: www.elsevier.com/locate/marpolbul

Abundance and distribution of large microplastics (1–5 mm) within beach sediments at the Po River Delta, northeast Italy

Sarah Piehl[a,1], Veronika Mitterwallner[a], Elizabeth C. Atwood[b,c], Mathias Bochow[a,2], Christian Laforsch[a,*]

[a] University Bayreuth, Dept. Animal Ecology I and BayCEER, Universitätsstr. 30, 95440 Bayreuth, Germany
[b] RSS Remote Sensing Solutions GmbH, Dingolfinger Str. 9, 81673 München, Germany
[c] Ludwig-Maximilians-Universität Munich, GeoBio-Center, Großhadernerstr. 2, 82152 Planegg-Martinsried, Germany

ARTICLE INFO

Keywords:
Microplastics
Beach sediment
Small-scale distribution
Monitoring
ATR-FTIR
Po River Delta

ABSTRACT

Coastal areas are especially prone to plastic debris, being subjected to various land- and sea-based sources. Nevertheless, knowledge about microplastic distribution on beaches is limited, as studies focused either on high tide lines, specific items, or relied on visual identification. Beaches exhibit several accumulation zones and microplastic deposition depends on particle properties. We thus studied microplastic distribution (1–5 mm), including various types and shapes, among three driftlines at three beaches within the Po River Delta. Particles were analyzed using ATR-FTIR spectroscopy. Abundances ranged from 2.92 (± 4.86 SD) to 23.30 (± 45.43 SD) microplastics per kilogram dry weight between the beaches. The accumulation of microplastics among driftlines showed no consistent pattern, besides expanded polystyrene tending to accumulate backshore. We observed that accumulation hotspots within a single driftline can disrupt a general observed accumulation pattern. Thus, microplastic monitoring guidelines should further include protocols for the handling of accumulation hotspots within datasets.

1. Introduction

As plastic pollution of marine ecosystems has become a widely acknowledged environmental problem, it has been placed on the agenda at the highest international levels (EU, 2018; G7, 2015; UNEP, 2016). Thereby, "microplastics", plastic pieces commonly defined as smaller than five millimeters, have particularly attracted the attention of scientists. Those fragments can reach the environment as primary microplastics, being intentionally produced for applications for example in cosmetics and cleansing products and released via wastewater effluents (Ziajahromi et al., 2016). Here, combined sewer overflows during heavy rainfall (Gasperi et al., 2014) or the spillage of pre-production pellets from industrial premises (Lechner and Ramler, 2015) are likely to be important input sources. Nevertheless, secondary microplastics, arising from fragmentation of plastic debris already present in the environment, currently seems to be the major input into the environment (Bergmann et al., 2015). Recent research efforts focusing on microplastic debris are driven by the ability of microplastics to infiltrate diverse matrices, as for example soil (Piehl et al., 2018; Van Cauwenberghe et al., 2015; Zhang et al., 2018), air (Dehghani et al., 2017; Dris et al., 2015a), and water (Dris et al., 2015b; Rezania et al., 2018; Wagner et al., 2014). Microplastics have also been found to enter food webs at various levels (Rezania et al., 2018), with yet unknown consequences for ecosystems and human health (Koelmans et al., 2017; Revel et al., 2018). Despite these unknowns, a precautionary principle should be adopted, as one of the major concerns with microplastic particles (MPPs) is that, once introduced into the environment, they hardly can be removed and will probably persist for centuries (Andrady, 2015).

Among the above-mentioned environmental compartments studied, beach sediments represent the interface between the ocean and terrestrial habitats. They are thus especially vulnerable for both land- as well as sea-based microplastic debris inputs, often exhibiting high numbers of MPPs (Hidalgo-Ruz et al., 2012; Rezania et al., 2018). Besides being an accumulation zone for microplastic debris, their relatively easy access makes them quite suitable areas for monitoring activities. Thereby, the assessment of MPP contamination levels within beach habitats is important for both a proper risk analysis and an

* Corresponding author.
E-mail address: christian.laforsch@uni-bayreuth.de (C. Laforsch).
[1] Present address: Coastal Research and Management Group, Leibniz-Institute for Baltic Sea Research Warnemuende (IOW), Seestr. 15, 18110 Rostock, Germany.
[2] Present address: Helmholtz Centre Potsdam - GFZ German Research Centre for Geosciences, Telegrafenberg, 14473 Potsdam, Germany

https://doi.org/10.1016/j.marpolbul.2019.110515
Received 3 May 2019; Received in revised form 10 August 2019; Accepted 11 August 2019

evaluation of plastic contamination trends. Currently, a full-scale investigation of MPP contamination levels of beaches with state-of-the-art methodologies is not feasible. Especially the investigation of small MPPs (< 1 mm) requires time- and cost-intensive sampling, sample processing, and analysis techniques. Here, the Technical Subgroup on Marine Litter (TSG-ML) suggests in their "Monitoring Guidance for Marine Litter in European Seas" to use adapted strategies for monitoring of large MPPs (1–5 mm) and small MPPs (0.02–1 mm), primarily lying in the use of different analytical techniques for identification and quantification (). In this context, some studies have already addressed the problem of a proper sampling strategy to reveal representative microplastic contamination levels on sandy beaches, even though the dynamic nature of beaches makes it a difficult task to undertake. For example, Turra et al. (2014) investigated the three-dimensional distribution of MPPs on sandy beaches in Brazil and found that the distribution of MPPs was neither uniform along the beach profile nor with depth. Additionally, Moreira et al. (2015) focused on driftlines during twelve consecutive tidal cycles and found high small-scale spatial and temporal variability. Nevertheless, both studies concentrated on "pellets" (industrial raw material) which, depending on the investigated area, constitute only a fraction of all MPPs > 1 mm (Bond et al., 2014; Fok et al., 2017; Young and Elliott, 2016). Other studies investigating all types of MPPs provide contradictory results. For example, Dekiff et al. (2014) detected a vertical homogenous distribution for MPPs < 1 mm, whereas Heo et al. (2013) found a non-uniform vertical distribution (MPPs from 1 to 20 mm).

Yet, there remains a high uncertainty about microplastic accumulation patterns given the recommended size classes by the MSFD as well as considering all polymer types and shapes. To extend current knowledge on MPP distribution on sandy beaches, we set a focus on large MPPs since this is the size class currently feasible for routine monitoring programs, and taking into consideration various polymer types and shapes. We investigated MPP abundance along three different accumulation zones (i.e. driftlines) at three beaches within the Po River Delta. The area was chosen for two reasons. On the one hand, it exhibits a unique habitat supporting an immense biodiversity and constituting one of the most important UNESCO "World Heritage sites" (Gaglio et al., 2017). On the other hand, it is vulnerable to plastic debris input from the Po River, listed as the second most important marine litter source into the Adriatic Basin, close behind shipping lanes whose density is also highest offshore of the Po River Delta (Liubartseva et al., 2016). We hypothesize, that (I) MPP abundance will increase with increasing distance to the waterline, due to relocation processes by wind and water towards the upper shore, and (II) the relative abundance of polymer types will differ among accumulation zones, due to different densities of polymers likely influencing their transportation behavior.

2. Materials and methods

2.1. Study area

The catchment basin of the Po River extends over almost the whole northwest of Italy, spanning around 74000 km^2 (Fig. 1), and is inhabited by about one quarter of the Italian population (Artioli et al., 2005). Providing 40% of the national GDP, 37% of industrial production, 55% of cattle raised, and 35% of the agricultural production, the Po River has a substantial relevance as water supply and livestock/industry effluent disposal (Artioli et al., 2005; Fox et al., 2004). As the longest Italian river, with a daily average discharge of 1500 m^3/s, the Po River provides the largest riverine influx to the northern Adriatic Sea (Falcieri et al., 2014). The highest river discharge occurs in the spring, due to high precipitation and snowmelt, and the lowest in autumn (Falcieri et al., 2014). Two further large rivers influencing the studied area are the Adige (average discharge of 235 m^3/s; Munari et al., 2017) and Brenta (average discharge of 71 m^3/s; Volf et al., 2013), both of which discharge < 50 km northwards from the Po River Delta (Fig. 1) and together produce a single freshwater plume (Falcieri et al., 2014).

The Po River Delta itself covers an area of around 685 km^2, with a coastline spanning 64 km from north to south (Jiménez et al., 1995). It is directly affected by seven active branches of the terminal river system: Po di Maistra, Po di Pila (splitting into Busa di Tramontana, Busa Dritta, and Busa di Scirocco), Po di Tolle, Po di Gnocca, and Po di Goro (Maicu et al., 2018) (Fig. 1).

The prevailing currents of the northern Adriatic Sea flow counterclockwise, which are comprised of two coastal currents defined along the whole basin: the Eastern Adriatic Current (EAC) flowing northwards along the Dalmatian coast and the Western Adriatic Current (WAC) flowing southwards along the Italian coast (Zavatarelli, 2002) (Fig. 1). Tidal fluctuation is around 30 cm, but under specific conditions can reach up to 140 cm, and within the investigated area a slight increase of around 8 cm of the tidal range from south to north is described (Maicu et al., 2018). The northern Adriatic Sea has an average depth of 40 m, is sharply stratified, and the residence time of the water is about two years (Artioli et al., 2005).

2.2. Sample design and sampling

Three different sites were chosen at approximately 15-km intervals. The sampling site "Levante" (sample date: 06-13-2016) was located between the two river mouths, Po di Levante and Po di Maistra, in the northern part of the delta. The sampling site "Pila" (sample date: 06-16-2016) was situated just north of the major river mouth of Po di Pila. The third sampling site "Allagemento" (sample date: 06-22-2016) was stationed north of Po di Tolle, at the southern part of the delta (Fig. 1).

At each site, three accumulation zones were identified within the intertidal zone of the beaches: the most recent high tide line (HTL), an extreme tide line (ETL), and the most distant accumulation line to the sea, here defined as backshore (BSH). The ETL was defined as the line with the highest visible amount of washed ashore material. The BSH line was determined by the beginning of small sand dunes, bushy vegetation and/or steeply rising terrain (a graph of the sampling design and images of the sites are provided within S1 and S2 Supplementary material).

Transect lines were placed at those accumulation zones within the window of time between high tide cycles. Samples were taken with 10-m intervals, resulting in a total of eleven replicates for the site "Levante", nine replicates for the site "Allagemento", and six replicates for the site "Pila". A defined amount of sediment was collected using a stainless steel frame (25 × 25 cm), and the upper 5 cm of sediment was extracted using a metal spatula. The weight of each sample was measured using a customary scale before the volume was reduced by wet-sieving the samples with filtered tap water over stainless steel sieves with mesh sizes of 5 and 1 mm (Retsch GmbH). Samples were transferred into polyethylene (PE) sample bags to facilitate transportation and storage, whereas sample contamination through the used PE bags was not observed (see Section 2.5). To standardize MPP numbers to dry weight, an additionally 1-liter sediment sample from each transect was collected and stored in PE bottles. To calculate dry weight, first the wet weight of each one liter sample was determined on a laboratory scale (Sartorius 1219 MP), followed by drying at 60 °C (Memmert, Typ O 50, DW 12880-Kl.2) until a stable weight was reached. The calculated wet weight content was then used to calculate the dry weight of the field samples for microplastic analysis.

2.3. Microplastic sample processing

During field work, not all material < 1 and > 5 mm could be removed. Thus, a second wet-sieving of the samples with filtered water over 1 and 5 mm stainless steel sieves was conducted in the laboratory. Thereby, sample material > 5 mm was discarded after visual screening for attached smaller particles. A density separation with $ZnCl_2$ was conducted to further separate inorganic material with a higher density

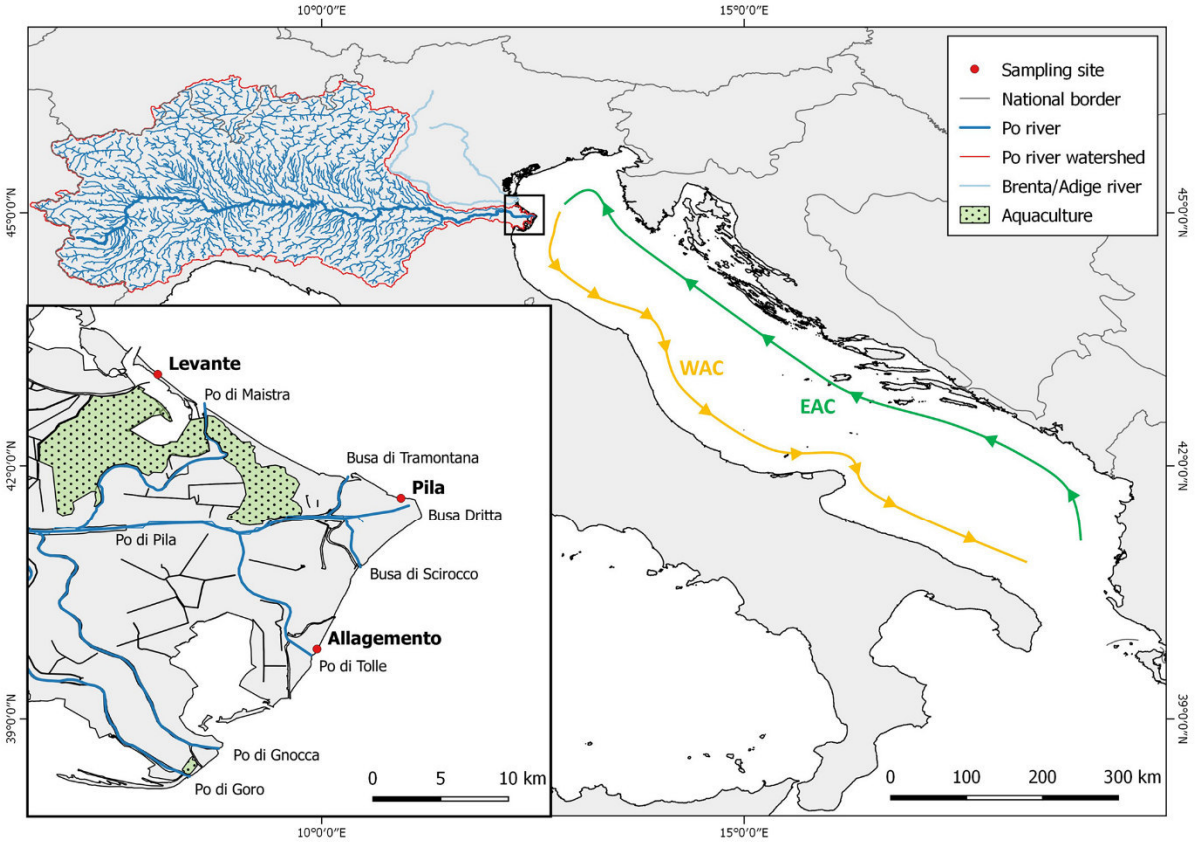

Fig. 1. Overview of the study system showing the Po River catchment area in northern Italy and the Adriatic Basin. The two coastal surface currents (EAC Eastern Adriatic Current, WAC Western Adriatic Current), as well as the two nearest rivers, Brenta and Adige are indicated. The enlarged study area (black box) displays the sampling sites, the seven active Po River branches, and areas used for aquaculture.

from polymer particles. As water within samples would reduce density of the $ZnCl_2$ solution, samples were first dried at 55 °C (Memmert, Typ O 50, DW 12880-Kl.2). To prevent light particles from getting lost, drying was conducted at the lowest ventilation setting. Afterwards, the samples were transferred into glass beakers and $ZnCl_2$ with a density of 1.6–1.8 g/cm^3 was added. Samples were stirred for 3 h followed by a 12h settling period. Next, the supernatant of each sample was extracted using a self-made mote spoon (stainless steel, mesh size < 1 mm) and rinsed with 98% ethanol. The extracted material was transferred into a petri dish for visual pre-sorting of potential MPPs. To categorize each particle according to shape, pictures of each potential polymer particle were taken under a stereomicroscope (Leica M50 with a cold light source Leica KL 300 LED, Leica Microsystems) equipped with a digital analysis system (camera: Olympus DP26, 5 Megapixel; software: cellSens, Olympus Corporation). For subsequent spectroscopic measurements, each particle was labelled and stored in a 1.5 ml Eppendorf tube.

2.4. Polymer identification

To identify polymer types, the spectrum of every potential polymer particle was measured with a Tensor 27 FTIR spectrometer further equipped with a Platinum-ATR-unit (Bruker Optik GmbH). To increase accuracy, eight pooled background scans were taken at the beginning and after each tenth measurement. Thereafter, eight co-added sample scans were recorded. Spectra were recorded in the wavelength range of 4000 cm^{-1} to 400 cm^{-1}, with a spectral resolution of 8 cm^{-1}. Obtained spectra were analyzed with the Software OPUS 7.5 (Bruker Optik GmbH). To identify the polymer type, a comparative analysis of the resulting spectra was done against a reference polymer library including the most common polymers as well as natural materials (Löder et al., 2015). For spectral search, spectra were first vector normalized and a correlation search algorithm of the first derivative was used. This allowed for more emphasis to be put at steep edges of spectrum peaks, which are typical for synthetic polymer materials. The identified polymer types were grouped into four different classes: PE, polypropylene (PP), polystyrene (PS; predominantly PS, but also includes one styrene-acrylonitrile and one acrylonitrile butadiene styrene particle), and "Others". The category "Others" included polymers with a minor contribution to the total abundance, namely ethylene vinyl alcohol/acetate (EVOH/EVA), polyethylene terephthalate (PET), polyurethane (PUR), polyamide (PA), polyvinyl chloride (PVC), polyester (PEST), polybutylene terephthalate (PBT), and one agglomeration of fibers which was marked as unknown due to the mixture of different polymers. Polymer particles were categorized by shape in five classes, namely spheres, pellets, fragments, ropes, and fibers.

2.5. Contamination prevention

Even though the probability of sample contamination with MPPs from the surroundings and used materials is negligible given the investigated size class of > 1 mm, several measures against

Table 1
Descriptive statistics of the three beaches for the different transects showing microplastics per kilogram dry weight and respective standard deviation (SD), standard error (SE) and relative standard error (%SE). BSH backshore, ETL extreme tide line, HTL high tide line.

Beach	Transect	Median	Mean	SD	SE	%SE
Levante	BSH	9.28	11.57	11.43	3.45	29.78
(n = 11)	ETL	17.43	52.61	70.78	21.34	40.57
	HTL	5.29	5.72	5.16	1.56	27.18
Total		9.28	23.30	45.43	7.91	33.94
Pila	BSH	9.08	10.47	7.47	3.05	29.12
(n = 6)	ETL	2.28	5.28	7.07	2.88	54.66
	HTL	3.94	4.35	1.33	0.54	12.45
Total		4.44	6.70	6.27	1.48	22.06
Allagemento	BSH	6.22	7.21	6.58	2.19	30.43
(n = 9)	ETL	0.24	0.47	0.50	0.17	35.89
	HTL	0.51	1.09	1.40	0.47	42.77
Total		0.72	2.92	4.86	0.94	32.00

contamination were taken. These included the usage of stainless steel and glassware whenever possible, coverage of the samples with aluminum foil or glass lids, filtering of all chemicals and water used for sample processing over stainless steel mesh (pore size of 5 µm), and use of laboratory coats made of cotton during sample processing. As the samples were stored in PE bags for transportation to the laboratory, all bags were carefully controlled for signs of abrasion after the sample material was transferred to the glass beakers. As no signs of abrasions were detected on the PE transport bags and weathering of the bags during the short storage time is unlikely, it can be assumed that possible contamination is negligible for the investigated size class of > 1 mm.

2.6. Statistical analysis

All statistical analyses were performed using the statistic software R (v3.5.0) with the platform RStudio (v1.1.447). To test hypothesis I, i.e. the abundance of MPPs will increase with increasing distance to the waterline, and hypothesis II, i.e. the relative abundance of different polymer types will differ between accumulation zones, the three beaches were analyzed separately using parametric analysis of variance (ANOVA). To meet the assumption of normally distributed errors, MPP abundance data was log(x + 1) transformed for hypothesis I and 4th root transformed for hypothesis II. Fulfillment of the assumption was checked using histograms and Shapiro-Wilk test. A Bartlett test was conducted to check for homogeneity of variances, or in case of a non-normal distribution of errors, Fligner-Killeen test was used. Significant differences of MPP abundance between the accumulation zones backshore (BSH), extreme tide line (ETL), and high tide line (HTL) were analyzed using one-tailed orthogonal contrasts for the directional hypothesis I. Two-tailed TukeyHSD post-hoc tests were conducted to evaluate non-directional hypothesis II of differences in the accumulation of different polymer types among the accumulation zones. In case assumptions were violated, the non-parametric Kruskal-Wallis rank sum test was used together with Games-Howell post-hoc test to identify significant differences among the accumulation zones. Differences were accepted as significant at $p < 0.05$, and all results are shown as average ± one standard deviation.

To analyze the effect of sampling frequency on variance, resampling with replacement was performed on the given replicates within an accumulation zone. More specifically, for each beach accumulation zone (BSH, ETL, and HTL), in a first step two values were randomly extracted from all replicates along a transect and the mean calculated, which was repeated 50 times. In a second step, the number of extracted values was increased by one (for a total of three) and the whole procedure repeated. Subsequent steps followed accordingly, always increasing the extracted values by one, until a modelled replication of 20 sample units was reached. To visualize the influence of sampling frequency on the precision of the obtained mean, margin of errors around the sample mean were calculated for the confidence levels 90% (Z = 1.65), 95% (Z = 1.96), and 99% (Z = 2.56) following Besley et al. (2017):

$$Z * SD/SQRT(N)$$

where SD is the standard deviation of the sample mean and N the number of extracted values. The margin of error around the mean, expressed in units of standard deviation, was subsequently plotted against number of samples.

3. Results

3.1. Microplastic abundance at sandy beaches of the Po River Delta

Of the 3451 total analyzed particles, 3395 particles (98%) were identified as a synthetic polymer. Most MPPs were found at the northern most sampling site Levante, with a total of 768.88 and an average abundance of 23.30 (± 45.43) MPPs per kilogram dry weight (DW). Pila followed with a total of 120.56 MPPs per kilogram DW (average of 6.70 ± 6.27 MPPs per kilogram DW) and 78.89 MPPs per kilogram DW (average of 2.92 ± 4.86 per kilogram DW) at Allagemento, located at the southernmost part of the delta. Tables 1 and 2 present an overview of these abundance densities.

Polyethylene was the polymer most often recorded at site Levante (54.2%) and the second most abundant polymer found at sites Pila (33.6%) and Allagemento (15.2%) (Table 2, Fig. 2). At these two sites, PS was the most common polymer found (Pila: 52.2%; Allagemento: 77.5%), while PS was the second most common polymer at site Levante (26.8%) (Table 2, Fig. 2). Another numerously occurring polymer was PP: Levante (13.7%), Pila (8.3%), and Allagemento (6.5%). Within the category "Others", totals of 131 EVOH/EVA particles, 21 PET particles, 8 PUR particles, 5 PA particles, 4 PVC particles, 2 PEST particles, 1 PBT particle, and the one unknown fiber agglomeration were found. These polymer types comprised little of the overall MPP abundance at the sites Levante (5.4%) and Pila (5.8%), and only 0.8% at the site Allagemento (Table 2, Fig. 2).

Regarding the shape of the MPPs, fragments were predominant (3224 particles; 95.0%) for all three beaches. At the site Levante, almost all MPPs were in the shape category fragment (96.5%), with further occurrences of spheres (49 particles; 1.9%), pellets (18 particles; 0.7%), fibers (14 particles; 0.5%), and ropes (11 particles; 0.4%). A slightly different pattern was observed at the site Pila, where fiber-conglomerates (24 particles; 5.2%) were the second most common shape,

Table 2
Microplastic particles per kilogram dry weight (± SD) for the different polymer types and within the three different transects of the investigated beaches. BSH backshore, ETL extreme tide line, HTL high tide line. PE polyethylene, PP polypropylene, PS polystyrene, Other (ethylene vinyl alcohol/acetate, polyethylene terephthalate, polyurethane, polyamide, polyvinyl chloride, polyester, polybutylene terephthalate).

Transect	Polymer	Levante (n = 11)	Pila (n = 6)	Allagemento (n = 9)
BSH	PE	46.92 ± 4.20	11.89 ± 1.30	5.13 ± 0.54
	PP	13.96 ± 1.48	4.70 ± 0.59	2.72 ± 0.28
	PS	63.81 ± 6.63	44.24 ± 5.60	57.01 ± 6.14
	Other	2.58 ± 0.29	2.00 ± 0.21	0.00 ± 0.00
Total		127.26 ± 4.47	62.82 ± 3.94	64.86 ± 3.97
ETL	PE	359.11 ± 46.52	19.62 ± 5.37	0.45 ± 0.10
	PP	83.32 ± 10.85	3.25 ± 0.45	0.23 ± 0.08
	PS	100.20 ± 10.92	6.83 ± 1.33	3.52 ± 0.38
	Other	36.05 ± 3.83	1.97 ± 0.43	0.00 ± 0.00
Total		578.68 ± 26.38	31.66 ± 2.86	4.19 ± 0.25
HTL	PE	10.41 ± 0.97	9.03 ± 0.70	6.41 ± 0.86
	PP	7.71 ± 0.69	2.09 ± 0.25	2.18 ± 0.42
	PS	41.64 ± 3.70	11.88 ± 0.92	0.61 ± 0.14
	Other	3.19 ± 0.47	3.08 ± 0.34	0.63 ± 0.21
Total		62.94 ± 2.35	26.08 ± 0.90	9.84 ± 0.54

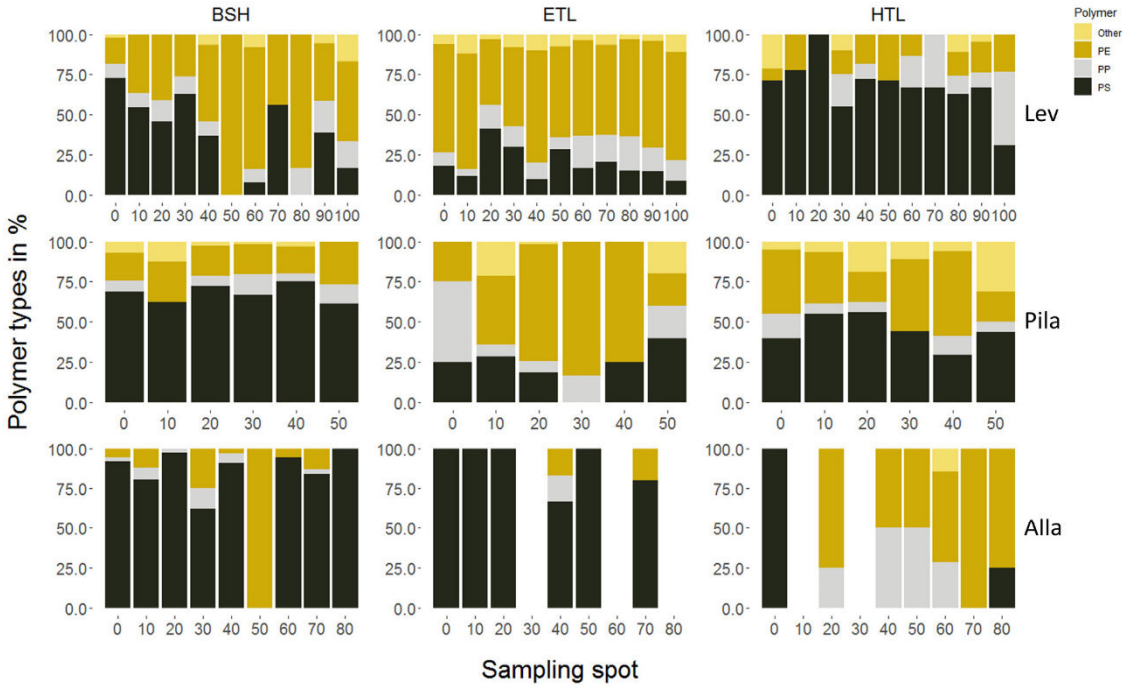

Fig. 2. Percentage share of the different polymer types for each sampling spot at the different sampled accumulation zones at the three sampling sites Levante (Lev; n = 11), Pila (n = 6), and Allagemento (Alla; n = 9). BSH backshore, ETL extreme tide line, HTL high tide line. PE polyethylene, PP polypropylene, PS polystyrene, Other (ethylene vinyl alcohol/acetate, polyethylene terephthalate, polyurethane, polyamide, polyvinyl chloride, polyester, polybutylene terephthalate.

followed by spheres (21 particles; 4.5%) and pellets (11 particles; 2.4%). At the site Allagemento, pellets were the second most common shape (15 particles; 4.4%), followed by five spheres (1.5%) and three ropes (0.9%). Generally, most spheres were made of PS (85.3%) and fibers were predominantly aggregated to conglomerates (81.6%).

3.2. Across-shore distribution among three accumulation zones

Across-shore variability was highest for the sampling site Levante, ranging from 5.72 (± 5.16) to 52.61 (± 70.78) MPPs per kilogram DW, followed by Allagemento ranging from 0.47 (± 0.50) to 7.21 (± 6.58) MPPs per kilogram DW, and lowest for the site Pila with MPP abundances ranging from 4.35 (± 1.33) to 10.47 (± 7.47) (Table 1). The abundance of MPPs among the three sampled accumulation zones (BSH, ETL, and HTL) was significantly different at the sampling sites Levante and Allagemento (Table 3, Fig. 3). Nevertheless, hypothesis I (abundance of MPPs will increase with increasing distance to the waterline) was only accepted for the sampling site Allagemento and rejected for the sites Levante and Pila. Contrast analysis for the sampling site Levante revealed significantly higher MPP abundance at the accumulation zone ETL compared to the accumulation zone HTL (Table 3, Fig. 3) but not for the BSH. At the sampling site Allagemento, a significantly higher abundance of MPPs was found at the accumulation zone BSH compared to the accumulation zone ETL (Table 3, Fig. 3). For the sampling site Pila with only six replicates per accumulation zone, no significant differences between MPP abundance were detected among the accumulation zones ($p = 0.14$) but it was noted that the MPP abundance was also higher at the accumulation zone BSH as compared to the zones ETL and HTL (Table 3, Fig. 3).

Highest numbers of MPPs were found within the accumulation zone ETL at the site Levante, with PE being the dominant polymer type, whereas for Pila and Allagemento PS was dominating and highest numbers of MPPs were found within the accumulation zone BSH (Table 2, Fig. 2). For the majority of the sampling sites, PS was found to be the dominant polymer type in the accumulation zone BSH. Polypropylene had the lowest abundance among all investigated accumulation zones and beaches, besides the accumulation zone HTL at the sampling site Allagemento.

Hypothesis II (the relative abundance of different polymer types will differ between accumulation zones) was accepted for the polymer types PE and PP at the sites Levante and Allagemento and for PS at the sites Pila and Allagemento. Polyethylene was significantly differently distributed among the three accumulation zones at Levante (Table 3; Fig. 4). Subsequent post-hoc test showed a trend towards higher abundance of PE at the BSH as compared to the accumulation zone HTL ($p = 0.06$). A similar pattern at Levante was found for the abundance of PP among the three accumulation zones (Table 3; Fig. 4), with a significantly higher abundance of PP at the ETL as compared to the accumulation zone HTL and a significantly higher abundance of PP at the ETL as compared to the BSH (Table 3, Fig. 4). The abundance of PS did not differ among the three investigated accumulation zones at Levante ($p = 0.36$).

For the sampling site Pila, neither the abundance of PE ($p = 0.69$) nor the abundance of PP ($p = 0.29$) was found to differ significantly among the three accumulation zones. Only the abundance of PS differed significantly among the three accumulation zones according to ANOVA results (Table 3, Fig. 4). Nevertheless, post-hoc test revealed only a marginally higher abundance of PS at the accumulation zone BSH as compared to the accumulation zone ETL ($p = 0.09$).

For the accumulation zones at the site Allagemento, a significant difference was found for the polymer PS (Table 3, Fig. 4). Thereby, significantly more PS was found at the accumulation zone BSH as compared to the accumulation zones HTL and ETL (Table 3, Fig. 4). Further, a significant difference for the polymers PE and PP were found (Table 3, Fig. 4) with higher abundance of PE and PP at the accumulation zone BSH as compared to the accumulation zone ETL (Table 3,

Table 3
Results of analysis of variance (ANOVA) and p-values of subsequent analysis of differences between groups. Significant differences were checked with orthogonal contrasts for H01 and TukeyHSD as post-hoc test for H02 (Bonferroni corrected p-values are shown). In case of violations of assumptions (marked with an asterisk), non-parametric Kruskal-Wallis test and according Games Howell post-hoc tests were conducted. BSH backshore, ETL extreme tide line, HTL high tide line. PE polyethylene, PP polypropylene, PS polystyrene.

	ANOVA/Kruskal-Wallis results					Orthogonal contrasts		Post-hoc comparisons		
	DF	Test-statistic	Adj. r^2	p-value	N	BSH-ETL/HTL	ETL-HTL	ETL-HTL	BSH-HTL	BSH-ETL
H01: No differences between microplastic abundance among the three transects BSH, ETL, and HTL										
Levante	2,30	7.45	0.30	0.002	11	0.324	0.001	–	–	–
Pila	2,15	2.26	0.13	0.138	6	–	–	–	–	–
Allagemento*	2	10.01	–	0.007	9	–	–	0.446	0.057	0.036
H02 (PE): No differences between polyethylene abundance among the three transects BSH, ETL, and HTL										
Levante*	2	21.04	–	< 0.001	11	–	–	0.109	0.064	0.158
Pila	2	0.75	–	0.688	6	–	–	–	–	–
Allagemento*	2	7.10	–	0.029	9	–	–	0.112	0.910	0.048
H02 (PP): No differences between polypropylene abundance among the three transects BSH, ETL, and HTL										
Levante	2,30	6.55	0.26	0.004	11	–	–	0.004	0.609	0.042
Pila	2	2.48	–	0.290	6	–	–	–	–	–
Allagemento	2,24	3.49	0.16	0.047	9	–	–	0.253	0.592	0.040
H02 (PS): No differences between polystyrene abundance among the three transects BSH, ETL, and HTL										
Levante	2,30	1.05	0.00	0.361	11	–	–	–	–	–
Pila*	2	8.56	–	0.014	6	–	–	0.442	0.137	0.089
Allagemento	2,24	15.08	0.52	< 0.001	9	–	–	0.185	< 0.001	0.004

Fig. 4).

3.3. Along-shore distribution

Smallest along-shore variation within a transect ranged from 0 to 1.36 MPPs per kilogram DW at the accumulation zone ETL at Allagemento (S3 Supplementary material). The highest along-shore variation from 3.05 to 235.41 MPPs per kilogram DW was found for the accumulation zone ETL at Levante (S3 Supplementary material). This heterogeneity is also expressed in high SDs, particularly at the accumulation zone ETL, where values of the SDs are always higher than the mean values (Table 1). For the sampling sites Levante and Pila, the accumulation zone HTL exhibited the lowest within-site variability. Contrarily, the accumulation zone HTL at Allagemento showed the highest variability (Table 1), probably influenced by the general low abundances found at this site. Along-shore distribution patterns of total MPP abundances per kilogram DW for the different accumulation zones and sampling sites are shown in S5 of the Supplementary material.

Those results are reflected by the resampling analysis, assessing how many replicates need to be taken to achieve a given standard deviation with a given confidence level (Fig. 5). For example, if a standard deviation of one from the mean is set as an acceptable value of spread for a given confidence level, then sampling the accumulation zone HTL requires the least numbers of samples within a transect (Fig. 5). Considering the accumulation zones ETL and BSH, a minimum of 10 samples are required to reach a confidence level of 90% for the sampling sites Pila and Allagemento (Fig. 5b and c). For the sampling site Levante, a standard deviation of one for the accumulation zone ETL could not be reached with the set upper limit of 20 samples. For the accumulation zone BSH at the site Levante, 14 samples would be required to

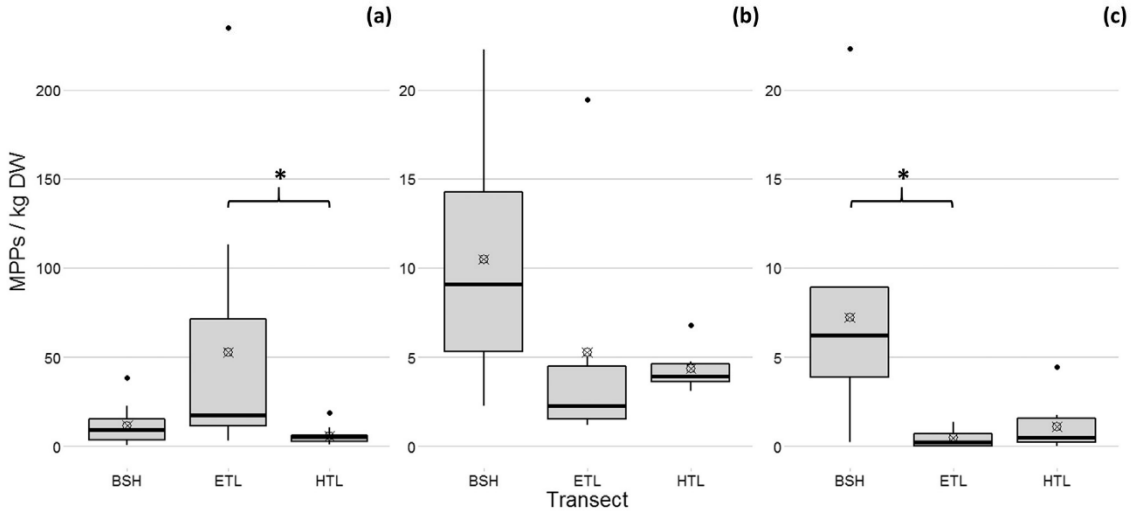

Fig. 3. Difference of microplastic abundance of the three accumulation zones. Microplastic particles (MPPs) per kilogram dry weight (DW) for sampling site (a) Levante (n = 11), (b) Pila (n = 6), and (c) Allagemento (n = 9). Mean values are indicated by a cross-circle symbol (⊠) and ANOVA resulting in significant differences ($p < 0.05$) are marked by an asterisk. Note the different scales of the y-axis. BSH backshore, ETL extreme tide line, HTL high tide line.

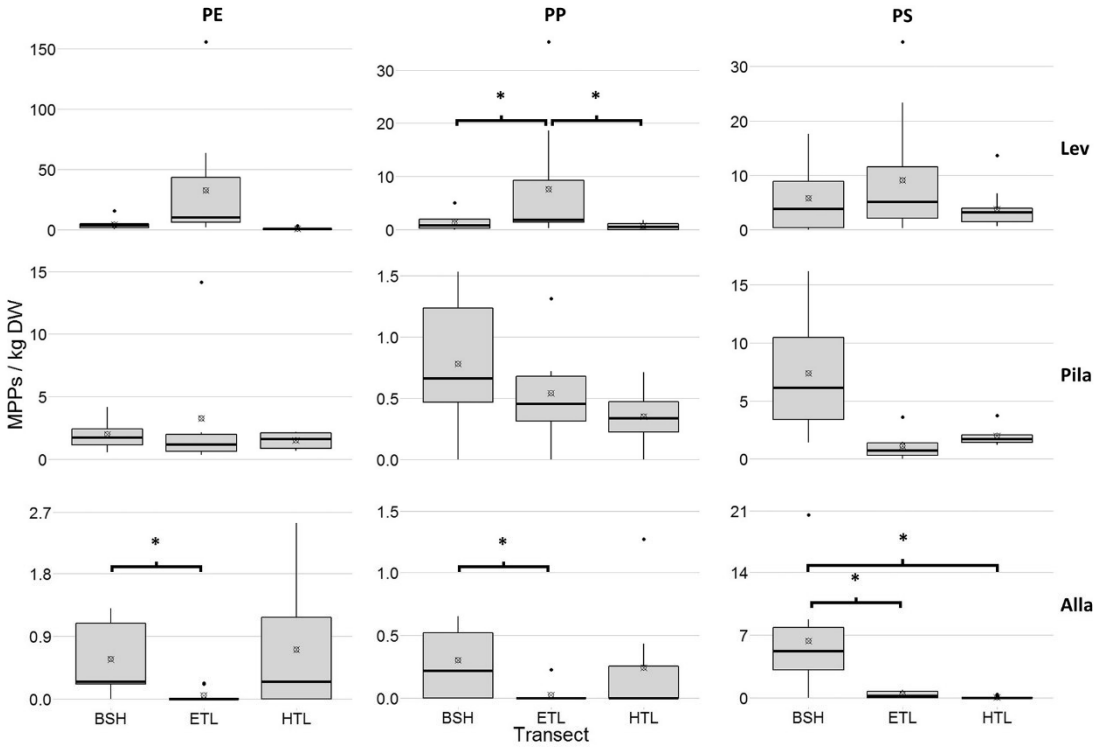

Fig. 4. Comparison of polymers of the different accumulation zones for sampling site Levante (Lev; n = 11), Pila (n = 6), and Allagemento (Alla; n = 9). Mean values are indicated by a cross-circle symbol (⊗). ANOVA resulting in a significant difference ($p < 0.05$) are marked with an asterisk. Note the different scales of the y-axis. BSH backshore, ETL extreme tide line, HTL high tide line. PE polyethylene, PP polypropylene, PS polystyrene.

achieve a standard deviation of one for a confidence level of 90% (Fig. 5a).

4. Discussion

4.1. Microplastic abundance on sandy beaches of the Po River Delta

The mean abundance of MPPs, within the size range from 1 to 5 mm, found at the three investigated beaches ranged from 2.92 (± 4.86) to 23.30 (± 45.43) MPPs per kilogram DW (Table 1). Considering only the mean MPP abundance at the HTL (ranging from 1.09 ± 1.40 to 5.72 ± 5.16 MPPs per kg DW), the found quantities are lower than numbers reported by Munari et al. (2017) (5.99 ± 3.53 to 21.63 ± 12.8 MPPs per kilogram DW) sampling large MPPs at the HTL north and south of the Po River Delta. The discrepancy between these results could be due to the time span of one year in between sampling campaigns, as the recent high tide line rather represents a snapshot of contamination and is known to exhibit daily variations (Imhof et al., 2017). It should also be noted that the samples in our study were taken at beaches with limited access for visitors, which could also explain differences in sampled MPP abundances among studies.

At our sampling sites, MPPs are likely to be transported from either nearby sources, like intensively practiced aquaculture within the lagoons and maritime recreational activities, or distant sources, like runoff from land-based industries, agriculture, effluents of sewage treatment plants, or sewer overflows. The higher MPP abundance found at the site Levante can potentially be attributed to the rivers Brenta and Adige, as well as the Venetian lagoon, all representing further close-by major microplastic sources. For the Venetian Lagoon, a study of subtidal sediment samples revealed already high MPP abundances (Vianello et al., 2013). The reported numbers of 672 to 2175 MPPs per kilogram DW point towards a substantial source of plastic debris in this area and possibly also for the nearby Po River Delta.

Accumulation at the beaches occurs due to the natural sedimentation process of the Po River Delta. Thereby, microplastic debris from the above-mentioned sources is transported via the southward flowing Western Adriatic Current (WAC) to the investigated sites (Fig. 1). Here, a general trend of decreasing MPP contamination from north (Levante) to south (Allagemento) was observed (Table 1). Through the protruding form of the delta, beaches north of Po di Pila are generally more exposed to the WAC, whereas beaches south of Po di Pila are more shaded from the current by the delta itself. Thus, MPPs transported by the WAC are more prone to beach at the sites Levante and Pila. For example, at the sampling site Levante more seashells were observed, spreading over the entire beach (S2 Supplementary material), which could point towards increased hydrodynamic energies (waves, currents) and lead to higher inputs of MPPs (Chubarenko et al., 2018). Nevertheless, the general observed decreasing trend of MPP contamination from north to south is not necessarily reflected on a smaller spatial scale as indicated by a study from Atwood et al. (2019). Here, local factors such as differing MPP export within the Po River branches probably play another important role.

Considering hydrodynamical factors at the sampling site Allagemento, its sheltered position with regard to the WAC could explain the lowest found abundance of MPPs at this site. Due to the smaller width of the beach, it could additionally be more influenced by tides and thus, MPPs are perhaps more often redistributed and the probability of export is increased. Especially at the site Allagemento, PS made up 77.5% of the total number of found MPPs. Here, density

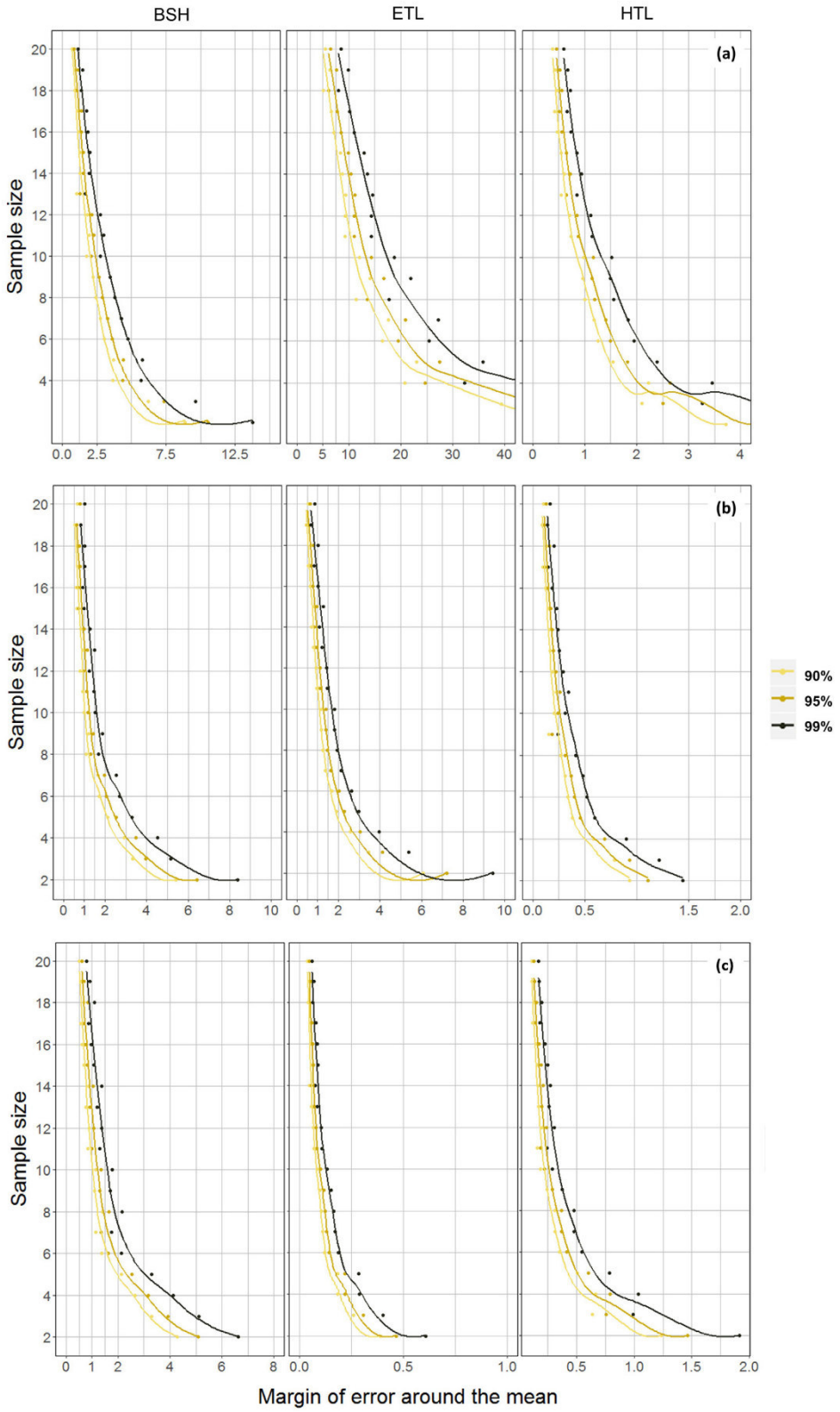

(caption on next page)

Fig. 5. Sampling frequency analysis for the three accumulation areas of the sampling site (a) Levante, (b) Pila, and (c) Allagemento. The impacts of different confidence levels on sample size for the three accumulation zones are shown with sample size on the y-axis and the margin of error around the mean expressed in units of standard deviation on the x-axis. BSH backshore, ETL extreme tide line, HTL high tide line. Note the different scales on the y-axis.

gradients between the river plume and the surrounding Adriatic Sea water could entrap higher density plastics inside the river plume, transporting them away from the shore, whereas expanded PS could be subjected to wind drift and thus overcome density-related water barriers and reach the beaches more easily.

Considering polymer types, FTIR spectroscopy revealed PE (468.97 particles per kilogram DW) as the most common polymer type, followed by PS (329.74 particles per kilogram DW), and PP (120.16 particles per kilogram DW) (Table 2). The high abundance of PE and PP can be explained by high production volumes and use, especially for packaging materials (PlasticsEurope, 2018) and thus its higher probability for becoming plastic litter. Furthermore, PS also has been found to constitute a major component of MPPs in previous published studies (Clunies-Ross et al., 2016; Imhof et al., 2017; Kang et al., 2015; Yu et al., 2016), and is associated with aquaculture (Heo et al., 2013), which is extensively conducted within the delta (Munari et al., 2017) and along the entire coast.

In accordance with the assumption that secondary microplastics are the major component of MPP contamination, fragments were the most abundant shape found within this study. Fibers on the other hand were rarely observed, which can be explained by the set lower size limit of 1 mm allowing fibers (usually exhibiting diameters between 6 and 175 µm: Cole et al., 2015; Dris et al., 2016, 2018) to pass. Similarly, spheres (such as primary MPPs used as ingredients of cosmetics and abrasive agents) are usually smaller than 50 µm (UNEP, 2015) and are most likely being underestimated by our analysis. Within this study, only pre-production pellets could be attributed as primary MPPs with certainty. The proportion of pellets in the present study was low (1.3%), even though three pellet-producing and pellet-processing plants are closely located to the study area (Munari et al., 2017). Either the industry is already sensitive considering spillage of pre-production pellets (Munari et al., 2017) or pellets reaching the river mouth are transported by the WAC further away to beaches south of the delta.

4.2. Across-shore distribution among three accumulation zones

Our first hypothesis (I) of increasing MPP abundance with increasing distance to the waterline could statistically not be confirmed (Table 3, Fig. 3). This is in accordance with a study of Lo et al. (2018), investigating MPP abundance among three tidal heights at ten sites, who also did not find a consistent pattern among the distribution of MPPs across three different sampled accumulation zones. Nevertheless, most studies have shown increasing MPP abundances towards the upper beach (Heo et al., 2013; Imhof et al., 2018; Turner and Holmes, 2011; Turra et al., 2014), which is in accordance with our study for the uppermost accumulation zone BSH at the sites Pila and Allagemento (Fig. 3).

Regarding polymer type distribution our second hypothesis (II) could be confirmed in most cases. Polystyrene for example, with the one exception of an extreme value at Levante (cook's distance > 4 times the mean; S4 Supplementary material), showed a consistent pattern of increasing abundances towards the upper beach for all three sites, reflecting the general pattern for the sites Pila and Allagemento due to the high share of this polymer type. These results are in accordance with a recent study by Lo et al. (2018), who found more foamed MPPs at the strandline furthest from the high tide mark (comparable to BSH in this study). Once cast ashore, secondary deposition of lower shore accumulated MPPs by wind-action is another process for MPP transport towards the upper shore (Heo et al., 2013; Imhof et al., 2018) and thus should have a higher influence on low-density particles. Consequently, PS particles accumulate more distant to the water and are therefore less impacted by wave action and tide cycles. Relocation by wind may play an important role for long-term accumulation processes (Imhof et al., 2017). At the Po River Delta, transport of particles to the upper shore for the northern and southern area is influenced by different wind regimes. The northeasterly Bora and northwesterly blowing Mistral winds, more frequently occurring during winter, have a higher influence on the northern beaches Levante and Pila, whereas the site Allagemento is more influenced by the east-southeasterly Scirocco winds, occurring more frequently between spring and autumn.

The polymer types PE and PP, exhibiting a density around 0.9 g/cm^{-3}, showed no clear accumulation patterns at the investigated sites. At the site Pila the accumulation patterns even differed among the polymer types (Fig. 4). Another interesting aspect which can be seen in Fig. 4 is that at site Levante PE and PP mostly accumulated at the ETL, whereas those polymers showed a contradictory pattern at the site Allagemento with higher abundances at the BSH and HTL as compared to the ETL.

At the site Levante, the higher abundance of PE and PP at the ETL as compared to the HTL could be due to higher export rates at the HTL given frequent water contact of the water-nearest accumulation zone results in direct input and output of MPPs (Imhof et al., 2018). Regarding accumulation patterns at the site Allagemento, the general lower MPP abundance at this site together with no MPPs being observed for some replicates needs to be considered. Wave-action and seastorm events further influence the dispersion of debris across the beach sediment, as storm waves redispose beach sediment and thus also move already stranded MPPs towards upper lines along the beach shore (Chubarenko et al., 2018). The smaller width of the sampling site Allagemento could enhance such redispersion rates, either moving particles to the upper shore or exporting particles within the intertidal back to the sea.

Considering monitoring strategies, one needs to consider exactly the purpose of the monitoring applied. If for example the focus is to assess the general trend of pollution, sampling the recent high tide line could bias the results due to high daily variations (Imhof et al., 2017) and thus, accumulation zones further away from the waterline should be considered. On the other hand, if the focus is to monitor the effectiveness of a certain mitigation strategy, one possible could focus on specific polymer types or items. For example, if expanded PS used in aquaculture would be the target of a mitigation measure one could possibly focus on areas at the backshore as indicated by our results.

4.3. Along-shore distribution

As seen for the site Levante, the occurrence of accumulation hotspots can influence the observed distribution patterns. The morphology of a beach as well as small scale topographic heterogeneities or barriers could contribute to the observed heterogenic abundances with occasionally occurring accumulation hotspots. Besides a general strong along-shore patchiness of total MPP abundances (S6 Supplementary material), the along-shore distribution of single polymer types was also highly variable (Fig. 2). This is in accordance with previous studies (Chubarenko et al., 2018; Imhof et al., 2017) and shows further the high distribution variability of MPP abundances on various levels.

Current circulation cells are a major influencing factor for alongshore patchiness of both natural materials and MPPs (Chubarenko and Stepanova, 2017). A further explanation could be that floating MPPs exhibit coherent properties and therefore accumulate in patches (Imhof et al., 2017). In addition, beach morphology and vegetation patterns will determine accumulation areas for stranding particles. Microplastic distribution was especially heterogeneous in the upper beach

accumulation zones (Table 1), where disturbances like dunes, vegetation, or detritus occurred much more often. These structures might act as natural separators or increase the probability of entanglement of particles (Imhof et al., 2018; Turner and Holmes, 2011). The abovementioned main wind directions further influence redistribution of particles and, in conjunction with disturbances at the beach, additionally contribute to along-shore patchiness.

Against this background and based on the collected and elsewhere published data it is not straight forward to derive recommendations on sample replication for monitoring strategies. Concerning replication within a transect, the resampling analysis presented in our study revealed a high variability among sites and accumulation zones. For example, considering a standard deviation of 0.5 at a confidence level of 90%, around five replicates (HTL at Pila and Allagemento) to > 20 replicates (BSH and ETL at Levante) would be required. For comparison, Besley et al. (2017) found that the CI around the mean decreased rapidly after a replication of five, and 11 replicates would be sufficient. The difference between results could be due to the fact that Besley et al. (2017) included four different transects located at one site whereas we analyzed the resampling frequency for each site and accumulation zone separately.

According to the above stated results the suggestion of five replicates at the strandline by TSG-MSFD (Galgani et al., 2013) seems reasonable for this accumulation zone (HTL in our study). Yet, for the zones ETL and BSH our results are in accordance with those of Besley et al. (2017) and indicate the necessity to take at least twice as much samples. As the along-shore variability cannot be assessed before sampling, it seems thus plausible to take at least 10 replicates for the accumulation zones ETL and BSH as a compromise between accuracy and feasibility (within this study, 10 replicates within one transect were the maximum achievable for one persons at one day).

Nevertheless, we did not investigate along-shore variability on a larger scale. For example, Fisner et al. (2017) investigated transect replication on a 7-km beach at southeastern Brazil (in total 20 replicate transects with each seven samples) and found that at least 96 transects would be required to derive a density estimate within 50% of the mean. Thus, further studies are needed to come up with recommendations on how transects and samples within a transect should be replicated.

5. Conclusions

Our hypothesis of increasing MPP abundance with increasing distance to the waterline (hypothesis I) could statistically only be accepted for one site. Nevertheless, our results on MPPs (> 1 mm) of different polymer types and shapes support previous studies recommending to include different accumulation zones in sampling designs to obtain representative contamination levels of MPPs (Heo et al., 2013; Lo et al., 2018; Naji et al., 2017; Turra et al., 2014).

Our second hypothesis (II), that the relative abundance of polymer types varies among accumulation zones, could partly be accepted with no distinct pattern for a given polymer type. We further show that the general observed trend of positively correlated PS abundance with increasing distance to the waterline can be obscured by sampling spots with extreme MPP abundances. Such spots were found to seemingly occur randomly within the different accumulation zones examined in this study. According to the high along-shore variability of MPP abundances, overall resampling analysis indicated that at least five replicates for the HTL and 10 replicates for the ETL and BSH need to be taken to achieve an acceptable precision (standard deviation of one at a confidence level of 90%). Results of this study provide further insights into MPP abundances and distributions of various polymer types and shapes within a deltaic system and can be used to improve monitoring strategies on sandy beaches. Concurrently, immediate actions to curb plastic pollution, adressing both land- and sea-based sources, are required. Ideally these actions are transnational, since litter introduced into the northern Adriatic Sea is predestinated to be washed ashore at the protruding delta.

Acknowledgements

The authors would like to thank Lena Löschel who played a very important role in the preparation and analysis of the microplastic samples, and Heghnar Martirosyan and Annika Heymann are thanked for their help with ATR measurements. We would like to extend our thanks to Claudio our boat captain for bringing us to the remote beaches and Peter Schad for construction of the sampling frames. Sebastian Steibl and Anja Ramsberger for providing advice and linguistic improvements on the manuscript.

Funding source declaration

This research has been conducted as part of the project “Sentinels4marine plastic waste” funded by the German Federal Ministry for Economic Affairs and Energy (Bundesministerium für Wirtschaft und Energie, or BMWi) via the DLR Space Administration under the grant numbers 50EE1301 and 50EE1269.

Declaration of competing interest

The authors declare that no competing interests exist. Although the author ECA is affiliated with a commercial entity (RSS Remote Sensing Solutions GmbH), this does not alter their adherence to journal policies on sharing data and materials.

Appendix A. Supplementary data

Supplementary data to this article can be found online at https://doi.org/10.1016/j.marpolbul.2019.110515.

References

Andrady, L.A., 2015. Plastics and Environmental Sustainability. Wiley (324 pp).
Artioli, Y., Bendoricchio, G., Palmeri, L., 2005. Defining and modelling the coastal zone affected by the Po river (Italy). Ecol. Model. 184, 55–68. https://doi.org/10.1016/j.ecolmodel.2004.11.008.
Atwood, E.C., Falcieri, F.M., Piehl, S., Bochow, M., Matthies, M., Franke, J., Carniel, S., Sclavo, M., Laforsch, C., Siegert, F., 2019. Coastal accumulation of microplastic particles emitted from the Po River, Northern Italy: comparing remote sensing and hydrodynamic modelling with in situ sample collections. Mar. Pollut. Bull. 138, 561–574. https://doi.org/10.1016/j.marpolbul.2018.11.045.
Bergmann, M., Gutow, L., Klages, M., 2015. Marine Anthropogenic Litter, Marine Anthropogenic Litter. Springer International Publishing, Cham. https://doi.org/10.1007/978-3-319-16510-3.
Besley, A., Vijver, M.G., Behrens, P., Bosker, T., 2017. A standardized method for sampling and extraction methods for quantifying microplastics in beach sand. Mar. Pollut. Bull. 114, 77–83. https://doi.org/10.1016/j.marpolbul.2016.08.055.
Bond, A.L., Provencher, J.F., Daoust, P.-Y., Lucas, Z.N., 2014. Plastic ingestion by fulmars and shearwaters at Sable Island, Nova Scotia, Canada. Mar. Pollut. Bull. 87, 68–75. https://doi.org/10.1016/j.marpolbul.2014.08.010.
Chubarenko, I., Stepanova, N., 2017. Microplastics in sea coastal zone: lessons learned from the Baltic amber. Environ. Pollut. 224, 243–254. https://doi.org/10.1016/j.envpol.2017.01.085.
Chubarenko, I.P., Esiukova, E.E., Bagaev, A.V., Bagaeva, M.A., Grave, A.N., 2018. Three-dimensional distribution of anthropogenic microparticles in the body of sandy beaches. Sci. Total Environ. 628–629, 1340–1351. https://doi.org/10.1016/j.scitotenv.2018.02.167.
Clunies-ross, P.J., Smith, G.P.S., Gordon, K.C., Gaw, S., 2016. Synthetic shorelines in New Zealand? Quantification and characterisation of microplastic pollution on Canterbury ' s coastlines characterisation of microplastic pollution on Canterbury' s. New Zeal. J. Mar. Freshw. Res. 8330. https://doi.org/10.1080/00288330.2015.1132747.
Cole, M., Webb, H., Lindeque, P.K., Fileman, E.S., Halsband, C., Galloway, T.S., 2015. Isolation of microplastics in biota-rich seawater samples and marine organisms. Sci. Rep. 4, 4528. https://doi.org/10.1038/srep04528.
Dehghani, S., Moore, F., Akhbarizadeh, R., 2017. Microplastic pollution in deposited urban dust, Tehran metropolis, Iran. Environ. Sci. Pollut. Res. 24, 20360–20371. https://doi.org/10.1007/s11356-017-9674-1.
Dekiff, J.H., Remy, D., Klasmeier, J., Fries, E., 2014. Occurrence and spatial distribution of microplastics in sediments from Norderney. Environ. Pollut. 186, 248–256. https://doi.org/10.1016/j.envpol.2013.11.019.
Dris, R., Gasperi, J., Rocher, V., Saad, M., Renault, N., Tassin, B., 2015a. Microplastic contamination in an urban area: a case study in Greater Paris. Environ. Chem. 12,

592. https://doi.org/10.1071/EN14167.
Dris, R., Imhof, H., Sanchez, W., Gasperi, J., Galgani, F., Tassin, B., Laforsch, C., 2015b. Beyond the ocean: contamination of freshwater ecosystems with (micro-)plastic particles. Environ. Chem. 12, 539. https://doi.org/10.1071/EN14172.
Dris, R., Gasperi, J., Saad, M., Mirande, C., Tassin, B., 2016. Synthetic fibers in atmospheric fallout: a source of microplastics in the environment? Mar. Pollut. Bull. 104, 290–293. https://doi.org/10.1016/j.marpolbul.2016.01.006.
Dris, R., Gasperi, J., Rocher, V., Tassin, B., 2018. Synthetic and non-synthetic anthropogenic fibers in a river under the impact of Paris Megacity: sampling methodological aspects and flux estimations. Sci. Total Environ. 618, 157–164. https://doi.org/10.1016/j.scitotenv.2017.11.009.
EU, 2018. A European Strategy for Plastics in a Circular Economy.
Falcieri, F.M., Benetazzo, A., Sclavo, M., Russo, A., Carniel, S., 2014. Po River plume pattern variability investigated from model data. Cont. Shelf Res. 87, 84–95. https://doi.org/10.1016/j.csr.2013.11.001.
Fisner, M., Majer, A.P., Balthazar-Silva, D., Gorman, D., Turra, A., 2017. Quantifying microplastic pollution on sandy beaches: the conundrum of large sample variability and spatial heterogeneity. Environ. Sci. Pollut. Res. 24, 13732–13740. https://doi.org/10.1007/s11356-017-8883-y.
Fok, L., Cheung, P.K., Tang, G., Li, W.C., 2017. Size distribution of stranded small plastic debris on the coast of Guangdong, South China. Environ. Pollut. 220, 407–412. https://doi.org/10.1016/j.envpol.2016.09.079.
Fox, J.M., Hill, P.S., Milligan, T.G., Boldrin, A., 2004. Flocculation and sedimentation on the Po River Delta. Mar. Geol. 203, 95–107. https://doi.org/10.1016/S0025-3227(03)00332-3.
G7, 2015. Leaders' Declaration G7 Summit 7–8 June 2015. G7 Summit, pp. 7–8.
Gaglio, M., Aschonitis, V.G., Gissi, E., Castaldelli, G., Fano, E.A., 2017. Land use change effects on ecosystem services of river deltas and coastal wetlands: case study in Volano–Mesola–Goro in Po river delta (Italy). Wetl. Ecol. Manag. 25, 67–86. https://doi.org/10.1007/s11273-016-9503-1.
Galgani, F., Hanke, G., Werner, S., Oosterbaan, L., Nilsson, P., Fleet, D., Kinsey, S., Thompson, R.C., van Franeker, J., Vlachogianni, T., Scoullos, M., Veiga, J.M., Palatinus, A., Matiddi, M., Maes, T., Korpinen, S., Budziak, A., Leslie, H., Gago, J., Liebezeit, G., 2013. Guidance on Monitoring of Marine Litter in European Seas: A Guidance Document Within the Common Implementation Strategy for the Marine Strategy Framework Directive. Publications Office of the European Union, Luxembourg.
Gasperi, J., Dris, R., Bonin, T., Rocher, V., Tassin, B., 2014. Assessment of floating plastic debris in surface water along the Seine River. Environ. Pollut. 195C, 163–166. https://doi.org/10.1016/j.envpol.2014.09.001.
Heo, N.W., Hong, S.H., Han, G.M., Hong, S., Lee, J., Song, Y.K., Jang, M., Shim, W.J., 2013. Distribution of small plastic debris in cross-section and high strandline on Heungnam beach, South Korea. Ocean Sci. J. 48, 225–233. https://doi.org/10.1007/s12601-013-0019-9.
Hidalgo-Ruz, V., Gutow, L., Thompson, R.C., Thiel, M., 2012. Microplastics in the marine environment: a review of the methods used for identification and quantification. Environ. Sci. Technol. 46, 3060–3075. https://doi.org/10.1021/es2031505.
Imhof, H.K., Sigl, R., Brauer, E., Feyl, S., Giesemann, P., Klink, S., Leupolz, K., Löder, M.G.J., Löschel, L.A., Missun, J., Muszynski, S., Ramsperger, A.F.R.M., Schrank, I., Speck, S., Steibl, S., Trotter, B., Winter, I., Laforsch, C., 2017. Spatial and temporal variation of macro-, meso- and microplastic abundance on a remote coral island of the Maldives, Indian Ocean. Mar. Pollut. Bull. 116, 340–347. https://doi.org/10.1016/j.marpolbul.2017.01.010.
Imhof, H.K., Wiesheu, A.C., Anger, P.M., Niessner, R., Ivleva, N.P., Laforsch, C., 2018. Variation in plastic abundance at different lake beach zones - a case study. Sci. Total Environ. 613–614, 530–537. https://doi.org/10.1016/j.scitotenv.2017.08.300.
Jiménez, J.A., Capobiango, M., Suanez, S., Ruol, P., Fraunié, P., Stive, M.J.F., 1995. Coastal processes along the Ebro, Po and Rhone Deltas. In: Proceedings of the Second International Conference on the Mediterranean Coastal Environment, MEDCOST 95.
Kang, J.-H., Kwon, O.Y., Lee, K.-W., Song, Y.K., Shim, W.J., 2015. Marine neustonic microplastics around the southeastern coast of Korea. Mar. Pollut. Bull. 96, 304–312. https://doi.org/10.1016/j.marpolbul.2015.04.054.
Koelmans, A.A., Besseling, E., Foekema, E., Kooi, M., Mintenig, S., Ossendorp, B.C., Redondo-Hasselerharm, P.E., Verschoor, A., van Wezel, A.P., Scheffer, M., 2017. Risks of plastic debris: unravelling fact, opinion, perception, and belief. Environ. Sci. Technol. 51, 11513–11519. https://doi.org/10.1021/acs.est.7b02219.
Lechner, A., Ramler, D., 2015. The discharge of certain amounts of industrial microplastic from a production plant into the River Danube is permitted by the Austrian legislation. Environ. Pollut. 200, 159–160. https://doi.org/10.1016/j.envpol.2015.02.019.
Liubartseva, S., Coppini, G., Lecci, R., Creti, S., 2016. Regional approach to modeling the transport of floating plastic debris in the Adriatic Sea. Mar. Pollut. Bull. 103, 115–127. https://doi.org/10.1016/j.marpolbul.2015.12.031.
Lo, H.-S., Xu, X., Wong, C.-Y., Cheung, S.-G., 2018. Comparisons of microplastic pollution between mudflats and sandy beaches in Hong Kong. Environ. Pollut. 236, 208–217. https://doi.org/10.1016/j.envpol.2018.01.031.
Löder, M.G.J., Kuczera, M., Mintenig, S., Lorenz, C., Gerdts, G., 2015. Focal plane array detector-based micro-Fourier-transform infrared imaging for the analysis of microplastics in environmental samples. Environ. Chem. 12, 563. https://doi.org/10.1071/EN14205.
Maicu, F., De Pascalis, F., Ferrarin, C., Umgiesser, G., 2018. Hydrodynamics of the Po River-Delta-Sea system. J. Geophys. Res. Ocean. https://doi.org/10.1029/2017JC013601.
Moreira, F.T., Lívio, A., Martini, B., Alves, M., Abreu, D., Biato, S., Turra, A., Prantoni, A.L., Martini, B., de Abreu, M.A., Stoiev, S.B., Turra, A., Lívio, A., Martini, B., Alves, M., Abreu, D., Biato, S., Turra, A., 2015. Small-scale temporal and spatial variability in the abundance of plastic pellets on sandy beaches: methodological considerations for estimating the input of microplastics. Mar. Pollut. Bull. 102, 114–121. https://doi.org/10.1016/j.marpolbul.2015.11.051.
Munari, C., Scoponi, M., Mistri, M., 2017. Plastic debris in the Mediterranean Sea: types, occurrence and distribution along Adriatic shorelines. Waste Manag. 67, 385–391. https://doi.org/10.1016/j.wasman.2017.05.020.
Naji, A., Esmaili, Z., Khan, F.R., 2017. Plastic debris and microplastics along the beaches of the Strait of Hormuz, Persian gulf. Mar. Pollut. Bull. 114, 1057–1062. https://doi.org/10.1016/j.marpolbul.2016.11.032.
Piehl, S., Leibner, A., Löder, M.G.J., Laforsch, C., Bogner, C., 2018. Identification and Quantification of Macro- and Microplastics on an Agricultural Farmland 1–9. https://doi.org/10.1038/s41598-018-36172-y.
PlasticsEurope, 2018. Plastics - the Facts 2018. In: An analysis of European plastics production, demand and waste data. Plast. Eur. Assoc. Plast. Manuf. Bruss..
Revel, M., Châtel, A., Mouneyrac, C., 2018. Micro (nano)plastics: a threat to human health? Curr. Opin. Environ. Sci. Health 1, 17–23. https://doi.org/10.1016/j.coesh.2017.10.003.
Rezania, S., Park, J., Md Din, M.F., Mat Taib, S., Talaiekhozani, A., Kumar Yadav, K., Kamyab, H., 2018. Microplastics pollution in different aquatic environments and biota: a review of recent studies. Mar. Pollut. Bull. 133, 191–208. https://doi.org/10.1016/j.marpolbul.2018.05.022.
Turner, A., Holmes, L., 2011. Occurrence, distribution and characteristics of beached plastic production pellets on the island of Malta (central Mediterranean). Mar. Pollut. Bull. 62, 377–381. https://doi.org/10.1016/j.marpolbul.2010.09.027.
Turra, A., Manzano, A.B., Dias, R.J.S., Mahiques, M.M., Barbosa, L., Balthazar-Silva, D., Moreira, F.T., 2014. Three-dimensional distribution of plastic pellets in sandy beaches: shifting paradigms. Sci. Rep. 4, 4435. https://doi.org/10.1038/srep04435.
UNEP, 2015. Plastic in Cosmetics: Are We Polluting the Environment Through Our Personal Care? 2015 UNEP.
UNEP, 2016. Marine Plastic Debris GLOBAL Lessons and Research to Inspire Action.
Van Cauwenberghe, L., Devriese, L., Galgani, F., Robbens, J., Janssen, C.R., 2015. Microplastics in sediments: a review of techniques, occurrence and effects. Mar. Environ. Res. 2009. https://doi.org/10.1016/j.marenvres.2015.06.007.
Vianello, a, Boldrin, A., Guerriero, P., Moschino, V., Rella, R., Sturaro, A., Da Ros, L., 2013. Microplastic particles in sediments of lagoon of Venice, Italy: first observations on occurrence, spatial patterns and identification. Estuar. Coast. Shelf Sci. 130, 54–61. https://doi.org/10.1016/j.ecss.2013.03.022.
Volf, G., Atanasova, N., Kompare, B., Ožanić, N., 2013. Modeling nutrient loads to the northern Adriatic. J. Hydrol. 504, 182–193. https://doi.org/10.1016/j.jhydrol.2013.09.044.
Wagner, M., Scherer, C., Alvarez-Muñoz, D., Brennholt, N., Bourrain, X., Buchinger, S., Fries, E., Grosbois, C., Klasmeier, J., Marti, T., Rodriguez-Mozaz, S., Urbatzka, R., Vethaak, A., Winther-Nielsen, M., Reifferscheid, G., 2014. Microplastics in freshwater ecosystems: what we know and what we need to know. Environ. Sci. Eur. 26, 12. https://doi.org/10.1186/s12302-014-0012-7.
Young, A.M., Elliott, J.A., 2016. Characterization of microplastic and mesoplastic debris in sediments from Kamilo Beach and Kahuku Beach, Hawai'i. Mar. Pollut. Bull. 113, 477–482. https://doi.org/10.1016/j.marpolbul.2016.11.009.
Yu, X., Peng, J., Wang, J., Wang, K., Bao, S., 2016. Occurrence of microplastics in the beach sand of the Chinese inner sea: the Bohai Sea. Environ. Pollut. 214, 722–730. https://doi.org/10.1016/j.envpol.2016.04.080.
Zavatarelli, M., 2002. Diagnostic and prognostic model studies of the Adriatic Sea general circulation: seasonal variability. J. Geophys. Res. 107, 3004. https://doi.org/10.1029/2000JC000210.
Zhang, S., Yang, X., Gertsen, H., Peters, P., Salánki, T., Geissen, V., 2018. A simple method for the extraction and identification of light density microplastics from soil. Sci. Total Environ. 616–617, 1056–1065. https://doi.org/10.1016/j.scitotenv.2017.10.213.
Ziajahromi, S., Neale, P.A., Leusch, F.D.L., 2016. Wastewater treatment plant effluent as a source of microplastics: review of the fate, chemical interactions and potential risks to aquatic organisms. Water Sci. Technol. 74, 2253–2269. https://doi.org/10.2166/wst.2016.414.

Article B2: Supplementary information

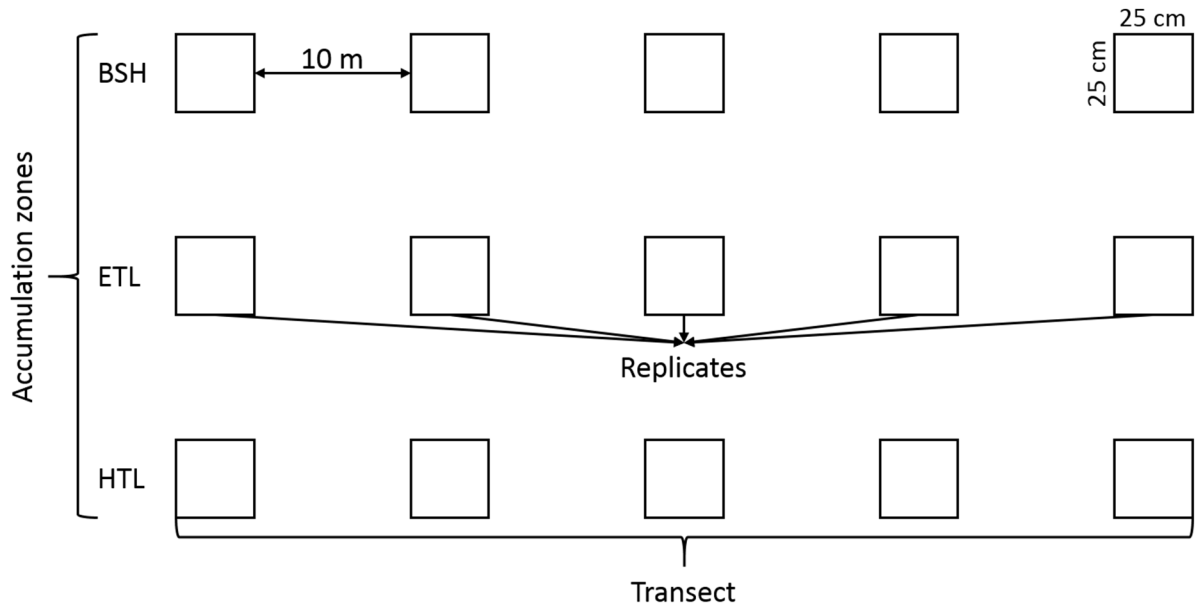

Supplementary material 1. Sampling design for microplastic sediment samples at the three investigated beaches. Samples were taken within the window between high tide cycles, resulting in a total of eleven replicates for the site Levante, six for the site Pila and nine for the site Allagemento. BSH: backshore, ETL: extreme tide line, HTL: high tide line.

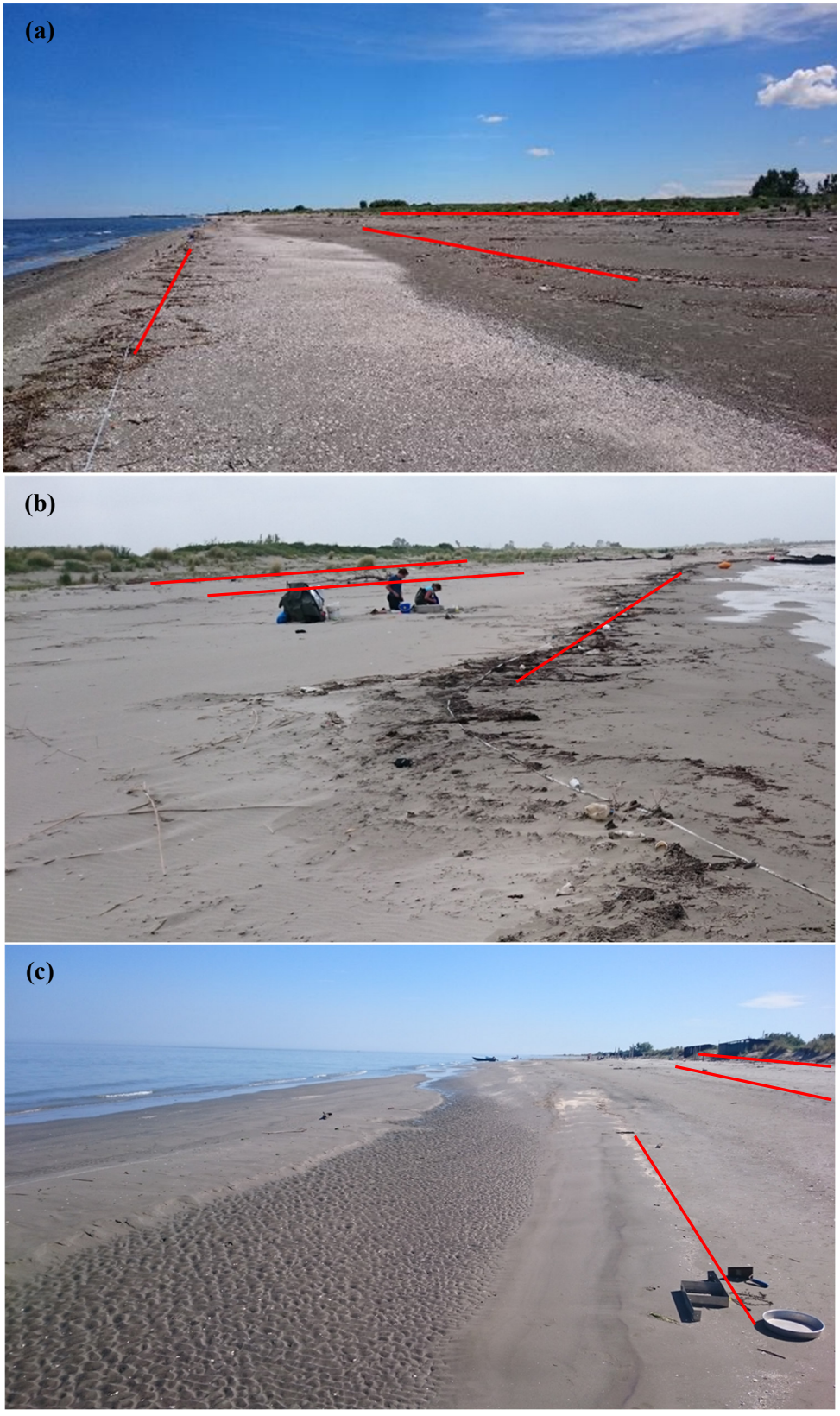

Supplementary material 2. Pictures of the three investigated beaches (a) Levante, (b) Pila, and (c) Allagemento, showing the sampled accumulation areas (red lines).

Supplementary material 3. Microplastic (MPP) abundances for single replicates per kilogram of dry weight (kg/DW). Cumulative sum, mean, and standard deviation (SD) are shown. Lev: Levante, Alla: Allagemento, BSH: backshore, ETL: extreme tide line, HTL: high tide line.

Sample ID	BSH				ETL				HTL			
	MPPs kg/DW	Sum	Mean	SD	MPPs kg/DW	Sum	Mean	SD	MPPs kg/DW	Sum	Mean	SD
Lev_0	22.61				17.43				5.29			
Lev_10	9.28	31.89	15.95	9.43	10.37	27.80	13.90	5.00	2.78	8.07	4.03	1.78
Lev_20	38.40	70.29	23.43	14.58	12.77	40.57	13.52	3.59	0.96	9.02	3.01	2.18
Lev_30	20.06	90.35	22.59	12.02	50.38	90.95	22.74	18.66	5.87	14.89	3.72	2.28
Lev_40	10.46	100.81	20.16	11.74	3.05	94.00	18.80	18.40	18.90	33.79	6.76	7.07
Lev_50	0.32	101.12	16.85	13.26	18.05	112.06	18.68	16.46	2.65	36.44	6.07	6.54
Lev_60	6.70	107.82	15.40	12.70	17.02	129.07	18.44	15.04	5.29	41.74	5.96	5.98
Lev_70	5.76	113.58	14.20	12.24	113.02	242.09	30.26	36.22	0.96	42.69	5.34	5.81
Lev_80	1.45	115.03	12.78	12.22	8.79	250.88	27.88	34.63	10.59	53.28	5.92	5.71
Lev_90	10.55	125.58	12.56	11.54	235.41	486.30	48.63	73.30	6.10	59.38	5.94	5.39
Lev_100	1.68	127.26	11.57	11.43	92.38	578.68	52.61	70.78	3.56	62.94	5.72	5.16
Pila_0	6.31				1.44				4.75			
Pila_10	2.26	8.58	4.29	2.86	5.05	6.49	3.24	2.55	6.80	11.55	5.78	1.45
Pila_20	22.34	30.91	10.30	10.61	19.41	25.90	8.63	9.51	3.74	15.29	5.10	1.56
Pila_30	11.84	42.76	10.69	8.70	1.79	27.69	6.92	8.48	3.09	18.38	4.60	1.62
Pila_40	15.08	57.84	11.57	7.79	1.20	28.89	5.78	7.78	4.13	22.51	4.50	1.42
Pila_50	4.98	62.82	10.47	7.47	2.77	31.66	5.28	7.07	3.57	26.08	4.35	1.33
Alla_0	22.38				0.72				0.22			
Alla_10	8.92	31.30	15.65	9.51	0.54	1.26	0.63	0.12	0.00	0.22	0.11	0.16
Alla_20	8.93	40.23	13.41	7.77	0.24	1.50	0.50	0.24	1.73	1.95	0.65	0.94
Alla_30	5.00	45.23	11.31	7.61	0.00	1.50	0.37	0.32	0.00	1.95	0.49	0.83
Alla_40	8.64	53.87	10.77	6.70	1.36	2.86	0.57	0.52	0.51	2.46	0.49	0.72
Alla_50	0.22	54.09	9.01	7.38	0.24	3.10	0.52	0.48	0.45	2.91	0.49	0.65
Alla_60	3.86	57.94	8.28	7.01	0.00	3.10	0.44	0.48	4.44	7.35	1.05	1.61
Alla_70	6.22	64.16	8.02	6.53	1.09	4.19	0.52	0.50	0.93	8.28	1.03	1.49
Alla_80	0.70	64.86	7.21	6.58	0.00	4.19	0.47	0.50	1.56	9.84	1.09	1.40

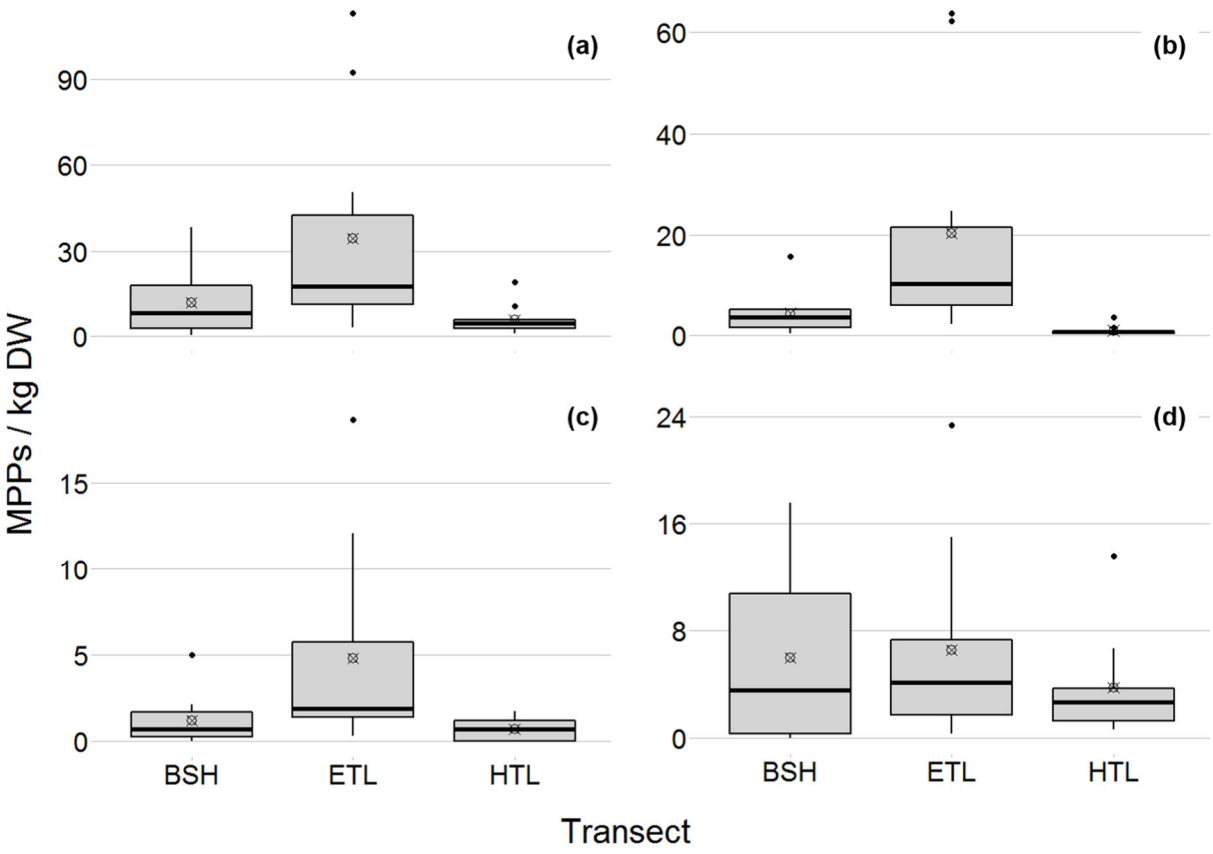

Supplementary material 4. Microplastic (MPP) abundance per kilogram dry weight (DW) of the three transects after removing an influential datapoint (cook's distance >4 times the mean) for the sampling site Levante (a). Comparison of polymer types of the different transects for (b) polyethylene, (c) polypropylene, and (d) polystyrene after removing an influential datapoint. Mean values are indicated by circle/cross symbol (⊠). BSH: backshore, ETL: extreme tide line, HTL: high tide line.

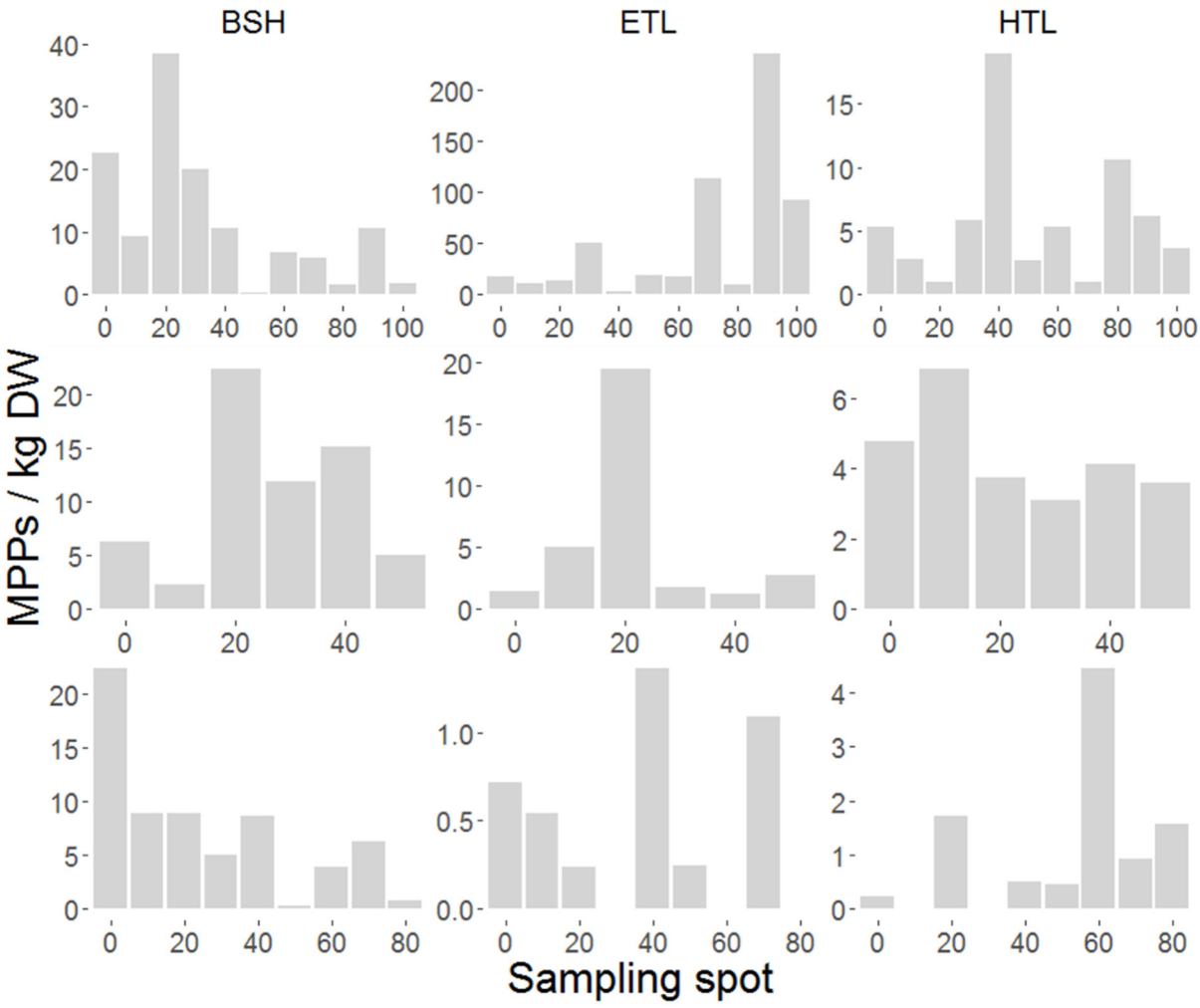

Supplementary material 5. Microplastic (MPP) abundances per kilogram dry weight (DW) at each replicate within the three different accumulation zones sampled for the three beaches. From top to bottom: Levante (n=11), Pila (n=6), and Allagemento (n=9). BSH: backshore, ETL: extreme tide line, HTL: high tide line.

Chapter C

Chapter C: Development of alternative monitoring methods for buoyant plastic debris in aquatic systems

Article C1: Coastal accumulation of microplastic particles emitted from the Po River, Northern Italy: Comparing remote sensing and hydrodynamic modelling with in-situ sample collections

Atwood EC, Falcieric F, Piehl S, Bochow M, Matthies M, Franke J, Carniel S, Sclavo M, Laforsch C, Siegert F (2018)

Marine Pollution Bulletin 138: 561-574

Marine Pollution Bulletin 138 (2019) 561–574

Contents lists available at ScienceDirect

Marine Pollution Bulletin

journal homepage: www.elsevier.com/locate/marpolbul

Coastal accumulation of microplastic particles emitted from the Po River, Northern Italy: Comparing remote sensing and hydrodynamic modelling with *in situ* sample collections

Elizabeth C. Atwood[a,b,*], Francesco M. Falcieri[c], Sarah Piehl[d], Mathias Bochow[d,e], Michael Matthies[f], Jonas Franke[a], Sandro Carniel[c], Mauro Sclavo[c], Christian Laforsch[d], Florian Siegert[a,b]

[a] RSS Remote Sensing Solutions GmbH, Isarstr. 3, 82065 Baierbrunn, Germany
[b] Ludwig-Maximilians-Universität Munich, GeoBio-Center, Großhadernerstr. 2, 82152 Martinsried, Planegg, Germany
[c] Consiglio Nazionale delle Ricerche – Istituto di Scienze Marine (CNR-ISMAR), Arsenale-Tesa 104, Castello 2737/F, 30122 Venezia, Italy
[d] University Bayreuth, Dept. Animal Ecology I, Universitätsstr. 30, 95440 Bayreuth, Germany
[e] Helmholtz Centre Potsdam - GFZ German Research Centre for Geosciences, Telegrafenberg, 14473 Potsdam, Germany
[f] University of Osnabrück, Institute of Environmental Systems Research, Barbarastr. 12, 49069 Osnabrück, Germany

ARTICLE INFO

Keywords:
Beach sediment
River plume
FT-IR
ROMS
Landsat-8
Sentinel-2

ABSTRACT

Microplastic research has mainly concentrated on open seas, while riverine plumes remain largely unexplored despite their hypothesized importance as a microplastic source to coastal waters. This work aimed to model coastal accumulation of microplastic particles (1–5 mm) emitted by the Po River over 1.5 years. We posit that river-induced microplastic accumulation on adjacent coasts can be predicted using (1) hydrodynamic-based and (2) remote sensing-based modelling. Model accumulation maps were validated against sampling at nine beaches, with sediment microplastic concentrations up to 78 particles/kg (dry weight). Hydrodynamic modelling revealed that discharged particle amount is only semi-coupled to beaching rates, which are strongly mouth dependent and occur within the first ten days. Remote sensing modelling was found to better capture river mouth relative strength, and accumulation patterns were found consistent with hydrodynamic modelling. This methodology lays groundwork for developing an operational monitoring system to assess microplastic pollution emitted by a major river.

1. Introduction

Marine plastic litter has long been recognized as an environmental problem (Azzarello and van Vleet, 1987; Law and Thompson, 2014; Sheavly and Register, 2007) but only recently has begun to receive international attention at a level adequate to the potential severity of the threat (G7 Germany, 2015; GESAMP, 2016; UNEP, 2016). Microplastics, commonly defined as particles < 5 mm in diameter (Galgani et al., 2013), are increasingly proving to be ubiquitous in all water systems. Roughly 70 to 80% of marine debris comes primarily from land-based sources (Wagner et al., 2014), much being passively collected in waterways which eventually flow to the sea. Mani et al. (2015) found river water concentrations up to 3.9 million particles/km^2 in metropolitan areas along the Rhine River. Annual input of plastic particles to the Great Laurentian Lakes is estimated at 9.8 thousand tonnes (Hoffman and Hittinger, 2017). Despite the fact that freshwater systems are at least as severely contaminated as the oceans (Dris et al., 2015), large rivers have to date received relatively little attention (Mani et al., 2015; Wagner et al., 2014). An estimated 1.15 and 2.41 million tonnes enter the oceans each year from rivers alone (Lebreton et al., 2017), representing up to 50% of land based plastic emissions estimate, which ranges from 4.8 to 12.7 million tonnes (Jambeck et al., 2015). Once microplastics reach coastal waters, their dispersion and transportation pathways are governed by ocean and atmosphere dynamics; our understanding of these physical processes is still limited. Some authors suggest that how these processes influence microplastic transport may, to some extent, be comparable to well-studied suspended sediment transportation systems (Zhang, 2017), which could offer a more established framework for modelling suspended microplastic transportation.

* Corresponding author at: RSS Remote Sensing Solutions GmbH, Isarstr. 3, 82065 Baierbrunn, Germany.
E-mail address: atwood@rssgmbh.de (E.C. Atwood).

https://doi.org/10.1016/j.marpolbul.2018.11.045
Received 24 July 2018; Received in revised form 21 September 2018; Accepted 19 November 2018

Microplastic transportation pathways are characterized by complex dynamics due to processes such as movement mechanisms (windage and sinking velocities) as well as changes in physical and chemical characteristics (loss of structural integrity, fragmentation and aggregation, see review Andrady, 2017) as well as interactions with biota (Law and Thompson, 2014). A combined hydrodynamic-Lagrangian transportation model effort would therefore be surely dependent upon necessary simplifying assumptions, as well as the quality of the hydrodynamic forcing data. Such models, with different degrees of realism, have been recently utilized to hindcast potential sources of stranded plastic litter in the Indian Ocean (Bouwman et al., 2016; Duhec et al., 2015), Aegean Sea (Politikos et al., 2017) and Adriatic Sea (Carlson et al., 2017). To date, little attention has been placed on local-scale river plume microplastic transport modelling in coastal seas (Browne et al., 2010; Carlson et al., 2017; Zhang, 2017). It is important to bear in mind that, due to the intrinsic model simplifications, dispersion pathways computed based on modelling results can accumulate errors over longer distances and times. Generally, modelling results should be considered qualitative rather than quantitative until validated against an independent dataset. A different type of model based on remote sensing acquisitions offers multiple depictions of the river plume that inherently include actual environmental conditions. While such an image displays the complex coastal ocean environment of the surface layer, it nevertheless offers restricted information for below the water surface and only represents the snapshot time period when the image was acquired.

In this paper, we implement and compare these two different types of models to assess how microplastics from a major river are spreading into a semi-enclosed sea and accumulate along its coastline. The objective is to create a coastal microplastic exposure map, which depicts accumulation of particles emitted from the Po River along the outer delta and covering southward the coastal area still under strong influence from the main Po River plume. Model (1) is a Lagrangian particle transportation model forced by a state-of-the-art hydrodynamic model, while model (2) is based on satellite remote sensing of river plume form and intensity along the coastline. We hypothesize that both models are able to capture coastal patterns in river plume emitted microplastic accumulation. Model results are validated against sediment sampling for microplastics from beaches with varying river plume exposure gradients. Development of a system to model coastal accumulation of microplastic debris from rivers would represent a very useful tool for agencies responsible for monitoring and reporting this pollution, as well as organization of clean-up activities and remediation strategies.

2. Materials and methods

2.1. Study area

The Adriatic Sea separates the Italian peninsula and Balkan coast, extending 800 km from the connection with the Ionian Sea over the Strait of Otranto northwest toward the Venice Lagoon (Fig. 1). The prevailing currents flow counterclockwise from the Strait of Otranto along the Balkan coastline and return southward with the Western Adriatic Current (WAC) along the Italian coastline (Artegiani et al., 1997a, 1997b; Carniel et al., 2016). The North Adriatic sub-basin is defined as the shallow area north of the 100 m isobath (Fig. 1).

The Po River provides the largest riverine influx to the Adriatic Sea, averaging daily 1500 m^3/s with streamflow ranging between 100 m^3/s and 11,550 m^3/s (Falcieri et al., 2014). Being the longest river in Italy, the Po River drainage area (74,000 km^2) encompasses much of the northern region of the country, with > 20 million inhabitants, and includes many large cities as well as areas of intensive industrial and agricultural activities (lower left inset Fig. 1). The river splits into many sub-rivers before flowing into the Adriatic Sea, the main recognized arms of which are the Po di Maistra, della Pila, delle Tolle, di Gnocca (or della Donzella) and di Goro (upper right inset Fig. 1). Additionally, there exist many side channels and lagoons, which also carry a portion of the river water to the sea. Notable among these side channels are the Busa di Scirocco and di Tramontana. The delta is an actively changing system with shifting sandbars that can obstruct outflow from a particular mouth (Simeoni and Corbau, 2009) and thus increase the outflow elsewhere. The highest river discharge occurs in the spring, associated with high precipitation and snow-melt runoff, and the lowest in autumn (Falcieri et al., 2014).

Both wind regime and freshwater influx play a deciding role in North Adriatic circulation patterns (Bignami et al., 2007; Bolaños et al., 2014; Falcieri et al., 2014). There are three main recognized wind regimes: Bora, Scirocco and Mistral. Bora events consist of strong, dry, northeasterly winds that tend to occur more often during the winter months, which together with low river discharge results in a small Po River plume that remains close to the coastline (Boldrin et al., 2009; Falcieri et al., 2014). As mentioned above, a Scirocco event comprises warm, humid, east-southeasterly winds that tend to occur more often during the spring to fall. This wind regime together with high river discharge results in a wider plume that can extend far across the Adriatic Basin. Mistral events are the least powerful of the wind regimes and are defined based on winds coming from the northwest, which have been found to minorly enhance WAC flow into the Ionian Sea (Bignami et al., 2007).

2.2. Sample design

The Po Delta field campaign was conducted from 4 to 25 June 2016, during which both water and sediment samples were taken. Water sample locations were selected to cover the main Po River, recognized river mouths and important subsidiary river mouths as well as the plume, ranging from near-coast waters to the plume outer edge (indicated by surface waters with salinity > 30 PSU). At each station, water samples used to estimate microplastic concentrations were collected from a small boat using a specially designed mini-manta trawl (300 μm mesh, further details available in S1 of the Supplementary material). A total of 24 water stations were sampled, the locations of which are indicated in Fig. 2 of the Results. The trawl net was rinsed before each sample collection by running the net without the cod end through the water for 5 min at the sampling location. One trawl pass per location was conducted alongside the boat for an average of 20 min and only when wind conditions were below Beaufort 2 (light breeze, 6–11 km/h). Samples were stored in glass jars until further processing in the lab. During trawling, *in situ* measurements were collected for sea surface temperature (°C) and salinity (PSU). Water clarity measurements (visibility depth with a Hydrobios secchi disk) were conducted both before and after each trawl. Additionally, 2 L water samples were concurrently collected from the water surface (top 40 cm) for later determination of the water parameters chlorophyll-*A* (Chl-*A*) and suspended particulate matter (SPM). Water samples were also processed for measurement of colored dissolved organic matter (CDOM, or Gelbstoff), but due to very low detected CDOM levels, these data were determined not useful for building a regionally calibrated remote sensing algorithm. Samples were kept dark while being stored in a cooler with ice until filtering later that the same day.

Chl-*A* samples were hand-pump filtered using Whatman GF/F glass microfiber filters (0.7 μm pore size), following the IOC and SCOR (1994) protocol. Filters were then wrapped in aluminum and stored at −20 °C for the duration of the field campaign, after which they were stored at −80 °C until further processing. Chl-*A* was extracted with 96% ethanol and analyzed with a JASCO FP-8600 fluorometer at an excitation wavelength of 435 nm and an emission wavelength of 670 nm. The fluorometer was calibrated using a photometer (JASCO V-670) and a Chl-*A* standard (C6144-1MG, Sigma-Aldrich). After the first measurements, samples were acidified with HCl and again measured to subtract phaeopigments from the chlorophylls to get concentration of Chl-*A* in mg/L following the JGOFS protocol (UNESCO, 1994).

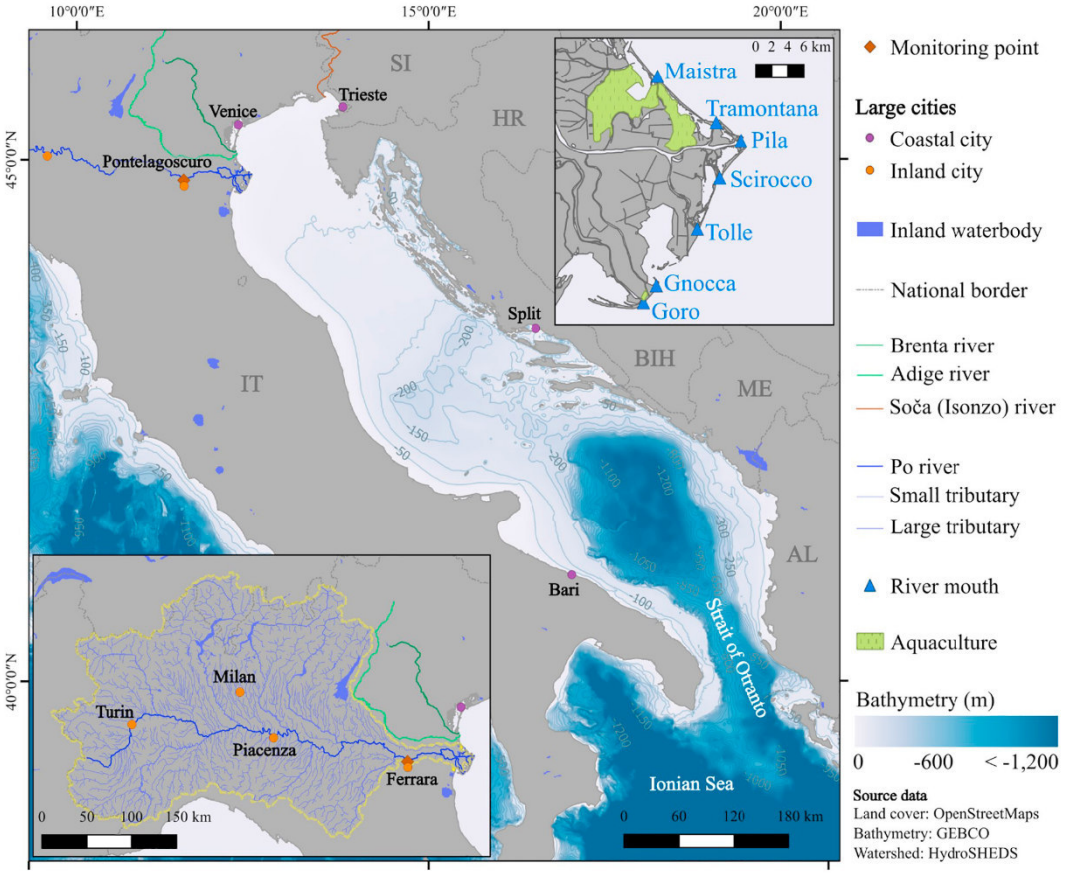

Fig. 1. Adriatic Sea overview map, showing bathymetry (contour lines follow 50 m depth intervals) along with large coastal cities and bordering countries: AL - Albania, ME - Montenegro, BIH - Bosnia and Herzegovina, HR - Croatia, SI - Slovenia, IT - Italy. Lower left inset shows Po River watershed (yellow dashed line) with large inland cities, as well as the Brenta (dark green line) and Adige (light green line) rivers. The Po Delta is displayed in the upper right inset, showing all five major river mouths (Maistra, Pila, Tolle, Gnocca and Goro) as well as important side channels (Tramontana and Scirocco) and dense aquaculture areas. (For interpretation of the references to color in this figure legend, the reader is referred to the web version of this article.)

SPM samples were hand-pump filtered using pre-weighed cellulose acetate filters with 0.45 µm pore size, air dried and stored in aluminum foil (Lindell et al., 1999). Filters were further dried in a 60–80 °C oven for 2 h and allowed to cool in a desiccator before weighting on a Sartorius R 200 D.

Surface reflectance measurements concurrent to each trawl were taken following the measurement methodology from Mobley (1999) and Fargion and Mueller (2000). An ASD FieldSpec 3 Hi-Res spectrometer was fitted with an 8° optic lens and set to measure raw digital numbers over an averaging of 50 rapid measurements. For each sampling location, a minimum of five measurement cycles were taken with the goal to collect as many cycles as possible during trawling. Each cycle consisted of a downwelling irradiance measurement over a white reference (nadir angle), an upwelling plus a sky radiance measurement both made following Mobley geometry (135° azimuth angle from sun, 40° off nadir for water and 40° off zenith for sky; Mobley, 1999), and lastly a repeated downwelling irradiance measurement to control for potential changes in lighting intensity conditions over the measurement cycle. All spectral measurement angles were estimated by hand and controlled by a second observer with a preset adjustable triangle. Measurement integration times were optimized for each measurement cycle in order to maximize signal. Downwelling irradiance was measured over a 90% Spectralon® white reference panel. Processing of raw digital numbers into remote sensing reflectance is discussed further in Section 2.5.

Sediment samples were collected from nine beaches in order to serve as a validation dataset for the hydrodynamic and remote sensing models (sample locations are indicated in the Results). Beach sample locations were selected so that three each of low, medium and high river plume impact areas would be represented. Estimates of river impact were based on the hydrodynamic modelling accumulation map (more details below in Section 2.4). At each location, samples were taken along the extreme high tide line, following protocols from Moreira et al. (2016) and Turra et al. (2014), and were only conducted between high tide cycles. The extreme tide line was defined visually as the area with the largest accumulation of drift material, which was found to always be a clearly separate line to the last high tide line. Samples were taken at equal intervals along a 100 m transect line, where the first 10 m were walked along the straight transect line and then turned at 90° for placement along the meandering drift line. Samples were taken with a 25 × 25 cm stainless steel quadrat and sampled to a depth of 5 cm. Wet weight of the samples were recorded and then sieved over 1 mm stainless steel mesh (matching model assumptions from the hydrodynamic model, more details below). Additionally, two 1 L bottles where filled with unsieved sand from the same transect line for later processing in the lab to convert the wet weight to dry weight.

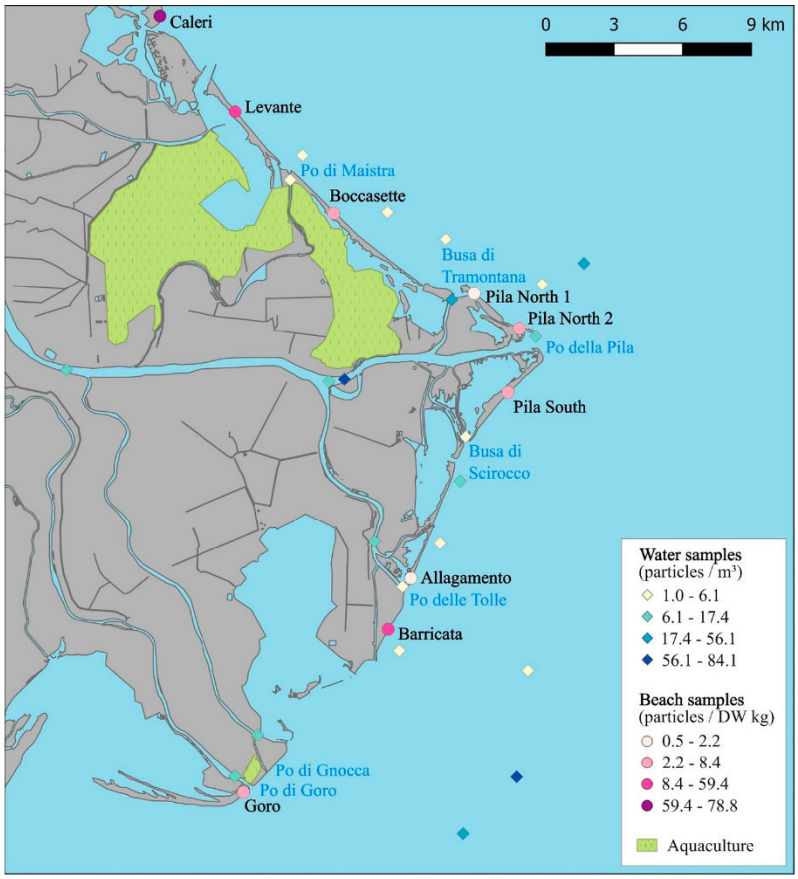

Fig. 2. Overview of water microplastic samples (diamonds, blue scale) and sediment microplastic samples (circles, pink scale) collected during the June 2016 field campaign. A total of 24 water locations and 9 beach locations were sampled, only beach locations are labeled (black text). Water samples are reported as particles/m^3 while sediment samples are reported as particles per dry weight kg (DW kg). River mouths are labeled in dark blue and dense aquaculture areas within lagoons are indicated. (For interpretation of the references to color in this figure legend, the reader is referred to the web version of this article.)

2.3. Microplastic sample processing

Water samples were first fractionated into two size classes: 5 mm–500 μm and 500–300 μm. To remove organic matter (which would disturb spectroscopic analysis) from the microplastic water samples, samples of the size class 500–300 μm were treated with enzymatic purification (Löder et al., 2017) and wet peroxide oxidation (Masura et al., 2015). For the latter class (size 5 mm–500 μm), samples with high organic content were treated solely with wet peroxide oxidation. All potential microplastic particles > 500 μm were visually presorted, photographed and stored for further analysis with Attenuated Total Reflectance (ATR) Fourier Transform Infrared (FT-IR) spectroscopy. For a full quantitative analysis of the fraction < 500 μm, samples were split. One subsample was filtered onto aluminum oxide membranes (Whatman Anodisc filters) and analyzed with Focal Plane Array (FPA) based Micro-FT-IR spectroscopy. The rest of the subsamples were filtered onto glass fiber filters (grade MN 85/90 BF) and analyzed with a newly developed shortwave infrared (SWIR) close-range imaging spectroscopy methodology called PlaMAPP (Schmidt et al., 2018) using a HySpex SWIR-320 m-e sensor (Norsk Elektro Optikk AS). This method allows counting microplastic particles, classifying the plastic type and determining particle size in a semi-automated way. Determination of plastic type is done by comparing the wavelength positions of the spectral absorption bands (local minima in the spectral signatures) of the recorded image spectra to those of plastic spectra from a reference spectral library.

Sediment samples along the 100 m transect were pooled, then processed by drying at 55 °C and separated from inorganic material using a zinc chloride solution (density 1.6–1.8 g/cm^3). The supernatant, which included both organic material and potential polymer particles, was collected using a self-made mote spoon (stainless steel, mesh size < 1 mm), rinsed with 98% ethanol and transferred into glass petri dishes. All potential microplastic particles were visually separated from organic material under a stereomicroscope (Leica M50 with cold light source Leica KL 300 LED, Leica Microsystems), photographed (attached Olympus DP26 camera, 5 Megapixel, Olympus Corp.) and identified to polymer type using ATR FT-IR spectroscopy.

Spectra of all potential microplastic particles > 500 μm, from both water and sediment samples, were recorded with a Tensor 27 FT-IR spectrometer (Bruker Optik GmbH) from 8 co-added scans within a spectral range from 4000 to 400 cm^{-1} and a spectral resolution of 8 cm^{-1}. Background scans were performed after every 10th measurement. Spectra were identified using the OPUS v7.5 software, correlating measured spectra against reference spectra from a custom in-house library (containing polymer spectra as well as spectra from both natural and lab materials used during sampling and processing, see Löder et al., 2015). Spectra of all potential microplastic particles < 500 μm were collected using the Tensor 27 FT-IR spectrometer further equipped with

a Hyperion 3000 FT-IR microscope that had a 15× cassegrain objective and a 64 × 64 FPA detector mounted. Spectra were obtained in transmission mode and measurement settings were as published by Löder and Gerdts (2015). Obtained chemical images were analyzed with the ImageLab v2.26 software and the BayreuthParticleFinder tool (developed during the project together with Epina Software Lab GmbH), which automatically highlights potential polymer particles on the chemical image obtained from the FT-IR measurements of the filter. Given that polymer spectra can diverge, dependent on factors such as particle size, thickness, color, polymer additives or adsorbed chemicals, all automatically detected particles were further manually controlled afterwards.

2.4. Hydrodynamic model

Simulations for microplastic dispersal from the Po River were performed from 1 January 2015 to 15 June 2016, to coincide with the field sampling campaign. A 3D Individual Based Lagrangian tracking model (ICHTHYOP; Lett et al., 2008) was implemented to simulate the dispersion of virtual microplastic particles (VMP) due to 3D currents and water column thermohaline structure. In the model, VMP behave as a Lagrangian drifter under the effect of horizontal/vertical advection and dispersion as well as buoyancy force due to the difference between the particle and surrounding water density. Particles were assigned a spherical shape (diameter of 1 mm) and density of 0.91 g/mL. Density was chosen to correspond with the averaged density of virgin polyethylene (both high and low density) and polypropylene, which together account for over 48% of EU demand (PlasticsEurope, 2014) and represent the majority of sampled microplastic debris (Imhof et al., 2013; Zbyszewski and Corcoran, 2011). Horizontal dispersion was included with a turbulent dissipation rate of $\epsilon = 10^{-7}\,m^2/s^3$, in agreement with turbulent kinetic energy observations in the Adriatic Sea. VMP were tracked for a total of 60 days, in excess of Adriatic particle half-life model estimates (Liubartseva et al., 2016) and drifter mean half-life observations (Poulain, 2001) of *circa* 40 days.

Simulations were based on the simplifying assumption of a constant concentration of 10 microplastic particles/m^3 in river waters, as reported in previous observations from the Po River (van der Wal et al., 2015; Vianello et al., 2015). Given that the river is represented as a point source inside the hydrodynamical model, VMP were released at the surface along straight 500 m transects located 250 m in front of each river mouth, with the goal being to mimic a direct discharge from the river itself. Po River mouths included Maistra, Pila, Tolle, Gnocca and Goro plus the Busa di Scirocco (given its presence in the hydrodynamic model). VMP were released over the entire simulation period at hourly intervals from all six locations, and the total number of VMP released at each mouth was determined based on the water discharge distribution among the main branches of the Po River.

Once released, a VMP was considered beached if it passed closer than 250 m from the coastline. This fixed distance was set based on the model spatial resolution (half the horizontal grid size) and in consideration that the model has difficulty representing complex nearshore processes. VMP were tagged with release date and river mouth, so that relative contribution from each river mouth could later be assessed. Once identified as beached, the VMP was removed from the dataset. VMP resuspension after beaching was not accounted for in the model, given the still existing amount of uncertainty surrounding this process (Hardesty et al., 2017; Zhang et al., 2017). This approach could lead to a small overestimation of beaching rates, but it was decided that a simplifying approach was preferable to setting an arbitrary factor meant to represent resuspension and similar nearshore processes.

ICHTHYOP simulations were run offline using as physical forcing an elaboration of the UNIVPM-Regione Marche operational hydrodynamic model that covers the northern Adriatic Sea (horizontal resolution of 500 m; 12 vertical sigma layers). The model (ROMS, Regional Ocean Modelling System; Haidvogel et al., 2008; http://myroms.org) was implemented in a coupled version with a surface wave model (SWAN, Simulating WAves Nearshore model; Booij et al., 1999; http://swan.tudelft.nl) through the COAWST (Coupled-Ocean-Atmosphere-Wave-Sediment Transport Modelling System; Warner et al., 2010; Warner et al., 2008). Surface forcings were derived from COSMO-I7, a local implementation of the Lokal Model (Steppeler et al., 2003) developed in the framework of the COSMO Consortium (http://cosmo-model.org) and run by the Agenzia Regionale per la Prevenzione, l'Ambiente e l'Energia dell'Emilia Romagna - Servizio Idro-Meteo-Clima (ARPA ER-SIMC). The UNIVPM-Regione Marche model implementation was chosen because it was the only freely available and operationally running forecast model with a high horizontal resolution for the Adriatic Sea.

A coastal reference grid was developed for displaying the distribution of beached particles along the Po Delta shore. To avoid artificial "shadowing" effects from corners of the hydrodynamic model grid cells located along the coastline, a smoothed grid was established based rather on the coastline. This grid was created with ArcGIS v9.31 software by projecting the coastline 250 m offshore, separating this into 500 m segments and buffering each segment with 250 m, producing grid cells variable in both shape and surface but without sharp angles or abrupt changes in direction. After post processing, distribution maps of estimated accumulation could be defined for each day up to the entire simulation period. Beach sediment sampling transect locations were placed as close as possible to the middle of the modelled accumulation pixel.

2.5. Near-range spectral measurements and remote sensing model

The remote sensing model for quantifying coastal exposure to riverine-based microplastic particles was based on the assumption that suspended microplastic particles are transported by the same mechanisms as other passive, suspended water constituents for which well-established remote sensing methodologies exist. With the goal being to optimally capture river plume water reflectance characteristics, near-range spectral measurements were used to build regionally calibrated remote sensing spectral reflectance water parameter algorithms for different satellite platforms.

First, raw digital number measurements from the spectroradiometer of downwelling irradiance plus upwelling and sky radiance were converted to irradiance, E(z, λ) in units of W/(m^2 nm), and radiance, L (z,θ,φ,λ) in units of W/(m^2 sr nm), using the software package RS^3 version 6.4.0 from ASD Inc. Radiance measurements were visually checked for abnormal behavior (such as saturation or detector jumps) before being converted to remote sensing reflectance (R_{RS}) following the methodology described by Heim (2005):

$$R_{RS}(0+,\lambda) = \frac{L_{total}(0+,\lambda) - r_{wa}xL_{sky}(\lambda)}{E_{down}(0+,\lambda)}\ [sr^{-1}]$$

where $R_{RS}(0+,\lambda)$ is the remote sensing reflectance directly above the water surface (0+) for a given wavelength (λ), L_{total} is the above water (upwelling) radiance measurement, r_{wa} is the proportion of directly back-reflected skylight at the air-water interface (taken here to be 0.021, following Heim, 2005), L_{sky} the sky radiance, and E_{down} the downwelling irradiance measurement.

The ASD R_{RS} dataset from the field campaign together with the *in situ* SPM measurements were used to calibrate various candidate algorithms to the Po River region and for a given satellite sensor, the best of which was then selected as the optimal regionally calibrated empirical algorithm for the time series analysis. Four separate algorithms for spectral detection of SPM were considered: (i) Jørgensen (1999) based on the CZCS band 3 detecting in the range 540–560 nm, (ii) Dekker (1993) based on *in situ* spectrometer measurements at 706 nm, and two different SPOT-3 ratio-based algorithms from Doxaran et al. (2002) based on (iii) band 3 (780–890 nm) divided by band 1 (500–590 nm)

and (iv) band 3 divided by band 2 (610–680 nm). All calibrated models were assessed for quality *via* Root Mean Square Error (RMSE) as well as goodness of fit statistics following the methods of the Ocean Color Group (Campbell and O'Reilly, 2005). This allowed determination of the best-calibrated SPM algorithm for Po River water with a particular satellite. Both the "Baseline" and "Calibrated" fits were also assessed for data overfitting using a leave-one-out cross-validation (LOOCV) technique (Michaelsen, 1987). Further details regarding the calibration and validation process are available in S2 of the Supplementary material.

Landsat 8 (L8), a joint mission of the U.S. Geological Survey (USGS) and National Aeronautics and Space Administration (NASA), is equipped with two push-broom sensors, the Operational Land Imager (OLI) and the Thermal Infrared Sensor (TIRS), which provide multispectral images with 30 m spatial resolution. The Po Delta study area is located in the overlap region between two Landsat flight paths, thus reducing the revisit time for this particular study to 7 days. The European Space Agency (ESA) Sentinel-2 (S-2) mission is a constellation of two identical satellites that are equipped with a push-broom MultiSpectral Instrument (MSI) sensor. S-2 provides multispectral images with 10, 20 and 60 m spatial resolution depending on the spectral band. S-2 has a revisit time of up to 2–3 days at midlatitudes. Usable images from L8 and S-2 acquired between 1 January 2015 and 30 June 2016 were compiled. Other platforms with coarser image spatial resolution (≥300 m) but proving daily (MODIS) to 2-day (Sentinel-3) acquisitions with much greater Signal-to-Noise Ratio (SNR) were considered but not implemented given that our goal was to capture the fine river plume structure as close to the coastline as possible.

Different atmospheric correction algorithms were tested to minimize the introduction of artifacts to the bands needed for detection of various water parameters, which was accomplished through comparison with concurrent *in situ* R_{RS} spectrometer measurements (further details in S3 and S4 of the Supplementary material).

The L8 and S-2 acquisitions were processed with a hierarchical object-based image analysis (OBIA) developed with eCognition software (Trimble Navigation Ltd.) to remove land, cloud, boats, white caps and breaking waves. The masked images were then used to create SPM concentration maps, which showed how the river plume was spreading into the surface coastal waters over the examined time period.

For each acquisition date, non-coastline pixels were masked and the remaining utilized as the basis for creating the coastline riverine microplastic exposure map. This was accomplished by converting pixel values to a similarity ratio using the average SPM concentration from all five river mouths for that acquisition date. The goal was to display how similar a given coastline pixel was to a pure river water pixel, which was then used to indicate influence from river plume waters along the coastline. Data were binned into hexagons to allow for combination of images with differing footprints as well as spatial resolution, at diameters of both 30 m and 100 m. This was accomplished using the "hexbin" package within the R software package (R Core Team, 2016). The first diameter represents the minimum allowable resolution and the second to match the sediment sampling scheme as well as easier visualization of the entire Po Delta coastline. Gaps in the dataset, produced through masking areas such as cloud cover or breaking waves, were filled in the time series using a combination of Nearest Neighbor Filtering and temporal linear interpolation. This was done again in R using the packages "raster", "rgdal", "rgeos", "sp" and "spacetime". SPM values between L8 and S-2 images were compared using standardized differences to check for any inherent bias between the different sensors. The time series was then summed to create a composite image of river plume influence along the Po Delta coastline for the entire modelled time period.

Po River gauge measurements were obtained for the modelling period from ARPA ER, taken at Pontelagoscuro. Wind regime in front of the Po Delta was estimated by extracting the zonal and meridional wind components from the COSMO I7 dataset (forcing field used in the hydrodynamic model) for eight points located 20 km in front of the coastline. For each point, the daily average magnitude and heading were first computed, and then all eight points averaged to obtain a single value representative of the whole area. Significant wind regime events were identified as days with an average wind speed over 5 m/s and consistently blowing from northeast (Bora), southeast (Scirocco) or northwest (Mistral).

2.6. Validation of the modelled microplastic exposure maps

Modelled microplastic accumulation values from both the remote sensing time series as well as the hydrodynamic particle tracking were compared to *in situ* beach sediment microplastic concentrations to assess model validity as well as identify weaknesses and strengths of each modelling method. Comparisons were made using both Pearson's Correlation r as well as Spearman's Rank Coefficient ρ. All calculations were carried out using R software. Model maps were also compared to one another by unit-base normalizing (also known as feature scaling) each map and then comparing difference values at regular latitudinal intervals along the coastline.

3. Results and discussion

3.1. Water parameter sampling

Water parameter field measurements are presented in Table 1. Chl-*A* measurements fell within 0.005–0.043 mg/L, and SPM values covered a moderate range as compared with ARPA ER monitoring measurements of SPM from Pontelagoscuro (for the time period January 2015 to June 2016, these ranged from 12 to 372 mg/L). Secchi depth measurements only reached a maximum of 163 cm, all located along the outer edge of the river plume.

3.2. Microplastic sampling

Water microplastic samples analyzed by ATR FT-IR and SWIR spectroscopy ranged from 1 to 84 particles/m^3 (Fig. 2), with the highest concentrations being found along the outer river plume edge, within the main arm of the river (Po della Pila) and the side channel Busa di Tramontana. The Maistra and central Tolle river mouths both had very low concentrations, < 6 particles/m^3. Repeated measures from a particular river section, such as where Po delle Tolle separates from Pila or where Tolle splits into three channels before entering the Adriatic, indicated large variability from one sampling time to another.

Some of the highest *in situ* water microplastic measurements were found along the outer edge of the Po River plume, which suggests that either microplastic concentrations in the open Adriatic are at least comparable with those from the river, or that there are local accumulation processes occurring along the front between fresh river water and much higher salinity ocean water. Given that rivers are considered one of the main sources of plastic debris to the ocean (Jambeck et al., 2015; Lebreton et al., 2017) together with evidence that the Adriatic Sea is a highly dissipative system (Horvat, 2015), the latter hypothesis is more likely. Furthermore, concentrations found in this study are an order of magnitude higher than values measured by Suaria et al. (2016) in the open Adriatic Sea. Using the median *in situ* measured microplastic

Table 1
Measured water parameters during the field campaign. Chlorophyll-*A* (Chl-*A*) and suspended particulate matter (SPM) reported in mg/L, Secchi depth average from before and after trawl in cm.

	Chl-*A* (mg/L)	SPM (mg/L)	Secchi (cm)
Mean/Median	0.011/0.009	30.2/21.1	67/51
Standard deviation	0.008	29.4	36
Maximum	0.043	127.9	163
Minimum	0.005	7.7	29

Table 2
Sediment microplastic overview for all 9 beaches sampled, listed north to south. Percent contribution from each plastic type identified is listed: PE polyethylene, PP polypropylene, PS polystyrene ([1] also includes ABS acrylonitrile butadiene styrene and SAN styrene acrylonitrile), PA polyamide, EV accounts for EVOH ethylene vinyl alcohol and EVA ethylene vinyl acetate, PEST polyester, PET polyethylene terephthalate, PVC polyvinyl chloride, PUR polyurethane, PVAL polyvinyl alcohol, SBR styrene butadiene rubber, C/U accounts for either composite particles or unknown plastic types. Total microplastic particles found as well as particles/DW kg is indicated for each beach sampled.

Beach	% contribution												Tot. part.	Part./DW kg
	PE	PP	PS[1]	PA	EV	PEST	PET	PVC	PUR	PVAL	SBR	C/U		
Caleri	45.0	8.6	28.0	< 1	18.0	< 1	< 1	< 1	< 1	0	0	< 1	3080	78.8
Levante	62.2	14.6	16.4	< 1	5.7	< 1	< 1	< 1	< 1	< 1	< 1	< 1	2032	59.4
Boccasette	42.9	13.2	42.9	0	< 1	0	0	0	0	0	0	< 1	182	3.9
Pila North 1	27.0	14.8	54.8	0	< 1	0	< 1	0	0	0	0	< 1	115	2.2
Pila North 2	60.2	9.7	20.4	1.9	0	< 1	4.9	0	< 1	0	0	< 1	103	3.6
Pila South	45.7	18.9	34.1	0	1.4	0	0	0	0	0	0	0	440	8.4
Allagamento	10.0	5.0	85.0	0	0	0	0	0	0	0	0	0	20	0.5
Barricata	19.2	13.8	66.3	< 1	< 1	0	0	0	0	0	0	0	652	14.3
Goro	52.0	19.0	27.8	0	< 1	0	0	0	0	0	0	< 1	248	5.2

concentration from this study together with average Po River discharge (1500 m^3/s) and estimates of microplastic particle count to weight in the Adriatic (1.68 to 3.00 mg/particle; Suaria et al., 2016; van der Wal et al., 2015; Vianello et al., 2015), a rough estimate of floating microplastic released by the Po River ranges between 2.2 and 3.8 t per day. This translates to between 785 and 1402 t/yr, coming close to the estimates of 1349 t/yr by Liubartseva et al. (2016), although it should be noted the latter estimate is based on vertical water column integrated estimates of all plastic debris (both macro and microplastics). Our estimate should be taken with care given that the microplastic sampling method utilized in this study only sampled microplastics floating at the water surface, which has been shown to often underestimate total floating microplastic concentrations (Brunner et al., 2015; Kooi et al., 2016).

The beach sediment microplastic samples (Fig. 2) ranged from 0 to 78 particles per dry weight (DW) kg. The highest measurement by far was on the northernmost beach, Caleri, where a total of 3080 microplastic particles were identified for the entire transect (Table 2). Polystyrene (PS), acrylonitrile butadiene styrene (ABS) and styrene acrylonitrile (SAN) were found to have similar spectral signatures, thus were pooled into a group called styrene-based polymers to avoid potential confusion between these types. The same was true for the polymer types ethylene vinyl alcohol (EVOH) and ethylene vinyl acetate (EVA). Polyethylene (PE), polypropylene (PP) and the styrene polymer group made up > 97% of all particles sampled on six beaches (Boccasette, Pila North 1, Pila South, Allagamento, Barricata and Goro). Beach sediment particles identified as belonging to the styrene polymer group were most often found in their foamed form, which is not surprising considering that the non-foamed polystyrene is less dense than seawater. The remaining three beaches had either an increased contribution from EVOH/EVA or, in the case of Pila North 2, elevated contributions for the polymer types polyamide (PA) and polyethylene terephthalate (PET).

The top three contributing polymer types from the beach sediment microplastic concentrations were PE, styrene-based polymers and PP, in step with general trends observed in both the Po River (van der Wal et al., 2015) and the Mediterranean Sea (Suaria et al., 2016) as well as coastal (Zhang, 2017) and global oceans (Andrady, 2017). PE and PP make up between 45 and 50% of total global plastic production (PlasticsEurope, 2016). Higher occurrence of other plastic types, especially the heavier polymers such as EVOH, PVAL, PET (polyethylene terephthalate) and PVC (polyvinylchloride), were found at Caleri, Levante and Pila North 2 (Fig. 2 and Table 2). Caleri in particular was found to have the most extreme microplastic concentration, exceeding the measurement by Munari et al. (2017) of 21 particles/DW kg at Volano, just south of the Po Delta. It is important to note that a possible explanation for this could be different sampling locations, as this study sampled the extreme high tide line in contrast to the most recent high tide line. Our measurements were lower than those made in the Venice Lagoon (672–2175 particles/DW kg; Vianello et al., 2013), although it should be noted that smaller size classes were under investigation in the study by Vianello et al. and it is often the case that particle abundances increase with decreasing size class (Imhof et al., 2018; Lee et al., 2013). The two northernmost beaches surveyed in this study (Caleri and Levante) were located close to either a public parking lot or a harbor. Heavier particles are known to be transported more slowly than particles which are less dense than surrounding seawater (Cable et al., 2017), which include the plastic types EVOH, PVAL, PET and PVC in their virgin form. This suggests that the higher concentration rates more likely result from local sources, rather than longer distance transportation by the Po River plume or other Adriatic currents.

3.3. Time series data and hydrodynamic model accumulation

River discharge and wind speed, overlain with wind regimes, are shown in Fig. 3 together with total daily beached VMP and a pictorial overview of satellite acquisition coverage (discussed in more detail in the following Section 3.4). The highest observed daily wind speeds (Fig. 3a) occurred in February, March and November 2015, and March 2016, which all corresponded to northeast winds (Bora events, light blue bars in Fig. 3). Scirocco events (southeast wind, green bars) were observed to have less strong wind speeds. Both Mistral and Scirocco events were found to have occurred less frequently than Bora events.

Comparing Po River average daily outflow with the total daily beached VMP (Fig. 3b), a loose connection between streamflow and number of beached VMP was evident. This comes as no great surprised since Po River streamflow was inherently linked to daily particle release rate in the model. High beaching rates in February, June and October 2015 were observed to follow high river discharge events, but this pattern was not always present. Beaching peaks in July 2015 and January 2016 did not correlate with high river discharge events, hinting that beaching is not only driven by the amount of released VMP but also by the surface current field close to the coast and winds.

Of all VMP released, only 18% were found to beach during the simulations. The ratio of released-to-beached VMP for each mouth was highly variable. Po della Pila, Busa di Scirocco and Po di Gnocca river mouths were found to beach < 10% of all VMP released, while Po di Maistra and delle Tolle presented higher rates (26% and 19% respectively). By far the highest rate of beaching was determined for the southernmost river mouth, Po di Goro, with 94% of all released VMP being found to have beached. In Fig. 4a, the percentage of beached VMP from a particular river mouth are compared with the total VMP beached for each model run day. The other river mouths (Maistra, Pila, Scirocco, Tolle and Gnocca) display similar behavior in that the majority of

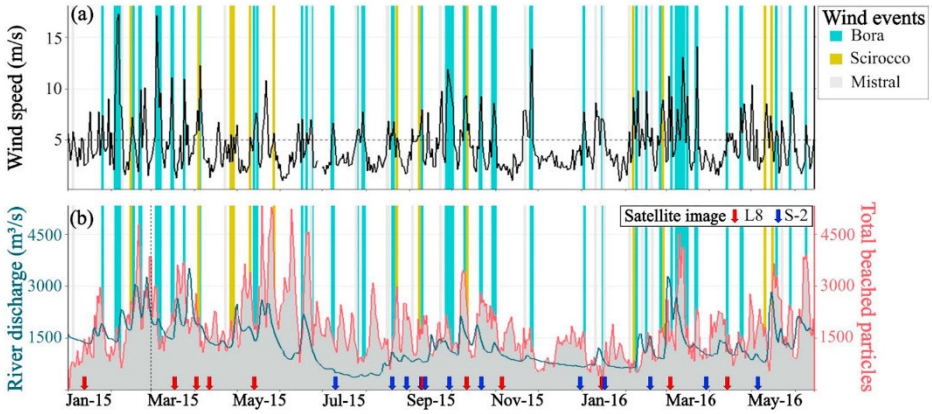

Fig. 3. (a) Average daily wind speed (m/s) in front of the Po Delta. Colored bars highlight wind events: Bora (light blue), Scirocco (green) and Mistral (light gray). Horizontal dashed line depicts the 5 m/s wind speed threshold. (b) Average daily Po River outflow (m^3/s) at Pontelagoscuro (dark blue line, left axis) compared with the average daily total of beached virtual microplastic particles (VMP, rose line, right axis). VMP were tracked in the model a total of 60 days, with the first day that satisfied this condition indicated by the vertical dashed black line. Usable satellite acquisitions are depicted by arrows (Landsat 8: L8, red; Sentinel-2: S-2, blue) along the temporal horizontal axis, ticked below to separate months. Wind events displayed as in (a). (For interpretation of the references to color in this figure legend, the reader is referred to the web version of this article.)

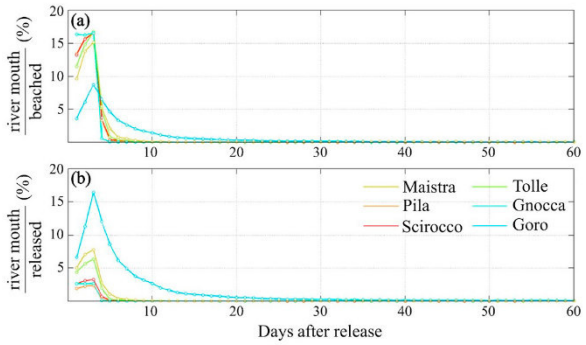

Fig. 4. Percent beached virtual microplastic particles (VMP) from each river mouth in comparison to (a) total daily beached VMP and (b) total daily released VMP. Days after release are depicted along the horizontal axis. Release events after April 15th, 2016, are not included since these were run for < 60 days.

beaching occurs within the first 3 days and was then followed by a sudden drop to low values, remaining close to zero after about 10 days. The Po di Goro mouth, on the other hand, also displayed high beaching rates in the first 5 days but thereafter a more gradual decline, reaching zero levels after *circa* 20 days. Thus, VMP released by the Po di Goro mouth were able to reach the coastline for a longer period of time (up to 30 days after release, as shown in Fig. 4a) and thus had higher probability to be beached than VMP released from the other mouths. Fig. 4b depicts the percentage of beached VMP per river mouth as compared to the total VMP released by the same river mouth. Here the much larger percentage of VMP to become beached from the total released by the Po di Goro mouth was quite clear, with over 34% of all VMP released from the river mouth being beached within the first three days after release. The elevated beaching rates of the Po di Maistra and delle Tolle were also more clearly depicted.

The hydrodynamic model beaching accumulation map for the entire simulation period is shown in Fig. 5. VMP release points in front of river mouths are indicated by the red arrows. Higher beached VMP accumulation was evident locally around each of the river mouth release points (Fig. 5a), as well as along the southern coast of the Po Delta and extending along the southward coast. The highest accumulation areas were modelled to be just south of the Po della Pila river mouth, and near to the Po di Gnocca and di Goro river mouths. The individual distribution from each river mouth is depicted in Fig. 5b, showing that the VMP beaching rates for all mouths remain quite local except for the southernmost Po di Goro mouth.

The hydrodynamic modelling results suggest that surface currents play a more deciding role in determining beaching rates, with the number of particles being released by the river only semi-coupled to beach accumulation. Surface currents in the northern Adriatic are determined by wind regime and freshwater influx, the Po River being the main contributor (Falcieri et al., 2014). VMP tracks from different river mouths revealed beaching rates of up to 18% for all modelled river mouths, with the exception of the southernmost mouth Po di Goro. This is a result of the Goro freshwater plume likely being held closer to the shoreline by the other plumes, thus allowing plume water to interact with the coastline for a longer period of time. For the other river mouths, VMP beaching was found to occur within 10 days following release, and beaching rate estimates suggests that over 80% of the microplastic particles being released by the Po River are being dispersed to the open Adriatic Sea system.

3.4. Remote sensing model accumulation

Results of all four assessed SPM algorithms are presented in Table 3, where the algorithm basis is listed along with the fitted algorithm and model fit statistics (RMSE, LOOCV-RMSE, bias). Model fit statistics were found to be reduced by an order of magnitude through the calibration/validation for both the Jørgensen and Dekker algorithms, only slight improvement was achieved for one of the band-ratio Doxaran algorithms while the other was found to be a non-significant predictor for the Po River water. Given the observed overlap of the Chl-*A* reflectance peak at 560 nm with the SPM signal saturation between 550 and 700 nm, the Dekker algorithm was selected as preferable to the Jørgensen algorithm (further details in S5 and S6 of the Supplementary material). Furthermore, the Dekker algorithm was found to be a significant predictor for both L8 as well as S-2 data.

A total of 26 usable images from L8 and S-2 (12 and 14 respectively) were compiled covering the modelling time period (as shown in Fig. 3 and Table 4). Usable images from two out of the total eighteen months considered could not be obtained. Of the compiled usable satellite images, five instances of Bora/low discharge were captured, as well as three instances of Scirocco/high discharge, only two instances of Bora/

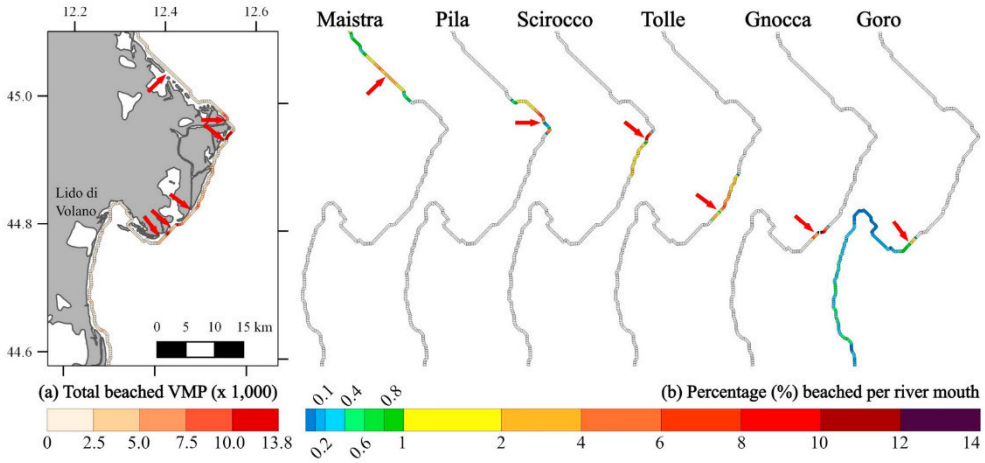

Fig. 5. (a) Distribution map for virtual microplastic particle (VMP) beaching accumulation over the entire 1.5-year simulation period, VMP release locations in front of river mouths are indicated by the red arrows. Color scale (beige low, red high) indicates total particles beached over entire modelling period. (b) Beached VMP for each river mouth displayed separately, color scale (blue low, red high) indicates percentage of total VMP beached from that particular river mouth. (For interpretation of the references to color in this figure legend, the reader is referred to the web version of this article.)

high and Mistral/high, and one instance each of Scirocco/low and Mistral/low discharge conditions. Images were atmospherically corrected (further details in S3 and S4 of the Supplementary material) and the optimal calibrated regional empirical algorithm for each sensor was implemented to create a time series of SPM river plume maps.

Examples from satellite image masking and implementation of the calibrated SPM algorithm are shown in Fig. 6. High/low river discharge was classified as daily average river discharge over/below the median discharge rate for the entire modelling period (1210 m^3/s). From the acquisition with high discharge, the strong effect of a wind event on river water transportation was quite evident. In the case of high discharge together with southeasterly Scirocco winds (Fig. 6b), plume water can be observed being pushed northward of the Po della Pila mouth. With northwesterly Mistral winds (Fig. 6c), the plume shape appears to be more heavily influenced by river outflow, with high river discharge producing a plume extending further into the Adriatic. But in the case of northeasterly Bora winds (Fig. 6a), the high discharge plume was kept closer to the coastline while primarily spreading high SPM waters toward the south. A somewhat different pattern was observed for the acquisitions concurrent to low discharge. The Bora wind event on January 16, 2016, was observed to again retain the plume close to the southern coastline (Fig. 6d). Plume form under low discharge and Scirocco wind was only demonstrated with one acquisition (Fig. 6e). SPM signal from the river water on this date were quite low, making the plume difficult to detect, but through utilizing a different stretch the plume could be observed to extend further into the Adriatic. The Mistral wind together with low discharge (Fig. 6f) was observed to retain the river plume close to the coastline, but much smaller than was observed with high discharge. Standard difference comparison between L8 and S-2 images revealed a slight sensor bias, in that detected L8 SPM values tended to be less (< 2 mg/L) than detected S-2 SPM values. This amount represented < 2% of the SPM range measured in the field (Table 1) and was thus taken to be negligible.

Results of the remote sensing composite hexagon binning processing are presented in Fig. 7, with red indicating coastal areas of high river water influence and green areas with less. Strong river water influence was detected around all five river mouths (Maistra, Pila, northern and central Tolle, Gnocca and Goro) as well as the Busa di Tramontana and di Scirocco. The southern arm of the Po delle Tolle was observed to have a lesser influence, while the northern section of coastline between river mouths presented very low rates of river water influence. Coastline sections near to the Po della Pila mouth and southward were observed to have higher rates, with the highest influence evidently being along the coastal section just north of Po della Pila. An area of very high river water influence (red) was detected between Po della Pila and Busa di Tramontana, which corresponds to an additional river mouth flowing out from the lagoon that was first observed during the field campaign.

Coastal exposure modelling using SPM derived from remote sensing images was able to well capture the signal of sediment heavy river plume waters spreading along the coastline (Fig. 6 and Fig. 7). Plume

Table 3
Calibrated algorithms for suspended particulate matter (SPM). Algorithm spectral basis and publication is indicated in the first column, standard fit algorithm in the second column together with model fit statistics: root mean square error (RMSE) and bias. Baseline and satellite specific algorithms are listed in the following columns, with fitted algorithm listed followed by fit statistics (RMSE, leave-one-out cross-validation RMSE, bias) in parentheses. Relationships that were found to be non-significant ($\alpha \geq 0.05$) during fitting are indicated with N/A. The satellite sensor band used is also indicated, *e.g.* Landsat 8 band 3 centered at 560 nm is indicated by $b3_{560}$.

Algorithm basis	Standard fit	Baseline fit	Landsat 8	Sentinel-2
Band at 555 nm (Jørgensen, 1999)	$0.09 + 56.19 * b_{555}$ (154.91; 148.22)	$\exp(1.47 + 0.60 * b_{555})$ (40.66; 29.98; 27.67)	$\exp(1.46 + 0.60 * b3_{560})$ (40.64; 29.35; 27.67)	$\exp(1.45 + 0.60 * b3_{561})$ (40.65; 29.63; 27.67)
Band at 706 nm (Dekker, 1993)	$2.69 + 3.31 * b_{706}$ (561.16; 488.92)	$\exp(1.92 + 0.79 * b_{706})$ (40.45; 21.72; 27.67)	$\exp(1.82 + 0.66 * b4_{655})$ (40.50; 22.91; 27.67)	$\exp(1.91 + 0.78 * b5_{706})$ (40.45; 21.65; 27.67)
SPOT bands XS3 (cen. 835 nm) and XS1 (cen. 545 nm) (Doxaran et al., 2002)	$\exp(3.01 + 3.13 * XS3_{835} / XS1_{545})$ (27.37; 21.06)	$\exp(2.37 + 3.25 * XS3_{835} / XS1_{545})$ (26.29; 29.62; 16.43)	N/A	$\exp(2.39 + 3.57 * b8_{843} / b3_{561})$ (26.42; 29.79; 16.49)
SPOT bands XS3 (cen. 835 nm) and XS2 (cen. 645 nm) (Doxaran et al., 2002)	$\exp(2.56 + 5.31 * XS3_{835} / XS2_{645})$ (83.15; 50.92)	N/A	N/A	N/A

Table 4
Temporal satellite image coverage from January 2015 to June 2016. Total images from each satellite (Sentinel-2: S-2; Landsat 8: L8) are listed in the table, note that S-2 images first became available July 2015. Satellite acquisitions also depicted in Fig. 4.

Platform	Jan	Feb	Mar	Apr	May	Jun	Jul	Aug	Sep	Oct	Nov	Dec	Jan	Feb	Mar	Apr	May	Jun	Total
L8	1	0	1	2	1	0	0	0	1	1	1	0	1	0	1	1	0	1	12
S-2	–	–	–	–	–	–	1	2	3	1	0	1	1	1	1	0	1	2	24

exposure was found to be highest locally around the five main river mouths (Maistra, Pila, Tolle, Gnocca and Goro), as well as by side channels (Scirocco, Tramontana). Different amounts of river plume exposure were determined for the three arms of the Tolle river mouth, with the highest signal coming from the middle arm and the lowest from the southern arm. Evidence of an extra river mouth with strong outflow between Tramontana and Pila from the remote sensing analysis follows observations made while collecting the field data. The Po della Pila mouth is supposed to transport over 60% of the entire river discharge (Correggiari et al., 2005), but based on the SPM exposure map, this river mouth appears to be on par with the effects from the Po delle Tolle and Busa di Tramontana. A persistent sand bank was observed at the opening of this river mouth, both in the remote sensing images and during sampling in the field. In images taken during high SPM events, it is clear that flow out of Po della Pila is being split into a northern and southern portion after encountering this sand bar. If flow is indeed being slowed out of Po della Pila by the presence of this sand bar, this would provide a mechanism to explain why the flow is high out of the Busa di Tramontana and the unnamed outlet just south of Tramontana. Although this can only be definitively tested with *in situ* hydrodynamic measurements, the potential of using remote sensing SPM images for identifying fine-scale river mouth dynamic patterns is nevertheless well demonstrated here. The time series was able to capture multiple acquisitions of Bora events with low river discharge and one instance with high river discharge. In all events, the river plume is observed to stay closer to the Italian coastline with Bora wind, following results and model predictions made by Falcieri et al. (2014). This is in stark contrast to the situation observed with Scirocco together with high discharge, where the river plume can be observed to extend further east and north (Fig. 6). River plume dynamics during Mistral events appear to be controlled more by river discharge than wind regime. The relationship between wind regime and freshwater outflow on northern Adriatic circulation patterns is complex, but remote sensing images of the river plume can certainly serve as a useful tool for testing hypotheses.

Very low *in situ* water microplastic concentrations were found for the Po di Maistra and delle Tolle mouths, as well as the Busa di Scirocco. Two of these river mouths, namely Maistra and Scirocco, were observed to also have low river plume influence from the remote sensing accumulation map. Maistra is expected to have the smallest outflow of all river mouths (Correggiari et al., 2005), and was thus also found to have the smallest impact from the hydrodynamic accumulation modelling (Fig. 5). The low *in situ* water microplastic concentration measurement from Po delle Tolle is less easily clarified, as this mouth was found to have a substantial influence by both the hydrodynamic and remote sensing accumulation models. There was also a discrepancy between the measured *in situ* concentrations from the middle Tolle mouth and before the Tolle arm divides into three. This suggests that

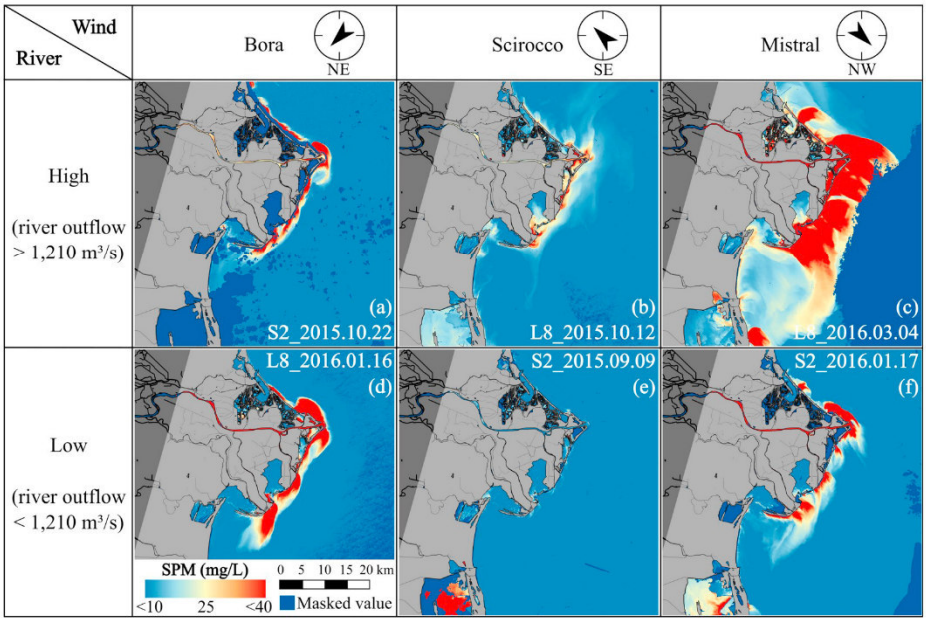

Fig. 6. Combined effect of different wind regimes (Bora, Scirocco or Mistral) with differing river discharge conditions on river plume transportation along the Western Adriatic. River discharge is termed "high" (panels a, b, c) or "low" (panels d, e, f) depending on daily discharge relative to the median (1210 m^3/s) over the entire simulation period. Wind events were classified based on wind direction (indicated by wind compass in each column, pointing in the direction that wind is blowing) and strength (winds in excess of 5 m/s). Suspended Particulate Matter (SPM) values, ranging from low in blue to high in red, depict river plume shape. Masked pixels are depicted in dark blue, land in light gray (outside of area of interest in dark gray). (For interpretation of the references to color in this figure legend, the reader is referred to the web version of this article.)

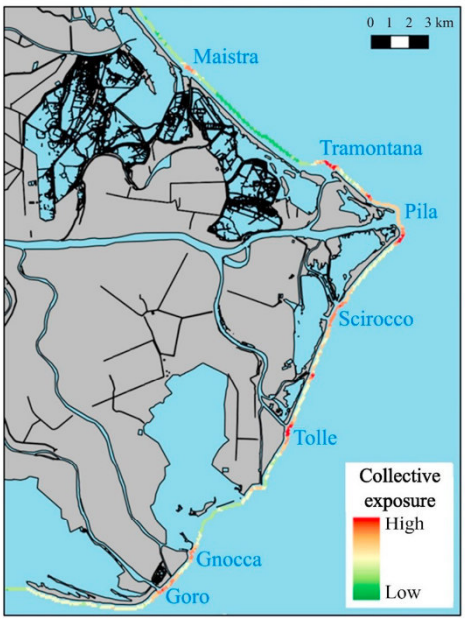

Fig. 7. Composite hexagon (100 m) map of SPM time series, colored by summed daily similarity values to river water. High rates of river plume influence (red) are observed at all five major river mouths and the Busa di Tramontana and di Scirocco, around Po della Pila. Low river plume influence (green) can be observed along the northern coast of the delta. (For interpretation of the references to color in this figure legend, the reader is referred to the web version of this article.)

further accumulation processes may be occurring within the Tolle subarm which have not been captured by the model, and thus warrants further investigation than was feasible within the scope of this study.

3.5. Model validation results

No significant relationship was found when comparing the *in situ* beach sediment microplastic concentrations to the nearest hydrodynamic model grid cell ($p > 0.10$ for Pearson's r and Spearman's ρ). Removal of beach locations that were under more influence from beach tourism and nearby aquaculture (namely Caleri, Levante, Boccasette and Barricata) resulted in a stronger correlation with the hydrodynamic results: Pearson's $r = 0.79$ and Spearman's $\rho = 0.80$ ($p < 0.07$ in both cases). Comparison of *in situ* beach sediment microplastic concentrations with the nearest remote sensing model 30 m hexagon revealed a moderate negative correlation, with Pearson's $r = -0.58$ ($p = 0.05$). No significant correlation was found at the 100 m hexagon resolution. Focusing the comparison to beaches with lesser influence from beach tourism and nearby aquaculture did not reveal an improved correlation. Removal of the styrene-based polymers from the *in situ* beach sediment microplastic concentrations was also considered, given that the majority of the styrene-based polymer group was composed of foamed polystyrene. This particular styrene polymer form is highly buoyant and thus very susceptible to windage during transport as well as potential higher susceptibility for further particle fractionation during beach sediment lab processing. Despite these considerations, removal of this group from *in situ* beach sediment microplastic concentrations was not found to provide any further model improvement.

Comparison between the two models is depicted in Fig. 8, where the normalized remote sensing exposure map is shown next to the hydrodynamic model accumulation map (Fig. 8a). General tendencies for lower normalized values along the coastline north of Pila di Maistra and south of Lido di Volano were similar between the two model results. Strong river mouth signal from Pila, the southern Tolle, Gnocca and Goro were also evident in both maps. Visual dissimilarities were most evident for the river mouths Maistra, Tramontana and Scirocco, where a strong signal was registered by the remote sensing model but not by the hydrodynamic model. In Fig. 8b, the difference of the normalized values (remote sensing normalized values, RS_{norm}, minus hydrodynamic normalized values, HD_{norm}) are displayed as a bar chart aligned along the latitudinal axis. The comparison was made along the full overlap extent of both maps and the distribution is indicated in Fig. 8b with one and two standard deviation gray shaded areas. A slight positive bias is observed, meaning that the RS_{norm} values tend to be higher than the HD_{norm} values, with 95% of all values lying between -0.07 and 0.49. Areas of exceptional variation, indicated by bars lying outside the shaded gray area, were notably the coastline located between Pila and Scirocco and between the northern and central Tolle mouths.

Validation of both accumulation models against all *in situ* measurements did not produce a significant relationship. This is likely due to additional microplastic processes (such as biofouling or sinking) and sources outside of the Po River water which were not included in either model. Artifacts may also have been introduced to the correlation through the *in situ* sediment sampling scheme. In an effort to circumvent potential temporal variability, the extreme high tide line was chosen for the field sampling over the most recent high tide line. Another factor to acknowledge is the assumption of beaching occurring after a particle passes within 250 m of the coastline, representing a substantial simplification of nearshore currents but which was necessary with the given modelling tools. A slightly significant correlation was found between the hydrodynamic accumulation map and *in situ* samples from beaches which were only accessible by boat and not located next to a large harbor. An inverse relationship between amount of beach litter and distance to nearest parking lot has already been established in the Adriatic (Munari et al., 2017), suggesting that beach tourism poses a significant plastic litter source not included in the models. The remote sensing river plume exposure model was not found to have a significant relationship with the *in situ* samples but was very useful in identifying which river mouths were significant outflow contributors during the simulation period. This information can be useful in the set-up of future ocean current models of the Po Delta. A number of factors not incorporated into either the hydrodynamic or the remote sensing model may largely explain the missing correlation. Refuse resulting from the major shipping corridors which cross the Adriatic are posited to account for 20% of all marine plastic litter introduced each year to the sea and the Po River for only 13.5% thereof (Liubartseva et al., 2016). Windage of particles was not accounted for in the hydrodynamic model, which can provide drift speeds up to 25% larger than the current speed (Chubarenko et al., 2016). After particles become beached, wind transportation may move particles laterally or further inland (Munari et al., 2016). Microplastic particle aging within the marine environment was also not represented, including processes of biofouling, further fragmentation, flocculation and aggregation, all which are recognized as important dynamic parameters influencing residence times and transportation pathways (Zhang, 2017). VMP density was simplified to 0.91 g/mL, representative of the average of virgin PE (both high and low density) and PP, which was a necessary assumption given the scope of the study. It would be quite interesting to test how differing particle density for each major plastic type would affect modelled coastal accumulation patterns, especially for the polymer groups most represented in the sediment samples (PE, PP and PS). Seasonality was accounted for in the hydrodynamic model through changing the amount of VMP released dependent upon Po River outflow, but the concentration of microplastic particles was held constant during the entire modelling period. It has been established that river mouth concentrations of microplastic particles can vary by up to three orders of magnitude at different times of the year (Lebreton et al., 2017) and that storm water runoff events can significantly increase river

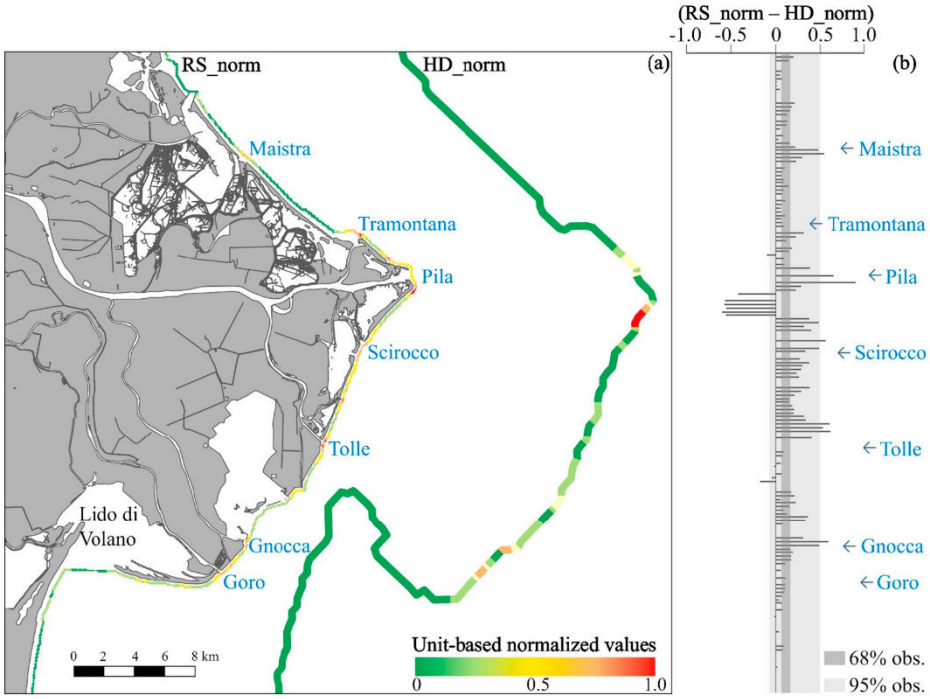

Fig. 8. (a) Remote sensing hexagon-binned (100 m) exposure map (left) next to hydrodynamic model accumulation map (right), both datasets have been unit-based normalized (green low to red high). (b) Difference normalized remote sensing model (RS_{norm}) to normalized hydrodynamic model (HD_{norm}), aligned along the latitudinal axis. Percentage all observations (obs.) at one standard deviation (1-σ, 68%, dark gray) or two (2-σ, 95%, light gray) is indicated, and river mouth position along bar chart is shown in blue italics. (For interpretation of the references to color in this figure legend, the reader is referred to the web version of this article.)

mouth microplastic load (Zhang, 2017). Beaching in this study's hydrodynamic model follows simplifying assumptions made in other studies (Lebreton et al., 2012; Politikos et al., 2017), since the mechanisms controlling onshore-offshore transport of microplastic particles remain unclear (Critchell et al., 2015; Hardesty et al., 2017; Hinata et al., 2017; Moreira et al., 2016). Despite this, these mechanisms likely play a driving role in determining small-scale and temporal variation in sediment microplastic deposition rates (Carlson et al., 2017; Hinata et al., 2017; Schulz et al., 2017; Zhang, 2017).

4. Conclusions and outlook

In situ sampling of both Po River and Adriatic Sea waters revealed microplastic concentrations up to 84 particles/m^3 and beach sediment concentrations up to 78 particles/DW kg. The hydrodynamic modelling approach was able to identify differing beaching rates between various river mouths and suggested that particle beaching mostly occurred within the first 10 days of release. Particles which do not beach within this initial time period (over 80% of all VMP emitted by the Po River) were transported away from the Po Delta coastline. Po River emitted particles that were moved offshore remained offshore, likely due to the continual freshwater input creating water density boundaries that inhibit westward transport. Especially the Po di Goro mouth was identified as effecting higher beaching rates over a much longer stretch of coastline. The suspended sediment remote sensing approach was able to well represent river mouth relative strength, such as the smaller contribution from the southernmost Po delle Tolle river arm or the much larger contribution of Busa di Tramontana in river outflow. Microplastic accumulation exposure maps were constructed from both approaches, which were found to be similar to one another but were not found to have a significant relationship to *in situ* beach sampling. This relationship changed when beaches that were closer to public parking lots and harbors were removed, suggesting that microplastic sources which were not accounted for in either modelling approach are also large contributors to beach microplastic accumulation.

There remain many uncertainties still in our understanding of the transportation and accumulation mechanisms of microplastics (Hardesty et al., 2017) and with this study we offer some insight into these mechanisms within the coastal environment. From the hydrodynamic modelling, we see how particles not beached within the first 10 days are transported away from the coastline. The hydrodynamic model also offers a continual track of VMP transportation and could be used to study VMP distribution in the open sea. The remote sensing model presents snapshots of surface river plume form at a finer spatial resolution over a larger area than computationally feasible with existing ocean current models. River plume exposure during the modelling period could be well captured but this is difficult to translate to actual microplastic accumulation rates. Model assimilation of remote sensing data into ocean current simulation models has begun to gain traction in other oceanographic modelling areas (Miyazawa et al., 2013; Stroud et al., 2009; Zhang et al., 2014), with up to 40% improvements in model forecast root square error. Hardesty et al. (2017) have already suggested the great improvements possible to our understanding of microplastic transportation pathways through integrating simulation model and empirical observations.

Deeper understanding of microplastic sources, pathways and accumulation areas is intrinsic to our ability to mitigate introduction of this pollutant to limnic and marine systems as well as organize clean-up activities. International agreements are already in place forbidding deposition of litter into the Mediterranean marine environment (Mistri et al., 2017; Munari et al., 2016), yet despite these steps this enclosed sea continues to have particularly high concentrations of marine debris

(Cozar et al., 2015; Suaria et al., 2016). Other modelling efforts within the Adriatic suggest that land-based sources of marine litter contribute the majority of marine litter entry into the sea each year (Munari et al., 2017). National borders are not a component of marine plastic debris transportation pathway mechanisms and finding middle ground in national agendas to support concerted legislation efforts are difficult. *In situ* microplastic sampling and sample processing is costly, thus modelling offers a methodology for upscaling point measurements to larger areas than could be feasibly sampled (Hardesty et al., 2017). Freshwater systems, in particular rivers, have been slower to receive the same microplastic research attention as attributed to marine systems (Wagner et al., 2014). Evidence exists that even low-density tourism can still create heavy consumer plastic pollution (Free et al., 2014). Methods for identifying marine debris sources and forecasting accumulation areas have already been put forward as a method to reduce the cost and optimize the effort of remediation activities (Krelling et al., 2017; UNEP, 2016). This study demonstrates the strengths and weaknesses of two separate modelling approaches, providing further tools aiming to answer the suggestion of Hardesty et al. (2017) to develop multipart solutions which can be applied at both local and regional scales to effect change.

Supplementary data to this article can be found online at https://doi.org/10.1016/j.marpolbul.2018.11.045.

Acknowledgements

The authors would like to thank Sandra Lohberger for providing advice and input to both the analysis and writing of the paper. This work was very kindly supported by numerous lab technicians and interns. Sabela Rodríguez Castaño, Sophia Wisböck and Moritz Altenbach in particular provided much appreciated support in image processing. Both Veronika Mitterwallner and Lena Löschel played very important roles in the preparation and analysis of the microplastic samples, and Heghnar Martirosyan and Annika Heymann are thanked for their help with ATR measurements. We would like to extend our thanks to our brave boat captains, Claudio and Sandro, who were willing to take a trio of crazy scientists repeatedly out into the open ocean. This study was partly funded by the German Federal Ministry for Economic Affairs and Energy (Bundesministerium für Wirtschaft und Energie, or BMWi) *via* the DLR Space Administration under the grant numbers 50EE1301 and 50EE1269, and by the Italian National Flagship Program RITMARE of the Italian Ministry of Education, University and Research.

References

Andrady, A.L., 2017. The plastic in microplastics: a review. Mar. Pollut. Bull. 119, 12–22. https://doi.org/10.1016/j.marpolbul.2017.01.082.

Artegiani, A., Paschini, E., Russo, A., Bregant, D., Raicich, F., Pinardi, N., 1997a. The Adriatic Sea general circulation. Part I: Air-sea interactions and water mass structure. J. Phys. Oceanogr. 27, 1492–1514. https://doi.org/10.1175/1520-0485(1997)027<1492:TASGCP>2.0.CO;2.

Artegiani, A., Paschini, E., Russo, A., Bregant, D., Raicich, F., Pinardi, N., 1997b. The Adriatic Sea general circulation. Part II: Baroclinic circulation structure. J. Phys. Oceanogr. 27, 1515–1532. https://doi.org/10.1175/1520-0485(1997)027<1515:TASGCP>2.0.CO;2.

Azzarello, M.Y., van Vleet, E.S., 1987. Marine birds and plastic pollution. Mar. Ecol. Prog. Ser. 37, 295–303. https://doi.org/10.3354/meps037295.

Bignami, F., Sciarra, R., Carniel, S., Santoleri, R., 2007. Variability of Adriatic Sea coastal turbid waters from SeaWiFS imagery. J. Geophys. Res. Oceans 112, C03S10. https://doi.org/10.1029/2006JC003518.

Bolaños, R., Sørensen, J.V.T., Benetazzo, A., Carniel, S., Sclavo, M., 2014. Modelling ocean currents in the northern Adriatic Sea. Cont. Shelf Res. 87, 54–72.

Boldrin, A., Carniel, S., Giani, M., Marini, M., Bernardi Aubry, F., Campanelli, A., Grilli, F., Russo, A., 2009. Effects of bora wind on physical and biogeochemical properties of stratified waters in the northern Adriatic. J. Geophys. Res. Oceans 114, 1492. https://doi.org/10.1029/2008JC004837.

Booij, N., Ris, R.C., Holthuijsen, L.H., 1999. A third-generation wave model for coastal regions: 1. Model description and validation. J. Geophys. Res. Oceans 104, 7649–7666.

Bouwman, H., Evans, S.W., Cole, N., Yive, Nee Sun Choong Kwet, Kylin, H., 2016. The flip-or-flop boutique: marine debris on the shores of St Brandon's rock, an isolated tropical atoll in the Indian Ocean. Mar. Environ. Res. 114, 58–64.

Browne, M.A., Galloway, T.S., Thompson, R.C., 2010. Spatial patterns of plastic debris along estuarine shorelines. Environ. Sci. Technol. 44, 3404–3409. https://doi.org/10.1021/es903784e.

Brunner, K., Kukulka, T., Proskurowski, G., Law, K.L., 2015. Passive buoyant tracers in the ocean surface boundary layer: 2. Observations and simulations of microplastic marine debris. J. Geophys. Res. Oceans 120, 7559–7573. https://doi.org/10.1002/2015JC010840.

Cable, R.N., Beletsky, D., Beletsky, R., Wigginton, K., Locke, B.W., Duhaime, M.B., 2017. Distribution and modeled transport of plastic pollution in the Great Lakes, the world's largest freshwater resource. Front. Environ. Sci. 5 (10377). https://doi.org/10.3389/fenvs.2017.00045.

Campbell, J.W., O'Reilly, J.E., 2005. Metrics for Quantifying the Uncertainty in a Chlorophyll Algorithm: Explicit Equations and Examples Using the OC4.v4 Algorithm and NOMAD data. Ocean Color Bio-optical Algorithm Mini-workshop, Durham, New Hampshire. 27–29 Sept. 2005.

Carlson, D.F., Suaria, G., Aliani, S., Fredj, E., Fortibuoni, T., Griffa, A., Russo, A., Melli, V., 2017. Combining litter observations with a Regional Ocean model to identify sources and sinks of floating debris in a semi-enclosed basin: the Adriatic Sea. Front. Mar. Sci. 4, 1–16. https://doi.org/10.3389/fmars.2017.00078.

Carniel, S., Benetazzo, A., Bonaldo, D., Falcieri, F.M., Miglietta, M.M., Ricchi, A., Sclavo, M., 2016. Scratching beneath the surface while coupling atmosphere, ocean and waves: analysis of a dense water formation event. Ocean Model 101, 101–112. https://doi.org/10.1016/j.ocemod.2016.03.007.

Chubarenko, I., Bagaev, A., Zobkov, M., Esiukova, E., 2016. On some physical and dynamical properties of microplastic particles in marine environment. Mar. Pollut. Bull. 108, 105–112. https://doi.org/10.1016/j.marpolbul.2016.04.048.

Correggiari, A., Cattaneo, A., Trincardi, F., 2005. The modern Po Delta system: lobe switching and asymmetric prodelta growth. Mar. Geol. 222-223, 49–74. https://doi.org/10.1016/j.margeo.2005.06.039.

Cozar, A., Sanz-Martín, M., Martí, E., Ignacio González-Gordillo, J., Ubeda, B., Gálvez, J.Á., Irigoien, X., Duarte, C.M., 2015. Plastic accumulation in the Mediterranean Sea. PLoS One 10, e0121762. https://doi.org/10.1594/PANGAEA.842054.

Critchell, K., Grech, A., Schlaefer, J., Andutta, F.P., Lambrechts, J., Wolanski, E., Hamann, M., 2015. Modelling the fate of marine debris along a complex shoreline: lessons from the Great Barrier Reef. Estuar. Coast. Shelf Sci. 167, 414–426. https://doi.org/10.1016/j.ecss.2015.10.018.

Dekker, A.G., 1993. Detection of Optical Water Quality Parameters for Eutrophic Waters by High Resolution Remote Sensing. Proefschrift Vrije Universiteit Amsterdam, Amsterdam, The Netherlands (237 pp).

van der Wal, M., van der Meulen, M., Tweehuijsen, G., Peterlin, M., Palatinus, A., Viršek, M.K., Coscia, L., Kržan, A., 2015. SFRA0025: Identification and Assessment of Riverine Input of (Marine) Litter. Eunomia Research & Consulting (208 pp).

Doxaran, D., Froidefond, J.-M., Lavender, S., Castaing, P., 2002. Spectral signature of highly turbid waters: application with SPOT data to quantify suspended particulatematter concentrations. Remote Sens. Environ. 81, 149–161.

Dris, R., Imhof, H., Sanchez, W., Gasperi, J., Galgani, F., Tassin, B., Laforsch, C., 2015. Beyond the ocean: contamination of freshwater ecosystems with (micro-)plastic particles. Environ. Chem. 12, 539. https://doi.org/10.1071/EN14172.

Duhec, A.V., Jeanne, R.F., Maximenko, N., Hafner, J., 2015. Composition and potential origin of marine debris stranded in the Western Indian Ocean on remote Alphonse Island, Seychelles. Mar. Pollut. Bull. 96, 76–86. https://doi.org/10.1016/j.marpolbul.2015.05.042.

Falcieri, F.M., Benetazzo, A., Sclavo, M., Russo, A., Carniel, S., 2014. Po River plume pattern variability investigated from model data. Cont. Shelf Res. 87, 84–95. https://doi.org/10.1016/j.csr.2013.11.001.

Fargion, G.S., Mueller, J.L., 2000. Ocean Optics Protocols for Satellite Ocean Color Sensor Validation, Revision 2: Sensor Intercomparison and Merger for Biological and Interdisciplinary Ocean Studies (SIMBIOS) Project Technical Memoranda. NASA/TM-2000-209966/REV2, Rept-2000-04041-0/REV2, NAS 1.15:209966/REV2. NASA, NASA Goddard Space Flight Center, Greenbelt, MD, USA (194 pp). https://ntrs.nasa.gov/search.jsp?R=20000097063.

Free, C.M., Jensen, O.P., Mason, S.A., Eriksen, M., Williamson, N.J., Boldgiv, B., 2014. High-levels of microplastic pollution in a large, remote, mountain lake. Mar. Pollut. Bull. 85, 156–163. https://doi.org/10.1016/j.marpolbul.2014.06.001.

G7 Germany, 2015. Leaders' Declaration G7 Summit, 7–8 June 2015. G7 Germany, Schloss Elmau, Germany (23 pp).

Galgani, F., Hanke, G., Werner, S., Oosterbaan, L., Nilsson, P., Fleet, D., Kinsey, S., Thompson, R.C., van Franeker, J., Vlachogianni, T., Scoullos, M., Veiga, J.M., Palatinus, A., Matiddi, M., Maes, T., Korpinen, S., Budziak, A., Leslie, H., Gago, J., Liebezeit, G., 2013. Guidance on Monitoring of Marine Litter in European Seas: A Guidance Document Within the Common Implementation Strategy for the Marine Strategy Framework Directive. Publications Office of the European Union, Luxembourg.

GESAMP, 2016. Sources, Fate and Effects of Microplastics in the Marine Environment: Part Two of a Global Assessment. Rep. Stud. GESAMP 93. IMO, FAO, UNESCO-IOC, UNIDO, WMO, IAEA, UN, UNEP, UNDP Joint Group of Experts on the Scientific Aspects of Marine Environmental Protection, Rome, Italy (221 pp).

Haidvogel, D.B., Arango, H., Budgell, W.P., Cornuelle, B.D., Curchitser, E., Di Lorenzo, E., Fennel, K., Geyer, W.R., Hermann, A.J., Lanerolle, L., Levin, J., McWilliams, J.C., Miller, A.J., Moore, A.M., Powell, T.M., Shchepetkin, A.F., Sherwood, C.R., Signell, R.P., Warner, J.C., Wilkin, J., 2008. Ocean forecasting in terrain-following coordinates: formulation and skill assessment of the Regional Ocean Modeling System. J. Comput. Phys. 227, 3595–3624.

Hardesty, B.D., Harari, J., Isobe, A., Lebreton, L., Maximenko, N., Potemra, J., van Sebille, E., Vethaak, A.D., Wilcox, C., 2017. Using numerical model simulations to improve the understanding of micro-plastic distribution and pathways in the marine environment. Front. Mar. Sci. 4 (30). https://doi.org/10.3389/fmars.2017.00030.

Heim, B., 2005. Qualitative and Quantitative Analyses of Lake Baikal's Surface-waters Using Ocean Colour Satellite Data (SeaWiFS). Doctoral Thesis. (142 pp).

Hinata, H., Mori, K., Ohno, K., Miyao, Y., Kataoka, T., 2017. An estimation of the average residence times and onshore-offshore diffusivities of beached microplastics based on

the population decay of tagged meso- and macrolitter. Mar. Pollut. Bull. 122, 17–26. https://doi.org/10.1016/j.marpolbul.2017.05.012.
Hoffman, M.J., Hittinger, E., 2017. Inventory and transport of plastic debris in the Laurentian Great Lakes. Mar. Pollut. Bull. 115, 273–281. https://doi.org/10.1016/j.marpolbul.2016.11.061.
Horvat, P., 2015. MICRO 2015 Seminar, Piran, Slovenia. May 2015.
Imhof, H.K., Ivleva, N.P., Schmid, J., Niessner, R., Laforsch, C., 2013. Contamination of beach sediments of a subalpine lake with microplastic particles. Curr. Biol. 23, R867–R868. https://doi.org/10.1016/j.cub.2013.09.001.
Imhof, H.K., Wiesheu, A.C., Anger, P.M., Niessner, R., Ivleva, N.P., Laforsch, C., 2018. Variation in plastic abundance at different lake beach zones - a case study. Sci. Total Environ. 613-614, 530–537. https://doi.org/10.1016/j.scitotenv.2017.08.300.
IOC, SCOR, 1994. Protocols for the Joint Global Ocean Flux Study (JGOFS) Core Measurements. IOC Manuals and Guides 29 (181 pp).
Jambeck, J.R., Geyer, R., Wilcox, C., Siegler, T.R., Perryman, M., Andrady, A., Narayan, R., Law, K.L., 2015. Plastic waste inputs from land into the ocean. Science 347, 768–771. https://doi.org/10.1126/science.1260352.
Jørgensen, P.V., 1999. Standard CZCS Case 1 algorithms in Danish coastal waters. Int. J. Remote Sens. 20, 1289–1301. https://doi.org/10.1080/014311699212731.
Kooi, M., Reisser, J., Slat, B., Ferrari, F.F., Schmid, M.S., Cunsolo, S., Brambini, R., Noble, K., Sirks, L.-A., Linders, T.E.W., Schoeneich-Argent, R.I., Koelmans, A.A., 2016. The effect of particle properties on the depth profile of buoyant plastics in the ocean. Sci. Rep. 6. https://doi.org/10.1038/srep33882.
Krelling, A.P., Souza, M.M., Williams, A.T., Turra, A., 2017. Transboundary movement of marine litter in an estuarine gradient: evaluating sources and sinks using hydrodynamic modelling and ground truthing estimates. Mar. Pollut. Bull. 119, 48–63. https://doi.org/10.1016/j.marpolbul.2017.03.034.
Law, K.L., Thompson, R.C., 2014. Oceans. Microplastics in the seas. Science 345, 144–145. https://doi.org/10.1126/science.1254065.
Lebreton, L.C.-M., Greer, S.D., Borrero, J.C., 2012. Numerical modelling of floating debris in the world's oceans. Mar. Pollut. Bull. 64, 653–661. https://doi.org/10.1016/j.marpolbul.2011.10.027.
Lebreton, L.C.M., van der Zwet, J., Damsteeg, J.-W., Slat, B., Andrady, A., Reisser, J., 2017. River plastic emissions to the world's oceans. Nat. Commun. 8, 15611. https://doi.org/10.1038/ncomms15611.
Lee, J., Hong, S., Song, Y.K., Hong, S.H., Jang, Y.C., Jang, M., Heo, N.W., Han, G.M., Lee, M.J., Kang, D., Shim, W.J., 2013. Relationships among the abundances of plastic debris in different size classes on beaches in South Korea. Mar. Pollut. Bull. 77, 349–354. https://doi.org/10.1016/j.marpolbul.2013.08.013.
Lett, C., Verley, P., Mullon, C., Parada, C., Brochier, T., Pierrick, P., Balnke, B., 2008. A lagrangian tool for modelling ichthyoplankton dynamics. Environ. Model. Softw. 23, 1210–1214.
Lindell, T., Pierson, D., Premazzi, G., Zilioli, E. (Eds.), 1999. Manual for Monitoring European Lakes Using Remote Sensing Techniques. Off. for Off. Publ. of the Europ. Communities, Luxembourg (161 pp).
Liubartseva, S., Coppini, G., Lecci, R., Creti, S., 2016. Regional approach to modeling the transport of floating plastic debris in the Adriatic Sea. Mar. Pollut. Bull. 103, 115–127. https://doi.org/10.1016/j.marpolbul.2015.12.031.
Löder, M.G.J., Gerdts, G., 2015. Methodology used for the detection and identification of microplastics—A critical appraisal. In: Bergmann, M., Gutow, L., Klages, M. (Eds.), Marine Anthropogenic Litter. Springer International Publishing, Cham, pp. 201–227.
Löder, M.G.J., Kuczera, M., Mintenig, S., Lorenz, C., Gerdts, G., 2015. Focal plane array detector-based micro-Fourier-transform infrared imaging for the analysis of microplastics in environmental samples. Environ. Chem. 12, 563. https://doi.org/10.1071/EN14205.
Löder, M.G.J., Imhof, H.K., Ladehoff, M., Löschel, L.A., Lorenz, C., Mintenig, S., Piehl, S., Primpke, S., Schrank, I., Laforsch, C., Gerdts, G., 2017. Enzymatic purification of microplastics in environmental samples. Environ. Sci. Technol. 51, 14283–14292. https://doi.org/10.1021/acs.est.7b03055.
Mani, T., Hauk, A., Walter, U., Burkhardt-Holm, P., 2015. Microplastics profile along the Rhine River. Sci. Rep. 5 (17988). https://doi.org/10.1038/srep17988.
Masura, J., Baker, J., Foster, G., Arthur, C., 2015. Laboratory Methods for the Analysis of Microplastics in the Marine Environment: Recommendations for Quantifying Synthetic Particles in Waters and Sediments Technical Memorandum NOS-OR&R-48. NOAA Marine Debris Program, NOAA Marine Debris Division, Silver Spring, MD, USA (39 pp).
Michaelsen, J., 1987. Cross-validation in statistical climate forecast models. J. Clim. Appl. Meteorol. 26, 1589–1600.
Mistri, M., Infantini, V., Scoponi, M., Granata, T., Moruzzi, L., Massara, F., de Donati, M., Munari, C., 2017. Small plastic debris in sediments from the Central Adriatic Sea: types, occurrence and distribution. Mar. Pollut. Bull. 124, 435–440. https://doi.org/10.1016/j.marpolbul.2017.07.063.
Miyazawa, Y., Murakami, H., Miyama, T., Varlamov, S.M., Guo, X., Waseda, T., Sil, S., 2013. Data assimilation of the high-resolution sea surface temperature obtained from the Aqua-Terra satellites (MODIS-SST) using an ensemble Kalman filter. Remote Sens. 5, 3123–3139. https://doi.org/10.3390/rs5063123.
Mobley, C.D., 1999. Estimation of the remote-sensing reflectance from above-surface measurements. Appl. Opt. 38, 7442. https://doi.org/10.1364/AO.38.007442.
Moreira, F.T., Prantoni, A.L., Martini, B., de Abreu, M.A., Stoiev, S.B., Turra, A., 2016. Small-scale temporal and spatial variability in the abundance of plastic pellets on sandy beaches: methodological considerations for estimating the input of microplastics. Mar. Pollut. Bull. 102, 114–121. https://doi.org/10.1016/j.marpolbul.2015.11.051.
Munari, C., Corbau, C., Simeoni, U., Mistri, M., 2016. Marine litter on Mediterranean shores: analysis of composition, spatial distribution and sources in north-western Adriatic beaches. Waste Manag. 49, 483–490. https://doi.org/10.1016/j.wasman.2015.12.010.
Munari, C., Scoponi, M., Mistri, M., 2017. Plastic debris in the Mediterranean Sea: types, occurrence and distribution along Adriatic shorelines. Waste Manag. 67, 385–391. https://doi.org/10.1016/j.wasman.2017.05.020.
PlasticsEurope, 2014. Plastics – The Facts 2014. An Analysis of European Plastics Production, Demand and Waste Data. PlasticsEurope (33 pp).
PlasticsEurope, 2016. Plastics – THE FACTS 2016. An Analysis of European Plastics Production, Demand and Waste Data. PlasticsEurope (38 pp). http://www.plasticseurope.org/Document/plastics—the-facts-2016-15787.aspx?Page=DOCUMENT&FolID=2.
Politikos, D.V., Ioakeimidis, C., Papatheodorou, G., Tsiaras, K., 2017. Modeling the fate and distribution of floating litter particles in the Aegean Sea (E. Mediterranean). Front. Mar. Sci. 4 (8). https://doi.org/10.3389/fmars.2017.00191.
Poulain, P.-M., 2001. Adriatic Sea surface circulation as derived from drifter data between 1990 and 1999. J. Mar. Syst. 29, 3–32. https://doi.org/10.1016/S0924-7963(01)00007-0.
R Core Team, 2016. R: A Language and Environment for Statistical Computing. R Foundation for Statistical Computing, Vienna, Austria.
Schmidt, L.K., Bochow, M., Imhof, H.K., Oswald, S.E., 2018. Multi-temporal surveys for microplastic particles enabled by a novel and fast application of SWIR imaging spectroscopy - study of an urban watercourse traversing the city of Berlin, Germany. Environ. Pollut. 239, 579–589. https://doi.org/10.1016/j.envpol.2018.03.097.
Schulz, M., van Loon, W., Fleet, D.M., Baggelaar, P., van der Meulen, E., 2017. OSPAR standard method and software for statistical analysis of beach litter data. Mar. Pollut. Bull. 122, 166–175. https://doi.org/10.1016/j.marpolbul.2017.06.045.
Sheavly, S.B., Register, K.M., 2007. Marine debris & plastics: environmental concerns, sources, impacts and solutions. J. Polym. Environ. 15, 301–305. https://doi.org/10.1007/s10924-007-0074-3.
Simeoni, U., Corbau, C., 2009. A review of the Delta Po evolution (Italy) related to climatic changes and human impacts. Geomorphology 107, 64–71. https://doi.org/10.1016/j.geomorph.2008.11.004.
Steppeler, J., Doms, G., Schattler, U., Bitzer, H.W., Gassmann, A., Damrath, U., Gregoric, G., 2003. Meso-gamma scale forecasts using the nonhydrostatic model LM. Meteorog. Atmos. Phys. 82, 75–96.
Stroud, J.R., Lesht, B.M., Schwab, D.J., Beletsky, D., Stein, M.L., 2009. Assimilation of satellite images into a sediment transport model of Lake Michigan. Water Resour. Res. 45 (202). https://doi.org/10.1029/2007WR006747.
Suaria, G., Avio, C.G., Mineo, A., Lattin, G.L., Magaldi, M.G., Belmonte, G., Moore, C.J., Regoli, F., Aliani, S., 2016. The Mediterranean Plastic Soup: synthetic polymers in Mediterranean surface waters. Sci. Rep. 6. https://doi.org/10.1038/srep37551.
Turra, A., Manzano, A.B., Dias, R.J.S., Mahiques, M.M., Barbosa, L., Balthazar-Silva, D., Moreira, F.T., 2014. Three-dimensional distribution of plastic pellets in sandy beaches: shifting paradigms. Sci. Rep. 4 (4435). https://doi.org/10.1038/srep04435.
UNEP, 2016. Marine Plastic Debris and Microplastics – Global Lessons and Research to Inspire Action and Guide Policy Change. United Nations Environment Programme, Nairobi, Kenya (274 pp).
UNESCO, 1994. Protocols for the Joint Global Ocean Flux Study (JGOFS) Core Measurements. UNESCO Publ. No 29. IOC Manuals and Guides, Paris, France. http://unesdoc.unesco.org/images/0009/000997/099739eo.pdf.
Vianello, A., Boldrin, A., Guerriero, P., Moschino, V., Rella, R., Sturaro, A., Da Ros, L., 2013. Microplastic particles in sediments of Lagoon of Venice, Italy: first observations on occurrence, spatial patterns and identification. Estuar. Coast. Shelf Sci. 130, 54–61. https://doi.org/10.1016/j.ecss.2013.03.022.
Vianello, A., Acri, F., Aubry, F.B., Boldrin, A., Camatti, E., Da Rosa, L., Marceta, T., Moschino, V., 2015. Occurrence and Distribution of Floating Microplastics in the North Adriatic Sea: Preliminary Results. MICRO 2015 Seminar, Piran, Slovenia. May 2015.
Wagner, M., Scherer, C., Alvarez-Muñoz, D., Brennholt, N., Bourrain, X., Buchinger, S., Fries, E., Grosbois, C., Klasmeier, J., Marti, T., Rodriguez-Mozaz, S., Urbatzka, R., Vethaak, A.D., Winther-Nielsen, M., Reifferscheid, G., 2014. Microplastics in freshwater ecosystems: what we know and what we need to know. Environ. Sci. Eur. 26 (12). https://doi.org/10.1186/s12302-014-0012-7.
Warner, J.C., Sherwood, C.R., Signell, R.P., Harris, C.K., Arango, H.G., 2008. Development of a three-dimensional, regionl coupled wave, current, and sediment-transport model. Comput. Geosci. 34, 1284–1306.
Warner, J.C., Armstrong, B., He, R., Zambon, J.B., 2010. Development of a coupled ocean–atmosphere–wave–sediment transport (COAWST) modeling system. Ocean Model 35, 230–244.
Zbyszewski, M., Corcoran, P.L., 2011. Distribution and degradation of fresh water plastic particles along the beaches of Lake Huron, Canada. Water Air Soil Pollut. 220, 365–372. https://doi.org/10.1007/s11270-011-0760-6.
Zhang, H., 2017. Transport of microplastics in coastal seas. Estuar. Coast. Shelf Sci. 199, 74–86. https://doi.org/10.1016/j.ecss.2017.09.032.
Zhang, P., Wai, O., Chen, X., Lu, J., Tian, L., 2014. Improving sediment transport prediction by assimilating satellite images in a Tidal Bay model of Hong Kong. Water 6, 642–660. https://doi.org/10.3390/w6030642.
Zhang, W., Zhang, S., Wang, J., Wang, Y., Mu, J., Wang, P., Lin, X., Ma, D., 2017. Microplastic pollution in the surface waters of the Bohai Sea, China. Environ. Pollut. 231, 541–548. https://doi.org/10.1016/j.envpol.2017.08.058.

Article C1: Supplementary information

Supplementary material 1: Mini-Manta trawl technical sheet

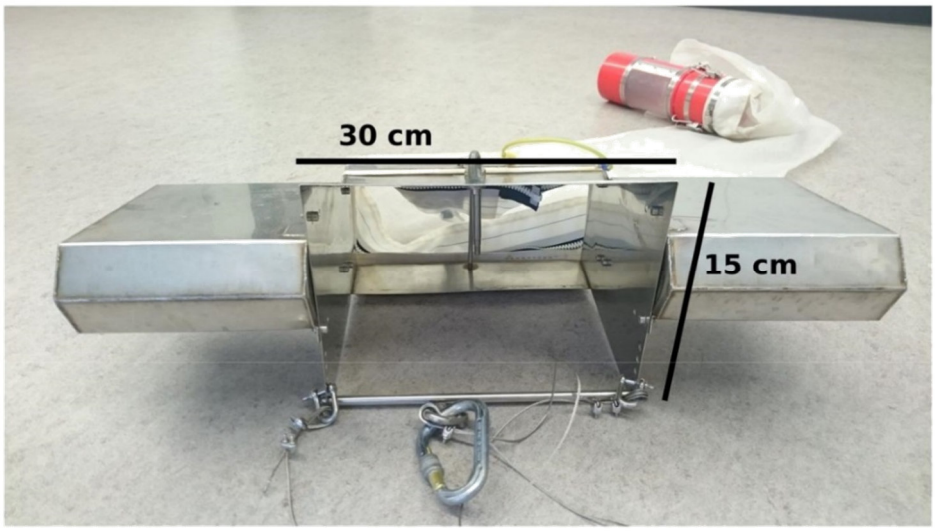

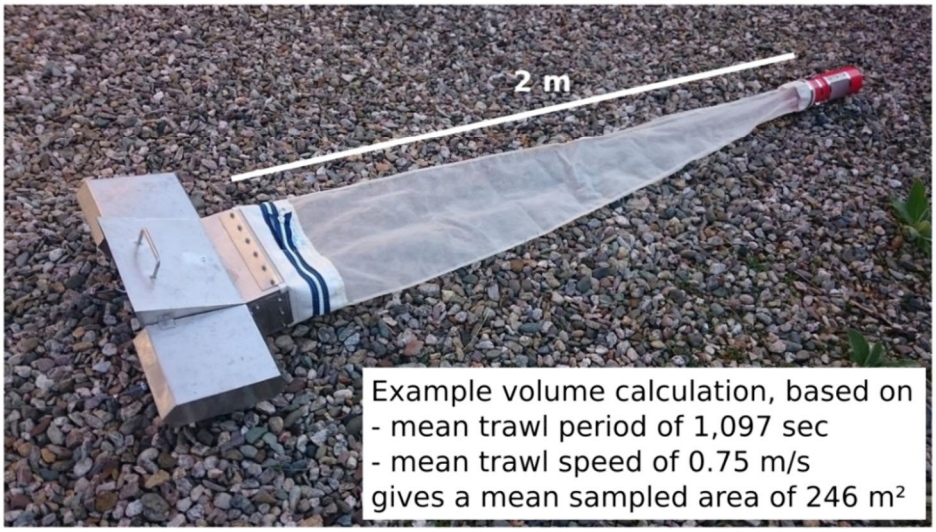

Supplementary material 2: Calibration and validation of empirical regional remote sensing algorithms of suspended particulate matter

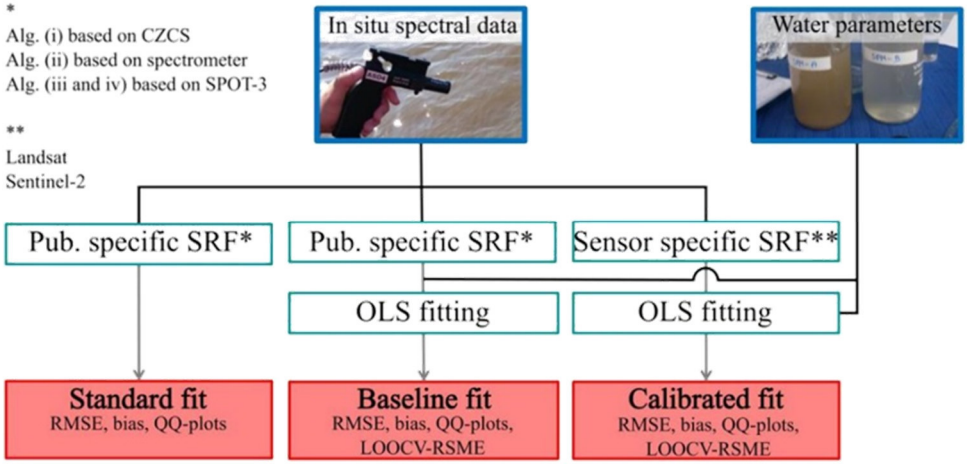

Flow diagram of water parameter algorithm calibration process. In situ spectral data (RRS) were used to create three fits: standard, baseline and calibrated. Spectral data were transformed to either match the publication specific algorithm (Alg.) or the targeted satellite, both accomplished using the sensor specific Spectral Response Function (SRF). SRF used for each step are indicated with (*) for Baseline and (**) for Calibrated. Baseline and calibrated fits were created using ordinary least squares (OLS) fitting of transformed spectral data to in situ water parameter measurements. Fits were compared using root mean square error (RSME), bias, quantile-quantile (QQ) plots and, in the case of the baseline and calibrated fits, the leave-one-out cross-validation (LOOCV) RSME.

Processing details:
The first step involved testing how the original algorithms, as they appeared in the publication, performed using the in situ RRS dataset and SPM measurements. This was termed “Standard fit”. When the original algorithm was fitted using reflectance data with a coarser spectral resolution, the in situ RRS data would be transformed using a weighted-average based on the sensor-specific Spectral Response Function (SRF) to emulate the required bands of the satellite sensors that were used in the original publication. In a next step, the algorithms were calibrated specifically to the Po Delta system using ordinary least squares. This was termed the “Baseline fit”, as this should be expected to represent the best performing form of each algorithm. It was necessary to introduce a log transform to the regressor in algorithms (i) and (ii) to avoid modelling of negative SPM values. In the final step, the algorithms were calibrated for each satellite sensor used to build the remote sensing timeseries (Landsat 8 and Sentinel-2). These were termed “Calibrated fit” for each satellite assessed. In order to accomplish this, the ASD RRS data were transformed using the respective SRF prior to running the regressions.

Supplementary material 3: Atmospheric correction algorithms

Atm corr algorithm	Dark object eval. basis	Addtional settings	Product
ATCOR	NIR	Atmospheric file maritime tropical, visibility estimate run, no cirrus correction	GeoTIFF, Bottom-of-Atmosphere (BOA) reflectance
Sen2Cor	SWIR	Aerosol type maritime, atmosphere auto, no cirrus correction	JPEG2000, Bottom-of-Atmosphere (BOA) reflectance
ACOLITE	SWIR	Resample smoothing before correction, full tile fixed ε, default Rayleigh correction	GeoTIFF (rhow_vnir, rhoam_nir), R_{RS}

Algorithms were compared for each sensor through the in situ RRS spectrometer measurements, taken within 2 hours of the satellite overpass, together with the corrected satellite RRS from the pixel corresponding to the same location. The atmospheric correction algorithms considered were ATCOR (ReSe Applications LLC), Sen2Cor (ESA, Science Toolbox Exploration Platform – STEP) and ACOLITE (Vanhellemont and Ruddick, 2015, 2014). ACOLITE is specially designed for turbid water remote sensing applications and can be implemented to use only SWIR bands.

Vanhellemont, Q., Ruddick, K., 2014. Turbid wakes associated with offshore wind turbines observed with Landsat 8. Remote Sensing of Environment 145, 105–115. 10.1016/j.rse.2014.01.009.
Vanhellemont, Q., Ruddick, K., 2015. Advantages of high quality SWIR bands for ocean colour processing: Examples from Landsat-8. Remote Sensing of Environment 161, 89–106. 10.1016/j.rse.2015.02.007

Supplementary material 4:

Overview

An S-2 image acquired on 15 June 2016, was taken the same day as *in situ* sampling, which allowed optimal comparison of R_{RS} measurements made by spectroradiometer from the boat with atmospherically corrected R_{RS} values from the satellite (see S4). Three *in situ* measurements could be achieved within two hours of the S-2 overpass, with one measurement from the middle of the Po della Pila mouth being taken directly following the satellite acquisition. The image was corrected separately using ATCOR, Sen2Cor and ACOLITE, and the pixel value from the same location as sampling was compared with *in situ* R_{RS} measurements. Variation of the eight neighboring atmospherically corrected pixels (3x3 window) was also considered. No L8 images could be acquired concurrent to *in situ* field sampling, thus comparisons with ATCOR and ACOLITE corrected pixel values had to be completed using *in situ* measurements from two days prior and one day posterior to the satellite acquisition.

S2: Atm corr compared to in situ R_rs

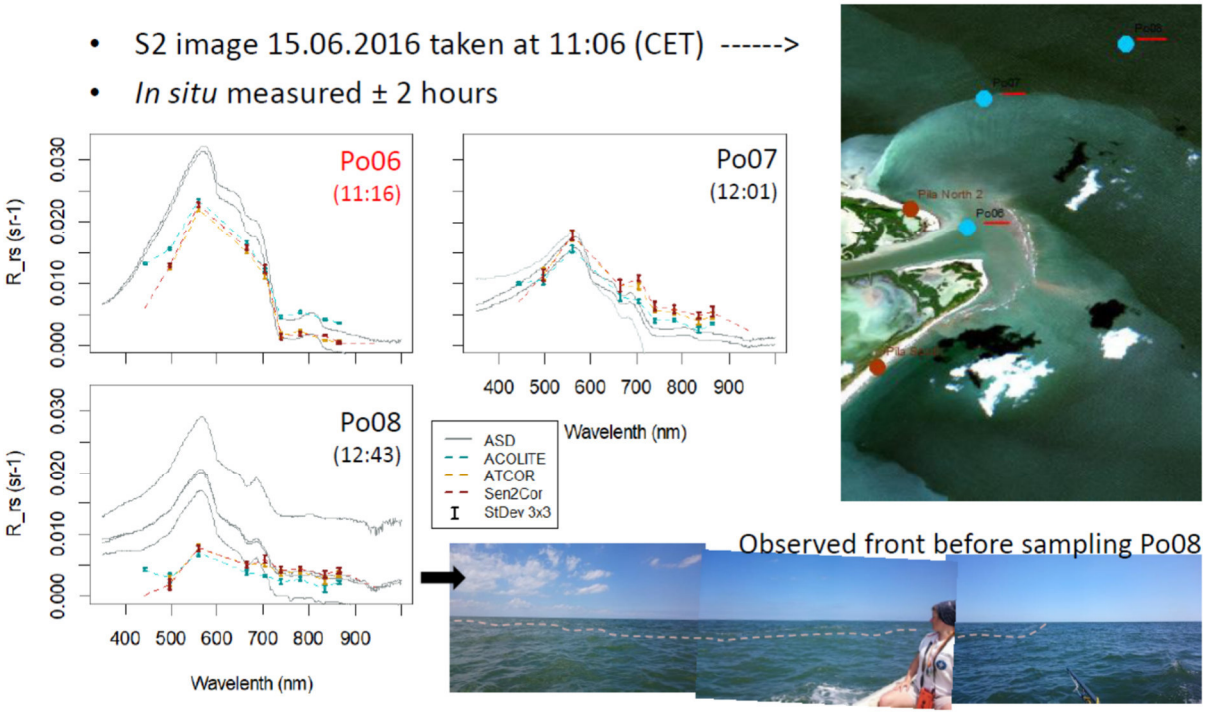

S2: Atm corr pixel comparison

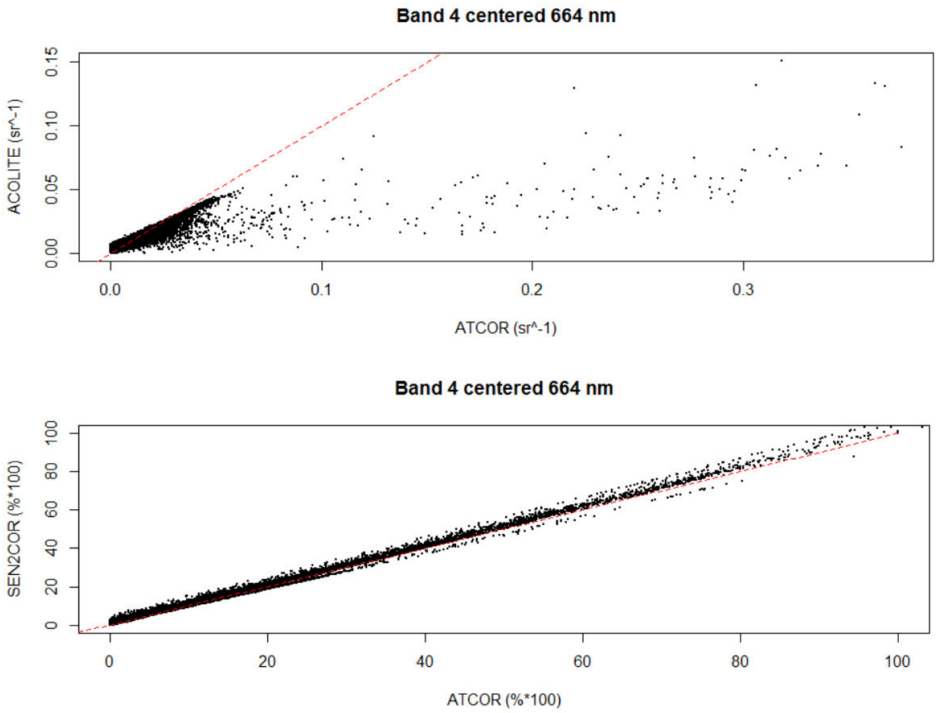

L8: Atm corr compared to in situ R_rs

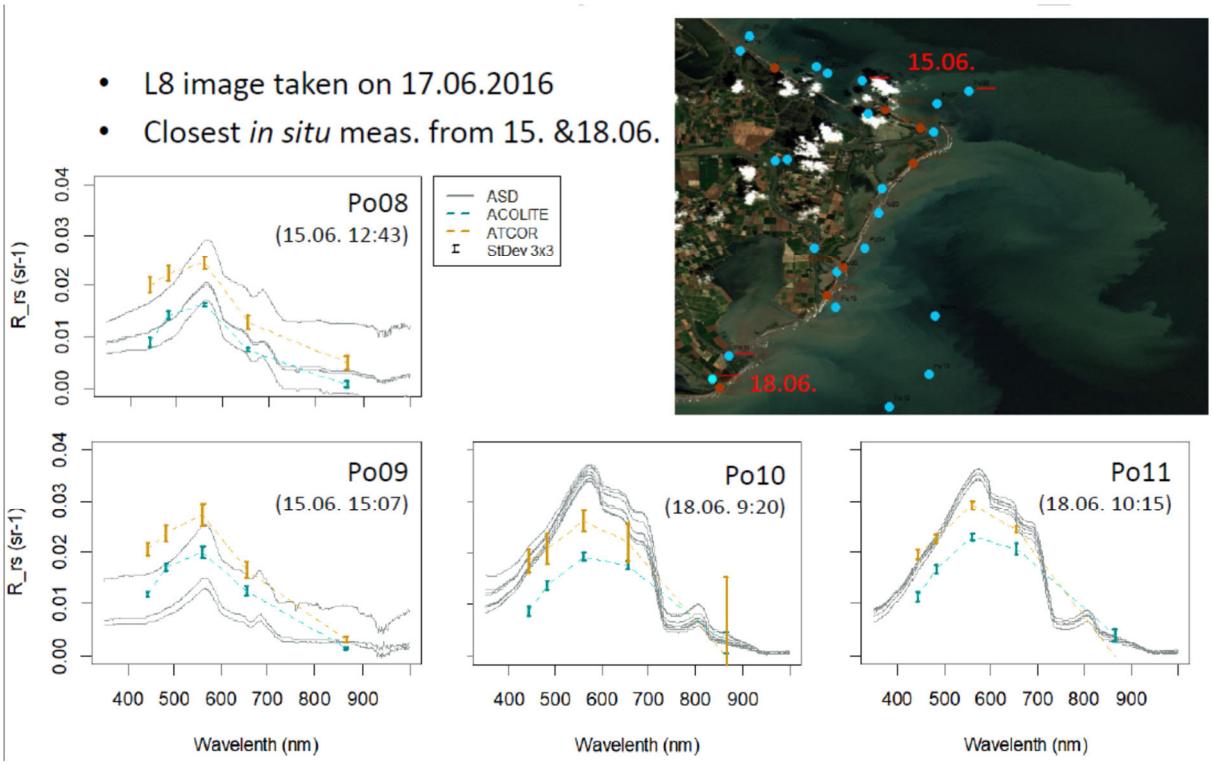

L8: Atm corr pixel comparison

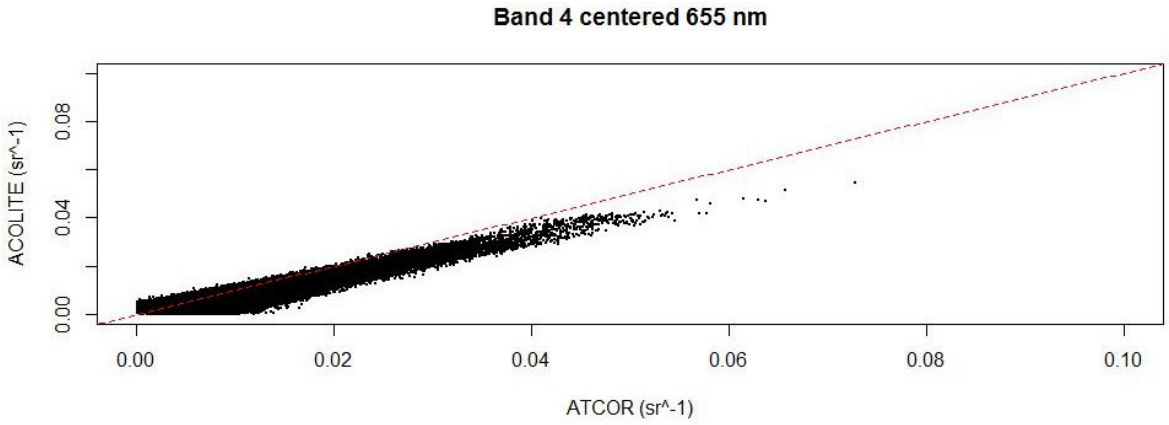

Conclusions

All atmospherically corrected RRS values were found to capture the same overall spectral signature characteristics observed from the in situ RRS measurements, performing especially well for the offshore clearer Adriatic water sampling location. Underestimation of RRS values were observed for the highly turbid Po della Pila waters. For the purposes of this study, Sen2Cor was determined to be the optimal atmospheric correction algorithm for S-2 data and ACOLITE for L8 data.

Supplementary material 5: ASD spectral curve analysis

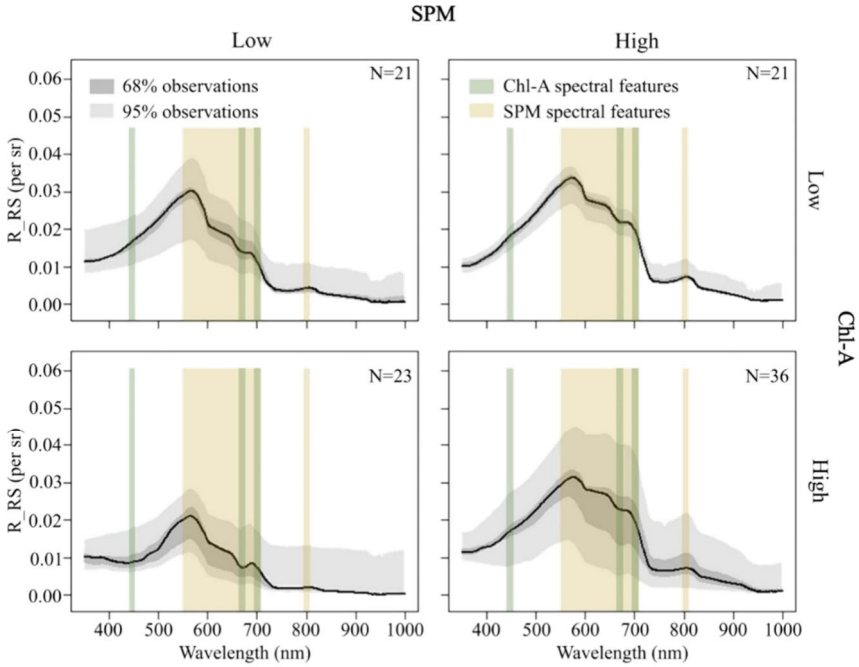

All spectral remote sensing reflectance (RRS) data, organized by relative in situ chlorophyll-A (Chl-A) and suspended particulate matter (SPM) measurements, grouped into "high" and "low" based on median of all Chl-A or SPM measurements. Number of individual reflectance measurements contributing to each curve is indicated (N), and percent of all observations at one standard deviation (1-σ, 68%, dark gray) or two (2-σ, 95%, light gray) is also indicated. Median RRS is indicated by a black line. Spectral features characteristic of Chl-A and SPM, as discussed in the text, are indicated in green and tan bars, respectively.

As expected, a decrease in RRS around 440 nm with low SPM and high Chl-A (lower left plot) was observed, which correlates to a known absorption peak of chlorophyll. Along the same curve, the augmented minimum at 665 nm was assumed to correspond to a second Chl-A absorption peak and the following maximum close to 700 nm likely to be the product of chlorophyll fluorescence. The low Chl-A, high SPM curve (upper right plot) showed no decrease around 440 nm, increased reflectance in the bands from 550-700 nm and augmentation of the reflectance maximum near 800 nm, all of which are similar to patterns documented by Doxaran et al. (2002) for the high turbidity waters from the Gironde river, France. The RRS measurements of samples with low Chl-A and high SPM content were also found to have the least variation, as indicated by the small deviations of the 1- and 2-σ curves from the median line. In the case of high Chl-A together with high SPM, variance among individual RRS measurements was found to be the highest (lower right plot in Figure 7). Reflectance between 600-700 nm was even more elevated relative to the maximum around 575 nm, but many of the Chl-A spectral signature features (such as a decrease in RRS at 440 nm and the min/max curve between 650-700 nm) were not as clearly evident.

Doxaran, D., Froidefond, J.-M., Lavender, S., Castaing, P., 2002. Spectral signature of highly turbid waters: Application with SPOT data to quantify suspended particulate matter concentrations. Remote Sensing of Environment 81, 149–161.

Supplementary material 6: Result of calibration and validation of empirical regional remote sensing algorithms of suspended particulate matter

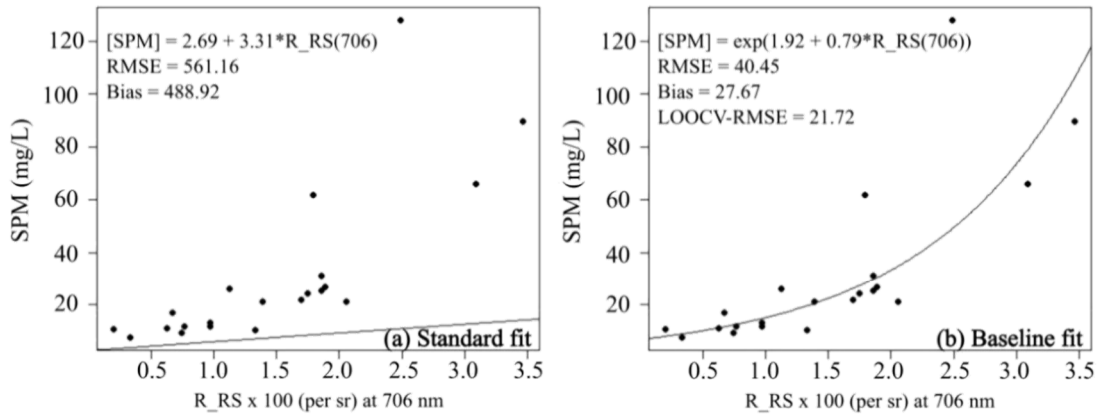

Comparison (a) published SPM Dekker algorithm with (b) baseline fit algorithm. Scaled spectral signal at 706 nm wavelength (RRS in sr-1) is depicted along the horizontal axis, measured in situ SPM (mg/L) along the vertical axis, and modelled values with the black line. In situ measured values are the black points. Algorithm is listed in upper left of each plot, along with model root mean square error (RMSE), bias and leave-one-out cross-validation RMSE (LOOCV-RMSE, right plot only).

The Dekker algorithm is based on the expected elevation of the RRS spectrum around 700 nm, as also observed from our data in the S5 plots with high SPM. A better fit to the measured values was observed, as is evident through the reduction of the RMSE and bias by an order of magnitude. The LOOCV-RMSE was found to be less than an order of magnitude different, suggesting that model overfitting is not an issue despite low sample numbers. Model fit statistics were found to be reduced by an order of magnitude through the calibration/ validation for both the Jørgensen and Dekker algorithms, only slight improvement was achieved for one of the band-ratio Doxaran algorithms while the other was found to be a non-significant predictor for the Po River water. An exponential relationship was determined preferential for the Jørgensen and Dekker algorithms to avoid modelling of negative values. Model fit statistics were relatively unaffected by fitting to satellite sensor specific bands with coarser spectral resolution. Given the observed overlap of the Chl-A reflectance peak at 560 nm with the SPM signal saturation between 550-700 nm (see S5), the Dekker algorithm was selected as preferable to the Jørgensen algorithm. Furthermore, the Dekker algorithm was found to be a significant predictor for both L8 as well as S-2 data.

Article C2: Can water constituents be used as proxy to map microplastic dispersal within transitional and coastal waters?

Piehl S, Atwood EC, Bochow M, Imhof HK, Franke J, Siegert F, Laforsch C

Frontiers in Environmental Science 8: 92

frontiers in Environmental Science

BRIEF RESEARCH REPORT
published: 26 June 2020
doi: 10.3389/fenvs.2020.00092

Can Water Constituents Be Used as Proxy to Map Microplastic Dispersal Within Transitional and Coastal Waters?

*Sarah Piehl[1,2], Elizabeth C. Atwood[3], Mathias Bochow[1,4], Hannes K. Imhof[1,5], Jonas Franke[3], Florian Siegert[3] and Christian Laforsch[1]**

[1] Department Animal Ecology I and BayCEER, University Bayreuth, Bayreuth, Germany, [2] Coastal Research and Management Group, Leibniz-Institute for Baltic Sea Research Warnemuende (IOW), Rostock, Germany, [3] RSS Remote Sensing Solutions GmbH, Munich, Germany, [4] Section 1.4 Remote Sensing and Geoinformatics, Helmholtz Centre Potsdam – GFZ German Research Centre for Geosciences, Potsdam, Germany, [5] Aquatic Systems Biology Unit, School of Life Sciences Weihenstephan, Technical University of Munich, Freising, Germany

OPEN ACCESS

Edited by:
André Ricardo Araújo Lima,
Center for Marine and Environmental Sciences (MARE), Portugal

Reviewed by:
Erik Van Sebille,
Utrecht University, Netherlands
Tomoya Kataoka,
Tokyo University of Science, Japan
Jesse Patrick Harrison,
CSC – IT Center for Science (Finland), Finland

***Correspondence:**
Christian Laforsch
christian.laforsch@uni-bayreuth.de

Specialty section:
This article was submitted to Toxicology, Pollution and the Environment, a section of the journal Frontiers in Environmental Science

Received: 12 March 2020
Accepted: 03 June 2020
Published: 26 June 2020

Citation:
Piehl S, Atwood EC, Bochow M, Imhof HK, Franke J, Siegert F and Laforsch C (2020) Can Water Constituents Be Used as Proxy to Map Microplastic Dispersal Within Transitional and Coastal Waters? Front. Environ. Sci. 8:92. doi: 10.3389/fenvs.2020.00092

Due to high spatiotemporal variability of aquatic systems, relationships between microplastic sources and sinks are highly complex and transportation pathways yet to be understood. Field data acquisitions are a necessary component for monitoring of microplastic contamination but alone cannot capture such complex relationships. Remote sensing is a key technology for environmental monitoring through which extrapolation of spatially limited field data to larger areas can be obtained. In this field study we tested whether microplastic distribution follows the same transport pattern as water constituents depictable from satellite images, namely chlorophyll-a, suspended particulate matter, and colored dissolved organic matter, and discuss their applicability as proxies. As rivers are a major source for marine microplastic contamination, we sampled three example river systems: the lower courses and river mouths of the Trave and Elbe estuary in Germany and the Po delta in Italy. For a full quantitative analysis of microplastics (>300 μm), ATR- and FPA-based μFT-IR spectroscopy and NIR imaging spectroscopy were utilized. Comparing water constituents with in-situ data using regression analysis, neither a relationship for the Elbe estuary nor for the Po delta was found. Only for the Trave river, a positive relationship between microplastics and water constituents was present. Differences in hydrodynamic conditions and spatiotemporal dynamics of water constituents and microplastic emissions among the river systems are possible explanations for the contrary results. Based on our results no conclusions on other river systems and likewise different seasons can be drawn. For remote sensing algorithms of water constituents to be used as microplastic proxy an adaption for each system as well as for different seasons would thus be necessary. The lower detection limit of 300 μm for microplastics could also have influenced relationships as microplastic abundance exponentially increases with decreasing size class. Further studies with improved sampling methods are necessary to assess our proposed method.

Keywords: microplastic, spectroscopy, remote sensing, HySpex, SPM, chlorophyll, CDOM

INTRODUCTION

Pollution of aquatic ecosystems with microplastic (MP) has recently gained particular attention due to its ability to accumulate in food webs and its potential threat to human health (Sharma and Chatterjee, 2017; Wang et al., 2019). To combat MP pollution in marine systems, MP (synthetic polymer particles <5 mm) litter has been included in several local and global directives for the protection of the marine environment (Directive of the European parliament, 2008; UN Resolution, 2020). Further, member states are required to adapt operational monitoring programs to assess sources, transport, and accumulation of MP within marine systems. As most plastic products are produced and consumed on land, rivers are a major transport pathway for MP litter to the oceans (van Wijnen et al., 2019). But to date, only limited data on MP abundances in estuaries and adjacent coastal areas exist (Rezania et al., 2018). Reported concentrations are highly variable, from less than one to over a thousand particles per cubic meter (Rezania et al., 2018) and are often accompanied by high standard deviations. Especially estuaries, as transition zone between fresh- and saltwater, are highly dynamic systems influenced by both local and global meteorological and hydrodynamical factors (e.g., local surface wind and waves, tidal influences, basin specific currents, regional precipitation). Consequently, in-situ sampling of MP within estuaries and adjacent coastal areas requires sufficient replication to cover the high spatiotemporal variability. Nevertheless, current field data collection of MP samples from estuaries and adjacent coastal areas are associated with high-cost ship expeditions. Further, the use of state-of-the-art sample processing and analytical methodologies for MP identification in environmental samples remains very time consuming (Enders et al., 2020). Thus, existing data of MP abundance at the water surface exhibits high uncertainties and are both spatially and temporally limited.

Remote sensing offers a promising monitoring tool to obtain data on large spatial and temporal scales, and thus could provide valuable data for improved microplastic monitoring approaches. One drawback is that the direct detection of MP is not possible due to its size and concentrations within the water surface layer which are too low to sufficiently influence the water surface reflectance signal. An indirect approach to investigate plastic litter transport was first conducted by Pichel et al. (2007) studying the sub-tropical convergence zone (STCZ) within the North Pacific. The STCZ accumulates floating materials due to its convergent current patterns, including plastic litter (Lebreton et al., 2012). Pichel et al. (2007) used chlorophyll-a (Chl-A) concentration as well as sea surface temperature (SST) derived from satellite images to identify the location of the STCZ. With this approach they were able to extrapolate single in-situ measurements of Chl-A and SST to a larger area. Moreover, a spatial correlation could be detected for Chl-A and SST with macroplastic litter (Pichel et al., 2007) but MP litter was not investigated. Additionally, a further spatial relationship of Chl-A and MP seems to be possible as it was shown that several species of algae attach to floating polymer particles (Masó et al., 2003) possibly due to the formation of extracellular polymeric substances enhancing aggregate formation (Xiao and Zheng, 2016). Besides Chl-A, further water constituents that can be derived from satellite images are suspended particulate matter (SPM) and colored dissolved organic matter (CDOM). As SPM comprises the same size range as MP and exhibits the same diversity of characteristics, i.e., consisting of a heterogenous mixture of particles of various sizes, densities and shapes, a spatial relationship due to similar transport pathways seems reasonable. A spatial correlation between CDOM (consisting of both decaying material of terrestrial origin and/or in-situ biological activity in the respective area) and MPs is further assumed likely as terrestrial inputs are thought to dominate the CDOM source in coastal areas (Stedmon and Nelson, 2014; Harvey et al., 2015) similar to MP litter inputs. Assuming that algae (Chl-A), SPM, CDOM and MPs are passive drifters which are mixed and transported by the same physical mechanisms (i.e., wind, waves, and currents) we tested the hypotheses that with (i) increasing Chl-A, (ii) SPM, and (iii) CDOM concentration, the concentration of MP increases. Moreover, an alternative indirect monitoring approach for floating MP through mapping proxies (the water constituents) measurable with remote sensing methods is proposed.

MATERIALS AND METHODS

Study Area

Sampling was conducted at three different terminal river systems (Trave, Elbe, and Po) entering different seas (North Sea, Baltic Sea, Northern Adriatic Sea), which were chosen as to cover a broad range of expected MP abundances (**Figure 1**).

The Trave river in northeastern Germany has a length of 113 km, a watershed of 1,804 km^2 (LM-MV and LM-SH, 2011) and exhibits an average annual discharge of 7.37 m^3/s into the western Baltic Sea. Samples were taken from 22.05.2014 to 25.05.2014 at the brackish river mouth, a riverine shallow water firth with an average depth of 5.5 meter. Sampling was conducted along a distance of approximately 5 km with river width varying from approximately 22 to 535 m (see **Supplementary Information 4**). Water exchange with the Baltic Sea is limited through a narrow connection at Lübeck Bay with salinity ranges from 0.2 to 17.3 PSU. Oscillations of the sea level (<20 cm) is a result of wind-induced water movements as well as the effect of buildup of water reaching the coast. The Trave drainage area is highly influenced by agriculture, and tourism is an additional important economic factor. The harbor of Lübeck, located ~18 km inland of the river mouth, serves as a shipyard location and a nationally important transfer point for passenger ferries and commercial goods.

The Elbe river in northwestern Germany is one of the largest rivers of Central Europe with a length of 1,100 km, an average yearly discharge of 844 m^3/s into the North Sea and a watershed of 148,000 km^2 which is home to 25 million people. Samples were taken from 19.08.2015 to 21.08.2015 within transitional waters of the tidally influenced river mouth (widths between ~0.2 and 21 km) and adjacent coastal waters spanning a total

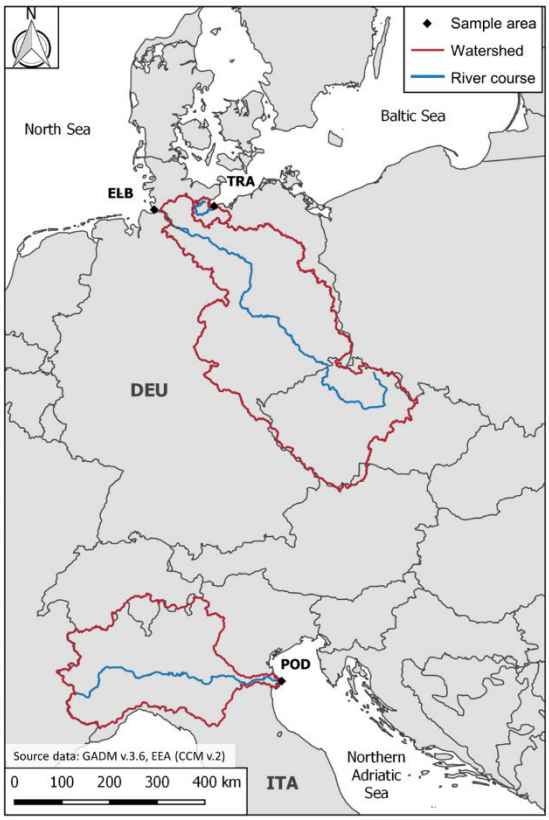

FIGURE 1 | Study areas of the Trave (TRA) and the Elbe estuary (ELB) in Germany (DEU) and the Po delta (POD) in Italy (ITA), course of the rivers and their respective watersheds.

length of ~32 km (see **Supplementary Information 5**). The Elbe estuary is a partly- to well-mixed mesotidal estuary with a tidal amplitude ranging between 2 to 4 m. Between a single tide, an average distance of 20 km is traveled between capsize points. As a hyper-synchronous estuary, the tidal amplitude increases to a maximum between the coast toward the city of Hamburg and thereafter decreases. The Elbe estuary morphology and hydrology leads to a so called "maximum turbidity zone" (MTZ) where concentrations of suspended matter reach their highest value. Inputs from upstream are supplemented with additional inputs from adjacent areas such as dike-free river branches and wastewater discharges. The investigated area is significantly influenced by ship traffic, as the harbor of Hamburg is the third largest container port in Europe.

The Po river in Italy has a watershed of 74,000 km^2 (Artioli et al., 2005) and a length of around 652 km (Lanzoni et al., 2015). Although exhibiting a smaller watershed as compared to the Elbe river, it contains a much higher population density representing almost half of the Italian population (~30 million people). It is the longest Italian river and has an average annual discharge of 1,500 m^3/s (Falcieri et al., 2014) flowing into the Northern Adriatic Sea (**Figure 1**). Given these factors, the Po river is thought to be the second most important marine litter source to the Adriatic basin (Liubartseva et al., 2016). Potential sources for MP include run-off and wastewater from intensively practiced agriculture, several industrial parks as well as large cities. The terminal river splits into seven active branches before entering the sea (**Supplementary Information 6**). As deltaic system, it exhibits a net sediment transport from the river to the delta. The Northern Adriatic Basin is influenced by tidal fluctuation of around 30 cm but under specific conditions can reach up to 140 cm (Maicu et al., 2018). Sampling was conducted from 10.06.2016 to 23.06.2016 at the terminal river branches with varying width from ~63 to 795 m and extending ~7.8 km offshore (see **Supplementary Information 6**).

Sampling

At each sampling location, water surface samples for MP and water constituents (Chl-A, SPM, CDOM), were simultaneously taken as described in detail by Atwood et al. (2019). Microplastic samples were concurrently collected from the top 15 cm of the water surface alongside motorboats and sailing ships using a mini-manta trawl equipped with a flowmeter (30 × 15 cm opening, 2 m long net with a mesh size of 300 µm). Water samples were always taken with flow direction of the river and in zigzag pattern perpendicular to the flow direction except for the Elbe estuary, where this maneuver was not possible due to intense ship traffic. Samples were stored in glass jars until processing in the laboratory. In total, 13 locations were sampled at the Trave river and 20 locations each at the Elbe estuary and the Po delta (see **Supplementary Information 4, 5, and 6**) as to cover a wide range of water constituents and MP concentrations. To assure similar conditions over the length of one trawl, water clarity was measured with a secchi disk at the beginning and the end of each trawl. For water constituents, 2 L water samples were concurrently collected with a glass flask from the water surface (top 40 cm) and kept both dark and cold until further processing. Later that same day, samples were separated and filtered on GF/F glass microfiber filters (0.7 µm pore size) for Chl-A following the JGOFS protocol (Knap et al., 1996) or pre-weighted cellulose acetate filters (0.45 µm pore size) for SPM following the protocol of Lindell et al. (1999).

Water Constituent Analysis

Chlorophyll pigments were extracted from the filters using 90% acetone [following JGOFS protocol (Knap et al., 1996)]. Extracted chlorophylls from the Trave river were analyzed with a fluorometer (Turner Designs, TD-700) with an excitation wavelength of 340–500 nm and an emission wavelength >665 nm. For the Elbe estuary and the Po delta, chlorophylls were extracted using 96% ethanol and extracts analyzed with a fluorometer (JASCO, FP-8600) at an excitation wavelength of 435 nm and an emission wavelength of 670 nm. The fluorometer was calibrated using a photometer (JASCO, V-670) and a Chl-A standard (Sigma-Aldrich, C6144-1MG). After each first measurement, samples were acidified with HCl and again measured to allow the subtraction of phaeopigments in order to obtain Chl-A concentration following the JGOFS protocol (Knap et al., 1996). Although extraction protocols slightly

differed, obtained results do not influence the general results, as regression analysis with MPs were performed separately for each river system.

Samples for SPM analysis were dried for 2 h at 60–80°C and cooled in a desiccator for 10–15 min before weighted on an analytical balance (Sartorius, R 200 D).

Absorbance analysis of CDOM was conducted using the filtrate of the SPM samples (material <0.45 μm). Duplicate samples were stored in glass flasks covered with aluminum foil and stored at a temperature of 7°C until spectrophotometric analysis. Measurements were taken with a UV-VIS-NIR spectroradiometer (PerkinElmer, LAMBDA 950) using 5 cm glass cuvettes. Absorbance measurements were performed at the wavelength positions 400, 412, 420, and 440 nm.

Microplastic Sample Processing

Each sample was first fractionated into two size classes: 5000–500 and 500–300 μm. All potential MP particles >500 μm were visually pre-sorted under a stereomicroscope (Leica, M50) using a counting chamber for zooplankton. For a more efficient visual pre-sorting, samples with a high organic content were additionally treated with a wet peroxide oxidation (Masura et al., 2015). Potential MPs were photographed (Olympus, DP 26), and stored in Eppendorf tubes for analysis with Attenuated Total Reflectance (ATR)-Fourier transform-infrared (FT-IR) spectroscopy (Löder et al., 2015).

The smaller size fraction (500–300 μm) of all samples was treated with an enzymatic purification protocol (Löder et al., 2017) and afterward with wet peroxide oxidation (Masura et al., 2015) to remove organic matter, which would interfere with subsequent spectroscopic analysis. As remaining particle numbers were still very high, subsamples were filtered onto 25 mm aluminum oxide filters (Whatman, Anodisc 25). Detailed information on the subsamples can be found in the **Supplementary Information** (see **Supplementary Information 1**). Subsamples were analyzed with a Focal Plane Array (FPA) based micro FT-IR (μFT-IR) spectroscope (Bruker, Tensor 27 FT-IR spectrometer equipped with a Hyperion 3000 FT-IR microscope with a 15× Cassegrain objective and a 64 × 64 FPA detector) according to Löder et al. (2015). In order to conduct a full quantitative analysis, the remainder of each sample was filtered onto glass fiber filters (Macherey-Nagel, MN 85/90 BF) and analyzed with a newly developed hyperspectral imaging methodology (Schmidt et al., 2018) using a near-infrared (NIR) imaging spectrometer (Norsk Elektro Optics AS, HySpex SWIR-320m-e).

To account for potential airborne contamination of the samples with small microplastics (500–300 μm), negative controls with filtered water were processed together with the microplastic samples for each set of samples from a river. In total, six negative controls were measured with the HySpex imaging spectrometer on which no MP particles were found. Mostly fibers were found (0.7 to 11.6 fibers on average for the three investigated data sets) within a total of 15 negative controls analyzed with FPA based μFT-IR spectroscopy (**Supplementary Information 3**). Only for the Po delta was one polypropylene particle found in one out of six negative controls corresponding to 0.17 particles on average. This amount was subtracted from measured polypropylene abundances in each sample within the Po delta data set. Synthetic fibers were generally not considered within this study as synthetic fibers normally exhibit diameters between 6 and 175 μm (Cole et al., 2015; Dris et al., 2016, 2018) which could not be sampled quantitatively with the utilized manta net. As no fibers or particles >500 μm were observed within the negative controls, it is assumed that airborne contamination of the larger size class can be neglected. Finally, obtained MP particle numbers from all three methods were added for each sample and standardized according to the filtered water volume to MP particles per cubic meter.

Statistical Analysis

All statistical analyses were performed using the software R v.3.5.2. Linear regression analyses were conducted to test the unidirectional null hypothesis that MP abundance will not increase with increasing water constituent abundance. To meet model assumptions for parametric linear regression analysis, the Trave data were square root transformed and for the Po delta data a log transformation was applied. Correlation analyses among all investigated water constituents were conducted to check for collinearity. Relationships were accepted as significant at $p < 0.05$, and all results are shown as average ± one standard deviation (SD).

To further investigate potential patterns within the datasets, principal component analyses (PCA) were applied. The packages "FactoMineR" (v.1.34) and "factoextra" (v.1.0.7) were used for PCA and biplots for visualization of the data. First the predictor variables were scaled to have a SD of one and a mean of zero. Two missing values within the Po delta dataset were excluded from the analysis, although imputing the two data points by predictive mean matching produced similar results. The function "prcomp" was used to calculate principal components (PCs) via singular value decomposition on the original data matrix.

To investigate potential spatial relationships between MP and water constituent abundance, subgroups according to sampling location were defined. For the Trave, the categories included river, wastewater treatment plant (WWTP), and coastal samples. For the Elbe data, a distinction between coastal and river samples was made, whereas the categories river, mouth (representing the seven distal branches of the delta), and coastal samples were defined for the Po delta data.

RESULTS

The three chosen river systems exhibited the assumed wide range of MP concentrations, ranging from 1 to 78 particles/m^3 at the Po delta, followed by the Elbe estuary with 0–11 particles/m^3 to only a few particles at the Trave river (0–1 particles/m^3; **Figure 2**, specific values in table **Supplementary Information 1**). For the Trave river generally higher MP concentrations were observed within the river than the coastal area (**Supplementary Information 4**) whereas for the Elbe estuary MP concentrations showed an increasing trend toward the coast (**Supplementary Information 5**). At the Po delta elevated MP concentrations

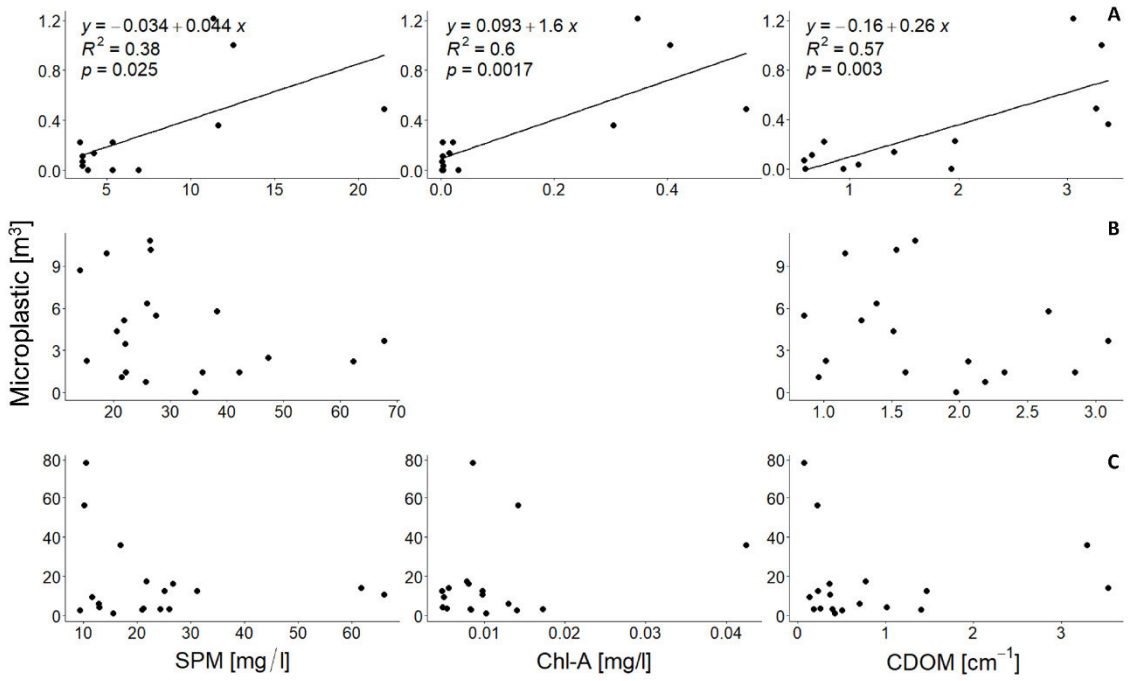

FIGURE 2 | Relationship between measured water constituents and microplastic (0.3–5 mm) at the Trave river **(A)**, the Elbe estuary **(B)**, and the Po delta **(C)**. Linear regression analysis revealed a significant positive relationship among the abundance of all three water constituents and microplastic abundance for the Trave river **(A)**. Chl-A, chlorophyll-a, SPM, suspended particulate matter, CDOM, colored dissolved organic matter.

were observed within the river branches, as well as the outer river plume (**Supplementary Information 6**). Linear regression analysis revealed a significant relationship between the abundance of MP and all three investigated water constituents for the Trave river, whereas Chl-A explaining the largest portion of the variance (**Figure 2**). Nevertheless, this result has to be interpreted with caution as MP abundances were generally low within this river system (**Figure 2**, **Supplementary Information 1**). PCA was conducted and results displayed within biplots to reveal further patterns within the data sets (**Figure 3**).

PCA of the Trave data revealed that the first PC, explaining 93.8% of the variance within the data, is almost equally represented by all three water constituents: Chl-A (35%), SPM (34%), and CDOM (32%) (**Figure 3A**). The second PC (explaining 5% of variance) instead is mostly represented by CDOM (65%) and SPM (28%). Microplastic abundances in coastal areas are better represented by CDOM with only a small angle between the main axis of the ellipse and the CDOM vector (**Figure 3A**).

Considering PCA results of the Elbe estuary a similar pattern can be seen with coastal samples better represented by CDOM (**Figure 3B**). The two predictor variables SPM and CDOM are equally represented (each 50%) by both PCs (**Figure 3B**).

Contrarily, none of the investigated water constituents could predict MP abundance for either the Elbe estuary (SPM: $F = 1.72$, $p = 0.21$ and CDOM: $F = 1.25$, $p = 0.28$) or the Po delta (Chl-A: $F = 1.14$, $p = 0.30$, SPM: $F = 1.71$, $p = 0.21$, and CDOM: $F < 0.001$, $p = 0.99$). For the Elbe estuary, the lacking relationship was further indicated by a second field data acquisition in June. Here, one of the highest MP values (4.44 MP particles/m^3) correlated with one of the highest SPM concentration (323.87 g/l) but the very highest MP value (4.60 MP particles/m^3) was sampled on a spot with a low SPM concentration (20.78 g/l) (**Supplementary Information 1**).

Furthermore, all water constituents showed a positive correlation among each other for both German river systems, whereas for the Po delta none of the investigated predictor variables correlated (**Supplementary Information 2**). Conducting PCA for the Po delta, the first PC is best represented by CDOM (57%) and Chl-A (31%), but only explaining around 49% of the variance (**Figure 3C**). The second PC is mostly represented by SPM (62%) and Chl-A (37%), explaining around 37% of the variance (**Figure 3C**). No clear differences in MP abundances between river mouth, river, and coastal samples can be seen (**Figure 3C**).

DISCUSSION

A clear relationship among water constituents and MP for all three investigated river systems could not be identified. The positive relationships between the three proxy water constituents

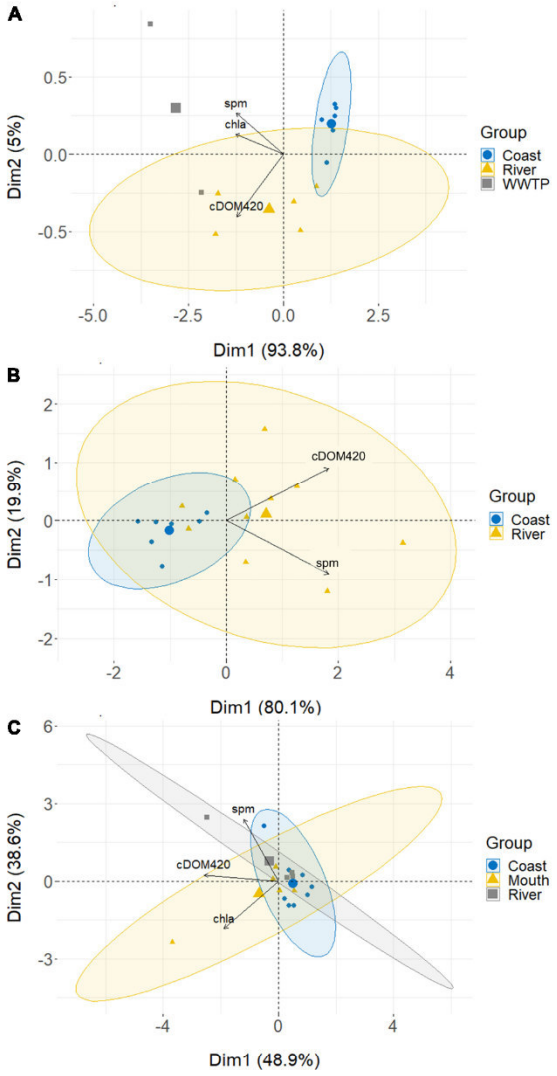

FIGURE 3 | Biplots of the Trave river **(A)**, the Elbe estuary **(B)**, and the Po delta **(C)** showing the scores of individual samples grouped by different symbols and colors. Loadings of the predictor variables chlorophyll-a (chla), suspended particulate matter (spm), and colored dissolved organic matter (cDOM420) on the first two principal components (Dim1 and Dim2) are represented as vectors. Larger symbols depict the center of the confidence ellipse (95% confidence level) drawn around the groups.

and MP abundances found for the Trave river needs to be verified in future studies, as the results are based on very low MP abundances within the obtained water samples (**Supplementary Information 1**). As indicated by the biplots, depending on the estuary type, spatial relationships between water constituents and MPs are further spatially limited. Thus, potential relationships need to be evaluated for various river systems separately and additionally for the river course and the coastal zone.

One factor influencing possible relationships between water constituents and MPs are the presence and location of their emission sources. In the Trave river, higher concentrations of MPs were found within the river, specifically close to the WWTP (**Supplementary Information 4**) and gradually decreasing toward the Baltic Sea. For the Baltic Sea, it is assumed that land-based litter inputs are dominating (Haseler et al., 2018) and thus the lower MP water surface concentrations at the coastal area may be a dilution effect. For the Elbe estuary, results show a tendency of higher abundance of MPs within the adjacent coastal area compared to the inner parts of the river (**Supplementary Information 5**). The increasing MP concentrations at the Elbe estuary toward the coastal area may be a consequence of additional inputs of sea-based sources. Both the study system of the Elbe estuary and the Po delta are highly influenced by fishing and aquaculture related litter inputs (Simeoni and Corbau, 2009; Kammann et al., 2018). Nevertheless, for the Po delta with its diverse terminal branches no pattern in MP abundance could be detected (**Figure 3C** and **Supplementary Information 6**). The protruding form of the Po delta plays an important role for dispersion of suspended material, as MP and water constituents emitted by the branches exhibit different hydrodynamical and meteorological conditions. The hydrodynamical conditions spanning from a mixed mesotidal estuary (Elbe) to nearly stratified systems (Trave, Po) generally influence spatial patterns of suspended materials and thus, further may explain observed differences.

For example, SPM showed no spatial relationship with MPs at the Elbe estuary. Nevertheless, a study on larger litter collected with bottom trawls and at the shore within an estuary in South America, reported that larger litter was accumulating in the MTZ (Acha et al., 2003). In our study, we focused on water surface MP concentrations at the Elbe estuary which also exhibits an MTZ. Even though our sampling did not cover the MTZ in August, during another sampling in June samples were taken closer to Hamburg city (**Supplementary Information 5**) and the MTZ was covered according to salinity measurements (**Supplementary Information 1**; located between 0.1 and 4 PSU; Herman and Heip, 1999). Here, a correlation analysis revealed a relationship between SPM and MPs (Spearman's rank correlation, $S = 154$, $p = 0.01$, rho = 0.66). The positive relationship of SPM and MPs at the Trave, explaining 38% of the variance, could be due to dominating riverine inputs for both. The missing relationship at the Po delta on the opposite could be the result of differing sources of SPM and MPs among the several distal branches at the investigated site. Suspended particulate matter dynamics are coupled to meteorological conditions and will vary on small temporal scales. For example, higher SPM inputs occur during high precipitation events due to increased terrestrial runoff as well as mobilization of riverbed sediments. Likewise, high MP export was already associated with high flow events in rivers (Hurley et al., 2018). Considering CDOM as proxy water constituent for MPs, only at the Trave river was a positive relationship found, whereas PCA showed that CDOM explained most of the variance in coastal samples (**Figure 3A**). A similar pattern was found for the Elbe estuary (**Figure 3B**) even though a relationship could

not be verified by regression analysis (**Figure 2B**). The absence of a relationship for the other two investigated sites can be explained by differing DOM dynamics among systems. For example, Berto et al. (2010) has shown an influence on DOM dynamics on a monthly and sub-monthly time scale at the Po delta. Processes leading to higher CDOM concentrations in spring and summer vary with higher inputs due to melt-water run-off from rivers in spring (Ferrari and Dowell, 1998; Stedmon and Nelson, 2014). Moreover, higher photo-bleaching in summer can alter the optical properties of surface waters and lead to decreased CDOM absorption and fluorescence (Vodacek et al., 1997). Both processes influence potential spatial as well as temporal relationships, in particular on a seasonal scale, of CDOM and MPs.

Even though a positive relationship between water constituents and MP abundance was found for the Trave river, the results need further validation since results are based on generally low MP abundances (**Supplementary Information 1**) as well as only one sampling campaign. Following linear regression, most variance was explained by Chl-A (62%). Contrarily, a correlation between MPs and Chl-A could not be detected for the Po delta. Although the slightly different extraction protocols used should not have influenced the observed results as samples were treated equally within a dataset, this source of potential error cannot be definitely excluded. Even though standard protocols for the analysis of chlorophyll exist, they vary in their results. A relationship would be further influenced by seasonal patterns, as well as the ability of some algae to influence their vertical position in the water column to counteract sinking out from the euphotic zone as well as resource acquisition (Raven and Doblin, 2014).

Remote sensing of water constituents in coastal systems is difficult due to the overlapping spectral signal from different optical components. The Trave provided the clearest CDOM signal of all three river systems, in that the SPM concentration was relatively low and the CDOM concentration relatively high. The Po delta was found to have the lowest CDOM concentrations and some of the highest SPM concentrations of all three study systems. Even though the least amount of variance was explained by SPM within the Trave data, from an in-situ monitoring point of view, SPM fulfills the requirements for an operational monitoring in being cost- and labor-effective, as well as easy to assess. A relationship between MP concentrations and sediment grain size as well as organic matter deposition has been proposed in previous studies (Vianello et al., 2013; Maes et al., 2017; Haave et al., 2019). Haave et al. (2019) further reported that particles <100 µm made up $>95\%$ of the MP concentration, whereas particles >500 µm showed different spatial distribution patterns. This points toward the importance of MP particles <300 µm not covered by our MP sampling method. Thus, it would be interesting in future studies to test the relationship of SPM and MPs with recently developed pumping systems which are able to extract MPs down to 1 µm (Lenz and Labrenz, 2018). In conjunction with the development of faster identification methods of MPs, higher sample replication can be achieved, resulting in more precise model results.

Further research in the field is desirable as satellite imagery has the potential to complement spatial and temporal limited point measurements and thus improve our current understanding of

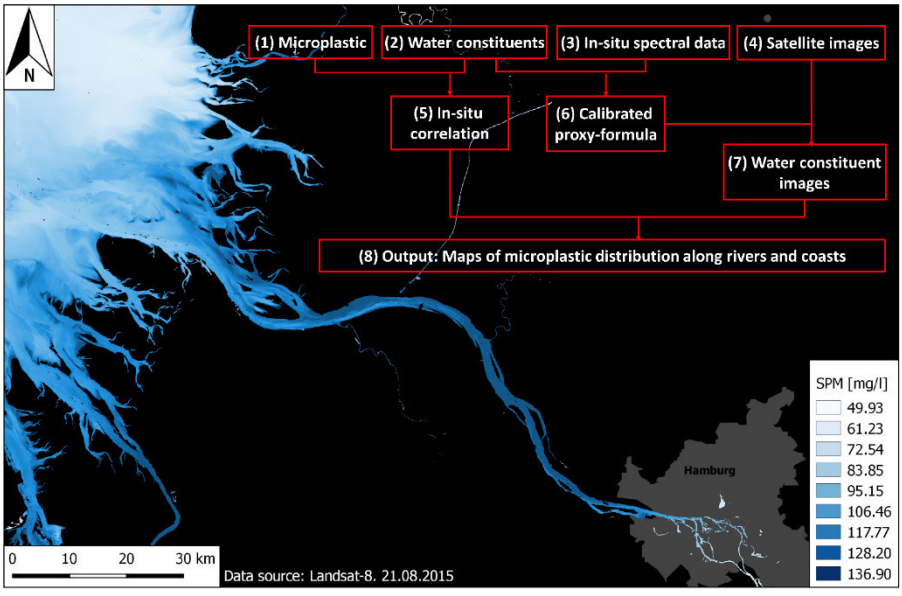

FIGURE 4 | Satellite image of suspended particulate matter (SPM) at the Elbe esturay. The diagram illustrates the proposed framework to track microplastic distribution via proxy water constituent maps (software: QGIS 2.14.8).

sources, transport, and accumulation of MPs within river courses and adjacent coastal areas.

In this study, we analyzed a spatial relationship (**Figure 4**) between in-situ MPs (**Figure 4**, component 1) and in-situ water constituents (**Figure 4**, component 2). Further steps are necessary to transfer remotely sensed water constituents into MP abundance to produce MP distribution maps along rivers and coasts which is described in detail by Atwood et al. (2019) and shown in **Figure 4** (components 3, 4, 6, and 7). Near-range spectral measurements (**Figure 4**, component 3) taken concurrent to sample collection would be needed to build regionally calibrated remote sensing spectral reflectance water parameter algorithms (**Figure 4**, component 6) for different satellite platforms (**Figure 4**, component 4) as specified in Atwood et al. (2019). Through the adaption of the remote sensing imagery of water constituents (**Figure 4**, component 7) with the calibrated algorithms, maps of the water constituents could then be used as proxy for MP. Existing single point measurements could thereby be extrapolated to large spatial scales to produce maps of MP distribution along rivers and coastal areas (**Figure 4**, component 8).

DATA AVAILABILITY STATEMENT

All datasets generated for this study are included in the article/**Supplementary Material**.

AUTHOR CONTRIBUTIONS

MB, JF, FS, and CL initiated the study. All authors designed the study. SP, EA, MB, and HI conducted the field sampling. SP prepared the microplastic samples with the help of four technichal assistants, conducted the microplastic particle identification with FT-IR spectroscopy, and wrote the first draft of the manuscript. MB conducted the NIR microplastic particle identification as well as did the analysis of CDOM. SP and HI did Chl-A and SPM analysis. EA processed the remote sensing data. SP analyzed the data. SP, EA, MB, HI, JF, and CL discussed and interpreted the data. SP and EA created the figures and tables. All authors were involved in revision and rewriting of the manuscript.

FUNDING

This publication was funded by the German Research Foundation (DFG) and the University of Bayreuth in the funding programme Open Access Publishing. This study was partly funded by the German Federal Ministry for Economic Affairs and Energy (Bundesministerium für Wirtschaft und Energie, or BMWi) via the DLR Space Administration under the grant numbers 50EE1301 and 50EE1269.

ACKNOWLEDGMENTS

The authors would like to thank the crew of the sailing ships "Bildungsschiff Niederelbe e.V." and "Aldebaran Marine Research and Broadcast" as well as our boat captains in Italy for flexible ship times and help during field data acquisitions. For storage and shipping of Chl-A samples, we would like to thank the Thünen Institut of Fisheries Ecology in Cuxhaven. For help with the analysis of the Chl-A samples, we thank Dr. Ben Gilfedder and Silke Hammer from the Limnological Station/chair of hydrology of the University of Bayreuth and Prof. Stibor of the Department Biology II/Aquatic Ecology of the Ludwig-Maximilians University Munich. For measurements of the SPM samples, thanks are extended to Prof. Dettner of the Department Animal Ecology II of the University of Bayreuth. Ursula Wilczek, Heghnar Martirosyan, Marion Preiß, and Lena Löschel are very heartfully thanked for their help in the lab with the microplastic samples. Finally, we would like to thank the reviewers for their valuable comments which substantially improved the manuscript.

SUPPLEMENTARY MATERIAL

The Supplementary Material for this article can be found online at: https://www.frontiersin.org/articles/10.3389/fenvs.2020.00092/full#supplementary-material

REFERENCES

Acha, E. M., Mianzan, H. W., Iribarne, O., Gagliardini, D., Lasta, C., and Daleo, P. (2003). The role of the Río de la Plata bottom salinity front in accumulating debris. *Mar. Pollut. Bull.* 46, 197–202. doi: 10.1016/s0025-326x(02)00356-9

Artioli, Y., Bendoricchio, G., and Palmeri, L. (2005). Defining and modelling the coastal zone affected by the Po river (Italy). *Ecol. Model.* 184, 55–68. doi: 10.1016/j.ecolmodel.2004.11.008

Atwood, E. C., Falcieri, F. M., Piehl, S., Bochow, M., Matthies, M., Franke, J., et al. (2019). Coastal accumulation of microplastic particles emitted from the Po River, Northern Italy: comparing remote sensing and hydrodynamic modelling with in situ sample collections. *Mar. Pollut. Bull.* 138, 561–574. doi: 10.1016/j.marpolbul.2018.11.045

Berto, D., Giani, M., Savelli, F., Centanni, E., Ferrari, C. R., and Pavoni, B. (2010). Winter to spring variations of chromophoric dissolved organic matter in a temperate estuary (Po River, northern Adriatic Sea). *Mar. Environ. Res.* 70, 73–81. doi: 10.1016/j.marenvres.2010.03.005

Cole, M., Webb, H., Lindeque, P. K., Fileman, E. S., Halsband, C., and Galloway, T. S. (2015). Isolation of microplastics in biota-rich seawater samples and marine organisms. *Sci. Rep.* 4:4528. doi: 10.1038/srep04528

Directive of the European parliament. (2008). Establishing a framework for Community action in the field of marine environmental policy (Marine Strategy Framework Directive). *Official J. Eur. Union* L164, 19–40.

Dris, R., Gasperi, J., Rocher, V., and Tassin, B. (2018). Synthetic and non-synthetic anthropogenic fibers in a river under the impact of Paris Megacity: sampling methodological aspects and flux estimations. *Sci. Total Environ.* 618, 157–164. doi: 10.1016/j.scitotenv.2017.11.009

Dris, R., Gasperi, J., Saad, M., Mirande, C., and Tassin, B. (2016). Synthetic fibers in atmospheric fallout: a source of microplastics in the environment? *Mar. Pollut. Bull.* 104, 290–293. doi: 10.1016/j.marpolbul.2016.01.006

Enders, K., Lenz, R., Ivar do Sul, J. A., Tagg, A. S., and Labrenz, M. (2020). When every particle matters: a QuEChERS approach to extract microplastics from environmental samples. *MethodsX* 7:100784. doi: 10.1016/j.mex.2020.100784

Falcieri, F. M., Benetazzo, A., Sclavo, M., Russo, A., and Carniel, S. (2014). Po River plume pattern variability investigated from model data. *Cont. Shelf Res.* 87, 84–95. doi: 10.1016/j.csr.2013.11.001

Ferrari, G. M., and Dowell, M. D. (1998). CDOM absorption characteristics with relation to fluorescence and salinity in coastal areas of the southern Baltic Sea. *Estuar. Coast. Shelf Sci.* 47, 91–105. doi: 10.1006/ecss.1997.0309

Haave, M., Lorenz, C., Primpke, S., and Gerdts, G. (2019). Different stories told by small and large microplastics in sediment - first report of microplastic concentrations in an urban recipient in Norway. *Mar. Pollut. Bull.* 141, 501–513. doi: 10.1016/j.marpolbul.2019.02.015

Harvey, E. T., Kratzer, S., and Andersson, A. (2015). Relationships between colored dissolved organic matter and dissolved organic carbon in different coastal gradients of the Baltic Sea. *Ambio* 44, 392–401. doi: 10.1007/s13280-015-0658-4

Haseler, M., Schernewski, G., Balciunas, A., and Sabaliauskaite, V. (2018). Monitoring methods for large micro- and meso-litter and applications at Baltic beaches. *J. Coast. Conserv.* 22, 27–50. doi: 10.1007/s11852-017-0497-5

Herman, P. M. J., and Heip, C. H. R. (1999). Biogeochemistry of the MAximum TURbidity Zone of Estuaries (MATURE): some conclusions. *J. Mar. Syst.* 22, 89–104. doi: 10.1016/S0924-7963(99)00034-2

Hurley, R., Woodward, J., and Rothwell, J. (2018). Microplastic contamination of river beds significantly reduced by catchment-wide flooding. *Nat. Geosci.* 11, 251–257. doi: 10.1038/s41561-018-0080-1

Kammann, U., Aust, M.-O., Bahl, H., and Lang, T. (2018). Marine litter at the seafloor – Abundance and composition in the North Sea and the Baltic Sea. *Mar. Pollut. Bull.* 127, 774–780. doi: 10.1016/j.marpolbul.2017.09.051

Knap, A., Michaels, A., Close, A., Ducklow, H., and Dickson, A. (eds) (1996). *Protocols for the Joint Global Ocean Flux Study (JGOFS) Core Measurements. JGOFS Report Nr. 19, vi+170 pp. Reprint of the IOC Manuals and Guides No. 29*. Paris: UNESCO, 1994.

Lanzoni, S., Luchi, R., and Bolla Pittaluga, M. (2015). Modeling the morphodynamic equilibrium of an intermediate reach of the Po River (Italy). *Adv. Water Resour.* 81, 95–102. doi: 10.1016/j.advwatres.2014.11.004

Lebreton, L. C.-M., Greer, S. D., and Borrero, J. C. (2012). Numerical modelling of floating debris in the world's oceans. *Mar. Pollut. Bull.* 64, 653–661. doi: 10.1016/j.marpolbul.2011.10.027

Lenz, R., and Labrenz, M. (2018). Small microplastic sampling in water: development of an encapsulated filtration device. *Water* 10:1055. doi: 10.3390/w10081055

Lindell, T., Pierson, D., and Premazzi, G. (1999). *Manual for Monitoring European Lakes using Remote Sensing Techniques*. Italy: Joint Research Centre.

Liubartseva, S., Coppini, G., Lecci, R., and Creti, S. (2016). Regional approach to modeling the transport of floating plastic debris in the Adriatic Sea. *Mar. Pollut. Bull.* 103, 115–127. doi: 10.1016/j.marpolbul.2015.12.031

LM-MV, and LM-SH. (2011). Vorläufige Bewertung des Hochwasserrisikos (gem. Art. 4) und Bestimmung der Gebiete mit potenziell signifikantem Hochwasserrisiko (gem. Art. 5). Schleswig-Holstein: Ministerium für Energiewende, Umwelt, Landwirtschaft, Natur und Digitalisierung. Available online at: https://www.schleswig-holstein.de/DE/Fachinhalte/H/hochwasserschutz/Downloads/Bewertung_SchleiTrave.pdf?__blob=publicationFile&v=1

Löder, M. G. J., Imhof, H. K., Ladehoff, M., Löschel, L. A., Lorenz, C., Mintenig, S., et al. (2017). Enzymatic purification of microplastics in environmental samples. *Environ. Sci. Technol.* 51, 14283–14292. doi: 10.1021/acs.est.7b03055

Löder, M. G. J., Kuczera, M., Mintenig, S., Lorenz, C., and Gerdts, G. (2015). Focal plane array detector-based micro-Fourier-transform infrared imaging for the analysis of microplastics in environmental samples. *Environ. Chem.* 12:563. doi: 10.1071/EN14205

Maes, T., Van der Meulen, M. D., Devriese, L. I., Leslie, H. A., Huvet, A., Frère, L., et al. (2017). Microplastics baseline surveys at the water surface and in sediments of the north-east atlantic. *Front. Mar. Sci.* 4:135. doi: 10.3389/fmars.2017.00135

Maicu, F., De Pascalis, F., and Ferrarin, C. (2018). Hydrodynamics of the po river-delta-sea system. *J. Geophys. Res.* 123, 6349–6372. doi: 10.1029/2017JC013601

Masó, M., Garcés, E., Pagès, F., and Camp, J. (2003). Drifting plastic debris as a potential vector for dispersing Harmful Algal Bloom (HAB) species. *Sci. Mar.* 67, 107–111. doi: 10.3989/scimar.2003.67n1107

Masura, J., Baker, J., Foster, G., and Arthur, C. (2015). "Laboratory Methods for the Analysis of Microplastics in the marine environment: recommendations for quantifying synthetic particles in waters and sediments," in *Proceedings of the Technical Memorandum NOS-OR&R-48* (Silver Spring, MD: NOAA Marine Debris Program, NOAA Marine Debris Division).

Pichel, W. G., Churnside, J. H., Veenstra, T. S., Foley, D. G., Friedman, K. S., Brainard, R. E., et al. (2007). Marine debris collects within the north pacific subtropical convergence zone. *Mar. Pollut. Bull.* 54, 1207–1211. doi: 10.1016/j.marpolbul.2007.04.010

Raven, J. A., and Doblin, M. A. (2014). Active water transport in unicellular algae: where, why, and how. *J. Exp. Bot.* 65, 6279–6292. doi: 10.1093/jxb/eru360

Rezania, S., Park, J., Md Din, M. F., Mat Taib, S., Talaiekhozani, A., Kumar Yadav, K., et al. (2018). Microplastics pollution in different aquatic environments and biota: a review of recent studies. *Mar. Pollut. Bull.* 133, 191–208. doi: 10.1016/j.marpolbul.2018.05.022

Schmidt, L. K., Bochow, M., Imhof, H. K., and Oswald, S. E. (2018). Multi-temporal surveys for microplastic particles enabled by a novel and fast application of SWIR imaging spectroscopy – Study of an urban watercourse traversing the city of Berlin. Germany. *Environ. Pollut.* 239, 579–589. doi: 10.1016/j.envpol.2018.03.097

Sharma, S., and Chatterjee, S. (2017). Microplastic pollution, a threat to marine ecosystem and human health: a short review. *Environ. Sci. Pollut. Res.* 24, 21530–21547. doi: 10.1007/s11356-017-9910-8

Simeoni, U., and Corbau, C. (2009). A review of the Delta Po evolution (Italy) related to climatic changes and human impacts. *Geomorphology* 107, 64–71. doi: 10.1016/j.geomorph.2008.11.004

Stedmon, C. A., and Nelson, N. B. (2014). *The Optical Properties of DOM in the Ocean. Second Edi*. Amsterdam: Elsevier Inc, doi: 10.1016/B978-0-12-405940-5.00010-8

UN Resolution (2020). *Transforming our World: the 2030 Agenda for Sustainable Development*. New York, NY: United Nations.

van Wijnen, J., Ragas, A. M. J., and Kroeze, C. (2019). Modelling global river export of microplastics to the marine environment: sources and future trends. *Sci. Total Environ.* 673, 392–401. doi: 10.1016/j.scitotenv.2019.04.078

Vianello, A., Boldrin, A., Guerriero, P., Moschino, V., Rella, R., Sturaro, A., et al. (2013). Microplastic particles in sediments of Lagoon of Venice, Italy: first observations on occurrence, spatial patterns and identification. *Estuar. Coast. Shelf Sci.* 130, 54–61. doi: 10.1016/j.ecss.2013.03.022

Vodacek, A., Blough, N. V., DeGrandpre, M. D., Peltzer, E. T., and Nelson, R. K. (1997). Seasonal variation of CDOM and DOC in the Middle Atlantic Bight: terrestrial inputs and photooxidation. *Limnol. Oceanogr.* 42, 674–686. doi: 10.4319/lo.1997.42.4.0674

Wang, W., Gao, H., Jin, S., Li, R., and Na, G. (2019). The ecotoxicological effects of microplastics on aquatic food web, from primary producer to human: a review. *Ecotoxicol. Environ. Saf.* 173, 110–117. doi: 10.1016/j.ecoenv.2019.01.113

Xiao, R., and Zheng, Y. (2016). Overview of microalgal extracellular polymeric substances (EPS) and their applications. *Biotechnol. Adv.* 34, 1225–1244. doi: 10.1016/j.biotechadv.2016.08.004

Conflict of Interest: EA, JF, and FS were employed by the company RSS Remote Sensing Solutions GmbH.

The remaining authors declare that the research was conducted in the absence of any commercial or financial relationships that could be construed as a potential conflict of interest.

Article C2: Supplementary information

Supplementary information 1: Raw data of in-situ water constituents and microplastic (MP) at the Trave river (T), the Elbe estuary (August: EA and June: EJ), and the Po delta (P). For the Trave all microplastics were analyzed with NIR spectroscopy. For the Elbe June campaign only FPA-based µFTIR analysis was conducted and the results of the subsamples correspondingly extrapolated. Values of chlorophyll-a (Chl-A) and suspended particulate matter (SPM) in mg/L, Secchi depth in cm, Temperature (Temp) in °C, Salinity in PSU, CDOM in cm^{-1}, volume and microplastic particles per m^3. Subsample refers to the percentage of the sample taken for FPA-based µFTIR spectroscopy.

Sample	Date	Area	Chl-A	SPM	Secchi	Temp	PSU	CDOM	Volume	Subsample	MPs
T14	23.05.2014	WWTP	0.4058	12.560	72.5	20.4	NaN	3.3186	1.00	NaN	1.000
T15	24.05.2014	Coast	0.0032	3.557	475	16.6	NaN	0.6581	36.02	NaN	0.111
T16	24.05.2014	River	0.0154	4.257	228.5	16.8	NaN	1.4081	29.52	NaN	0.136
T17	24.05.2014	River	0.0213	5.371	215	18.1	NaN	1.9699	26.67	NaN	0.225
T18	24.05.2014	Coast	0.0047	3.557	350	16.6	NaN	1.0814	30.96	NaN	0.032
T19	24.05.2014	Coast	0.0035	3.414	550	16.6	NaN	0.7659	31.78	NaN	0.220
T20	24.05.2014	Coast	0.0022	3.871	600	16.4	NaN	0.593	27.47	NaN	0.000
T21	24.05.2014	Coast	0.0022	3.571	550	16.9	NaN	0.5828	29.31	NaN	0.068
T22	24.05.2014	Coast	0.0048	5.343	535	19.6	NaN	0.9412	31.93	NaN	0.000
T23	24.05.2014	River	0.0315	6.900	122.5	18.1	NaN	1.9382	14.35	NaN	0.000
T24	25.05.2014	River	0.3046	11.640	125	18.5	NaN	3.3792	33.38	NaN	0.360
T25	25.05.2014	River	0.3473	11.380	115	18.7	NaN	3.0557	23.92	NaN	1.213
T27	25.05.2014	WWTP	0.5399	21.560	50	22.7	NaN	3.2692	8.22	NaN	0.487
AL01	19.08.2015	Coast	NaN	21.489	55	18.97	25.62	0.967	21.414	100	1.090
AL02	19.08.2015	Coast	NaN	14.191	95	18.60	25.60	NaN	10.122	100	8.672
AL03	19.08.2015	Coast	NaN	22.172	65	18.08	26.67	NaN	20.619	50	3.443
AL04	19.08.2015	Coast	NaN	18.839	75	18.75	22.44	1.163	19.850	50	9.907
AL05	19.08.2015	Coast	NaN	21.956	65	19.13	22.23	1.28	25.770	50	5.131
AL06	20.08.2015	Coast	NaN	15.392	105	19.41	25.48	1.018	12.817	50	2.254
AL07	20.08.2015	Coast	NaN	27.639	70	19.19	26.63	0.859	18.022	50	5.487
AL08	20.08.2015	Coast	NaN	26.592	80	19.67	23.55	1.675	20.787	50	10.797

AL09	20.08.2015	Coast	NaN	26.622	65	19.67	21.24	1.539	20.713	50	10.138
AL10	20.08.2015	River	NaN	25.972	70	20.05	19.29	1.389	25.102	50	6.330
AL11	20.08.2015	River	NaN	42.272	50	19.82	17.79	1.606	18.083	100	1.413
AL12	20.08.2015	River	NaN	20.739	60	20.78	14.36	1.517	22.653	50	4.365
AL13	21.08.2015	River	NaN	67.838	25	20.57	7.56	3.094	24.216	10	3.671
AL14	21.08.2015	River	NaN	22.272	55	21.09	11.47	2.849	23.465	100	1.421
AL15	21.08.2015	River	NaN	25.789	60	20.84	9.69	2.189	13.282	100	0.753
AL16	21.08.2015	River	NaN	35.804	30	21.13	7.69	2.331	20.162	50	1.433
AL17	21.08.2015	River	NaN	34.524	60	21.30	6.41	1.978	17.201	100	0.000
AL18	21.08.2015	River	NaN	62.352	35	21.23	5.33	2.065	22.460	50	2.177
AL19	21.08.2015	River	NaN	38.385	30	22.04	2.65	2.654	23.172	50	5.754
AL20	21.08.2015	River	NaN	47.407	30	21.97	1.78	NaN	16.651	100	2.469
EL01	14.06.2015	River	NaN	49.476	38.75	20.4	0.5	2.446	38.638	50	1.006
EL02	15.06.2015	River	NaN	26.815	38.75	19.2	0.5	1.721	48.688	50	0.799
EL03	15.06.2015	River	NaN	23.048	48.75	18.7	0.5	1.820	50.184	50	0.376
EL04	16.06.2015	River	NaN	122.656	20	17.7	0.7	1.709	30.328	50	2.002
EL05	16.06.2015	River	NaN	130.322	15.5	18.1	0.6	1.625	23.915	50	1.742
EL06	16.06.2015	River	NaN	73.322	21.2	18.1	0.6	1.764	43.792	50	0.707
EL07	17.06.2015	River	NaN	323.867	9	16.9	1.2	1.327	17.018	50	4.440
EL08	17.06.2015	River	NaN	74.089	16	16.6	2.4	0.741	32.25	50	1.654
EL09	23.06.2015	Coast	NaN	4.452	NaN	15.2	28.7	1.727	64.381	50	0.052
EL10	23.06.2015	Coast	NaN	10.746	NaN	15.3	27.1	1.131	63.936	50	0.104
EL11	23.06.2015	Coast	NaN	25.624	65	15.4	25	1.457	78.279	50	0.298
EL12	25.06.2015	River	NaN	51.659	44.25	16.1	16	1.601	39.189	50	1.616
EL13	25.06.2015	River	NaN	90.348	27.75	16.2	17.9	1.393	51.436	50	2.506
EL14	25.06.2015	River	NaN	20.778	42.5	16.4	10.7	1.692	52.207	50	4.597
Po01	10.06.2016	River	0.008	21.839	81.25	21.45	0.14	0.775	12.091	12.5	17.354
Po02	10.06.2016	Mouth	0.008	20.992	55	22.05	0.26	1.409	24.393	25	2.986

Po03	10.06.2016	Coast	0.005	11.698	65	22.86	6.91	0.139	26.383	25	9.204
Po04	10.06.2016	Coast	0.013	12.922	112.5	22.56	26.67	0.704	39.162	25	6.099
Po05	10.06.2016	Mouth	0.010	15.604	47.5	21.89	0.28	0.424	47.652	50	1.004
Po06	15.06.2016	Mouth	0.005	25.180	45	22.00	1.20	1.467	43.582	12.5	12.295
Po07	15.06.2016	Coast	0.005	13.039	72.5	22.58	17.02	1.014	41.449	25	4.122
Po08	15.06.2016	Coast	0.014	10.263	90	22.94	23.74	0.224	53.207	1.6	56.061
Po09	15.06.2016	Coast	0.014	9.470	92.5	22.72	27.02	0.509	33.895	6.3	2.444
Po10	18.06.2016	Coast	0.010	31.290	38.75	21.95	0.29	0.231	55.060	12.5	12.275
Po11	18.06.2016	River	0.008	26.748	35	22.32	0.26	0.362	37.196	6.3	16.153
Po12	18.06.2016	Mouth	0.043	17.051	80	21.72	23.56	3.296	36.136	25	35.749
Po13	18.06.2016	Coast	0.009	10.593	162.5	23.12	31.91	0.074	32.374	12.5	78.299
Po14	18.06.2016	Coast	0.006	11.814	125	22.85	31.93	NaN	39.199	25	4.817
Po15	18.06.2016	Coast	0.005	21.276	46.25	22.88	9.61	0.259	27.628	50	3.360
Po16	18.06.2016	Coast	0.010	66.067	33.75	22.51	0.15	0.370	28.621	25	10.546
Po18	23.06.2016	River	0.006	61.816	36.25	21.58	0.12	3.541	30.565	1.6	13.887
Po19	23.06.2016	River	0.008	24.380	32.5	22.82	0.14	0.398	38.945	25	3.257
Po20	23.06.2016	Mouth	0.017	26.133	40	24.01	11.11	0.187	41.710	25	3.273
Po21	23.06.2016	Coast	NaN	7.689	122.5	25.99	23.91	1.326	42.417	25	3.590

Supplementary information 2: Pearson's correlation coefficient for analyzed water constituents of the three investigated river systems. Chl-A: chlorophyll-a, SPM: suspended particulate matter, CDOM: colored dissolved organic matter.

TRAVE			
	Chl-A	**SPM**	**CDOM**
Chl-A	-	-	-
SPM	0.96	-	-
CDOM	0.9	0.86	-
ELBE AUG			
	SPM		
CDOM	0.6		
PO DELTA			
	Chl-A	**SPM**	**CDOM**
Chl-A	-	-	-
SPM	-0.06	-	-
CDOM	0.27	0.08	-

Supplementary information 3: Fibers and particles (*) in negative controls for analyzed microplastic size class <0.5 mm. PP: Polypropylene, PET: Polyethylene terephthalate, PAN: Polyacrylonitrile, PBT: Polybutylene terephthalate.

Study site	**ID Sample**	**PP**	**PET**	**PAN**	**PBT**	**SUM**
Elbe Aug	Blank1	0	2	2	0	4
Elbe Aug	Blank2	0	1	0	0	1
Elbe Aug	Blank3	0	1	0	0	1
Elbe Aug	Blank4	0	0	0	0	0
Elbe Aug	Blank5	0	1	0	0	1
Elbe Jun	Blank0	0	2	0	0	2
Elbe Jun	Blank1	0	2	0	0	2
Elbe Jun	Blank2	0	0	1	0	1
Elbe Jun	Blank3	0	2	3	0	5
Po delta	Blank2	0	10	0	0	10
Po delta	Blank3	0	5	0	1	6
Po delta	Blank4	1*	11	0	0	11
Po delta	Blank5	0	7	2	0	9
Po delta	Blank6	0	21	0	0	21
Po delta	Blank7	0	1	0	0	1

Conclusion

If current socio-economic trends continue, global solid waste generation is expected to increase from 3.5 million tons/day in 2010 to over 11 million tons/day in 2100 (Hoornweg et al. 2013). If no regulation and management plans are implemented, environmental plastic pollution will continue to rise. Not to mention the damage to the environment, plastic debris has tremendous socio-economic impacts for many industries, such as fishing, aquaculture, shipping, and tourism. Thus, plastic pollution of the environment is addressed at the highest international levels (G7 2015, EU 2018). In Europe, several international and regional instruments at sea (i.e. Annex V MARPOL 73/78, HELCOM, OSPAR, MSFD), along with initiatives on land-based waste management, exist (i.e. Waste Frame Directive (Directive 2008/98/EC), Packaging and Packaging Waste Directive (Directive 94/62/EC), Landfill Directive (Directive 99/31/EC), Urban Waste Water Treatment Directive (Directive 91/271/EEC). As most MP debris is the result of fragmentation of larger plastic debris already present in the environment, measures targeting large plastic debris are thus also relevant for MPs. Interestingly, MPs are exclusively addressed within directives concerning marine litter (MSFD, HELCOM, OSPAR). Even though the debate regarding the harm of MPs is ongoing, it is important to adopt a precautionary principle soon, as plastic debris persists in the environment for centuries (Andrady 2015) and there are limited removal options (especially for MPs).

To curb plastic debris pollution, politicians, industries, and consumers need to be addressed equally. Management strategies should focus not only on preventing, mitigating, and removing plastic debris, but also on behavior-changing activities. For scientists, it is crucial to communicate results in a responsible and clear way, as the topic is a sensitive one and misconceptions can arise easily. Nevertheless, the topic has the potential to increase public environmental awareness, as it demonstrates society's enormous impact on the planet. Therefore, it possibly could help to transpose the implemented "throwaway living" in the 50s into a sustainable consumer behavior in the future.

References

Accinelli C, Abbas HK, Little NS, Kotowicz JK, Mencarelli M, Shier WT (2016) A liquid bioplastic formulation for film coating of agronomic seeds. Crop Prot 89:123–128.

Accinelli C, Abbas HK, Shier WT, Vicari A, Little NS, Aloise MR, Giacomini S (2019) Degradation of microplastic seed film-coating fragments in soil. Chemosphere 226:645–650.

Acha EM, Mianzan HW, Iribarne O, Gagliardini D a, Lasta C, Daleo P (2003) The role of the Río de la Plata bottom salinity front in accumulating debris. Mar Pollut Bull 46:197–202.

Andrady AL (2003) Plastics and the environment. Andrady AL (eds) John Wiley & Sons, New Jersey.

Andrady AL (2015) Plastics and environmental sustainability. Andrady AL (eds) John Wiley & Sons, New Jersey.

Andrady AL (2017) The plastic in microplastics: A review. Mar Pollut Bull 119:12–22.

Arthur C, Baker J, Bamford H (2009) Proceedings of the International Research Workshop on the Occurrence, Effects and Fate of Microplastic Marine Debris. Arthur C, Baker J, Bamford H (eds) Sept 9-11, 2008. NOAA Technical Memorandum NOS-OR&R-30.

Auta HS, Emenike C., Fauziah S. (2017) Distribution and importance of microplastics in the marine environment: A review of the sources, fate, effects, and potential solutions. Environ Int 102:165–176.

Basnet K (1993) Solid Waste Pollution Versus Sustainable Development in High Mountain Environment: A Case Study of Sagarmatha National Park of Khumbu Region, Nepal. Contrib Nepalese Stud 20:131–139.

Bergmann M, Gutow L, Klages M (2015) Marine Anthropogenic Litter. Bergmann M, Gutow L, Klages M (eds) Springer International Publishing, Cham.

Bergmann M, Wirzberger V, Krumpen T, Lorenz C, Primpke S, Tekman MB, Gerdts G (2017) High Quantities of Microplastic in Arctic Deep-Sea Sediments from the HAUSGARTEN Observatory. Environ Sci Technol 51:11000–11010.

Berto D, Giani M, Savelli F, Centanni E, Ferrari CR, Pavoni B (2010) Winter to spring variations of chromophoric dissolved organic matter in a temperate estuary (Po River, northern Adriatic Sea). Mar Environ Res 70:73–81.

Besley A, Vijver MG, Behrens P, Bosker T (2017) A standardized method for sampling and extraction methods for quantifying microplastics in beach sand. Mar Pollut Bull 114:77–83.

Besseling E, Quik JTK, Sun M, Koelmans AA (2017) Fate of nano- and microplastic in freshwater systems: A modeling study. Environ Pollut 220:540–548.

Briassoulis D, Dejean C (2010) Critical review of norms and standards for biodegradable agricultural plastics part I. Biodegradation in soil. J Polym Environ 18:384–400.

Briassoulis D, Hiskakis M, Scarascia G, Picuno P, Delgado C, Dejean C (2010) Labeling scheme for agricultural plastic wastes in Europe. Qual Assur Saf Crop Foods 2:93–104.

Browne MA, Chapman MG, Thompson RC, Amaral-Zettler L a., Jambeck J, Mallos NJ (2015) Spatial and temporal patterns of stranded intertidal marine debris: is there a picture of global change? Environ Sci Technol 49:7082-7094.

Browne MA, Crump P, Niven SJ, Teuten E, Tonkin A, Galloway T, Thompson R (2011) Accumulation of Microplastic on Shorelines Woldwide: Sources and Sinks. Environ Sci Technol 45:9175–9179.

Buffington JM, Montgomery DR (1999) A procedure for classifying textural facies in gravel-bed rivers. Water Resour Res 35:1903–1914.

Carpenter EJ, Anderson SJ, Harvey GR, Miklas HP, Peck BB (1972) Polystyrene spherules in coastal waters. Science 178:749–50.

Carson HS, Lamson MR, Nakashima D, Toloumu D, Hafner J, Maximenko N, McDermid KJ (2013) Tracking the sources and sinks of local marine debris in Hawai'i. Mar Environ Res 84:76–83.

Castañeda RA, Avlijas S, Simard MA, Ricciardi A (2014) Microplastic pollution in St. Lawrence River sediments. Can J Fish Aquat Sci 71:1767–1771.

Van Cauwenberghe L, Devriese L, Galgani F, Robbens J, Janssen CR (2015) Microplastics in sediments: A review of techniques, occurrence and effects. Mar Environ Res 111:5-17.

Chubarenko I, Stepanova N (2017) Microplastics in sea coastal zone: Lessons learned from the Baltic amber. Environ Pollut 224:243–254.

Chubarenko IP, Esiukova EE, Bagaev AV, Bagaeva MA, Grave AN (2018) Three-dimensional distribution of anthropogenic microparticles in the body of sandy beaches. Sci Total Environ 628–629:1340–1351.

Cole M, Lindeque P, Fileman E, Halsband C, Goodhead R, Moger J, Galloway TS (2013) Microplastic ingestion by zooplankton. Environ Sci Technol 47:6646–55.

Cole M, Lindeque P, Halsband C, Galloway TS (2011) Microplastics as contaminants in the marine environment: A review. Mar Pollut Bull 62:2588–2597.

Cole M, Webb H, Lindeque PK, Fileman ES, Halsband C, Galloway TS (2015) Isolation of microplastics in biota-rich seawater samples and marine organisms. Sci Rep 4:4528.

Colton JB, Burns BR, Knapp, FD (1974) Plastic Particles in Surface Waters of the Northwestern Atlantic. Science 185:491–497.

Dris R, Gasperi J, Rocher V, Saad M, Renault N, Tassin B (2015) Microplastic contamination in an urban area: a case study in Greater Paris. Environ Chem 12:592.

Dris R, Gasperi J, Saad M, Mirande C, Tassin B (2016) Synthetic fibers in atmospheric fallout: A source of microplastics in the environment? Mar Pollut Bull 104:290–293.

Duis K, Coors A (2016) Microplastics in the aquatic and terrestrial environment: sources (with a specific focus on personal care products), fate and effects. Environ Sci Eur 28:2.

Eerkes-Medrano D, Thompson RC, Aldridge DC (2015) Microplastics in freshwater systems: A review of the emerging threats, identification of knowledge gaps and prioritisation of research needs. Water Res 75:63–82.

Enders K, Lenz R, Beer S, Stedmon CA (2017) Extraction of microplastic from biota: Recommended acidic digestion destroys common plastic polymers. ICES J Mar Sci 74:326–331.

Espí E, Salmerón A, Fontecha A, García Y, Real AI (2006) Plastic Films for Agricultural Applications. J Plast Film Sheeting 22:85–102.

EU (2018) EC (European Commission), Communication from the Commission: A European Strategy for Plastics in a Circular Economy – Strategy, COM/2018/028, 2018.

European Parliament and Council Directive, 91/271/EEC of 21 May 1991 concerning urban wastewater treatment, 1991, pp.40-52.

European Parliament and Council Directive, 94/62/EC of 20 December 1994 on packaging and packaging waste, as amended, 1994, p. 11.

European Parliament and of the Council Directive, 2008/98/EC of 19 November 2008 on waste and repealing certain Directives, 2008, p. 19.

European Union Council Directive 1999/31/EC of 16 July 1999 on the landfill of waste, 1991, pp.1–19.

Fazey FMC, Ryan PG (2016) Biofouling on buoyant marine plastics: An experimental study into the effect of size on surface longevity. Environ Pollut 210:354–360.

Ferrari GM, Dowell MD (1998) CDOM absorption characteristics with relation to fluorescence and salinity in coastal areas of the southern Baltic Sea. Estuar Coast Shelf Sci 47:91–105.

Filella M (2015) Questions of size and numbers in environmental research on microplastics: methodological and conceptual aspects. Environ Chem 12:527.

Fischer V, Elsner NO, Brenke N, Schwabe E, Brandt A (2014) Plastic pollution of the Kuril-Kamchatka-trench area (NW pacific). Deep Sea Res Part II Top Stud Oceanogr 111:399-405.

Fisner M, Majer AP, Balthazar-Silva D, Gorman D, Turra A (2017) Quantifying microplastic pollution on sandy beaches: the conundrum of large sample variability and spatial heterogeneity. Environ Sci Pollut Res 24:13732–13740.

Foley CJ, Feiner ZS, Malinich TD, Höök TO (2018) A meta-analysis of the effects of exposure to microplastics on fish and aquatic invertebrates. Sci Total Environ 631–632:550–559.

Frias JPGL, Nash R (2019) Microplastics: Finding a consensus on the definition. Mar Pollut Bull 138:145–147.

G7 (2015) Leaders' Declaration G7 Summit 7-8 June 2015. G7 Summit, pp.7–8..

Gall SC, Thompson RC (2015) The impact of debris on marine life. Mar Pollut Bull 92:170–179.

Galloway TS, Cole M, Lewis C (2017) Interactions of microplastic debris throughout the marine ecosystem. Nat Ecol Evol 1:0116.

Gatidou G, Arvaniti OS, Stasinakis AS (2019) Review on the occurrence and fate of microplastics in Sewage Treatment Plants. J Hazard Mater 367:504–512.

Gebhardt C, Forster S (2018) Size-selective feeding of Arenicola marina promotes long-term burial of microplastic particles in marine sediments. Environ Pollut 242:1777–1786.

Geyer R, Jambeck JR, Law KL (2017) Production, use, and fate of all plastics ever made. Sci Adv 3:25–29.

Goddijn-Murphy L, Peters S, van Sebille E, James NA, Gibb S (2018) Concept for a hyperspectral remote sensing algorithm for floating marine macro plastics. Mar Pollut Bull 126:255–262.

Guilherme MR, Aouada FA, Fajardo AR, Martins AF, Paulino AT, Davi MFT, Rubira AF, Muniz EC (2015) Superabsorbent hydrogels based on polysaccharides for application in agriculture as soil conditioner and nutrient carrier: A review. Eur Polym J 72:365–385.

Haave M, Lorenz C, Primpke S, Gerdts G (2019) Different stories told by small and large microplastics in sediment - first report of microplastic concentrations in an urban recipient in Norway. Mar Pollut Bull 141:501–513.

Halle A, Ladirat L, Gendre X, Goudouneche D, Pusineri C, Routaboul C, Tenailleau C, Duployer B, Perez E (2016) Understanding the Fragmentation Pattern of Marine Plastic Debris. Environ Sci Technol 50:5668–5675.

Hanke G, Galgani F, Werner S, Oosterbaan L, Nilsson P, Fleet D, Kinsey S, Thompson R, Van Franeker JA, Vlachogianni T (2013) Guidance on Monitoring of Marine Litter in European Seas. MSFD GES Technical Subgroup on Marine Litter (TSG-ML), Publications Office of the European Union.

Hanvey JS, Lewis PJ, Lavers JL, Crosbie ND, Pozo K, Clarke BO (2017) A review of analytical techniques for quantifying microplastics in sediments. Anal Methods 9:1369–1383.

Hardesty BD, Harari J, Isobe A, Lebreton L, Maximenko N, Potemra J, van Sebille E, Vethaak AD, Wilcox C (2017) Using Numerical Model Simulations to Improve the Understanding of Micro-plastic Distribution and Pathways in the Marine Environment. Front Mar Sci 4:1–9.

Harvey ET, Kratzer S, Andersson A (2015) Relationships between colored dissolved organic matter and dissolved organic carbon in different coastal gradients of the Baltic Sea. Ambio 44:392–401.

Haseler M, Schernewski G, Balciunas A, Sabaliauskaite V (2018) Monitoring methods for large micro- and meso-litter and applications at Baltic beaches. J Coast Conserv 22:27–50.

HELCOM (2008) Marine Litter within the Baltic Region. Helsinki Convention (HELCOM) Recommendation 29/2, adopted 5 March 2008.

Heo NW, Hong SH, Han GM, Hong S, Lee J, Song YK, Jang M, Shim WJ (2013) Distribution of small plastic debris in cross-section and high strandline on Heungnam beach, South Korea. Ocean Sci J 48:225–233.

Hidalgo-Ruz V, Gutow L, Thompson RC, Thiel M (2012) Microplastics in the Marine Environment: A Review of the Methods Used for Identification and Quantification. Environ Sci Technol 46:3060–3075.

Hoellein TJ, McCormick AR, Hittie J, London MG, Scott JW, Kelly JJ (2017) Longitudinal patterns of microplastic concentration and bacterial assemblages in surface and benthic habitats of an urban river. Freshw Sci 36:491–507.

Hoornweg D, Bhada-Tata P, Kennedy C (2013) Waste production must peak this century. Nature 502: 615-617.

Horton AA, Walton A, Spurgeon DJ, Lahive E, Svendsen C (2017) Microplastics in freshwater and terrestrial environments: Evaluating the current understanding to identify the knowledge gaps and future research priorities. Sci Total Environ 586:127–141.

Huerta Lwanga E, Mendoza Vega J, Ku Quej V, Chi J de los A, Sanchez del Cid L, Chi C, Escalona Segura G, Gertsen H, Salánki T, van der Ploeg M, Koelmans AA, Geissen V (2017) Field evidence for transfer of plastic debris along a terrestrial food chain. Sci Rep 7:14071.

Hussain N, Jaitley V, Florence AT (2001) Recent advances in the understanding of uptake of microparticulates across the gastrointestinal lymphatics. Adv Drug Deliv Rev 50:107–142.

Imhof HK, Ivleva NP, Schmid J, Niessner R, Laforsch C (2013) Contamination of beach sediments of a subalpine lake with microplastic particles. Curr Biol 23:R867-R868.

Imhof HK, Schmid J, Niessner R, Ivleva NP, Laforsch C (2012) A novel, highly efficient method for the separation and quantification of plastic particles in sediments of aquatic environments. Limnol Oceanogr Methods 10:524–537.

Imhof HK, Sigl R, Brauer E, Feyl S, Giesemann P, Klink S, Leupolz K, Löder MGJ, Löschel LA, Missun J, Muszynski S, Ramsperger AFRM, Schrank I, Speck S, Steibl S, Trotter B, Winter I, Laforsch C (2017) Spatial and temporal variation of macro-, meso- and microplastic abundance on a remote coral island of the Maldives, Indian Ocean. Mar Pollut Bull 116:340–347.

Imhof HK, Wiesheu AC, Anger PM, Niessner R, Ivleva NP, Laforsch C (2018) Variation in plastic abundance at different lake beach zones - A case study. Sci Total Environ 613–614:530–537.

Jambeck JR, Geyer R, Wilcox C, Siegler TR, Perryman M, Andrady A, Narayan R, Law KL (2015) Plastic waste inputs from land into the ocean. Science 347:768–771.

Kaiser D, Estelmann A, Kowalski N, Glockzin M, Waniek JJ (2019) Sinking velocity of sub-millimeter microplastic. Mar Pollut Bull 139:214–220.

Kaiser D, Kowalski N, Waniek JJ (2017) Effects of biofouling on the sinking behavior of microplastics. Environ Res Lett 12:124003.

Kako S, Isobe A, Magome S (2012) Low altitude remote-sensing method to monitor marine and beach litter of various colors using a balloon equipped with a digital camera. Mar Pollut Bull 64:1156–62.

Kako S, Isobe A, Magome S (2010) Sequential monitoring of beach litter using webcams. Mar Pollut Bull 60:775–779.

Kammann U, Aust MO, Bahl H, Lang T (2017) Marine litter at the seafloor - Abundance and composition in the North Sea and the Baltic Sea. Mar Pollut Bull 127:774-780.

Karami A (2017) Gaps in aquatic toxicological studies of microplastics. Chemosphere 184:841–848.

Kawecki D, Nowack B (2019) Polymer-Specific Modeling of the Environmental Emissions of Seven Commodity Plastics As Macro- and Microplastics. Environ Sci Technol 53:9664–9676.

Kershaw PJ, Turra A, Galgani F (2019) Guidelines for the monitoring and assessment of plastic litter in the ocean. GESAMP Reports Stud 99:126.

Khatmullina L, Isachenko I (2017) Settling velocity of microplastic particles of regular shapes. Mar Pollut Bull 114:871–880.

Kole PJ, Löhr AJ, Van Belleghem F, Ragas A (2017) Wear and Tear of Tyres: A Stealthy Source of Microplastics in the Environment. Int J Environ Res Public Health 14:1265.

Kooi M, Besseling E, Kroeze C, Wezel AP Van, Koelmans AA (2018) Freshwater Microplastics. Wagner M, Lambert S (eds) Springer International Publishing, Cham.

Kowalski N, Reichardt AM, Waniek JJ (2016) Sinking rates of microplastics and potential implications of their alteration by physical, biological, and chemical factors. Mar Pollut Bull 109:310–319.

Krelling AP, Souza MM, Williams AT, Turra A (2017) Transboundary movement of marine litter in an estuarine gradient: Evaluating sources and sinks using hydrodynamic modelling and ground truthing estimates. Mar Pollut Bull 119:48–63.

Law KL (2017) Plastics in the Marine Environment. Ann Rev Mar Sci 9:205–229.

Law KL, Morét-Ferguson SE, Goodwin DS, Zettler ER, DeForce E, Kukulka T, Proskurowski G (2014) Distribution of Surface Plastic Debris in the Eastern Pacific Ocean from an 11-Year Data Set. Environ Sci Technol 48:4732–4738.

Lebreton LC-M, Borrero JC (2012) Modeling the transport and accumulation floating debris generated by the 11 March 2011 Tohoku tsunami. Mar Pollut Bull 66:53–58.

Lebreton LC-M, Greer SD, Borrero JC (2012) Numerical modelling of floating debris in the world's oceans. Mar Pollut Bull 64:653–61.

Lebreton LCM, van der Zwet J, Damsteeg J, Slat B, Andrady A, Reisser J (2017) River plastic emissions to the world's oceans. Nat Commun 8:15611.

Lechner A, Ramler D (2015) The discharge of certain amounts of industrial microplastic from a production plant into the River Danube is permitted by the Austrian legislation. Environ Pollut 200:159–160.

Lehner R, Weder C, Petri-Fink A, Rothen-Rutishauser B (2019) Emergence of Nanoplastic in the Environment and Possible Impact on Human Health. Environ Sci Technol 53:1748–1765.

Lenz R, Labrenz M (2018) Small Microplastic Sampling in Water: Development of an Encapsulated Filtration Device. Water 10:1055.

Li J, Liu H, Paul Chen J (2018) Microplastics in freshwater systems: A review on occurrence, environmental effects, and methods for microplastics detection. Water Res 137:362–374.

Liu EK, He WQ, Yan CR (2014) 'White revolution' to 'white pollution' – agricultural plastic film mulch in China. Environ Res Lett 9:091001.

Lo H-S, Xu X, Wong C-Y, Cheung S-G (2018) Comparisons of microplastic pollution between mudflats and sandy beaches in Hong Kong. Environ Pollut 236:208–217.

Löder MGJ, Kuczera M, Mintenig S, Lorenz C, Gerdts G (2015) Focal plane array detector-based micro-Fourier-transform infrared imaging for the analysis of microplastics in environmental samples. Environ Chem 12:563.

Mace TH (2012) At-sea detection of marine debris: overview of technologies, processes, issues, and options. Mar Pollut Bull 65:23–7.

Magazine, Life. (1955) Throwaway living: Disposable items cut down household chores. Life, 39; 43-44.

Mai L, Bao L-J, Shi L, Wong CS, Zeng EY (2018) A review of methods for measuring microplastics in aquatic environments. Environ Sci Pollut Res 25:11319–11332.

Martín-Closas L, Costa J, Pelacho AM (2017) Soil Degradable Bioplastics for a Sustainable Modern Agriculture. Malinconico M (ed) Springer Berlin Heidelberg.

Massicotte P, Asmala E, Stedmon C, Markager S (2017) Science of the Total Environment Global distribution of dissolved organic matter along the aquatic continuum : Across rivers , lakes and oceans. Sci Total Environ 609:180–191.

Maximenko N, Hafner J, Niiler P (2012) Pathways of marine debris derived from trajectories of Lagrangian drifters. Mar Pollut Bull 65:51–62.

Michels J, Stippkugel A, Lenz M, Wirtz K, Engel A (2018) Rapid aggregation of biofilm-covered microplastics with marine biogenic particles. Proceedings Biol Sci 285:20181203.

Mintenig SMM, Int-Veen I, Löder MGJ, Primpke S, Gerdts G (2016) Identification of microplastic in effluents of waste water treatment plants using focal plane array-based micro-Fourier-transform infrared imaging. Water Res 108:365–372.

Morris AW, Hamilton EI (1974) Polystyrene spherules in the Bristol Channel. Mar Pollut Bull 5:26–27.

Nakashima E, Isobe A, Magome S, Kako S, Deki N (2011) Using aerial photography and in situ measurements to estimate the quantity of macro-litter on beaches. Mar Pollut Bull 62:762–9.

Neumann D, Callies U, Matthies M (2014) Marine litter ensemble transport simulations in the southern North Sea. Mar Pollut Bull 86:219–228.

Ogonowski M, Gerdes Z, Gorokhova E (2018) What we know and what we think we know about microplastic effects – A critical perspective. Curr Opin Environ Sci Heal 1:41–46.

OSPAR (2010) Guideline for Monitoring Marine Litter on the Beaches in the OSPAR Maritime Area. OSPAR Commision 2010.

Peeken I, Primpke S, Beyer B, Gütermann J, Katlein C, Krumpen T, Bergmann M, Hehemann L, Gerdts G (2018) Arctic sea ice is an important temporal sink and means of transport for microplastic. Nat Commun 9:1505.

Pichel WG, Churnside JH, Veenstra TS, Foley DG, Friedman KS, Brainard RE, Nicoll JB, Zheng Q, Clemente-Colón P (2007) Marine debris collects within the North Pacific Subtropical Convergence Zone. Mar Pollut Bull 54:1207–11.

Raven JA, Doblin MA (2014) Active water transport in unicellular algae: where , why , and how. 65:6279–6292.

Rech S, Macaya-Caquilpán V, Pantoja JF, Rivadeneira MM, Jofre Madariaga D, Thiel M (2014) Rivers as a source of marine litter – A study from the SE Pacific. Mar Pollut Bull 82:66–75.

Rezania S, Park J, Md Din MF, Mat Taib S, Talaiekhozani A, Kumar Yadav K, Kamyab H (2018) Microplastics pollution in different aquatic environments and biota: A review of recent studies. Mar Pollut Bull 133:191–208.

PlasticsEurope (2018) Plastics – the Facts 2018. https://www.plasticseurope.org, accessed October 2019.

Rochman CM (2018) Microplastics research—from sink to source. Science 360:28–29.

Rodrigues FHA, Spagnol C, Pereira AGB, Martins AF, Fajardo AR, Rubira AF, Muniz EC (2014) Superabsorbent hydrogel composites with a focus on hydrogels containing nanofibers or nanowhiskers of cellulose and chitin. J Appl Polym Sci 131:39725.

Rummel CD, Jahnke A, Gorokhova E, Kühnel D, Schmitt-Jansen M (2017) Impacts of Biofilm Formation on the Fate and Potential Effects of Microplastic in the Aquatic Environment. Environ Sci Technol Lett 4:258–267.

Scarascia-Mugnozza G, Sica C, Russo G (2012) Plastic materials in European agriculture: actual use and perspectives. J Agric Eng 42:15.

Schmidt LK, Bochow M, Imhof HK, Oswald SE (2018) Multi-temporal surveys for microplastic particles enabled by a novel and fast application of SWIR imaging spectroscopy – Study of an urban watercourse traversing the city of Berlin, Germany. Environ Pollut 239:579–589.

Schrank I, Trotter B, Dummert J, Scholz-Böttcher BM, Löder MGJ, Laforsch C (2019) Effects of microplastic particles and leaching additive on the life history and morphology of Daphnia magna. Environ Pollut 255:113233.

Schwarz AE, Ligthart TN, Boukris E, van Harmelen T (2019) Sources, transport, and accumulation of different types of plastic litter in aquatic environments: A review study. Mar Pollut Bull 143:92–100.

Statistisches Bundesamt (2019) FS 3 Land- und Forstwirtschaft, Fischerei, R. 5.1 Bodenfläche nach Art der tatsächlichen Nutzung 2017, Statistische Ämter des Bundes und der Länder, Deutschland, Version 2.0, Stand: 01.06.2019.

van Sebille E, Griffies SM, Abernathey R, Adams TP, Berloff P, Biastoch A, Blanke B, Chassignet EP, Cheng Y, Cotter CJ, Deleersnijder E, Döös K, Drake HF, Drijfhout S, Gary SF, Heemink AW, Kjellsson J, Koszalka IM, Lange M, Lique C, MacGilchrist GA, Marsh R, Mayorga Adame CG, McAdam R, Nencioli F, Paris CB, Piggott MD, Polton JA, Rühs S, Shah SHAM, Thomas MD, Wang J, Wolfram PJ, Zanna L, Zika JD (2018) Lagrangian ocean analysis: Fundamentals and practices. Ocean Model 121:49–75.

van Sebille E, Wilcox C, Lebreton L, Maximenko N, Hardesty BD, van Franeker JA, Eriksen M, Siegel D, Galgani F, Law KL (2015) A global inventory of small floating plastic debris. Environ Res Lett 10:124006.

Sharma S, Chatterjee S (2017) Microplastic pollution, a threat to marine ecosystem and human health: a short review. Environ Sci Pollut Res 24:21530–21547.

Sheavly SB, Register KM (2007) Marine Debris & Plastics: Environmental Concerns, Sources, Impacts and Solutions. J Polym Environ 15:301–305.

Sherman P, van Sebille E (2016) Modeling marine surface microplastic transport to assess optimal removal locations. Environ Res Lett 11:014006.

Siegfried M, Koelmans AA, Besseling E, Kroeze C (2017) Export of microplastics from land to sea. A modelling approach. Water Res 127:249–257.

Simeoni U, Corbau C (2009) A review of the Delta Po evolution (Italy) related to climatic changes and human impacts. Geomorphology 107:64–71.

Singh B, Sharma N (2008) Mechanistic implications of plastic degradation. Polym Degrad Stab 93:561–584.

Taylor AG, Allen PS, Bennett MA, Bradford KJ, Burris JS, Misra MK (1998) Seed enhancements. Seed Sci Res 8:245–256.

Tekman MB, Krumpen T, Bergmann M (2017) Marine litter on deep Arctic seafloor continues to increase and spreads to the North at the HAUSGARTEN observatory. Deep Res Part I Oceanogr Res Pap 120:88–99.

Topouzelis K, Papakonstantinou A, Garaba SP (2019) Detection of floating plastics from satellite and unmanned aerial systems (Plastic Litter Project 2018). Int J Appl Earth Obs Geoinf 79:175–183.

Turner A, Holmes L (2011) Occurrence, distribution and characteristics of beached plastic production pellets on the island of Malta (central Mediterranean). Mar Pollut Bull 62:377–381.

Turra A, Manzano AB, Dias RJS, Mahiques MM, Barbosa L, Balthazar-Silva D, Moreira FT (2014) Three-dimensional distribution of plastic pellets in sandy beaches: shifting paradigms. Sci Rep 4:4435.

Unice KM, Kreider ML, Panko JM (2013) Comparison of tire and road wear particle concentrations in sediment for watersheds in France, Japan, and the United States by quantitative pyrolysis GC/MS analysis. Environ Sci Technol 47:8138–8147.

Vianello A, Boldrin A, Guerriero P, Moschino V, Rella R, Sturaro A, Da Ros L (2013) Microplastic particles in sediments of Lagoon of Venice, Italy: First observations on occurrence, spatial patterns and identification. Estuar Coast Shelf Sci 130:54–61.

Vodacek A, Blough N V., DeGrandpre MD, Peltzer ET, Nelson RK (1997) Seasonal variation of CDOM and DOC in the Middle Atlantic Bight: Terrestrial inputs and photooxidation. Limnol Oceanogr 42:674–686.

Wagner M, Scherer C, Alvarez-Muñoz D, Brennholt N, Bourrain X, Buchinger S, Fries E, Grosbois C, Klasmeier J, Marti T, Rodriguez-Mozaz S, Urbatzka R, Vethaak AD, Winther-Nielsen M, Reifferscheid G (2014) Microplastics in freshwater ecosystems: what we know and what we need to know. Environ Sci Eur 26:12.

Waldschläger K, Schüttrumpf H (2019) Effects of Particle Properties on the Settling and Rise Velocities of Microplastics in Freshwater under Laboratory Conditions. Environ Sci Technol 53:1958–1966.

Wang W, Gao H, Jin S, Li R, Na G (2019) The ecotoxicological effects of microplastics on aquatic food web, from primary producer to human: A review. Ecotoxicol Environ Saf 173:110–117.

Waters CN, Syvitski JPM, Gałuszka A, Hancock GJ, Zalasiewicz J, Cearreta A, Grinevald J, Jeandel C, McNeill JR, Summerhayes C, Barnosky A (2015) Can nuclear weapons fallout mark the beginning of the Anthropocene Epoch? Bull At Sci 71:46–57.

Wiewel BV, Lamoree M (2016) Geotextile composition, application and ecotoxicology – A review. J Hazard Mater 317:640–655.

WORLDBANK (2015) World Development Indicators. https://data.worldbank.org/indicator, accessed on 2018-07-31 (2018).

World Economic Forum (2016) Ellen MacArthur Foundation and McKinsey & Company: The New Plastics Economy – Rethinking the future of plastics, http://www.ellenmacarthurfoundation.org/publications, accessed October 2019.

Zalasiewicz J, Waters CN, Ivar do Sul JA, Corcoran PL, Barnosky AD, Cearreta A, Edgeworth M, Gałuszka A, Jeandel C, Leinfelder R, McNeill JR, Steffen W, Summerhayes C, Wagreich M, Williams M, Wolfe AP, Yonan Y (2016) The geological cycle of plastics and their use as a stratigraphic indicator of the Anthropocene. Anthropocene 13:4–17.

Zalasiewicz J, Waters CN, Williams M, Barnosky AD, Cearreta A, Crutzen P, Ellis E, Ellis MA, Fairchild IJ, Grinevald J, Haff PK, Hajdas I, Leinfelder R, McNeill J, Odada EO, Poirier C, Richter D, Steffen W, Summerhayes C, Syvitski JPM, Vidas D, Wagreich M, Wing SL, Wolfe AP, An Z, Oreskes N (2015) When did the Anthropocene begin? A mid-twentieth century boundary level is stratigraphically optimal. Quat Int 383:196–203.

Zarfl C (2019) Promising techniques and open challenges for microplastic identification and quantification in environmental matrices. Anal Bioanal Chem 411:3743–3756.

Zhang S, Yang X, Gertsen H, Peters P, Salánki T, Geissen V (2018) A simple method for the extraction and identification of light density microplastics from soil. Sci Total Environ 616–617:1056–1065.

Zylstra ER (2013) Accumulation of wind-dispersed trash in desert environments. J Arid Environ 89:13–15.

Appendix

Microplastic in aquatic systems – Monitoring Methods and Biological Consequences

As science communication is an integral part of research, I presented preliminary results during my PhD at both national and international conferences. Together with two fellow researchers, we organized the Session "Microplastics in aquatic habitats – environmental concentrations and consequences" at the YOUMARES 8 conference, held in Kiel in 2017. One reason for the still existing knowledge gaps concerning abundances, sources, sinks, and transportation pathways, is the lack of cost- and labor-efficient standardized operational procedures for MP identification and quantification. To close these gaps and to generate comparable data in the future, we invited young scientists to present innovative methodologies along with studies assessing the concentration of MPs in the environment or their impact on aquatic life. An additional outcome was a book published in Springer of the conference proceedings. Here, we summarized the last three years of research on MP sample extraction, preparation, and analysis of MPs in the environment, providing an overview of the potential effects of MP exposure on biota.

Microplastics in Aquatic Systems – Monitoring Methods and Biological Consequences

Thea Hamm, Claudia Lorenz, and Sarah Piehl

Abstract

Microplastic research started at the turn of the millennium and is of growing interest, as microplastics have the potential to affect a whole range of organisms, from the base of the food web to top predators, including humans. To date, most studies are initial assessments of microplastic abundances for a certain area, thereby generally distinguishing three different sampling matrices: water, sediment and biota samples. Those descriptive studies are important to get a first impression of the extent of the problem, but for a proper risk assessment of ecosystems and their inhabitants, analytical studies of microplastic fluxes, sources, sinks, and transportation pathways are of utmost importance. Moreover, to gain insight into the effects microplastics might have on biota, it is crucial to identify realistic environmental concentrations of microplastics. Thus, profound knowledge about the effects of microplastics on biota is still scarce. Effects can vary regarding habitat, functional group of the organism, and polymer type for example, making it difficult to find quick answers to the many open questions. In addition, microplastic research is accompanied by many methodological challenges that need to be overcome first to assess the impact of microplastics on aquatic systems. Thereby, a development of standardized operational protocols (SOPs) is a pre-requisite for comparability among studies. Since SOPs are still lacking and new methods are developed or optimized very frequently, the aim of this chapter is to point out the most crucial challenges in microplastic research and to gather the most recent promising methods used to quantify environmental concentrations of microplastics and effect studies.

T. Hamm
GEOMAR Helmholtz Center for Ocean Research, Kiel, Germany
e-mail: thamm@geomar.de

C. Lorenz (✉)
Alfred Wegener Institute (AWI), Helmholtz Centre for Polar and Marine Research, Biologische Anstalt Helgoland, Helgoland, Germany
e-mail: claudia.lorenz@awi.de

S. Piehl
Department of Animal Ecology I and BayCEER, University of Bayreuth, Bayreuth, Germany
e-mail: sarah.piehl@uni-bayreuth.de

Introduction

Literature on microplastic (MP) abundance in aquatic environments and observed effects on biota has exponentially increased over the last 7 years (Connors et al. 2017). Within the current literature, MP sampling is imbalanced and studies are most often conducted on sandy beaches and the sea surface, followed by bottom sediment samples and water column samples (Duis and Coors 2016; Bergmann et al. 2017). Individual studies examining MP abundance, i.e., deep sea sediments (Van Cauwenberghe et al. 2013b; Woodall et al. 2014), sea ice (Obbard et al. 2014) or marine snow (Zhao et al. 2017) exist. Thereby, attempts to compare data taken from similar sampling matrices have been made in almost every study (Filella 2015), whereas for most studies this is often hampered by the various sampling methods applied (Hidalgo-Ruz et al. 2012; Filella 2015; Löder and Gerdts 2015; Costa and Duarte 2017). Hidalgo-Ruz et al. (2012) was the first article that showed the huge variety of different methods used for MP data collection and suggested the need for standardized operational protocols (SOPs). In the "Guidelines for Monitoring of marine litter" published by Hanke et al. (2013) the authors suggested methods based on the most often used techniques but also stressed that further standardization is needed. The NOAA made initial attempts of standardization in laboratory methods (Masura et al. 2015). Moreover, Löder and Gerdts (2015), as well as more recently Costa and Duarte (2017), took up the issue and critically assessed the different methods used for MP analysis. However, different environments can only be compared

S. Jungblut et al. (eds.), *YOUMARES 8 – Oceans Across Boundaries: Learning from each other*,
https://doi.org/10.1007/978-3-319-93284-2_13

to a certain extent, as the different sample matrices require different sampling methods. Moreover, as replication of samples is limited within a project, the high spatial and temporal variability of MPs in the various environments poses another major challenge in MP research (Goldstein et al. 2013; Moreira et al. 2016; Imhof et al. 2017). Whereas some recommendations for spatial replication have been made, no general consensus exists about temporal replication (Hanke et al. 2013). As a next step, the impact of the determined environmental concentrations of MP on biota is interesting. Parallel to monitoring studies, the toxicological implications for biota have been addressed in many studies. So far, we know that MPs are ingested by a wide range of organisms from the base of the food web up to top predators. As the environmental concentrations have not yet been sufficiently analyzed, exposure to MPs in laboratory studies are applying high concentrations to get first insights into possible effects following ingestion. This chapter aims to summarize the main results of the latest 3 years of research on sampling and monitoring methods as well as to give an overview about observed effects of MP exposure on biota.

Sampling Design

Previous research already addressed the problem of an appropriate sampling design (Browne et al. 2015; Löder and Gerdts 2015; Costa and Duarte 2017). A detailed review on the topic is given by Underwood et al. (2017). Over the last years, some studies focused on improving sampling design (Chae et al. 2015; Kang et al. 2015; Barrows et al. 2017) and aimed to investigate spatial and temporal patterns of MPs (Goldstein et al. 2013; Heo et al. 2013; Besley et al. 2017; Fisner et al. 2017; Imhof et al. 2017). Moreover, a few recommendations and protocols for sampling exist (Hanke et al. 2013; GESAMP 2016; Kovač Viršek et al. 2016). Potential factors which need to be considered when sampling beach sediments are summarized in Fig. 1. Some of the main issues are discussed in the following for both, water and sediment samples.

In each study, scientists should first determine the appropriate study area suitable for their research question. Thereby, factors such as, for example, proximity to potential sources (i.e., cities, harbors, industry), ocean currents and sampled sediment type need to be considered, as they can influence composition of MPs as well as the abundances (Hanvey et al. 2017). As a next step, a sampling design needs to be chosen, which suits the study question and is representative of the study area. Although most studies are initial assessments of MP concentrations, most often potential accumulation sites have been sampled (e.g., high tide line on beaches or ocean surface) (Filella 2015; Bergmann et al. 2017; Hanvey et al. 2017). Therefore, results cannot be extrapolated to the whole study area, as this kind of sampling is designed to find MP contamination. If the objective of the study is to assess the contamination level of the whole area, the sampling design could be improved by expanding the sampling to spots, which are not expected to have high amounts of MPs. Thus, random

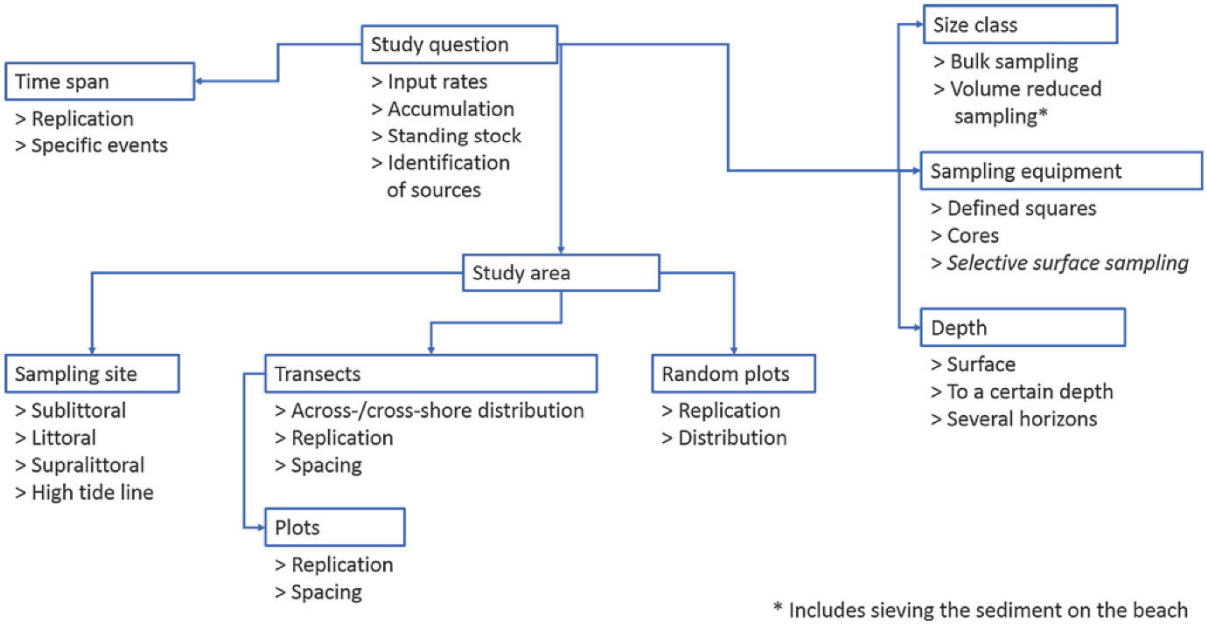

Fig. 1 Overview of factors, which need to be considered when planning a microplastics sampling campaign, exemplary for beach sediment samples

sampling, e.g., of a section of a beach, including the whole vertical and horizontal dimension, could be an option, although not yet conducted for MPs. In any case, care should be taken when formulating research questions, as this will set the framework for considerations regarding the sampling design.

Spatial and Temporal Replication

To get a representative sample, care needs to be taken with respect to appropriate replication as well as the amount of sample, which will be taken. If study areas of various sizes are compared, it needs to be considered, whether the number of replicates is kept the same or whether they are adjusted to the area (balanced vs. unbalanced sampling design). For beach sediment, Kim et al. (2015) adjusted sampling effort to beach size, whereas the majority of studies kept replicate numbers the same. In the current literature, replicate samples for one beach can range from one to 88 (Besley et al. 2017), whereas recommendations suggest a replication of at least five (Hanke et al. 2013). For beach sediments, Dekiff et al. (2014) found no significant variability in MP abundance within a 100 m transect, taking six replicate samples. Low spatial variability on a small scale (within tens of m) was further found in a recent study from Fisner et al. (2017) on plastic pellets (~ 1–6 mm; (Hidalgo-Ruz et al. 2012), whereas this study further found a high spatial variability on a large scale (within km). Contrary, Besley et al. (2017), including smaller MPs (300–5000 µm), found a high spatial variability among ten samples on a transect of 100 m. Confidence intervals around the mean in this study decreased rapidly after a replication of five, and 11 replicates would be needed to reach a 0.5 standard deviation at a confidence level of 90% (Besley et al. 2017). Those results are supported by a further study concentrating on large MPs (1–5 mm) on a 100 m transect on a tropical beach (six replicates; (Imhof et al. 2017). For surface water samples there is one study investigating spatial variability within the eastern North Pacific, off California (~ 20°–40°N, 120°–155°W; (Goldstein et al. 2013). They found that MP concentrations were highly variable over relatively small scales (tens of km) as well as for large scales (hundreds to thousands of km).

It is also stated that MP abundance varies over numerous temporal scales and detection of temporal trends are often hampered by the sampling design (Browne et al. 2015). Recent studies conducted on beaches found high daily variability due to tidal dynamics (Moreira et al. 2016; Imhof et al. 2017). One possibility to improve knowledge about temporal patterns could be through ice or sediment cores (Costa and Duarte 2017), by analyzing different layers separately. For the water surface, high inter-annual variability was found (Law et al. 2010; Doyle et al. 2011; Law et al. 2014), whereas Law et al. (2010), investigating a 22-year dataset of surface plankton net tows, found no strong temporal trends in MP concentrations within this data set. Nevertheless, the time span needed for a sampling campaign should be considered beforehand. For example for beach sediment sampling, sampling periods range over several hours to years (Browne et al. 2015).Whereas for some study questions, sampling over a certain period of time may not be a problem, for others it could lead to biased results. This might, for instance, apply to the sampling of various river mouths at a delta over several days. Strongly changing precipitation between sampling days could hamper comparability, as MP runoff could be enhanced during days of heavy rainfall, similar to what was hypothesized in a recent study comparing MP load of waste water treatment plants effluents on two different dates with differing participation events (Primpke et al. 2017a).

Sampling Depth

For both, sediments and water column, the optimal sampling depth remains another open question. Sediment sampling is recommended to a depth of at least 5 cm (Hanke et al. 2013; Besley et al. 2017), whereas studies report that a potential proportion can be lost if deeper sediment layers are not sampled (Carson et al. 2011; Claessens et al. 2011). Thus, it has already been stated that samples should be taken at a depth to 1 m, to get a more precise picture of MP abundances (Turra et al. 2014; Fisner et al. 2017). For the water column, only few studies exist where different depths were concurrently sampled (Lattin et al. 2004; Reisser et al. 2015). In one study, no significant differences were found between the sea surface, the water column (5 m depth), and above the bottom (Lattin et al. 2004), whereas the other found that MP concentrations decreased exponentially, with highest amounts within the first 0.5 m of the water column (Reisser et al. (2015). This is confirmed by Goldstein et al. (2013), detecting the highest concentrations of MPs during low wind conditions, when minimal mixing occurs between shallow and deeper water layers. The optimal sampling depth will finally be a compromise between increasing sampling surface and sampling depth and thus will also be determined by the research question.

Reporting of Data

Though different methods are necessary depending on the research question, researchers should aim for standardization, the most important one being size classes and reporting units. Regarding size classes the upper limit for MPs is 5 mm, whereas the lower limit will be defined by the sampling device, as well as the analytical method. Initial

studies investigating size distribution found generally increasing abundances with decreasing size classes (Imhof et al. 2016). Even though the applied methodology will define the lower size limit, the post-sampling procedures will allow for classification into different size classes. Thereby, Hanke et al. (2013) recommended to allocate MP particles into size bins of 100 µm. Although this recommendation would provide high resolution datasets, in practice this is almost not feasible, as the preparation of microplastic samples is already very time consuming and, for instance, additional sieving steps would further increase analysis time. Further, depending on the research question different size categories are of importance. If, for example, pictures of the microplastic particles are taken during analysis, it is possible to obtain data on the size at a later time point in case the data would be requested for comparative analysis.

Standardization of reporting units is a further necessity to increase comparability among data sets. So far, different sampling strategies have led to various reporting units (e.g., m^2, m^3, ml, l, g, kg) (Hidalgo-Ruz et al. 2012; Löder and Gerdts 2015; Costa and Duarte 2017). For MPs in the environment (excluding biota samples) either bulk or volume reduced samples are taken. Thus, a volume measurement can always be obtained and should be the minimum information reported. Additional reporting of sampling depth as well as weight measurements for sediment samples will further increase data quality.

Finally, reporting of meta data like prevailing wind direction, sea state, beach morphology, rainfall, and so on would improve the interpretation of the data collected (Barrows et al. 2017). In the current literature, missing information range from unreported size ranges, replication, detected numbers of particles to sampling locations (Filella 2015; Besley et al. 2017). Comprehensive reporting of the applied methods is a crucial part and not only a requirement for reproducibility, but further gives the reader the ability to judge about the representativeness of the study, as well as the conclusions drawn from the results.

Sampling Equipment

Further considerations should be made on the sampling equipment, as this will define the size range of MPs in the study, as well as reporting units. For beach sediments, sampling equipment is well established (Hidalgo-Ruz et al. 2012; Hanvey et al. 2017), it only remains important to consider, whether to collect a bulk or a volume reduced sample. For the latter, a lower size limit is defined. For bottom sediments corers, Van Veen or Ekman grabs can be used, however, grabs disturb the surface layer of the sediment and corers do not only take the sediment but also the water layer above the sediment (Löder and Gerdts 2015).

For water samples, nets of various types have been used (Table 1 gives an overview of the used equipment found in the current literature). Most commonly, manta nets are the device of choice (Costa and Duarte 2017), where the reduced sample volume limits the lowest size class of investigated MPs mostly to 300–350 µm (Filella 2015). Thus, some researchers used bottles to take bulk samples of the water surface (Dubaish and Liebezeit 2013; Barrows et al. 2017), which, however, results in small sample volumes. Nevertheless, sampling lower size ranges, Barrows et al. (2017) found MP concentrations were several orders of magnitude higher in bottle samples than manta samples. To obtain larger sample volumes, others took several bottles or buckets of surface water and concentrated the material on filters with smaller mesh sizes on board (hand-nets; Chae et al. 2015; Kang et al. 2015). Moreover, contamination issues through high air exposure times during a manta trawl, as well as filtering samples on board, motivated researchers to further develop pumping systems (Desforges et al. 2014; Lusher et al. 2014; Enders et al. 2015). One of the first studies comparing different methodologies for the same size class (300–5000 µm) was conducted by Setälä et al. (2016) comparing their custom-made pump to manta trawls. Preliminary results from the pump (collecting surface water in a depth of 0–0.5 m) did not significantly differ from the results obtained by the manta net. Another interesting solution to decrease sampling effort has been published by Edson and Patterson (2015). They designed an automated sampling device (MantaRay), which automatically pumps sea surface water at a depth of 30 cm, while drifting through the water. Thereby, particles are concentrated on a filter and 28 successive samples can be taken. For the prototype, 500 µm stainless steel sieves were used. Such an instrument can decrease sampling effort and airborne contamination, which is often a challenge when conducting trawls. One drawback could be the autonomous operation of the MantaRay, which limits the control over the area sampled. Moreover, an optical sensor is implemented to ensure that only water containing particulate matter is filtered. Thereby, especially small MP particles could be overlooked so the influence on the obtained results must be further evaluated.

Independent of the applied method, decreasing mesh sizes will increase the content of organic and inorganic material, which could lead to smaller sample sizes as meshes will become clogged faster, but also to increased sample preparation time in the laboratory. In any case, negative controls should be run, as most of the used methods may contain polymer materials which are a further source for contamination.

Table 1 Comparison of various methods used to collect water samples for the analysis of microplastics (MP) in different compartments. Pro and contra are always relative with regard to the sampling devices used for the specific compartment

Sampled compartment	Most common used equipment	General description	Pro	Contra	References
Sea surface microlayer (SML)	Rotating drum sampler	Drum is towed over the water surface and SML is sampled under capillary force by the rotating drum and collected in glass containers	reduced contamination issues large sample volume	only a small part of SML is sampled (50-60 µm)* water adhering to the drum may dilute the sample device materials need to be considered	Ng and Obbard (2006)
	Screen sampler	Water surface is gently touched with a metal sieve with specific pore size; MP particles and SML water is trapped within the metal sieve mesh by surface tension	easy handling and transport larger part of SML is covered compared to rotating drum sampler	only a part of SML is sampled (150-400 µm)* variation can be caused by different operators contamination through higher air exposure times	Song et al. (2014)
Water surface	Manta or plankton/ neuston nets with flowmeter	Net is towed over the water surface to a certain depth (depending on mouth opening) and volume recorded with a flowmeter	large sample sizes exact for the water surface layer integrates a high area of sea surface	investigated size class limited (mesh size often ~300 µm) contamination through higher air exposure times and material of equipment plankton/neuston nets: opening obstructed by ropes for towing	Barrows et al. (2017) and Costa and Duarte (2017)
	Bulk sampling with bottles	Water samples are taken directly from water surface and bottles closed below surface to reduce contamination	whole size range of MPs can be sampled reduced contamination issues	small sample sizes may result in a high variability varying sampling depth	Dubaish and Liebezeit (2013) and Barrows et al. (2017)
	Bulk sampling with hand-net	Water sample is taken with a container and poured over stainless steel meshes on board	whole size range of MPs can be sampled pre-separation of size classes possible large sample sizes can be obtained	varying sampling depth contamination through higher air exposure times device materials need to be considered	Chae et al. (2015) and Kang et al. (2015)
	Pumping systems	Seawater is either collected via the intake of a ship, a hose or a submersible pump	whole size range of MPs can be sampledpre-separation of size classes possible large sample sizes can be obtained reduced contamination issues	varying sampling depth smaller mesh sizes lead to faster blocking of the filters device materials need to be considered	Desforges et al. (2014), Enders et al. (2015), Lusher et al. (2014) and Setälä et al. (2016)
Water column	Bongo nets	Paired zooplankton nets joined by a central axle	large sample sizes integrates a high area of water column unobstructed by towing ropes	investigated size class is limited through mesh size contamination through material of equipment	Lattin et al. (2004)
	Continuous plankton recorder (CPR)	A box for filtering particles at a depth between 5–10 m; material is concentrated on continuously moving bands of filter silk	low operation effort archived data records available	smaller MP particles, which cannot be hand-picked can probably not be recovered from the silk material	Reid et al. (2003) and Thompson et al. (2004)
	Epibenthic sled	A sled which is towed over the sea bottom with a net placed at a certain distance (20 cm) over the bottom such that no resuspended sediment is collected	large sample volumesintegrates a high area of water column	high operation effort obstacles on the ground could block the net or make the sample useless due to resuspended material investigated size class is limited through mesh size contamination through material of equipment	Lattin et al. (2004)

Sample Preparation

The environmental samples taken for MP analysis usually contain a high amount of biogenic material (biota and detritus) and inorganic material (clay, silicates). Therefore, extraction of MPs from the environmental matrix is crucial to facilitate the subsequent identification of MPs. Sometimes, sieving is used to remove larger particles (> 5 mm) from the samples as well as to divide them into distinct size fractions that might be further analyzed differently (Löder and Gerdts 2015). Especially for bulk sediment samples, MPs have to be extracted from the inorganic sediment matrix first while for water and biota samples the removal of the biogenic matrix is put first.

Extraction Techniques

Removing inorganic material from environmental samples is based on the fact that most MPs possess a considerably lower density (0.90–1.55 g cm^{-3}; Table 2) than the inorganic components of sediments like quartz sand or other silicates (2.65 g cm^{-3}) (Hidalgo-Ruz et al. 2012). The most prominent extraction techniques are density separation or fluidization/elutriation. According to Hanvey et al. (2017) density separation is by far the most prevalent one and is defined by the liquid used, the mixing time, the time for settling and the limits of subsequent size fractionation (Hanvey et al. 2017). The most common salt solution for separation is sodium chloride (NaCl) with a density of 1.2 g/cm^3 (Thompson et al. 2004; Hidalgo-Ruz et al. 2012; Hanvey et al. 2017). Due to being inexpensive and non-hazardous, the use of NaCl is also recommended by Hanke et al. (2013), despite its relatively low density. By raising the density of the separation fluid, mainly by using other salt solutions, a better density gradient can be obtained (Filella 2015). These solutions include zinc chloride ($ZnCl_2$) with a density of 1.5–1.7 g cm^{-3} (Imhof et al. 2012; Imhof et al. 2013; Imhof et al. 2016; Mintenig et al. 2017), sodium iodide (NaI) with a density of 1.6 g cm^{-3} (Van Cauwenberghe et al. 2013a; Van Cauwenberghe et al. 2013b; Dekiff et al. 2014; Nuelle et al. 2014; Fischer and Scholz-Böttcher 2017), sodium polytungstate with a density of 1.4–1.5 g cm^{-3} (Corcoran et al. 2009; Corcoran 2015), zinc bromide ($ZnBr_2$) with a density of 1.71 g cm^{-3} (Quinn et al. 2017) and calcium chloride ($CaCl_2$) with a density of 1.30–1.46 g cm^{-3} (Stolte et al. 2015; Courtene-Jones et al. 2017). Samples are added to the separation fluid and either stirred or shaken for a defined time to separate MPs from the sediment matrix (Hanvey et al. 2017). These periods vary considerably between studies if indicated at all (Hidalgo-Ruz et al. 2012; Filella 2015; Hanvey et al. 2017). This is also true for settling times after mixing (Besley et al. 2017; Hanvey et al. 2017) which vary between several minutes (Nuelle et al. 2014; Corcoran 2015) and hours (Stolte et al. 2015; Imhof et al. 2016; Mintenig et al. 2017). Since the aim is to allow for all the sediment particles to sink and all MPs to rise through the whole fluid column according to their respective density, Besley et al. (2017) suggested a minimum settling time of 5–8 hours. Especially for small sample amounts, density separation can be done simply in a

Table 2 Density, heat deflection temperature (HDT), and chemical resistance of common plastic types (Osswald et al. 2006; Bürkle GmbH 2015; Qiu et al. 2016)

Plastic type	Density ρ	HDT	Chemical resistance									
			HCl		H_2SO_4	HNO_3		NaOH		KOH	H_2O_2	NaClO
	g cm^{-3}	°C	5% 2 M	35% 11 M	40%	5%	66%	4% 1 M	30% 10 M	10%	30%	12.5% Cl
Acrylonitrile butadiene styrene (ABS)	1.04–1.06	95–105	–	–	–	–	–	–	–	–	–	–
High-density polyethylene (HDPE)	0.94–0.96	~50	1/1	1/1	1/1	1/1	2/4	1/1	1/1	1/1	1/1	2/3
Low-density polyethylene (LDPE)	0.91–0.92	~35	1/1	1/1	1/1	1/1	3/4	1/1	1/1	1/1	1/2	2/3
Polyamide (PA)	1.02–1.14	55–120	4/4	4/4	4/4	4/4	4/4	1/–	1/–	1/–	4/4	4/4
Polybutylene terephthalate (PBT)	1.31	60	–	–	–	–	–	–	–	–	–	–
Polycarbonate (PC)	1.20	125–135	1/1	4/4	2/–	1/2	4/4	3/4	4/4	4/4	1/1	2/3
Polyethylene terephthalate (PET)	1.37	80	2	4	4	2	4	3	4/4	4/4	1/–	3
Polymethyl methacrylate (PMMA)	1.17–1.20	75–105	–	–	–	–	–	–	–	–	–	–
Polyoxymethylene (POM)	1.41–1.42	100–160	4/4	4/4	4/4	4/4	4/4	1/1	1/3	1/1	4/4	4/4
Polypropylene (PP)	0.90–0.91	55–70	1/1	1/2	1/1	1/1	4/4	1/1	1/1	1/1	1/3	2/3
Polystyrene (PS)	1.05	65–85	1/1	3/3	2/–	2/4	4/4	2/2	1/–	–	1/2	1/3
Polysulfone (PSU)	1.24	170–175	1/1	1/1	3/–	1/3	4/4	1/1	1/–	–	1/1	1/1
Polytetrafluoroethylene (PTFE)	2.15–2.20	50–60	1/1	1/1	1/1	1/1	1/1	1/1	1/1	1/1	1/1	1/1
Polyurethane (PUR)	1.05	–	–	–	–	–	–	–	–	–	–	–
Polyvinyl chloride (PVC)	1.16–1.55	65–75	1/1	2/3	1/3	1/2	3/4	1/1	1/3	–	1/1	1/3
Styrene acrylonitrile (SAN)	1.08	95–100	1/3	1/3	1/1	1/3	–	–	–	–	1/–	1/1

Chemical resistances are listed for temperatures of +20 °C (left digit and color code) and + 50 °C (right digit): – = no data available, 1/green = resistant, 2/yellow = practically resistant, 3/orange = partially resistant, 4/red = not resistant

beaker or flask where the supernatant is decanted or removed with a pipette or in a separatory funnel, where the inorganic material is removed via the bottom valve (Maes et al. 2017b; Mintenig et al. 2017; Zobkov and Esiukova 2017). Constructed devices like the Munich/MicroPlastic Sediment Separator (MPSS) by Imhof et al. (2012), designed for the extraction of MPs from large quantities of sediment (up to 6 kg), and the small-scale Sediment-Microplastic Isolation (SMI) unit by Coppock et al. (2017) usually achieve very good recovery rates (96%) even for small MPs (< 1 mm; (Imhof et al. 2012), when applied with $ZnCl_2$. According to Kedzierski et al. (2017), it is possible to extract 54% of the plastics produced in Europe with NaCl of 1.18 g cm^{-3} density while with a 1.8 g cm^{-3} solution (achievable with, e.g., NaI, polytungstate, $ZnCl_2$) the extraction of 93–98% is feasible. Therefore, achieved recovery rates are not only dependent on the device but mainly on the separation liquid used.

Another density based technique to separate MPs from sediment matrix is elutriation/fluidization, where water or air is pumped through the fluid column containing the sample and water or a salt solution (Claessens et al. 2013; Nuelle et al. 2014; Zhu 2015; Kedzierski et al. 2016). Recently, a non-density based extraction approach with canola oil has been developed by Crichton et al. (2017). The approach makes use of the oleophilic properties of MPs. So far it has only been tested with MPs larger than 500 µm, but showed high recovery rates of 96% (Crichton et al. 2017). When choosing one of the available methods, factors like sample volume or mass, time needed, costs, safety, toxicity, and extraction efficiency have to be considered.

For small amounts of sediment, approaches in flasks or funnels can be used or the novel developed SMI unit (Coppock et al. 2017; Maes et al. 2017b). If larger sediment volumes (1–6 L) are processed, elutriation systems or the MPSS would be a better choice (Imhof et al. 2012; Nuelle et al. 2014).

The time necessary for shaking should be adjusted to the sediment amount. The more sediment, the longer the mixing interval should be to assure that all MP particles are separated from the sediment particles. For settling, the span depends on the density gradient between MPs and liquid as well as the length of the fluidization column. Furthermore, the settling times have to be adjusted to the solutions used since particles rise and settle more slowly in more viscous solutions like $CaCl_2$ or $ZnCl_2$ (Crichton et al. 2017).

The most inexpensive approaches are simple setups with flasks and NaCl or oil. Zinc chloride is more expensive in relation to NaCl, especially when adjusted to higher densities but by far less expensive than NaI and polytungstate (Coppock et al. 2017). At best, an effective and cost efficient setup is used with a high density solution that can be refurbished and that allows for a proper mixing of the sediment as well as a proper settling time.

Concentrated NaCl solutions as well as canola oil do not pose any hazard to the environment. Other salt solutions are more hazardous to health and the environment in ascending order: NaI, $CaCl_2$, polytungstate, $ZnCl_2$. These solutions should therefore be recycled as far as possible due to financial and environmental reasons (Löder and Gerdts 2015). Kedzierski et al. (2017) showed that NaI can effectively be recycled without major density loss. Zinc chloride can be refurbished in large quantities quite easily via pressure filtration (Löder and Gerdts 2015). Miller et al. (2017) did an extensive comparison of different separation techniques on the basis of current literature and listed advantages and disadvantages. Based on this list, the authors recommended the use of $ZnBr_2$ (Miller et al. 2017). Nevertheless, $ZnBr_2$ has to date just been used by one study (Quinn et al. 2017) and $ZnCl_2$ is not included in the list although it is suitable for the same density range, less expensive ($ZnBr_2$: 165 € kg^{-1}, $ZnCl_2$: 92.50 € kg^{-1}, Merck Millipore, December 2017) and more widely used. Therefore, other authors have recommended the use of $ZnCl_2$ as well (Löder and Gerdts 2015; Ivleva et al. 2016; Primpke et al. 2017a).

Independent of the extraction method chosen the next step is to filter the residual fluid or the supernatant of the (density) separation containing MPs to remove the respective salt solution and to concentrate the sample to certain size fractions.

Sample Purification

Before the samples can be analyzed the biogenic matter has to be removed. Sediment samples after density separation contain usually a relatively low amount of biogenic matter (benthic diatoms, copepods, polychaetes, bivalves, etc.). In contrast, samples from the sea surface, mostly taken with plankton nets, are normally very rich in biogenic matter (phyto- and zooplankton) as well as biota samples. The main digesting agents used for the removal of biogenic matter are acids like hydrochloric acid (HCl), nitric acid (HNO_3) and sulphuric acid (H_2SO_4) (Claessens et al. 2013; De Witte et al. 2014; Klein et al. 2015), bases like sodium hydroxide (NaOH) and potassium hydroxide (KOH) (Foekema et al. 2013; Dehaut et al. 2016; Karami et al. 2017; Wagner et al. 2017), oxidative agents like sodium hypochlorite (NaClO) and hydrogen peroxide (H_2O_2) (Nuelle et al. 2014; Avio et al. 2015; Collard et al. 2015; Tagg et al. 2017) and enzymes (Cole et al. 2014; Löder and Gerdts 2015; Courtene-Jones et al. 2017; Fischer and Scholz-Böttcher 2017; Mintenig et al. 2017). Several studies showed the destructive effects, i.e., discoloration, embrittlement or a loss in surface area, of acids (e.g., HNO_3) and bases (e.g., NaOH) on MPs especially at high temperatures (Cole et al. 2014; Nuelle et al. 2014; Bürkle GmbH 2015; Karami et al. 2017). Heat deflection

temperatures of some plastics are around 50–80 °C or even below for PE (Osswald et al. 2006; Qiu et al. 2016). Therefore, it is generally recommended to use temperatures of less than 50 °C.

For H_2O_2, negative effects on synthetic polymers have been shown by Nuelle et al. (2014), but just after a week-long treatment. The needed incubation time and effectiveness can be further improved by a new approach from Tagg et al. (2017) who used Fenton's reagent, a mixture of iron sulphate ($FeSO_4$) and H_2O_2. The digestion with enzymes is regarded to be non-destructive to MPs, targeting specifically proteins, polysaccharides and lipids. Cole et al. (2014) presented an approach with Proteinase-K and an up to 97.7% effective removal of biogenic matter. Courtene-Jones et al. (2017) digested mussel tissue with trypsin with an efficiency of 88%. The biggest disadvantage of these treatments is the high cost of these specific enzymes. The succession of several technical enzymes in combination with sodium dodecyl sulphate (SDS) and an oxidative agent (i.e., H_2O_2) seems to be an effective, inexpensive, and non-hazardous alternative (Löder and Gerdts 2015; Löder et al. 2015; Fischer and Scholz-Böttcher 2017; Mintenig et al. 2017; Primpke et al. 2017b).

When choosing the most suitable digestion method several factors have to be considered: time, cost, destructiveness, and effectiveness.

Purification can take several minutes (Tagg et al. 2017), several hours (Cole et al. 2014; Dehaut et al. 2016) or several days (Foekema et al. 2013; Löder and Gerdts 2015; Karami et al. 2017). Generally, longer incubation times improve the effectiveness but might also negatively impact MPs. For example, Nuelle et al. (2014) showed a negative effect of a week-long treatment with H_2O_2 while no significant effect has been shown for shorter application periods (Nuelle et al. 2014; Tagg et al. 2017). Application time should be reduced to the maximum time before causing negative effects and to the minimum time necessary to cause the highest possible effectiveness.

Specific enzymes like Proteinase-K and trypsin are very expensive. Technical enzymes, on the other hand, can be used as an inexpensive alternative (Löder and Gerdts 2015; Löder et al. 2017; Mintenig et al. 2017).

It is noticeable that methods using acids are more destructive, especially at higher temperatures, than other methods. Only at low concentrations and low temperatures (5%, 25 °C) HCl and HNO_3 are less destructive than non-acid based methods, although they are also less effective at low temperatures and concentrations. For the alkaline treatments, KOH is more effective than NaOH with the same level of destructiveness. When comparing two oxidative treatments most frequently used, H_2O_2 is more effective than NaClO and less destructive.

Next to the potential destructiveness, the effectiveness of the treatment has to be taken into account when considering the most suitable digesting agent (Fig. 2). For most treatments, an increase in temperature provokes an increase in effectiveness but often also an increase in destructiveness. Some treatments might be very effective but also relatively destructive to MPs like HNO_3 (69%) and HCl (37%) and other treatments are less destructive but also less effective like NaOH and NaClO (Karami et al. 2017). Enzymatic treatments represent the best choice in terms of being non-destructive to MPs. Several working groups have shown the high effectiveness of enzymatic digestion with different enzymes (Cole et al. 2014; Courtene-Jones et al. 2017; Karlsson et al. 2017; Löder et al. 2017; Mintenig et al. 2017).

Microplastics Identification

Once the environmental samples have been purified and concentrated by removing the biogenic and inorganic matter the MPs within the samples have to be identified. This identification is most easily performed by visual inspection either with the naked eye or with the use of a (stereo) microscope (Shim et al. 2017). The sorting is based on several criteria defined in a pilot-study by Norén (2007), which include having no visible cell-structure, homogenous coloration, and equal thickness for fibers (Enders et al. 2015). Nonetheless, Hidalgo-Ruz et al. (2012) stated that up to 70% of particles that potentially resembled MPs based on merely visual inspection could not be confirmed to be of synthetic origin. These limits of visual identification, even by experienced operators, have been shown by several studies (Eriksen et al. 2013; Dekiff et al. 2014; Lenz et al. 2015; Löder and Gerdts 2015; Song et al. 2015). Despite this high proneness to errors, many studies still rely on the visual identification of MPs. An overestimation can be avoided when a chemical characterization is subsequently performed to confirm plastics. If the chemical characterization is based on a prior visual sorting of potential MPs, an underestimation, especially of very small particles is still very likely (Song et al. 2015). Stains can be used to facilitate visual analysis, like Nile Red (Desforges et al. 2014; Shim et al. 2016; Erni-Cassola et al. 2017; Maes et al. 2017a) or rose bengal (Ivleva et al. 2016). Maes et al. (2017a) presented an approach using Nile Red that enabled for a reliable identification of MPs (96.6% recovery for MPs of a 100–500 µm size range). Nevertheless, this approach does not allow for a differentiation of distinct polymer types (Maes et al. 2017a), and may only be suitable for identification of MPs used in organism studies, where the specific polymer type is known. For environmental samples, chemical characterization is needed and can be achieved by spectroscopic analyses like Fourier transform infrared (FTIR), Raman and energy dispersive X-ray (EDX) spectroscopy or thermal analysis (Ivleva et al. 2016; Shim et al. 2017).

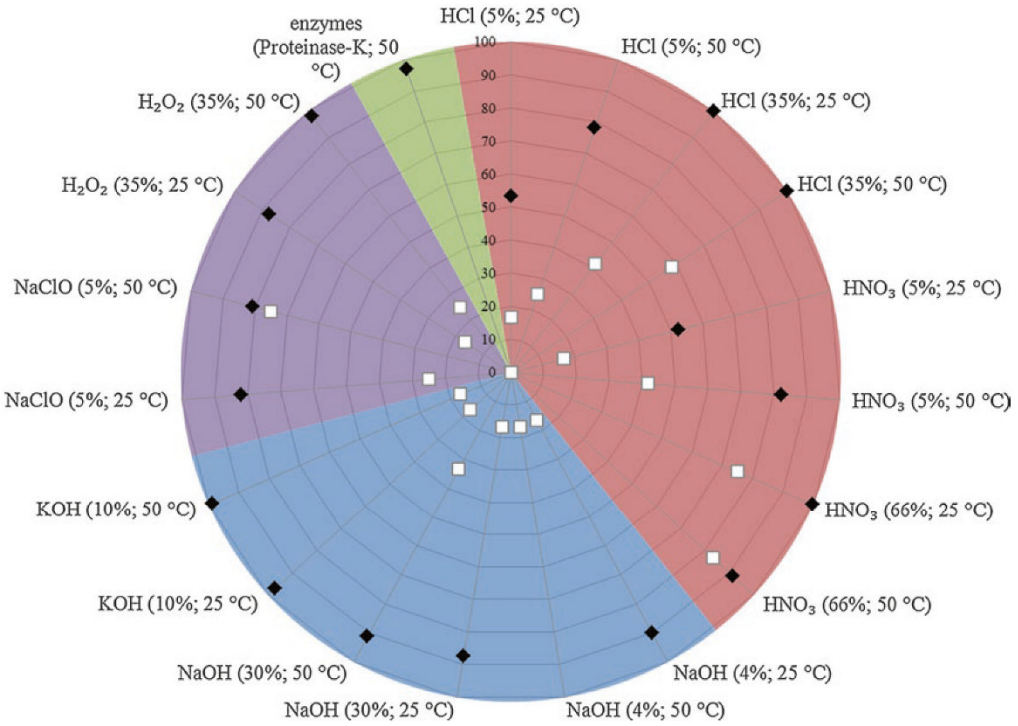

Fig. 2 Effectiveness of different digestion treatments (black symbols, in %) and maximum percentage of microplastics negatively affected by the treatments (white symbols, based on 12 polymers). Different colored sectors highlight the different treatments = red: acid, blue = alkaline, violet = oxidative, green = enzymatic (based on Cole et al. 2014; Bürkle GmbH 2015; Karami et al. 2017)

When combining EDX with scanning electron microscopy (SEM), this technique can provide information on the elemental composition of a particle and therefore distinguish plastics from inorganic materials (Eriksen et al. 2013; Vianello et al. 2013; Ivleva et al. 2016; Wagner et al. 2017; Wang et al. 2017). The identification of different plastic types is limited and therefore this method is recommended to be used for surface characterization and visualization additional to previous FTIR analysis (Vianello et al. 2013; Shim et al. 2017). FTIR analysis is a vibrational spectroscopic technique based on infrared radiation that excites molecular bonds resulting in vibrations that can be detected and transferred into characteristic absorbance spectra. These spectra can further be compared to a database of reference spectra allowing for the reliable identification of different polymer types. FTIR spectroscopy can be used in different modes, namely transmission (Löder et al. 2015; Käppler et al. 2016; Mintenig et al. 2017; Primpke et al. 2017b), reflection (Harrison et al. 2012; Vianello et al. 2013; Tagg et al. 2015) and attenuated total-reflectance (ATR) (Song et al. 2015; Käppler et al. 2016; Crichton et al. 2017; Imhof et al. 2017; Wagner et al. 2017). To measure very small particles FTIR spectroscopy can be coupled to microscopy (μFTIR) and be used in all three modes as well (Ivleva et al. 2016; Shim et al. 2017). All these modes have several advantages and limitations. While the transmission mode provides high quality spectra it is restricted to a certain thickness of material to allow infrared radiation to pass through the sample without being fully absorbed (Löder and Gerdts 2015; Ivleva et al. 2016). Reflectance mode on the other hand provides spectra of thick and opaque particles but does depend on the surface properties since uneven surfaces can cause scattering effects which cause refractive errors (Löder and Gerdts 2015; Shim et al. 2017). High quality spectra can be achieved by μATR-FTIR with the disadvantage of potentially damaging particles since a crystal has to be pressed on the sample (Ivleva et al. 2016; Shim et al. 2017). Another vibrational spectroscopy, that is complementary to FTIR, is Raman spectroscopy (Käppler et al. 2016). Monochromatic light, usually provided by a laser, irradiates the sample and vibrations are resulting in a Raman shift, which can be presented as substance characteristic spectra (Ivleva et al. 2016; Shim et al. 2017). Raman micro-spectrometry has successfully been used to identify MPs in environmental samples (Enders et al. 2015; Fischer et al. 2015; Frère et al. 2016; Imhof et al. 2016; Wagner et al. 2017). For thermal analysis, pyrolysis-gas chromatography-mass spectrometry (Pyr-GC-MS) and thermoextraction and desorption (TED) coupled with GC-MS are the most prevalent and promising ones (Fries et al. 2013; Dümichen et al. 2015; Fischer and Scholz-Böttcher 2017).

Both methods provide the chemical composition based on heating the sample and analyzing the decomposition products (Ivleva et al. 2016). Pyrograms or ion chromatograms are obtained that can be compared to references, equivalent to spectra of spectroscopic techniques (Löder and Gerdts 2015; Dümichen et al. 2017; Shim et al. 2017).

Most studies use these methods to analyze preselected particles. Recently Fischer and Scholz-Böttcher (2017) presented also for Pyr-GC-MS an approach independent of a prior visual sorting by analysing whole filters on which previously purified samples had been concentrated. That also TED-GC-MS can be used to analyze subsamples of environmental samples without pre-selection to identify MPs has been shown by Dümichen et al. (2017). An advantage of TED-GC-MS presented by Dümichen et al. (2017) is that a relatively high sample amount of up to 100 mg can be processed, which, depending on the condition of the environmental sample, obviates the need for sample purification.

Chemical imaging approaches developed for µFTIR and Raman spectroscopy eliminate the need for a visual preselection. Therefore, the purified samples are concentrated on filters that are directly scanned. The filter chosen for the analysis has to be compatible to the method by not interfering with the sample analysis (Käppler et al. 2015; Löder et al. 2015). For µFTIR the use of Focal plane array (FPA) detectors have substantially improved the time needed for the analysis of whole filter areas (Löder et al. 2015; Tagg et al. 2015; Käppler et al. 2016; Mintenig et al. 2017; Primpke et al. 2017b). Although the imaging using FPA is independent of a prior visual selection of potential MPs, the approach presented by Löder et al. (2015) still involves an operator-based selection of MPs based on their spectral signature. Therefore, advances are automated approaches independent of human bias like it has been recently presented by Primpke et al. (2017b).

Shim et al. (2017) recently reviewed the advantages and disadvantages of currently used methods for identification of MPs. Furthermore, Elert et al. (2017) added to the comparison a classification of the different techniques in terms of restrictions, requirements and the analytical information received.

The major advantage of thermal analysis is the simultaneous analysis of polymer and containing additives, while the major disadvantage is the destruction of the sample by combustion. While thermal analyses provide mass-related results only, spectroscopic analyses are normally non-destructive and provide particle-related results (Shim et al. 2017). The lower size limit for µFTIR is at 10 µm due to the diffraction limit (Löder and Gerdts 2015; Shim et al. 2017), whereas for Raman spectroscopy particles down to 1 µm size can be analyzed (Ivleva et al. 2016). Residual water hampers FTIR analysis while for Raman spectroscopy fluorescence of residues of the environmental matrix is a problem as well as the interference from pigments (Imhof et al. 2016; Käppler et al. 2016; Shim et al. 2017). Käppler et al. (2016) showed that Raman imaging provides a better identification of MPs < 20 µm when compared to using FPA-µFTIR in transmission mode but with the major drawback for Raman imaging that the measurement time was more than 100-times higher than the µFTIR analysis. Currently, µFTIR imaging of large filter areas is considerably faster than Raman imaging, even when reducing the resolution for Raman imaging, resulting in a comparable quality to FTIR imaging (Käppler et al. 2016).

All above mentioned methods share the commonality that to avoid misinterpretation of spectra and programs alike as well as identifying dyed MPs, efficient sample purification is of utmost importance (Löder and Gerdts 2015; Crichton et al. 2017; Fischer and Scholz-Böttcher 2017; Maes et al. 2017b). When choosing the most appropriate method: time demand, size range, and sample preparation have to be considered. Furthermore, thermal analysis should be used when a fast assessment of mass-related data is required, while spectroscopic analysis provides particle-related data but might take considerably longer. A holistic approach would involve FTIR-analysis of MPs down to 10 µm, Raman-analysis for MPs below 10 µm and a subsequent thermal analysis.

Biological Effects of Microplastics on Biota

Although research on MPs in aquatic systems regarding monitoring and abundance in animals has dramatically increased in the last years, profound knowledge about the effects of MPs on biota is still scarce (Ribeiro et al. 2017). Here, we give a short overview about investigated consequences of MP exposure, methods, and their effects on organisms.

Images circulating the media of sea turtles, dolphins or seals entangled in plastic bags and other macroplastics are well known, but what about the plastic we do not see? Microplastics can pose a danger to organisms, when they are ingested (Avio et al. 2017). Reasons for ingestion in the first place are either MPs being mistaken for food or prey due to similarities in size, shape or color (Wright et al. 2013) or because the organism is not selective with food particles, which is, for example, the case for most filter and deposit feeders (Van Cauwenberghe et al. 2015). Although filter feeders often possess some mechanisms to avoid particles that are too big or inedible, MPs are very similar to actually nutritious food and thus sorting mechanisms might not work (Ward and Shumway 2004).

The Risk of Exposure to Microplastics

When trying to assess the danger of MPs in the marine environment, various things have to be taken into consideration. The risk to be exposed to MPs varies a lot with compartments, usually divided into water surface, water column and sediments. Sediments are thought of as being the most affected compartment, because they function as a sink for MPs (Hidalgo-Ruz et al. 2012; Duis and Coors 2016). All compartments considerably vary spatially and temporally and distribution of MPs is, therefore, difficult to assess (Chubarenko et al. 2016).

Risk of exposure is different for the different types of polymers (buoyancy, fragmentation rate) and the habitat of the organism (surface layer, water column, sediment) (Andrady 2017). Polymers with low density tend to stay longer in the surface layer, possibly aggregating with phytoplankton in the euphotic zone (Long et al. 2017). They can also be overgrown by microbes and other fouling organisms and sink down in the water column together with MPs of neutral buoyancy. Higher density polymers such as polyvinyl chloride sink quickly and are readily available for benthic filter feeders or deposit feeders such as bivalves and polychaetes (Avio et al. 2017).

The hazard that MP poses for organisms also varies depending on the functional group such as the trophic level of the organism. So far, mainly low trophic levels such as filter feeders, deposit feeders and planktivorous fish have been found to be contaminated with MPs, but recently MP particles have also been detected in predatory pelagic fish such as tuna (Romeo et al. 2015) and even filter feeding mammals such as humpback whales (Besseling et al. 2015).

Studies have accumulated on examining fish guts for MPs and have found evidence of MPs among multiple species and life stages across different functional groups (Vendel et al. 2017). Transfer to higher trophic levels, such as fish preying on zooplankton that has ingested MPs, has been hypothesized but no clear evidence has been found yet (Santana et al. 2017). So far, studies give contradictory results with some claiming that MPs cascade to higher trophic levels (Setälä et al. 2014) while others disagree or argue that they travel to predators but do not persist in the gut (Santana et al. 2017).

Effects Due to the Specific Properties of Microplastic Particles

All types of MPs are hypothesized to cause gut blockage or a false sense of fullness, if not excreted within reasonable time span (Gall and Thompson 2015). Most MPs are so-called secondary MPs resulting from fragmentation of larger particles. Therefore, the shape of MPs can cause internal ruptures and injuries. Most studies have been conducted with primary MPs: spherical, highly defined microbeads not reflecting the situation in the environment, as the most commonly found types are fragments and fibers. This calls for the use of fragments or fibers in laboratory studies to enhance significance of the obtained results.

The effects of MPs on an organism depend a lot on its size. Seabirds often take up colorful plastic particles that fill up their stomach and can be too large for gut passage (van Franeker et al. 2011). Contrarily, very small particles (1–400 nm) (GESAMP 2015), called nanoplastics if <100 nm (Löder and Gerdts 2015), can potentially be implemented in body cells after ingestion as they are small enough to pass pores in membranes. Inside the cell, the particles can potentially disturb other tissues than the digestive system such as the liver or lymph system (von Moos et al. 2012).

Impacts on biota can vary depending on the polymer type of the encountered MPs. Some polymers such as silicone are sturdier and break down slower under the influence of temperature and wave action than others due to their chemical composition. They fragment slower and are also less likely to leach pollutants as leaching of additives is dependent on surface area which increases with decreasing particle size (Suhrhoff and Scholz-Böttcher 2016). Other polymers, however, are already toxic in themselves by leaching monomers or oligomers such as polyvinyl chloride (PVC) or polystyrene (PS). These monomers have been shown to act as endocrine disruptors (Espinosa et al. 2016).

When MPs are introduced into the environment they are free of microorganisms and have not yet been impacted by waves or UV light. With time, MPs weather, pollutants adsorb and leach, and microorganisms start growing on the particles. These processes lead to changed characteristics of the MPs. With growing or adhering organisms the buoyancy changes and low density polymers start to sink and become available for a different range of organisms. Furthermore, biofilm-coated particles might not be recognizable anymore as MPs or seem more palatable due to chemical cues emitted from the microorganisms and are ingested with higher probability. Bacterial assemblages on MPs have also been found to be different from other surfaces with yet unknown consequences (Kesy et al. 2016).

Considering all of the above, there are various things to be accounted for when working with MP in the laboratory. Glass containers or glass material should be used as much as possible to reduce contamination sources. As this is only possible to a certain extent, negative controls should also account for plastic materials used within the experimental set-up. To assess the effects of MPs in experiments, the concentrations have to be determined, to which the organisms are exposed. Using spherical beads, this can be calculated via diameter, density and mass of the spheres. Irregular beads are more difficult to handle. Simple methods usually involve counting chambers (Syberg et al. 2015), light microscopy

(Nobre et al. 2015) and quantitative filtering of the water samples. Other common methods are flow cytometer (Sussarellu et al. 2016) and the use of a coulter counter (Syberg et al. 2015). For characterization of the beads, FTIR (Lusher et al. 2017), Raman spectroscopy and electron microscopy (Murray and Cowie 2011) are the preferred methods. The next step is to determine the presence of MPs in the organism. This is usually achieved by dissecting to check for presence in gut systems or histological analysis of tissue samples (Farrell and Nelson 2013). Effects on the organism can be directly determined via deformations of larvae. Potentially, MPs can induce epigenetic effects, e.g., in copepods (Heindler et al. 2017). Epigenetics are usually viewed as a quick and advantageous mechanism for an F1 generation to adapt to a stressor to which the F0 generation was exposed. Microplastics can also cause a decrease in reproduction (Heindler et al. 2017) and are therefore directly affecting fitness. Sussarellu et al. (2016) also reported reductions in feeding activity, accumulation and inhibition of acetylcholinesterase activity in bivalves.

Microplastics as Vector for Pollutants

The effects of the combination of MPs with pollutants are ambivalently discussed. First, it is important to differentiate between pollutants adhering to plastics, which belong to the group of persistent organic pollutants (POPs), originating from the water, and between additives leaching from the MP particles or emittance of monomers or oligomers from the MPs themselves. The difference here is that pollutants that adhere to plastics are usually already widespread in the environment, while pollutants associated with plastic have only been around since the production of plastics, so roughly the 1950s (Hammer et al. 2012). Both groups of chemicals suggest a role of MPs as a vector to organisms. This is very debatable for pollutants already present in the environment as some argue that other pathways such as food and water are several magnitudes higher than the intake via MPs, simply due to the fact that MPs are still not that abundant in the ocean and, therefore, bioaccumulation of this POPs is not increased by MPs yet. Additionally, it is also discussed if leaching additives from MPs are of major concern. Here, it is important to differentiate between primary MPs and secondary MPs. Primary MPs are introduced already in the size range of MPs whereas secondary MPs are often introduced into the environment as macroplastics that fragment over time into MPs. They weather over time and it remains an open question how much additives are still present within those fragments.

Heindler et al. (2017) revealed in a study on the toxicity effects of polyethylene terephthalate (PET) and the common plasticizer diethylhexyl phthalate (DEHP) that copepod nauplii are far more sensitive to exposure than adults. This stresses the need for assessing the toxicity of MPs at different life stages and focusing on juveniles or larvae, which are usually more sensitive to stressors than adults. Effects of MPs on younger life-stages can have knock-on effects on populations if for example mortality is significantly higher and fewer individuals reach sexual maturity and reproduce.

Regarding laboratory methods, again, glassware should be used where appropriate to make sure that no pollutant is adhered to the experimental container and, therefore, removed from the experiment. Toxin burdens can for example be assessed in different compartments (water, plastic, and biota) via high throughput liquid chromatography (HPLC) (Brennecke et al. 2015).

Conclusion

Although intensive research activities have already resolved some methodological issues in MP research, there are still some challenges, which need to be overcome before standardized operational protocols (SOPs) can be defined. Sampling effort (spatial and temporal replication, as well as sample volume) within a project is still limited by the high demand for personnel and physical resources as well as the long analysis time for MP samples. Thereby, an adequate sampling design should be chosen to answer pre-defined research questions as precisely as possible. It is obvious that different research questions require the use of different methods, which in turn will hamper complete standardization of methods. Nevertheless, a comprehensive and proper data recording, as well as gathering additional information, e.g., environmental data, will contribute to high quality datasets.

In addition, the extraction of MPs from environmental matrices is a crucial step, as inorganic and organic substances concurrently sampled with the potential MPs, can interfere with the subsequent analysis. Lately, many protocols have been proposed to remove inorganic or organic materials from samples. Thereby, developments were made to improve extraction efficiency, while not affecting fragile MPs, i.e., applying high density solutions for density separation of inorganic material or enzymatic purification of organic material. Finally, for a reliable identification of MPs a solely visible analysis is insufficient, and a chemical characterization is highly recommended. Spectroscopic methods like Raman- or FTIR-spectroscopy are state-of-the-art, providing particle related data (e.g., numbers, sizes) as well as thermal extraction methods like Pyr-GC-MS and TED-GC-MS, which provide mass related data and information about absorbed pollutants or contained additives.

Both methods will provide relevant information for further studies on the effects of MPs on organisms. There is still a huge lack of knowledge and besides evidence that MPs are

ingested, either by mistake or because the organism is not selective in feeding, information about the effects is limited. The exposure to MPs will largely depend on the habitat of the organism (water surface, water column, sediment) and the feeding type (predatory, herbivory, planktivory). How the MPs affect the organism after ingestion is largely unknown but depends most likely very much on specific properties of the MPs (polymer type, size, shape) as well as life stage of the organism. The interaction of MPs with adsorbed pollutants seems to be negligible compared to already existing pathways (food, water), however, the effect of leaching additives is not yet determined. Thus, the effects of MPs on organisms still need intense research activities to come up with proper risk assessments for different life stages of different species to determine, who is most at risk and how to protect them.

Appendix

This article is related to the YOUMARES 8 conference session no. 13: "Microplastics in Aquatic Habitats – Environmental Concentrations and Consequences". The original Call for Abstracts and the abstracts of the presentations within this session can be found in the appendix "Conference Sessions and Abstracts", chapter "12 Microplastics in Aquatic Habitats – Environmental Concentrations and Consequences", of this book.

References

Andrady AL (2017) The plastic in microplastics: a review. Mar Pollut Bull 119:12–22. https://doi.org/10.1016/j.marpolbul.2017.01.082

Avio CG, Gorbi S, Regoli F (2015) Experimental development of a new protocol for extraction and characterization of microplastics in fish tissues: first observations in commercial species from Adriatic Sea. Mar Environ Res 111:18–26. https://doi.org/10.1016/j.marenvres.2015.06.014

Avio CG, Gorbi S, Regoli F (2017) Plastics and microplastics in the oceans: from emerging pollutants to emerged threat. Mar Environ Res 128:2–11. https://doi.org/10.1016/j.marenvres.2016.05.012

Barrows APW, Neumann CA, Berger ML et al (2017) Grab vs. neuston tow net: a microplastic sampling performance comparison and possible advances in the field. Anal Methods 9:1446–1453. https://doi.org/10.1039/C6AY02387H

Bergmann M, Tekman MB, Gutow L (2017) LITTERBASE: an online portal for marine litter and microplastics and their implications for marine life. In: Baztan J, Jorgensen B, Pahl S et al (eds) Fate and impact of microplastics in marine ecosystems. Elsevier, MICRO 2016, Amsterdam, pp 106–107. https://doi.org/10.1016/B978-0-12-812271-6.00104-6

Besley A, Vijver MG, Behrens P et al (2017) A standardized method for sampling and extraction methods for quantifying microplastics in beach sand. Mar Pollut Bull 114:77–83. https://doi.org/10.1016/j.marpolbul.2016.08.055

Besseling E, Foekema EM, Van Franeker JA et al (2015) Microplastic in a macro filter feeder: humpback whale *Megaptera novaeangliae*. Mar Pollut Bull 95:248–252. https://doi.org/10.1016/j.marpolbul.2015.04.007

Brennecke D, Ferreira EC, Costa TMM et al (2015) Ingested microplastics (>100 μm) are translocated to organs of the tropical fiddler crab *Uca rapax*. Mar Pollut Bull 96:491–495. https://doi.org/10.1016/j.marpolbul.2015.05.001

Browne MA, Chapman MG, Thompson RC et al (2015) Spatial and temporal patterns of stranded intertidal marine debris: is there a picture of global change? Environ Sci Technol 49:7082–7094. https://doi.org/10.1021/es5060572

Bürkle GmbH (2015) Chemische Beständigkeit von Kunststoffen. Bürkle GmbH. URL:www.buerkle.de/files_pdf/wissenswertes/chemical_resistance_en.pdf. Accessed 03 Aug 2017

Carson HS, Colbert SL, Kaylor MJ et al (2011) Small plastic debris changes water movement and heat transfer through beach sediments. Mar Pollut Bull 62:1708–1713. https://doi.org/10.1016/j.marpolbul.2011.05.032

Chae D-H, Kim I-S, Kim S-K et al (2015) Abundance and distribution characteristics of microplastics in surface seawaters of the Incheon/Kyeonggi coastal region. Arch Environ Contam Toxicol 69:269–278. https://doi.org/10.1007/s00244-015-0173-4

Chubarenko I, Bagaev A, Zobkov M et al (2016) On some physical and dynamical properties of microplastic particles in marine environment. Mar Pollut Bull 108:105–112. https://doi.org/10.1016/j.marpolbul.2016.04.048

Claessens M, Meester SD, Landuyt LV et al (2011) Occurrence and distribution of microplastics in marine sediments along the Belgian coast. Mar Pollut Bull 62:2199–2204. https://doi.org/10.1016/j.marpolbul.2011.06.030

Claessens M, Van Cauwenberghe L, Vandegehuchte MB et al (2013) New techniques for the detection of microplastics in sediments and field collected organisms. Mar Pollut Bull 70:227–233. https://doi.org/10.1016/j.marpolbul.2013.03.009

Cole M, Webb H, Lindeque PK et al (2014) Isolation of microplastics in biota-rich seawater samples and marine organisms. Sci Rep 4:4528. https://doi.org/10.1038/srep04528

Collard F, Gilbert B, Eppe G et al (2015) Detection of anthropogenic particles in fish stomachs: an isolation method adapted to identification by Raman spectroscopy. Arch Environ Contam Toxicol 69:331–339. https://doi.org/10.1007/s00244-015-0221-0

Connors KA, Dyer SD, Belanger SE (2017) Advancing the quality of environmental microplastic research. Environ Toxicol Chem 36:1697–1703. https://doi.org/10.1002/etc.3829

Coppock RL, Cole M, Lindeque PK et al (2017) A small-scale, portable method for extracting microplastics from marine sediments. Environ Pollut 230:829–837. https://doi.org/10.1016/j.envpol.2017.07.017

Corcoran PL (2015) Benthic plastic debris in marine and fresh water environments. Env Sci Process Impact 17:1363–1369. https://doi.org/10.1039/c5em00188a

Corcoran PL, Biesinger MC, Grifi M (2009) Plastics and beaches: a degrading relationship. Mar Pollut Bull 58:80–84. https://doi.org/10.1016/j.marpolbul.2008.08.022

Costa MF, Duarte AC (2017) Microplastics sampling and sample handling. Compr Anal Chem 75:25–47. https://doi.org/10.1016/bs.coac.2016.11.002

Courtene-Jones W, Quinn B, Murphy F et al (2017) Optimisation of enzymatic digestion and validation of specimen preservation methods for the analysis of ingested microplastics. Anal Methods 9:1437–1445. https://doi.org/10.1039/C6AY02343F

Crichton EM, Noel M, Gies EA et al (2017) A novel, density-independent and FTIR-compatible approach for the rapid extraction of microplastics from aquatic sediments. Anal Methods 9:1419–1428. https://doi.org/10.1039/C6AY02733D

De Witte B, Devriese L, Bekaert K et al (2014) Quality assessment of the blue mussel (*Mytilus edulis*): comparison between com-

mercial and wild types. Mar Pollut Bull 85:146–155. https://doi.org/10.1016/j.marpolbul.2014.06.006

Dehaut A, Cassone A-L, Frère L et al (2016) Microplastics in seafood: benchmark protocol for their extraction and characterization. Environ Pollut 215:223–233. https://doi.org/10.1016/j.envpol.2016.05.018

Dekiff JH, Remy D, Klasmeier J et al (2014) Occurrence and spatial distribution of microplastics in sediments from Norderney. Environ Pollut 186:248–256. https://doi.org/10.1016/j.envpol.2013.11.019

Desforges J-PW, Galbraith M, Dangerfield N et al (2014) Widespread distribution of microplastics in subsurface seawater in the NE Pacific Ocean. Mar Pollut Bull 79:94–99. https://doi.org/10.1016/j.marpolbul.2013.12.035

Doyle MJ, Watson W, Bowlin NM et al (2011) Plastic particles in coastal pelagic ecosystems of the Northeast Pacific Ocean. Mar Environ Res 71:41–52. https://doi.org/10.1016/j.marenvres.2010.10.001

Dubaish F, Liebezeit G (2013) Suspended microplastics and black carbon particles in the jade system, southern North Sea. Water Air Soil Pollut 224:1352–1359. https://doi.org/10.1007/s11270-012-1352-9

Duis K, Coors A (2016) Microplastics in the aquatic and terrestrial environment: sources (with a specific focus on personal care products), fate and effects. Environ Sci Eur 28:2

Dümichen E, Barthel A-K, Braun U et al (2015) Analysis of polyethylene microplastics in environmental samples, using a thermal decomposition method. Water Res 85:451–457. https://doi.org/10.1016/j.watres.2015.09.002

Dümichen E, Eisentraut P, Bannick CG et al (2017) Fast identification of microplastics in complex environmental samples by a thermal degradation method. Chemosphere 174:572–584. https://doi.org/10.1016/j.chemosphere.2017.02.010

Edson EC, Patterson MR (2015) MantaRay: a novel autonomous sampling instrument for in situ measurements of environmental microplastic particle concentrations. Paper presented at the OCEANS 2015 – MTS/IEEE Washington, DC, pp 19–22 Oct 2015

Elert AM, Becker R, Duemichen E et al (2017) Comparison of different methods for MP detection: what can we learn from them, and why asking the right question before measurements matters? Environ Pollut 231:1256–1264. https://doi.org/10.1016/j.envpol.2017.08.074

Enders K, Lenz R, Stedmon CA et al (2015) Abundance, size and polymer composition of marine microplastics ≥ 10 μm in the Atlantic Ocean and their modelled vertical distribution. Mar Pollut Bull 100:70–81. https://doi.org/10.1016/j.marpolbul.2015.09.027

Eriksen M, Mason S, Wilson S et al (2013) Microplastic pollution in the surface waters of the Laurentian Great Lakes. Mar Pollut Bull 77:177–182. https://doi.org/10.1016/j.marpolbul.2013.10.007

Erni-Cassola G, Gibson MI, Thompson RC et al (2017) Lost, but found with Nile red: a novel method for detecting and quantifying small microplastics (1 mm to 20 μm) in environmental samples. Environ Sci Technol. https://doi.org/10.1021/acs.est.7b04512

Espinosa C, Esteban MÁ, Cuesta A (2016) Microplastics in aquatic environments and their toxicological implications for fish. In: Soloneski S, Larramendy ML (eds) Toxicology – new aspects to this scientific conundrum. InTech, Rijeka, pp 113–145. https://doi.org/10.5772/64815

Farrell P, Nelson K (2013) Trophic level transfer of microplastic: *Mytilus edulis* (L.) to *Carcinus maenas* (L.). Environ Pollut 177:1–3. https://doi.org/10.1016/j.envpol.2013.01.046

Filella M (2015) Questions of size and numbers in environmental research on microplastics: methodological and conceptual aspects. Environ Chem 12:527–538. https://doi.org/10.1071/EN15012

Fischer M, Scholz-Böttcher BM (2017) Simultaneous trace identification and quantification of common types of microplastics in environmental samples by pyrolysis-gas chromatography–mass spectrometry. Environ Sci Technol 51:5052–5060. https://doi.org/10.1021/acs.est.6b06362

Fischer D, Kaeppler A, Eichhorn K-J (2015) Identification of microplastics in the marine environment by Raman microspectroscopy and imaging. Am Lab 47:32–34

Fisner M, Majer AP, Balthazar-Silva D et al (2017) Quantifying microplastic pollution on sandy beaches: the conundrum of large sample variability and spatial heterogeneity. Environ Sci Pollut Res 24:13732–13740. https://doi.org/10.1007/s11356-017-8883-y

Foekema EM, De Gruijter C, Mergia MT et al (2013) Plastic in North Sea fish. Environ Sci Technol 47:8818–8824. https://doi.org/10.1021/es400931b

Frère L, Paul-Pont I, Moreau J et al (2016) A semi-automated Raman micro-spectroscopy method for morphological and chemical characterizations of microplastic litter. Mar Pollut Bull 113:461–468. https://doi.org/10.1016/j.marpolbul.2016.10.051

Fries E, Dekiff JH, Willmeyer J et al (2013) Identification of polymer types and additives in marine microplastic particles using pyrolysis-GC/MS and scanning electron microscopy. Environ Sci Processes Impact 15:1949–1956. https://doi.org/10.1039/C3EM00214D

Gall SC, Thompson RC (2015) The impact of debris on marine life. Mar Pollut Bull 92:170–179. https://doi.org/10.1016/j.marpolbul.2014.12.041

GESAMP (2015) Sources, fate and effects of microplastics in the marine environment: a global assessment. In: Kershaw PJ (ed) (IMO/FAO/UNESCO-IOC/UNIDO/WMO/IAEA/UN/UNEP/UNDP Joint Group of Experts on the Scientific Aspects of Marine Environmental Protection). Rep. Stud. GESAMP No. 90

GESAMP (2016) Sources, fate and effects of microplastics in the marine environment: part two of a global assessment. In: Kershaw PJ, Rochmann CM (eds) (IMO/FAO/UNESCO-IOC/UNIDO/WMO/IAEA/UN/UNEP/UNDP Joint Group of Experts on the Scientific Aspects of Marine Environmental Protection). Rep. Stud. GESAMP No. 93

Goldstein MC, Titmus AJ, Ford M (2013) Scales of spatial heterogeneity of plastic marine debris in the Northeast Pacific Ocean. PLoS One 8:e80020. https://doi.org/10.1371/journal.pone.0080020

Hammer J, Kraak MHS, Parsons JR (2012) Plastics in the marine environment: the dark side of a modern gift. In: Whitacre DM (ed) Reviews of environmental contamination and toxicology, vol 220. Springer, New York, pp 1–44. https://doi.org/10.1007/978-1-4614-3414-6_1

Hanke G, Galgani F, Werner S et al (2013) MSFD GES technical subgroup on marine litter. Guidance on Monitoring of marine litter in European Seas European Commission. https://doi.org/10.2788/99475

Hanvey JS, Lewis PJ, Lavers JL et al (2017) A review of analytical techniques for quantifying microplastics in sediments. Anal Methods 9:1369–1383. https://doi.org/10.1039/C6AY02707E

Harrison JP, Ojeda JJ, Romero-González ME (2012) The applicability of reflectance micro-Fourier-transform infrared spectroscopy for the detection of synthetic microplastics in marine sediments. Sci Total Environ 416:455–463. https://doi.org/10.1016/j.scitotenv.2011.11.078

Heindler FM, Alajmi F, Huerlimann R et al (2017) Toxic effects of polyethylene terephthalate microparticles and Di(2-ethylhexyl) phthalate on the calanoid copepod, *Parvocalanus crassirostris*. Ecotoxicol Environ Saf 141:298–305. https://doi.org/10.1016/j.ecoenv.2017.03.029

Heo N, Hong S, Han G et al (2013) Distribution of small plastic debris in cross-section and high strandline on Heungnam beach, South Korea. Ocean Sci J 48:225–233. https://doi.org/10.1007/s12601-013-0019-9

Hidalgo-Ruz V, Gutow L, Thompson RC, Thiel M (2012) Microplastics in the marine environment: a review of the methods used for identification and quantification. Environ Sci Technol 46:3060–3075. https://doi.org/10.1021/es2031505

Imhof HK, Schmid J, Niessner R et al (2012) A novel, highly efficient method for the separation and quantification of plastic particles in sediments of aquatic environments. Limnol Oceanogr Methods 10:524–537. https://doi.org/10.4319/lom.2012.10.524

Imhof HK, Ivleva NP, Schmid J et al (2013) Contamination of beach sediments of a subalpine lake with microplastic particles. Curr Biol 23:R867–R868

Imhof HK, Laforsch C, Wiesheu AC et al (2016) Pigments and plastic in limnetic ecosystems: a qualitative and quantitative study on microparticles of different size classes. Water Res 98:64–74. https://doi.org/10.1016/j.watres.2016.03.015

Imhof HK, Sigl R, Brauer E et al (2017) Spatial and temporal variation of macro-, meso- and microplastic abundance on a remote coral island of the Maldives, Indian Ocean. Mar Pollut Bull 116:340–347. https://doi.org/10.1016/j.marpolbul.2017.01.010

Ivleva NP, Wiesheu AC, Niessner R (2016) Microplastic in aquatic ecosystems. Angew Chem Int Ed 56:1720–1739. https://doi.org/10.1002/anie.201606957

Kang J-H, Kwon OY, Lee K-W et al (2015) Marine neustonic microplastics around the southeastern coast of Korea. Mar Pollut Bull 96:304–312. https://doi.org/10.1016/j.marpolbul.2015.04.054

Käppler A, Windrich F, Löder MJ et al (2015) Identification of microplastics by FTIR and Raman microscopy: a novel silicon filter substrate opens the important spectral range below 1300 cm^{-1} for FTIR transmission measurements. Anal Bioanal Chem 407:6791–6801. https://doi.org/10.1007/s00216-015-8850-8

Käppler A, Fischer D, Oberbeckmann S et al (2016) Analysis of environmental microplastics by vibrational microspectroscopy: FTIR, Raman or both? Anal Bioanal Chem 408:8377–8391. https://doi.org/10.1007/s00216-016-9956-3

Karami A, Golieskardi A, Choo CK et al (2017) A high-performance protocol for extraction of microplastics in fish. Sci Total Environ 578:485–494. https://doi.org/10.1016/j.scitotenv.2016.10.213

Karlsson TM, Vethaak AD, Almroth BC et al (2017) Screening for microplastics in sediment, water, marine invertebrates and fish: method development and microplastic accumulation. Mar Pollut Bull 122:403–408. https://doi.org/10.1016/j.marpolbul.2017.06.081

Kedzierski M, Le Tilly V, Bourseau P et al (2016) Microplastics elutriation from sandy sediments: a granulometric approach. Mar Pollut Bull 107:315–323. https://doi.org/10.1016/j.marpolbul.2016.03.041

Kedzierski M, Le Tilly V, César G et al (2017) Efficient microplastics extraction from sand. A cost effective methodology based on sodium iodide recycling. Mar Pollut Bull 115:120–129. https://doi.org/10.1016/j.marpolbul.2016.12.002

Kesy K, Oberbeckmann S, Müller F et al (2016) Polystyrene influences bacterial assemblages in *Arenicola marina*-populated aquatic environments in vitro. Environ Pollut 219:219–227. https://doi.org/10.1016/j.envpol.2016.10.032

Kim I-S, Chae D-H, Kim S-K et al (2015) Factors influencing the spatial variation of microplastics on high-tidal coastal beaches in Korea. Arch Environ Contam Toxicol 69:299–309. https://doi.org/10.1007/s00244-015-0155-6

Klein S, Worch E, Knepper TP (2015) Occurrence and spatial distribution of microplastics in river shore sediments of the Rhine-main area in Germany. Environ Sci Technol 49:6070–6076. https://doi.org/10.1021/acs.est.5b00492

Lattin GL, Moore CJ, Zellers AF et al (2004) A comparison of neustonic plastic and zooplankton at different depths near the southern California shore. Mar Pollut Bull 49:291–294. https://doi.org/10.1016/j.marpolbul.2004.01.020

Law KL, Morét-Ferguson S, Maximenko NA et al (2010) Plastic accumulation in the North Atlantic subtropical gyre. Science 329:1185–1188. https://doi.org/10.1126/science.1192321

Law KL, Morét-Ferguson SE, Goodwin DS et al (2014) Distribution of surface plastic debris in the eastern Pacific Ocean from an 11-year data set. Environ Sci Technol 48:4732–4738. https://doi.org/10.1021/es4053076

Lenz R, Enders K, Stedmon CA (2015) A critical assessment of visual identification of marine microplastic using Raman spectroscopy for analysis improvement. Mar Pollut Bull 100:82–91. https://doi.org/10.1016/j.marpolbul.2015.09.026

Löder MGJ, Gerdts G (2015) Methodology used for the detection and identification of microplastics—a critical appraisal. In: Bergmann M, Gutow L, Klages M (eds) Marine anthropogenic litter. Springer, Cham, pp 201–227. https://doi.org/10.1007/978-3-319-16510-3_8

Löder MGJ, Kuczera M, Mintenig S et al (2015) Focal plane array detector-based micro-Fourier-transform infrared imaging for the analysis of microplastics in environmental samples. Environ Chem 12:563–581. https://doi.org/10.1071/EN14205

Löder MGJ, Imhof HK, Ladehoff M et al (2017) Enzymatic purification of microplastics in environmental samples. Environ Sci Technol. https://doi.org/10.1021/acs.est.7b03055

Long M, Paul-Pont I, Hégaret H et al (2017) Interactions between polystyrene microplastics and marine phytoplankton lead to species-specific hetero-aggregation. Environ Pollut 228:454–463. https://doi.org/10.1016/j.envpol.2017.05.047

Lusher AL, Burke A, O'Connor I et al (2014) Microplastic pollution in the Northeast Atlantic Ocean: validated and opportunistic sampling. Mar Pollut Bull 88:325–333. https://doi.org/10.1016/j.marpolbul.2014.08.023

Lusher AL, Welden NA, Sobral P et al (2017) Sampling, isolating and identifying microplastics ingested by fish and invertebrates. Anal Methods 9:1346–1360. https://doi.org/10.1039/C6AY02415G

Maes T, Jessop R, Wellner N et al (2017a) A rapid-screening approach to detect and quantify microplastics based on fluorescent tagging with Nile Red. Sci Rep 7:44501. https://doi.org/10.1038/srep44501

Maes T, Van der Meulen MD, Devriese LI et al (2017b) Microplastics baseline surveys at the water surface and in sediments of the north-East Atlantic. Front Mar Sci 4:135. https://doi.org/10.3389/fmars.2017.00135

Masura J, Baker J, Foster G et al (2015) Laboratory methods for the analysis of microplastics in the marine environment: recommendations for quantifying synthetic particles in waters and sediments. NOAA Technical Memorandum, Silver Spring

Miller ME, Kroon FJ, Motti CA (2017) Recovering microplastics from marine samples: a review of current practices. Mar Pollut Bull 123:6–18. https://doi.org/10.1016/j.marpolbul.2017.08.058

Mintenig SM, Int-Veen I, Löder MGJ et al (2017) Identification of microplastic in effluents of waste water treatment plants using focal plane array-based micro-Fourier-transform infrared imaging. Water Res 108:365–372. https://doi.org/10.1016/j.watres.2016.11.015

Moreira FT, Prantoni AL, Martini B et al (2016) Small-scale temporal and spatial variability in the abundance of plastic pellets on sandy beaches: methodological considerations for estimating the input of microplastics. Mar Pollut Bull 102:114–121. https://doi.org/10.1016/j.marpolbul.2015.11.051

Murray F, Cowie PR (2011) Plastic contamination in the decapod crustacean *Nephrops norvegicus* (Linnaeus, 1758). Mar Pollut Bull 62:1207–1217. https://doi.org/10.1016/j.marpolbul.2011.03.032

Ng KL, Obbard JP (2006) Prevalence of microplastics in Singapore's coastal marine environment. Mar Pollut Bull 52:761–767. https://doi.org/10.1016/j.marpolbul.2005.11.017

Nobre CR, Santana MFM, Maluf A et al (2015) Assessment of microplastic toxicity to embryonic development of the sea urchin *Lytechinus variegatus* (Echinodermata: Echinoidea). Mar Pollut Bull 92:99–104. https://doi.org/10.1016/j.marpolbul.2014.12.050

Norén F (2007) Small plastic particles in Coastal Swedish waters. KIMO Sweden, Lysekil

Nuelle M-T, Dekiff JH, Remy D et al (2014) A new analytical approach for monitoring microplastics in marine sediments. Environ Pollut 184:161–169. https://doi.org/10.1016/j.envpol.2013.07.027

Obbard RW, Sadri S, Wong YQ et al (2014) Global warming releases microplastic legacy frozen in Arctic Sea ice. Earth's Future 2:315–320. https://doi.org/10.1002/2014EF000240

Osswald TA, Baur E, Brinkmann S et al (2006) International plastics handbook. Hanser, München

Primpke S, Imhof H, Piehl S et al (2017a) Mikroplastik in der Umwelt. Chem unserer Zeit 51:402–412. https://doi.org/10.1002/ciuz.201700821

Primpke S, Lorenz C, Rascher-Friesenhausen R et al (2017b) An automated approach for microplastics analysis using focal plane array (FPA) FTIR microscopy and image analysis. Anal Methods 9:1499–1511. https://doi.org/10.1039/C6AY02476A

Qiu Q, Tan Z, Wang J et al (2016) Extraction, enumeration and identification methods for monitoring microplastics in the environment. Estuar Coast Shelf Sci 176:102–109. https://doi.org/10.1016/j.ecss.2016.04.012

Quinn B, Murphy F, Ewins C (2017) Validation of density separation for the rapid recovery of microplastics from sediment. Anal Methods 9:1491–1498. https://doi.org/10.1039/C6AY02542K

Reid PC, Colebrook JM, Matthews JBL et al (2003) The Continuous Plankton Recorder: concepts and history, from Plankton Indicator to undulating recorders. Prog Oceanogr 58:117–173. https://doi.org/10.1016/j.pocean.2003.08.002

Reisser J, Slat B, Noble K et al (2015) The vertical distribution of buoyant plastics at sea: an observational study in the North Atlantic Gyre. Biogeosciences 12:1249–1256. https://doi.org/10.5194/bg-12-1249-2015

Ribeiro F, Garcia AR, Pereira BP et al (2017) Microplastics effects in *Scrobicularia plana*. Mar Pollut Bull 122:379–391. https://doi.org/10.1016/j.marpolbul.2017.06.078

Romeo T, Pietro B, Pedà C et al (2015) First evidence of presence of plastic debris in stomach of large pelagic fish in the Mediterranean Sea. Mar Pollut Bull 95:358–361. https://doi.org/10.1016/j.marpolbul.2015.04.048

Santana MFM, Moreira FT, Turra A (2017) Trophic transference of microplastics under a low exposure scenario: insights on the likelihood of particle cascading along marine food-webs. Mar Pollut Bull 121:154–159. https://doi.org/10.1016/j.marpolbul.2017.05.061

Setälä O, Fleming-Lehtinen V, Lehtiniemi M (2014) Ingestion and transfer of microplastics in the planktonic food web. Environ Pollut 185:77–83. https://doi.org/10.1016/j.envpol.2013.10.013

Setälä O, Magnusson K, Lehtiniemi M et al (2016) Distribution and abundance of surface water microlitter in the Baltic Sea: a comparison of two sampling methods. Mar Pollut Bull 110:177–183. https://doi.org/10.1016/j.marpolbul.2016.06.065

Shim WJ, Song YK, Hong SH et al (2016) Identification and quantification of microplastics using Nile Red staining. Mar Pollut Bull 113:469–476. https://doi.org/10.1016/j.marpolbul.2016.10.049

Shim WJ, Hong SH, Eo SE (2017) Identification methods in microplastic analysis: a review. Anal Methods 9:1384–1391. https://doi.org/10.1039/C6AY02558G

Song YK, Hong SH, Jang M et al (2014) Large accumulation of micro-sized synthetic polymer particles in the sea surface microlayer. Environ Sci Technol 48:9014–9021. https://doi.org/10.1021/es501757s

Song YK, Hong SH, Jang M et al (2015) A comparison of microscopic and spectroscopic identification methods for analysis of microplastics in environmental samples. Mar Pollut Bull 93:202–209. https://doi.org/10.1016/j.marpolbul.2015.01.015

Stolte A, Forster S, Gerdts G et al (2015) Microplastic concentrations in beach sediments along the German Baltic coast. Mar Pollut Bull 99:216–229. https://doi.org/10.1016/j.marpolbul.2015.07.022

Suhrhoff TJ, Scholz-Böttcher BM (2016) Qualitative impact of salinity, UV radiation and turbulence on leaching of organic plastic additives from four common plastics – a lab experiment. Mar Pollut Bull 102:84–94. https://doi.org/10.1016/j.marpolbul.2015.11.054

Sussarellu R, Suquet M, Thomas Y et al (2016) Oyster reproduction is affected by exposure to polystyrene microplastics. Proc Natl Acad Sci U S A 113:2430–2435. https://doi.org/10.1073/pnas.1519019113

Syberg K, Khan FR, Selck H et al (2015) Microplastics: addressing ecological risk through lessons learned. Environ Toxicol Chem 34:945–953. https://doi.org/10.1002/etc.2914

Tagg AS, Sapp M, Harrison JP et al (2015) Identification and quantification of microplastics in wastewater using focal plane array-based reflectance micro-FT-IR imaging. Anal Chem 87:6032–6040. https://doi.org/10.1021/acs.analchem.5b00495

Tagg AS, Harrison JP, Ju-Nam Y et al (2017) Fenton's reagent for the rapid and efficient isolation of microplastics from wastewater. Chem Commun 53:372–375. https://doi.org/10.1039/C6CC08798A

Thompson RC, Olsen Y, Mitchell RP et al (2004) Lost at sea: where is all the plastic? Science 304:838. https://doi.org/10.1126/science.1094559

Turra A, Manzano AB, Dias RJS et al (2014) Three-dimensional distribution of plastic pellets in sandy beaches: shifting paradigms. Sci Rep 4:4435. https://doi.org/10.1038/srep04435

Underwood AJ, Chapman MG, Browne MA (2017) Some problems and practicalities in design and interpretation of samples of microplastic waste. Anal Methods 9:1332–1345. https://doi.org/10.1039/C6AY02641A

Van Cauwenberghe L, Claessens M, Vandegehuchte MB et al (2013a) Assessment of marine debris on the Belgian Continental Shelf. Mar Pollut Bull 73:161–169. https://doi.org/10.1016/j.marpolbul.2013.05.026

Van Cauwenberghe L, Vanreusel A, Mees J et al (2013b) Microplastic pollution in deep-sea sediments. Environ Pollut 182:495–499. https://doi.org/10.1016/j.envpol.2013.08.013

Van Cauwenberghe L, Claessens M, Vandegehuchte MB et al (2015) Microplastics are taken up by mussels (*Mytilus edulis*) and lugworms (*Arenicola marina*) living in natural habitats. Environ Pollut 199:10–17. https://doi.org/10.1016/j.envpol.2015.01.008

van Franeker JA, Blaize C, Danielsen J et al (2011) Monitoring plastic ingestion by the northern fulmar Fulmarus glacialis in the North Sea. Environ Pollut 159:2609–2615. https://doi.org/10.1016/j.envpol.2011.06.008

Vendel AL, Bessa F, Alves VEN et al (2017) Widespread microplastic ingestion by fish assemblages in tropical estuaries subjected to anthropogenic pressures. Mar Pollut Bull 117:448–455. https://doi.org/10.1016/j.marpolbul.2017.01.081

Vianello A, Boldrin A, Guerriero P et al (2013) Microplastic particles in sediments of lagoon of Venice, Italy: first observations on occurrence, spatial patterns and identification. Estuar Coast Shelf Sci 130:54–61. https://doi.org/10.1016/j.ecss.2013.03.022

Viršek MK, Palatinus A, Koren Š et al (2016) Protocol for microplastics sampling on the sea surface and sample analysis. J Vis Exp 118:55161. https://doi.org/10.3791/55161

von Moos N, Burkhardt-Holm P, Kohler A (2012) Uptake and effects of microplastics on cells and tissue of the blue mussel *Mytilus edulis* L. after an experimental exposure. Environ Sci Technol 46:11327–11335. https://doi.org/10.1021/es302332w

Wagner J, Wang Z-M, Ghosal S et al (2017) Novel method for the extraction and identification of microplastics in ocean trawl and fish gut matrices. Anal Methods 9:1479–1490. https://doi.org/10.1039/C6AY02396G

Wang Z-M, Wagner J, Ghosal S et al (2017) SEM/EDS and optical microscopy analyses of microplastics in ocean trawl and fish guts. Sci Total Environ 603:616–626. https://doi.org/10.1016/j.scitotenv.2017.06.047

Ward EJ, Shumway SE (2004) Separating the grain from the chaff: particle selection in suspension- and deposit-feeding bivalves. J Exp Mar Biol Ecol 300:83–130. https://doi.org/10.1016/j.jembe.2004.03.002

Woodall LC, Sanchez-Vidal A, Canals M et al (2014) The deep sea is a major sink for microplastic debris. R Soc open Sci 1:140317. https://doi.org/10.1098/rsos.140317

Wright SL, Thompson RC, Galloway TS (2013) The physical impacts of microplastics on marine organisms: a review. Environ Pollut 178:483–492. https://doi.org/10.1016/j.envpol.2013.02.031

Zhao S, Danley M, Ward JE et al (2017) An approach for extraction, characterization and quantitation of microplastic in natural marine snow using Raman microscopy. Anal Methods 9:1470–1478. https://doi.org/10.1039/C6AY02302A

Zhu X (2015) Optimization of elutriation device for filtration of microplastic particles from sediment. Mar Pollut Bull 92:69–72. https://doi.org/10.1016/j.marpolbul.2014.12.054

Zobkov M, Esiukova E (2017) Microplastics in Baltic bottom sediments: quantification procedures and first results. Mar Pollut Bull 114:724–732. https://doi.org/10.1016/j.marpolbul.2016.10.060

List of publications

PUBLICATIONS IN PEER-REVIEWD JOURNALS

2020 **Piehl S,** Atwood EC, Bochow M, Imhof HK, Franke J, Siegert F, Laforsch C: Can water constituents be used as proxy to map microplastic dispersal within transitional and coastal waters? Front. Environ. Sci. 8: 92.

2019 **Piehl S,** Mitterwallner V, Atwood EC, Bochow M, Laforsch C: Abundance and distribution of large microplastics (1-5 mm) within beach sediments at the Po River Delta, northeast Italy. Mar. Pollut. Bull. 149.

Frei S, **Piehl S,** Gilfedder BS, Löder MGJ, Krutzke J, Wilhelm L, Laforsch C: Occurrence of microplastics in the hyporheic zone of rivers. Sci. Rep. 9.

2018 **Piehl S,** Leibner A, Löder MGJ, Dris R, Bogner C, Laforsch C: Identification and quantification of macro- and microplastics on an agricultural farmland. Sci. Rep. 8.

Atwood EC, Falcieric F, **Piehl S**, Bochow M, Matthies M, Franke J, Carniel S, Sclavo M, Laforsch C, Siegert F: Coastal accumulation of microplastic particles emitted from the Po River, Northern Italy: Comparing remote sensing and hydrodynamic modelling with in-situ sample collections. Mar. Pollut. Bull. 138: 561-574.

Weithmann N, Möller JN, Löder MGJ, **Piehl S**, Laforsch C, Freitag R: Organic fertilizer as a vehicle for the entry of microplastic into the environment. Sci. Adv. 4: 1-7.

2017 Löder MGJ, Imhof HK, Ladehoff M, Löschel L, Lorenz C, Mintenig S, **Piehl S**, Primpke S, Schrank I, Laforsch C, Gerdts G: Enzymatic purification of microplastics in environmental samples. Environ. Sci. Technol. 51: 14283–14292s.

2013 Seibold S, Hempel A, **Piehl S**, Bässler C, Brandl R, Rösner S, Müller J: Forest vegetation structure has more influence on predation risk of artificial ground nests than human activities. Basic and Applied Ecology 14: 687-693.

BOOK CHAPTER

2018 Hamm T, Lorenz C, **Piehl S**: Microplastics in Aquatic Systems – Monitoring Methods and Biological Consequences. In: YOUMARES 8 – Oceans Across Boundaries: Learning from each other [Jungblut S et al. (eds.)], 1st edt.: 179-195, Springer.

NON-PEER REVIEWED CONTRIBUTIONS

2019 **Piehl S,** Hauk R, Robbe E, Haseler M, Klaeger F, Labrenz M, Schernewski G: Mikroplastik in der Umwelt - Eintrag, Verbleib und Konsequenzen. Tagungsband 12. Rostocker Abwassertagung.

Moses SR, **Piehl S**, Ramsperger AFRM, Löder MGJ, Laforsch C: Plastik im aquatischen Ökosystem. Sammelband „Ressourcen im globalen Wandel“.

2018 Möller JN, Laforsch C, Löder MGJ, Schrank I, **Piehl S**: Von der Tonne auf den Acker. Entsorga Magazin 5, Oktober 2018.

2017 Primpke S, Imhof HK, **Piehl S**, Lorenz C, Löder MGJ, Laforsch C, Gerdts G: Mikroplastik in der Umwelt. Chemie in unserer Zeit 51: 402-412.

CONFERENCE CONTRIBUTIONS

2018 **Poster**
SETAC, Rom
Applicability of remote sensing methods for indirect mapping of microplastic distribution within aquatic ecosystems

2017 **Session chair**
YOUMARES, Kiel
Microplastics in aquatic habitats – environmental concentrations and consequences

2015 **Talk**
Piehl S, Bochow M, Atwood E, Franke J, Siegert F, Laforsch C: Contamination of aquatic ecosystems with plastic debris: global and local monitoring using remote sensing methods. ASLO 22nd-27th February, Granada, Spain.

Talk
Piehl S, Bochow M, Atwood E, Imhof H, Schrank I, Franke J, Englhart S, Siegert F and Laforsch C: Satelliten-gestützte Methoden zur Erfassung von Quellen und Verbreitungsmuster von Mikroplastik in aquatischen Ökosystemen. DGL 21st-25th September, Essen, Germany.

Talk
Piehl S, Bochow M, Atwood E, Imhof H, Schrank I, Franke J, Engelhart S, Siegert F, and Laforsch C: Applicability of Remote Sensing Methods for Monitoring Floating Microplastic. YOUMARES 16th-18th September, Bremen, Germany.

2014 **Talk**
Piehl S, Siamsuni Y, Lenz M, Neviaty PZ, Juterzenka K: Effects of Microplastic Ingestion on the Performance of the Mangrove Whelk Terebralia palustris (Gastropoda; Potamididae). YOUMARES 10th-12th September, Stralsund, Germany.

Danksagung

Diese Doktorarbeit ist nur mit Hilfe und Unterstützung vieler Personen zu Stande gekommen, denen ich hier meinen Dank ausdrücken möchte. Prof. Dr. Christian Laforsch und Prof. Dr. Florian Siegert haben mir durch ihren Antrag für das Projekt „Sentinels4MarinePlastics“ erst die Möglichkeit gegeben mich dieser Thematik zu widmen. Christian möchte ich zudem für die Möglichkeit in einer tollen Arbeitsgruppe und einem gut ausgestatteten Labor meine Arbeit durchführen zu können danken. In der Arbeitsgruppe Tierökologie möchte ich mich bei allen Kollegen/Innen für die herzliche Aufnahme und die Unterstützung bedanken. Christian und Martin zudem für die fachliche Betreuung und, zusammen mit der gesamten „Mikroplastik-Gruppe“ und meinen Projektpartnern Liz und Mathias, für die kreativen Diskussionsrunden, durch die neue Ideen zu Stande gekommen sind und damit den Inhalt der Arbeit bereichert haben.

Während der Feldarbeiten in Indonesien waren vor allem Pak Kurnia, Haris und Reza, und in Italien unser Bootskapitän Claudio, eine große Unterstützung. Da die Arbeit im großen Umfang Laborarbeit beinhaltete möchte ich mich vor allem auch bei Uschi, Heghnar, Marion und Mechthild bedanken, die als Ansprechpartner für Laborgeräte, Verbrauchsmaterialien, Einweisungen, etc. eine enorm große Hilfe waren und einem immer unterstützend zur Seite standen. Danke auch an Isabella, Martina, Jens, und Liz die immer ein offenes Ohr für mich hatten.

Für die sprachliche Überarbeitung möchte ich zudem Mark meinen Dank ausdrücken, sowie Franziska und Mareike für die inhaltlichen Anmerkungen.

Zuletzt gilt mein tiefster Dank meinen Eltern, meinem Bruder, Peter und meinen Freunden, sowie meiner „Bayreuther-Familie“ den Alexens, die während der gesamten Studien- und Doktorandenzeit immer an mich geglaubt haben, darüber hinaus eine enorme Stütze waren und mir meine in extremen Stressphasen auftretende Verwirrtheit stets verziehen haben.

(Eidesstattliche) Versicherungen und Erklärungen

(§ 9 Satz 2 Nr. 3 PromO BayNAT)

Hiermit versichere ich eidesstattlich, dass ich die Arbeit selbständig verfasst und keine anderen als die von mir angegebenen Quellen und Hilfsmittel benutzt habe (vgl. Art. 64 Abs 1 Satz 6 BayHSchG).

(§ 9 Satz 2 Nr. 3 PromO BayNAT)

Hiermit erkläre ich, dass ich die Dissertation nicht bereits zur Erlangung eines akademischen Grades eingereicht habe und dass ich nicht bereits diese oder eine gleichartige Doktorprüfung endgültig nicht bestanden habe.

(§ 9 Satz 2 Nr. 4 PromO BayNAT)

Hiermit erkläre ich, dass ich Hilfe von gewerblichen Promotionsberatern bzw. -vermittlern oder ähnlichen Dienstleistern weder bisher in Anspruch genommen habe noch künftig in Anspruch nehmen werde.

(§ 9 Satz 2 Nr. 7 PromO BayNAT)

Hiermit erkläre ich mein Einverständnis, dass die elektronische Fassung meiner Dissertation unter Wahrung meiner Urheberrechte und des Datenschutzes einer gesonderten Überprüfung unterzogen werden kann.

(§ 9 Satz 2 Nr. 8 PromO BayNAT)

Hiermit erkläre ich mein Einverständnis, dass bei Verdacht wissenschaftlichen Fehlverhaltens Ermittlungen durch universitätsinterne Organe der wissenschaftlichen Selbstkontrolle stattfinden können.

……

Ort, Datum, Unterschrift